

**Advances in directed monooxygenase evolution:
From diversity generation and flow cytometry screening
to tailor-made monooxygenases**

Von der Fakultät für Mathematik, Informatik und Naturwissenschaften der RWTH Aachen University zur Erlangung des akademischen Grades einer Doktorin der Naturwissenschaften genehmigte Dissertation

vorgelegt von

Diplom-Biologin

Anna Joëlle Ruff

aus Aachen

Berichter: Universitätsprofessor Dr. Ulrich Schwaneberg

Juniorprofessorin Dr. Miriam Agler-Rosenbaum

Tag der mündlichen Prüfung: 30. August 2012

Diese Dissertation ist auf den Internetseiten der Hochschulbibliothek online verfügbar.

Parts of this thesis have been previously published:

Publications:

- 1) Anna Joëlle Ruff, Jan Marienhagen, Rajni Verma, Danilo Roccatano, Hans-Gottfried Genieser, Percy Niemann, Amol V. Shivange, Ulrich Schwaneberg, dRTP and dPTP a complementary nucleotide couple for the Sequence Saturation Mutagenesis (SeSaM) method, 2012, Journal of Molecular Catalysis B: Enzymatic 84, 40-47
- 2) Anna Joëlle Ruff, Alexander Dennig, Georgette Wirtz, Milan Blanusa, Ulrich Schwaneberg, Ultra-high throughput screening system for accelerated directed evolution of P450 monooxygenases, 2012, ACS-Catalysis 2, 2724-2728
- 3) Alexander Dennig, Jan Marienhagen, Anna Joëlle Ruff, Lukas Guddat, Ulrich Schwaneberg, Directed Evolution of P 450 BM3 into a p-Xylene Hydroxylase, 2012, ChemCatChem 4, 771-773
- 4) Andreas Braun, Bettina Halwachs, Martina Geier, Katrin Weinhandl, Michael Guggemos, Jan Marienhagen, Anna Joëlle Ruff, Ulrich Schwaneberg, Vincent Rabin, Daniel E. Torres Pazmino, Gerhard G. Thallinger, Anton Glieder, MuteinDB: The mutein database linking substrates, products and enzymatic reactions directly with genetic variants of enzymes, 2012, Databases Vol. 2012, doi:10.1093/database/bas028

Posters:

- 5) Anna Joëlle Ruff, Jan Marienhagen, Ulrich Schwaneberg, A redesigned monooxygenase P450 BM3 directly driven by a conductive polymer, 2010, 10th International Symposium on Cytochrome P450 Biodiversity and Biotechnology, Woods Hole MA, USA
- 6) Anna Joëlle Ruff, Jan Marienhagen, Hemanshu Mundhada, Ulrich Schwaneberg, Ribavarin: A complementary universal base to P for Sequence Saturation Mutagenesis Method (SeSaM), 2011, Biotrans 2011, Giardini Naxos, Italy
- 7) Anna Joëlle Ruff, Alexander Dennig, Ulrich Schwaneberg, Ultra-high throughput screening system for accelerated directed evolution of P450 monooxygenases, 2012, 11th International Symposium on Cytochrome P450 Biodiversity and Biotechnology, Torino, Italy
- 8) Claudia Ley, Dirk Holtmann, Anna Joëlle Ruff, Ulrich Schwaneberg, Jens Schrader, A microtiter plate based technique for the fast optimization of electroenzymatic processes, 2012, Symposium "Catalyzing Bio-Economy - Biocatalysts for Industrial Biotechnology", Dechema, Frankfurt

Parts of this thesis will be published:

Publication:

- 9) Claudia Ley, Anna Joëlle Ruff, Hendrik Schewe, Ulrich Schwaneberg, Jens Schrader, Dirk Holtmann, Coupling of electrochemical and optical measurements in a microtiter plate for the fast optimization of electro enzymatic processes with P450s, 2012, (submitted to Applied Microbiology and Biotechnology)

ABSTRACT

Advances in directed monooxygenase evolution: From diversity generation and flow cytometry screening to tailor-made monooxygenases

Directed Evolution became a powerful tool for proteins engineers to generate tailor-made biocatalyst. Directed protein evolution consist of the following three consecutive main steps, which are performed in iterative cycles; Step 1 the gene diversity generation, Step 2 the screening for improved variants and Step 3 the isolation of gene encoding for improved proteins. In this thesis, methodological advancements in the two key steps of the directed evolution, the diversity generation (SeSaM method) and high throughput screening (flow cytometer based screening technology) were performed and complemented by the evolution of P450 BM3 for alternative cofactor systems. Step 1 consisting of generation of high quality mutant libraries was advanced by developing an improved SeSaM protocol in which a universal base complementary to the P-base was employed to generate more diverse libraries. Step 2 was advanced by generating a whole cell high throughput screening assay for monooxygenases allowing to efficiently sample the diversity generated in Step1. Subsequently, the advanced protocols were applied to evolve P450 BM3 for alternative cofactor systems in iterative rounds (Step 3). These developed methods (flow cytometer assay for P450 BM3 and advanced SeSaM method) are of main interest for the researchers focusing on protein engineering.

In Chapter I of the thesis, the application of the R-base as universal base complementary to P-base increase the amino acid sequence space that can be covered with the SeSaM method. SeSaM-P/R allows for the first time to introduce at all four nucleotides transversion mutations which are homogeneously distributed over the targeted gene and which mutate in an ideal case each nucleotide of a gene. Second approach to advance the SeSaM method has been undertaken via a modified base at the 3' position of the sugar backbone. Through a chemical cleavable block the number of added bases was aimed to be controlled. The advanced SeSaM protocol is of general interest for researchers performing directed evolution experiments since a high quality mutant library with superior diversity than the standard epPCR is provided.

In Chapter II of the thesis, the first flow cytometer based ultra-high throughput screening platform that can be applied in directed evolution campaigns of P450 monooxygenases was developed. A whole cell high throughput screening assay for P450 BM3 based on a coumarin derivative (7-Benzoxy-3-Carboxy-Coumarin Ethyl ester (BCCE)) was established. Furthermore, the presented screening platform is not only restricted to P450 BM3, the reported BCCE screening system will very likely be applicable to all P450 monooxygenases that can be expressed in *E. coli* and catalyze an *O*-dealkylation of coumarin derivatives (e.g. human CYP3A4). However, the flow cytometer-based ultra-high throughput screening assay for directed evolution of P450 BM3 towards improved mediated electron transfer with Zn-dust could not be developed. The inhibitory effect of the Zn-dust on the microbial grow was pre-dominant and excluded the use of the double emulsion technology for the evolution of P450 BM3 for mediated electron transfer (MET).

In Chapter III, the advanced methods developed in Chapter I and II were employed to generate P450 BM3 libraries to evolve the catalyst towards alternative cofactor systems. P450 monooxygenases have a remarkable catalytic capability of inserting one atom from molecular oxygen into inert CH bonds. This unique oxygen chemistry makes the P450s very attractive for organic synthesis in the chemical and pharmaceutical industries. The evolution of P450 BM3 for improved alternative cofactor systems allows a step forward to liberate P450 BM3 from the requirement of expensive NADPH addition as cofactor which restricts the industrial use. The enzyme was evolved by generating random mutant libraries with the SeSaM method and by epPCR. The libraries were enriched with the flow cytometer screening system and subsequent screening in MTP format for improved mediated electron transfer. P450 BM3 M3 could further be engineered towards increased activity in presence of the alternative cofactor system Zn/Co(III)-sep. Indeed, new hot spots which were not reported before as relevant for the mediated electron transfer, could be identified. The second investigated alternative cofactor system, the direct electron transfer was explored by directed evolution to enhance the activity of the monooxygenase P450 BM3 in presence of a conducting polymer. Focus mutagenesis as well as random approach were performed, but no P450 BM3 variants with improved activity or new hot spots could be identified. Instead, an inhibitory effect by the conductive polymer could be demonstrated. Concluding, the P450 BM3 has no activity with the conductive polymer Clevios P. The selected mutants in the screening were improved for resistance towards Clevios P or stability with NADPH but the activity for direct electron transfer and the electron transfer rate did not increase.

Subsequently, collaborative P450 BM3 projects are summarized: the monooxygenase mutein database (muteinDB) was supported in which muteins altering substrate specificity are collected, the evolution of P450 BM3 for substrate specificity was contributed and P450 BM3 muteins with surface modifications for electrochemical characterization were generated.

INDEX

I.	List of abbreviations	V
II.	List of figures	VI
III.	List of tables	X
1.	Introduction	1
1.1	Monooxygenase P450 BM3 from <i>Bacillus megaterium</i>	1
1.1.1	Cytochrome P450 catalyzed reactions	2
1.1.2	Synthetic potential of P450 monooxygenases	3
1.1.3	Alternative cofactor systems for P450 BM3	5
1.1.3.1	Mediated electron transfer system	6
1.1.3.2	Direct electron transfer using conductive polymers	8
1.2	Directed evolution and generation of high quality mutant libraries	11
1.3	Sequence Saturation Mutagenesis method (SeSaM)	15
1.4	High throughput screening systems	19
1.5	Objectives	21
2.	Material and Methods	23
2.1	Chemicals	23
2.2	Devices	23
2.3	Other materials	24
2.4	Enzymes	24
2.5	Kits	24
2.6	Media	25
2.7	Media additives	25
2.8	Nucleotides	26
2.9	Primers	26
2.10	Vectors and strains	26
2.11	Microbiological methods	27
2.11.1	<i>E. coli</i> cultivation and P450 BM3 expression	27
2.11.2	Fluorescence microscopy	28
2.11.3	Cryocultures	28
2.12	Molecular biological methods	28
2.12.1	Validation of dRTP as universal base for SeSaM method	28
2.12.2	SeSaM-R method	33
2.12.3	SeSaM-P/R method	35
2.12.4	Agarose gel electrophoresis	35
2.12.5	Polymerase Chain Reaction (PCR)	36
2.12.5.1	Standard PCR	36
2.12.5.2	Colony PCR	36
2.12.5.3	Overlap extension PCR	36
2.12.5.4	EpPCR library generation	37
2.12.5.5	Site directed (SDM) and site saturation mutagenesis (SSM) - PCR	37

2.12.6	Cloning	38
2.12.6.1	Preparation of chemical competent cells	38
2.12.6.2	Digestion with restriction enzymes	38
2.12.6.3	PLICing	38
2.12.6.4	Transformation	39
2.12.6.5	Sequencing	39
2.13	Biochemical methods	39
2.13.1	Activity assay in MTP format	39
2.13.1.1	NADPH consumption assay	39
2.13.1.2	4-Aminoantypirin activity assay (4- AAP assay)	40
2.13.1.3	BCCE activity assay	40
2.13.1.4	pNCA activity assay	41
2.13.2	Flow cytometry screening systems	41
2.13.2.1	Whole cells flow cytometry screening system	41
2.13.2.2	Flow cytometry activity assay with w/o/w-emulsion	42
2.13.3	Protein purification	43
2.13.4	Polyacrylamide gel electrophoresis (SDS-page)	43
2.13.5	Determination of P450 concentration by CO-gassing	44
2.13.6	Kinetic characterization of P450 BM3 variants	44
2.14	Analytic and chemical methods	45
2.14.1	GC and GC-MS	45
2.14.2	Substrate synthesis	46
3.	Results and Discussions	49
Chapter I:	Advancement of SeSaM	49
I.1	dRTP and dPTP a complementary nucleotide couple for the Sequence Saturation Mutagenesis (SeSaM) method	50
1.1	SeSaM Step 2 optimization of dRTP incorporation	51
1.2	SeSaM Step 3 optimization: Polymerases for elongating R-tails	52
1.3	SeSaM Step 4 optimization: Polymerases for nucleotide incorporation opposite of the R-base	53
1.4	SeSaM-R method of <i>EGFP</i>	54
1.5	SeSaM-P/R method	54
1.6	MAP analysis of amino acid substitution patterns for SeSaM-R and SeSaM-P/R	57
1.7	Discussion	58
1.8	Conclusions	61
I.2	Advancement of the SeSaM method including nucleotide analogs	62
2.1	Nucleotide analogs with chemical cleavable blocks	62
2.1.1	MANT-dATP and 3'-ac-2' dRTP	63
2.1.2	3'-I-dATP	64
2.1.3	3'-O-NH ₂ -2'-dATP	64
2.2	Discussion	67
2.3	Conclusions	68

Chapter II: Flow cytometry based screening system for P450 BM3	69
II.1 High throughput screening system for accelerated directed evolution of P450 monooxygenases	69
1.1 Assay development and proof of principle	69
1.2 Conclusions	74
II.2 Flow cytometry assay based on w/o/w-emulsification for mediated electron transfer	75
2.1 Emulsification of P450 BM3 in presence of Zinc-dust	75
2.2 Discussion	79
2.3 Conclusions	81
Chapter III: Evolution of P450 BM3 for alternative cofactor systems	82
III.1 Evolution of P450 BM3 towards improved Mediated Electron Transfer (MET)	82
1.1 Activity assays for P450 BM3 in presence of Zn-dust and protein purification	83
1.1.1 Fluorescent MTP assay in presence of Zn/Co(III)-sep	83
1.1.2 Calibration curve of 7-Hydroxy-3-Carboxy-Coumarin Ethyl ester (3-CCE)	83
1.1.3 Thin Layer Chromatography analysis of the BCCE conversion	84
1.1.4 P450 BM3 purification and concentration determination	85
1.2 Saturation mutagenesis at positions N543 and R471	87
1.3 Directed evolution towards improved MET	89
1.3.1 Generation and screening of error-prone Polymerase Chain Reaction (epPCR) libraries	89
1.3.2 Generation and screening of SeSaM libraries	91
1.4 Saturation and iterative recombination of selected hot spots (R255, R203, I401, F423) for improved MET	97
1.5 Discussion	100
1.6 Conclusions	105
III.2 Evolution of P450 BM3 towards improved Direct Electron Transfer (DET)	106
2.1 Colorimetric screening assay for activity detection in presence of a conductive polymer as alternative cofactor	106
2.1.1 Optimization of 4-AAP assay	108
2.1.1.1 Removal of the conductive polymer	109
2.1.1.2 Influence of the conductive polymer formulation	111
2.1.2 Linear detection range of the 4-AAP assay	113
2.1.3 Activity check and standard deviation in 96 well plate format	113
2.2 Protein engineering of P450 BM3 for improved direct electron transfer (DET)	115
2.2.1 Role of the FMN in P450 BM3 Y51F T577G	115

2.2	Structure guided mutant libraries	118
2.2.2.1	Screening of SSM libraries	119
2.2.2.2	Simultaneous saturation of position G488 and W574	121
2.2.2.3	Iterative SSM libraries	122
2.2.2.4	Summary of results from structure guided mutant libraries	123
2.2.3	Random mutagenesis libraries	125
2.2.3.1	First round of directed evolution - mutagenesis and screening	125
2.2.3.2	Second round of directed evolution	127
2.2.3.3	Summary of the random mutagenesis libraries	131
2.2.4	Summary of the P450 BM3 evolution for improved DET	132
2.3	Activity measurements with purified protein in the presence of the conducting polymer Clevios P	133
2.3.1	Activity of purified P450 variant Y51F T577G	133
2.3.2	Product detection by GC and GC-MS	138
2.4	NADPH or mediator based conversion	140
2.5	Discussion	143
2.6	Conclusions	151
4.	Appendix Chapter: Summarizing collaborative projects with P450 BM3	154
4.1	Directed Evolution of P450 BM3 into a p-Xylene Hydroxylase	154
4.2	Electrochemical characterization of P450 BM3 variants	154
4.3	Surface modification of P450 BM3 for immobilization on gold particles	155
4.4	Monooxygenase mutain database (MuteinDB)	156
5.	Summary	158
6.	Appendix	161
6.1	List of strains and primers	161
6.2	Supplementary information of Chapter I	166
6.3	Vector maps	170
7.	References	172

I. List of abbreviations

4-AAP	4-Aminoantipyrin	NADPH	Nicotinamid Adenin Dinucleotide-Phosphate (reduced)
ALA	Aminolevulinic acid	OD₆₀₀	Optical Density at 600 nm
APS	Ammoniumpersulfate	P450 BM3	Cytochrome P450 BM3 from <i>Bacillus megaterium</i>
A_{x nm}	Absorption at x nm	PBS	Phosphate Buffer Saline
BCC acid	7-Benzoxo-3-Carboxy Coumarin acid	PLICing	Phosphorothioate-based Ligase-Independent gene Cloning
BCCE	7-Benzoxo-3-Carboxy Coumarin Ethyl ester	pNCA	para-nitrophenoxycarboxylic acid
BMP	Heme domain of P450 BM3	Rev	Reverse
bp	base pairs	RT	Room Temperature
CMC	Carboxy Methyl Cellulose	rpm	rotations per minute
Co(III)-sep	Cobalt(III)sepulchrates	SDM	Site Directed Mutagenesis
DET	Direct Electron Transfer	SDS- PAGE	Sodium Dodecyl Sulfate polyacrylamide gel electrophoresis
DMSO	Dimethyl Sulfoxide	SEL	Trace elements solution
dNTP	desoxynucleotide triphosphate	SeSaM	Sequence Saturation Mutagenesis
<i>E. coli</i>	Escherichia coli	SSC	Side Scattering
EGFP	Enhanced Green Fluorescent Protein	SSM	Site Saturation Mutagenesis
epPCR	error prone Polymerase Chain Reaction	TB	Terrific Broth
FAD	Flavin Adenin Dinucleotide	TdT	Terminal deoxynucleotidyl Transferase
FITC	Fluorescein isothiocyanate	TEMED	Tetramethylethylenediamine
FMN	Flavin Mononucleotide	Ts	Transitions
FSC	Forward Scattering	Tv	Transversions
Fwd	Forward	UV	Ultra Violet
IPTG	Isopropyl-β-D thiogalactopyranoside		
Kan	Kanamycin		
LB	Lysogeny Broth		
LMO	Light Mineral Oil		
MAP	Mutagenesis Assistant Program		
MET	Mediated Electron Transfer		
MCS	Multiple Cloning Site		
MTP	Microtiter plate		

II. List of figures

Fig. 1: Electron transfer mechanism of P450 BM3.	2
Fig. 2: Reaction catalyzed by P450 monooxygenases.	3
Fig. 3: Reaction scheme of mediated electron transfer.	7
Fig. 4a: Chemical structure of the conductive polymer Clevios P.	9
Fig. 4b: Reaction scheme of the electrochemical driven conversion of pNCA by P450 BM3 with CoSep as mediator.	10
Fig. 5: Directed evolution scheme.	11
Fig. 6: Classification of current random mutagenesis methods in the three main classes.	13
Fig. 7: SeSaM Step 1: Generation of ssDNA fragment pool with random length distribution.	15
Fig. 8: SeSaM Step 2: Enzymatic elongation of single stranded DNA with universal base.	16
Fig. 9: SeSaM Step 3: Synthesis of the full length gene.	16
Fig. 10: SeSaM Step 3: Replacement of universal bases.	16
Fig. 11: Mutational bias obtained when the P-base is used at A position (1) or T position (2).	17
Fig. 12: Mutational bias obtained when the R-base is used at T position (1) or A position (2).	19
Fig. 13: Step one to five of the “read” and “write” activity assay.	32
Fig. 14: Graphical abstract summarizing the work performed in Chapter II.	50
Fig. 15: Phosphorimager analysis of 3'-tailed FITC-oligonucleotides.	51
Fig. 16: Gel electrophoresis of the PCR Products generated in the Read activity assay.	52
Fig. 17: Polyacrylamid gels of R-base tailed nucleotides.	53
Fig. 18: PCR product of 250 bp generate in the write activity assay and used for cloning and sequencing analysis.	53
Fig. 19: Obtained amino acid substitution patterns of <i>EGFP</i> .	55
Fig. 20: Distribution of the mutations generated by the SeSaM-P/R method for <i>EGFP</i> .	55
Fig. 21: Scheme of the SeSaM method.	56
Fig. 22: Amino acid substitution patterns for <i>EGFP</i> calculated by MAP server.	57
Fig. 23: Overview of the by BIOLOG synthesized blocked bases.	63
Fig. 24: Terminal transferase (TdT) catalyzed 3'-tailing with the blocked base 8-xylo-dATP.	64
Fig. 25: Terminal transferase (TdT) catalyzed 3'-tailing with the blocked base 3'-O-NH ₂ -2'-dATP at different concentration.	65
Fig. 26: Terminal transferase (TdT) catalyzed 3'-tailing with the blocked base 3'-O-NH ₂ -2'-dATP.	65
Fig. 27: Terminal transferase (TdT) catalyzed 3'-tailing with the blocked base 3'-O-NH ₂ -2'-dATP with addition of Na-acetate.	66
Fig. 28: Structure of TdT with I-dATP in the active center.	68
Fig. 29: Scheme of the 7-Benzoxo-3-Carboxy-Coumarin Ethyl ester (BCCE) conversion catalysed by P450 BM3 and P450 BM3 DM variants.	70
Fig. 30: Conversion over time of BCCE using whole cells and cell free lysates with adjusted protein concentration by CO titration.	71
Fig. 31: Flow cytometer analysis of P450 BM3 whole cells.	71

Fig. 32: Light microscopy (a1, b1) and fluorescence microscopy (a2, b2) of <i>E. coli</i> cells after incubation with BCCE.	72
Fig. 33: BCCE conversion with purified P450 BM3 M3 DM-1 (R255H) with varied concentration.	73
Fig. 34: Scheme of the BCC-acid conversion by P450 BM3 in presence of the alternative cofactor system Zn/Co(III)-sep instead of the natural cofactor NADPH.	76
Fig. 35: FACS-plots of double emulsions, containing cells, BCC-acid and Zn/Co(III)-sep after 0 min, 30 min, 90 min and 120 min incubation.	77
Fig. 36: FACS-plots of double emulsions, containing <i>E. coli</i> P450 BM3 M3 cells, BCC-acid and Zn/Co(III)-sep after 30 min, 1 h and 4.0 h incubation.	78
Fig. 37: Fluorescence microscopy (a ₁ , a ₁) and phase contrast (b ₁ , b ₂) of w/o/w-emulsion with P450 BM3, BCC-acid and Zn/Co(III)-sep.	79
Fig. 38: Coefficient of variation of the fluorescent BCCE assay in continuous measurements and as endpoint measurement.	83
Fig. 39: Scheme of the BCCE conversion catalyzed by P450 BM3.	83
Fig. 40: Calibration curve of 3-CCE in presence of NADPH or Zn/Co(III)-sep in the reaction mixture monitored at λ_{ex} 400 nm, λ_{em} 440 nm.	84
Fig. 41: TLC analysis of the BCCE conversion by P450 BM3 F87A, monitored under UV-light.	85
Fig. 42: Elution fraction of P450 BM3 purification separated on 10% acrylamide gel and stained with coomassie brilliant blue.	86
Fig. 43: Chromatogramm monitored during the purification of P450 BM3 WT by anion exchange chromatography.	86
Fig. 44: Absorption spectra of P450 BM3 (dilution 1:8) after CO gassing and with subtracted background.	87
Fig. 45: Plot of the activity measurements used to determine the kinetic parameters of P450 BM3 M3 N543S R471C and P450 BM3 M3.	88
Fig. 46: PCR products separated by agarose gel electrophoresis and stained with GelRed.	89
Fig. 47: Flow cytometry plot of the negative control, cells containing pET28 a(+) lacking P450 BM3 gene; cells expressing P450 BM3 epPCR library after three rounds of enrichment.	90
Fig. 48: Scheme of the generated SeSaM libraries.	91
Fig. 49: Agarose gel of the optimal phosphorothiolated nucleotides concentration determination.	93
Fig. 50: Agarose gel stained with GelRed of the preliminary template generation for Step 1 and Step 3.	93
Fig. 51: Automated gel electrophoresis pictures of the ssDNA fragment pool with random length distribution analyzed with the RNA-chip-Kit.	94
Fig. 52: Agarose gel of the generated PCR products in step 4 of SeSaM mutagenesis method.	95
Fig. 53: Flow cytometry plot of the negative control, cells containing pET28 a(+) lacking P450 BM3 gene; Positive control, cells expressing P450 BM3 F87A; SeSaM library of P450 BM3 M3 after two rounds of enrichment (sort 1 and sort 2).	96
Fig. 54: Activity of P450 BM3 variants selected in the SeSaM library screening and re-screening.	96

Fig. 55: PCR product of the site saturation mutagenesis at position R255 and F423.	97
Fig. 56: Activity of the P450 BM3 variants generated in the iterative site saturation mutagenesis libraries or by site directed mutagenesis and compared to the improved variants selected in the first round of directed evolution.	98
Fig. 57: Scheme of the evolution pathway starting from P450 BM3 M3 and summarizing the selected variants improved for MET.	99
Fig. 58: Crystal structure of P450 BM3. The interaction between amino acid N543 and G488 are displayed.	101
Fig. 59: Crystal structure of P450 BM3: Displayed are the amino acids beneficial for the MET.	102
Fig. 60: Scheme of the 4-AAP detection system.	107
Fig. 61: Scheme of the P450 BM3 catalyzed reaction used in the screening assay to improve the catalyze for the direct electron transfer.	108
Fig. 62: Reaction mixture of the 3-phenoxytoluene conversion by P450 BM3 (cell free supernatant) with Clevios P, after centrifugation.	109
Fig. 63: Absorption spectrum of oxidized and reduced Clevios P (1:10 dilution).	110
Fig. 64: Reaction mixture after Clevios P precipitation.	111
Fig. 65: Influence of Clevios P formulation on the enzymatic activity.	112
Fig. 66: Calibration curve of the 4-AAP assay for phenol detection.	113
Fig. 67: Standard deviation in 96 well plates format of the 3-phenoxytoluene conversion in presence of the conductive polymer Clevios P as alternative cofactor system.	114
Fig. 68: Scheme of the generated FAD deficient P450 BM3 variant.	116
Fig. 69: SDS-page of the purified P450 BM3 Y51F T577G truncated protein.	116
Fig. 70: Fluorescence emission spectra from 460–700 nm of FMN, purified Heme-FMN-domain of P450 BM3 Y51F and purified Heme-FMN-domain of P450 BM 3 Y51F T577G (λ_{ex} 440 nm).	117
Fig. 71: Absorption spectra from 350–600 nm of Buffer (KPI 0.1M pH 7.5), purified Heme-FMN-domain of P450 BM3 Y51F and purified Heme-FMN-domain of P450 BM3 Y51F T577G.	118
Fig. 72: Crystal structure of the P450 BM3 FMN-binding site.	119
Fig. 73: Example of screening results from one 96 well plate from SSM 471 library.	120
Fig. 74: Relative activities of several P450 muteins with the conducting polymer PEDOT/PSS and the 4-AAP assay compared to the parent P450 BM3 Y51F T577G.	120
Fig. 75: Sequencing results of selected variants of structure guided mutant libraries.	121
Fig. 76: Scheme of the overlap extension PCR used to generate a multiple SSM at position G488 and W574 in the variant P450 BM3 Y536S T533E A534E.	122
Fig. 77: Relative activity of improved variants in presence of the conductive polymer Clevios P compared to P450 BM3 Y51F T577G after CO normalization.	124
Fig. 78: Four epPCR products separated by agarose gel electrophoresis.	125
Fig. 79: The relative activity of the muteins compared to the template gene P450 BM3 Y51F T577G is displayed.	126
Fig. 80: SDS page of the expressed muteins from the first evolution round.	127

Fig. 81: Experion automated gel electrophoresis analysis of the selected improved variants from second directed evolution round.	128
Fig. 82: Absorption spectra of the selected variants after CO-gassing used to determine the P450 concentration.	129
Fig. 83: Result of the 4-AAP activity assay with CO-normalized enzyme concentration or normalized enzyme concentration by automated gel electrophoresis system.	129-130
Fig. 84: Activity with NADPH and Clevios P of the purified variants selected in the epPCR library screening (B4-P3-G10 and B4-P4-H2) by the 4-AAP assay.	130
Fig. 85: a) NADPH consumption assay with purified P450 BM3 Y51F T577G, b) Detection of 3-phenoxytoluene conversion products determined by the 4-AAP assay.	134
Fig. 86: BCCE conversion by purified P450 BM3 WT-T577G.	137
Fig. 87: BCCE conversion recorded at λ_{ex} 400 nm, λ_{em} 440 nm with P450 BM3 WT-T577G cell lysate.	137
Fig. 88: GC chromatograms of the 3-phenoxytoluene conversion by P450 BM3.	138
Fig. 89: GC-MS spectra used for the peak identification of the 3-phenoxytoluene conversion by P450 BM3.	139
Fig. 90: GC peak area correlated to an internal standard to determine and compare the product formation rate of the 3-phenoxytoluene conversion in presence of Clevios P, no electron donor or NADPH.	140
Fig. 91: BCCE conversion recorded at λ_{ex} 400 nm, λ_{em} 440 nm with P450 BM3 WT-T577G cell lysate after storage of the cell lysate for 48h at 4°C.	141
Fig. 92: SDS-page of the collected fraction during purification.	142
Fig. 93: BCCE conversion by P450 BM3 T577G crude extract after GSSG reductase treatment.	142
Fig. 94: Structure model of the P450 BM3.	148
Fig. 95: PCR product of variant P450 BM3 M4 and M5 generated by SDM and separated by agarose gel electrophoresis.	155
Fig. 96: (a) Lysins displayed on the surfaces of P450 BM3. (b) S450 and S555 located on the surfaces of P450 BM3 and displayed in red.	156
Fig. 97: Vector map of pET28a(+).	170
Fig. 98: Vector map of pCWori(+) a derivative of plasmid pHSe5.	170
Fig. 99: Vector map of pALXtreme-1a, derivative of plasmid pET28a(+).	171

III. List of tables

Table 1: Key performance parameters of SeSaM-P, SeSaM-R and SeSaM-P/R.	60
Table 2: Kinetic characterization of P450 variants converting 7-Benzoxo-3-Carboxy-Coumarin Ethyl ester.	70
Table 3: Kinetic characterization of P450 BM3 variants hydroxylating 12-pNCA in presence of Zn/Co(III)-sep.	88
Table 4: Kinetic characterization of P450 variants converting BCCE in presence of Zn/Co(III)-sep.	90
Table 5: Generated and selected variants which were compared in the activity assay with Zn/Co(III)-sep.	98
Table 6: Overview of the available Clevios formulations and the specifications.	112
Table 7: Overview and sequencing results of the generated iterative SSM libraries.	123
Table 8: Sequencing results of the improved variants selected in the second directed evolution round.	131
Table 9: Generated variants used to compare the activity assay employed with purified protein.	135

1. Introduction

1.1 Monooxygenase P450 BM3 from *Bacillus megaterium*

Monooxygenases are present nearly in all organism (Bernhardt, 2006). They have been found in all eukaryotes, animals, plants and fungi as well as in some prokaryotes (Lewis and Lake, 1996). In mammals, cytochromes are membrane-associated, but in several bacteria they can be found as cytosolic proteins (Peters et al., 2003). The cytochrome P450 superfamily was discovered in 1955 (Brodie et al., 1955). The term “cytochrome P450” was described for the first time in literature in 1962 (Omura, 1999). The name cytochrome P450 originates from its spectral properties, which reflects the presence of the heme b bound in the active center of the enzyme, the "P" stands for pigment and "450" refers to the wavelength absorption maximum of the reduced CO-bound complex (Nelson et al., 1996). These properties are also used for the determination of the P450-concentration. The new nomenclature used the term CYP to specify the class, followed by a series of numbers and letters, to classify the enzymes and identification of their degree of similarity (Example: P450 BM3 is coded as CYP102A1).

Cytochrome P450s are part of the family of the external monooxygenases, involved in oxygen metabolism (Bernhardt, 2006). P450s are grouped in 10 classes, depending on the electron delivering system from NAD(P)H to the active site. Mitochondrial and most bacterial P450s are three-component systems comprising a P450, a ferredoxin and a NADH-dependent, FAD-containing ferredoxin reductase (Hollmann et al., 2011; Whitehouse et al., 2012).

Cytochrome P450 BM3 (CYP102) from *Bacillus megaterium* is a 118 kDa size, water soluble, NADPH-dependent fatty acid hydroxylase, that catalyzes the subterminal oxidation of saturated and unsaturated long-chain fatty acids (Narhi et al., 1988; Budde et al., 2004, 2004; Bernhardt, 2006). P450 BM3 is more thermostable and easier to handle compared to other P450s (Bernhardt, 2006). P450 BM3 can be recombinantly expressed in *E. coli* (Narhi et al., 1988), facilitating the investigation its potential applications in synthesis of chemical precursors for pharmaceutical products or industrially relevant substrates. P450 BM3 is compared to other monooxygenases highly active with natural substrates, reaching turnover rates of thousands of substrate molecules per minute for specific fatty acids (arachidonic acid 17 000 turnover min⁻¹) (Cirino and Arnold, 2002).

Structurally, P450 BM3 contains two distinct domains, the heme- and the reductase-domain, containing the FAD (Flavinadeninucleotide) and the FMN (Flavinmononucleotide) binding domain, fused as a single polypeptide chain (Whitehouse et al., 2012). The structure

of P450 heme binding domain is fully resolved (Ravichandran et al., 1993) as well as the complex heme/FMN-binding domain (Sevrioukova et al., 1999a). However, the crystal structure of the full-length enzyme is currently not available (Sevrioukova et al., 1999b). The heme domain has been crystallized in the presence and absence of various substrates allowing to extend the understanding of structure-function relationships (Sevrioukova et al., 1999a). Recently, the crystal structure of the FAD/NADPH-binding domain of P450 BM3 has been reported (Joyce et al., 2012).

P450 BM3 is described “to experience a substrate-induced thermodynamic switch that regulates the electron transfer” (Wong and Schwaneberg, 2003) (Fig. 1). In absence of substrate, no electron transfer from flavin mononucleotide (FMN) to heme occurs. “This control mechanism prevents the consumption of the electron donor (NADPH) avoiding the production of reactive and cell-damaging reactive oxygen species, such as hydrogen peroxide” (Wong and Schwaneberg, 2003). The electron transfer path is not yet defined; however, relevant amino acids are identified providing valuable information contributing to the investigation of P450s electron transfer properties and channel (Whitehouse et al., 2012).

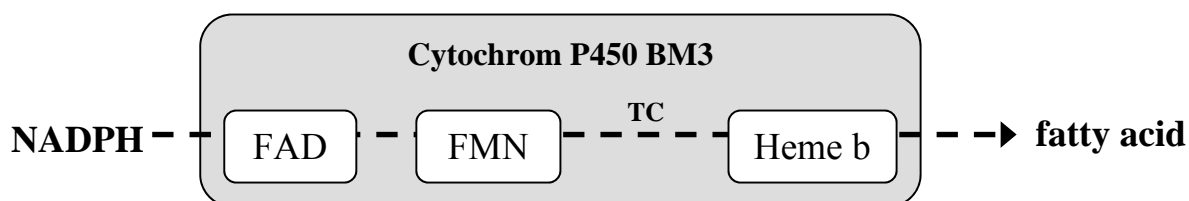


Fig. 1: Electron transfer mechanism of P450 BM3. TC = Thermodynamic control (adapted from Wong et al. (Wong and Schwaneberg, 2003)).

1.1.1 Cytochrome P450 catalyzed reactions

Cytochrome P450 monooxygenases have a remarkable catalytic capability of inserting one atom from molecular oxygen into inert C-H bonds (Bernhardt, 2006). The enzymes contain heme b in their active center, where the reaction (2) is taking place.



The catalytic mechanism was summarized by Urlacher et al. as follows: “The oxygen binds to the heme iron where the enzyme catalyzes the cleavage of the oxygen O-O bond. The essential step in the oxidation of substrate by P450 is the addition of one atom of molecular oxygen, which is activated by reduced heme iron, to the substrate. This reaction is usually a

hydroxylation reaction (2). The second oxygen atom is reduced to water, through accepting electrons from NAD(P)H via a flavoprotein or a ferredoxin” (Urlacher et al., 2004b).

Divers reactions are catalyzed by more than 5000 monooxygenases already described, and constantly new enzymes are reported (Bernhardt, 2006). The sequence identity is often less than 20 % (Urlacher and Schmid, 2004) between P450 monooxygenases with similar structural organization. Only a few amino acids are conserved, which play a key role in catalysis (Munro et al., 2002).

P450s can hydroxylate a broad range of substrates, from alkanes, phenols to complex molecules, such as steroids and fatty acids (Budde et al., 2006). Included are hydroxylation, epoxidation, deamination, desulphuration, dehalogenation, peroxidation (Bernhardt, 2006). An additional reaction that has also found an application in high-throughput screening methods of mutant libraries is the dealkylation reaction, using fluorogenic substrates such as alkyl-coumarins (Urlacher and Eiben, 2006) (Fig. 2).

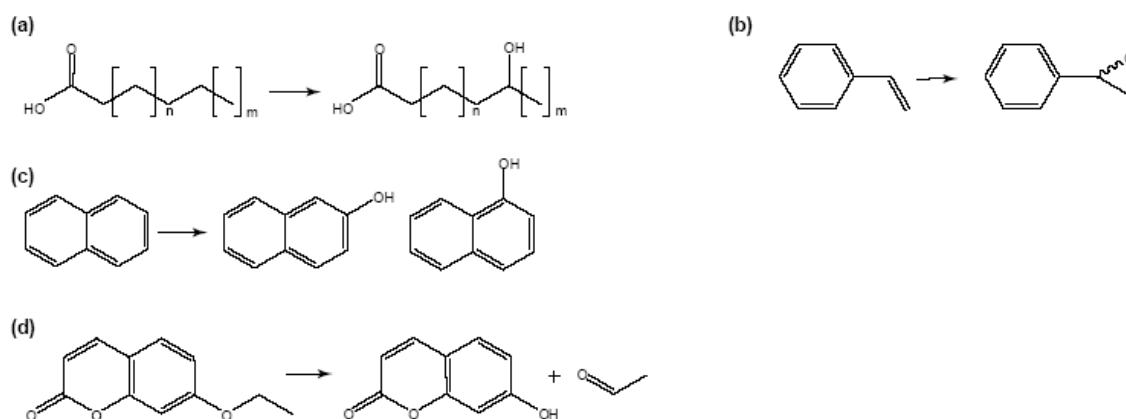


Fig. 2: Reaction catalyzed by P450 monooxygenases: C-H activation of sp^3 hybridized C-atoms (a), epoxidation of C=C double bonds (b), hydroxylation of aromatic compounds (c), dealkylation reaction (d). (Urlacher and Eiben, 2006).

1.1.2 Synthetic potential of P450 monooxygenases

The unique oxygen chemistry makes P450s very attractive for organic synthesis in the chemical and pharmaceutical industries (Juchau, 1990). P450-catalyzed reactions are often stereoselective and difficult to achieve by chemical means, especially in aqueous environment, room temperature, under atmospheric pressure, and with molecular oxygen as oxygenation agent (Guengerich et al., 1996).

Application of P450s in industrial scales already exists, the most prominent being: the 11 β -hydroxylation of Reichstein s, a progesterone derivative to hydrocortisone, a process using P450s from the fungi *Curcularia* sp. (Petzoldt, 1982) [www.schering.de], produced at a scale

of 100 tons/year. A similar example is the conversion of progesterone to cortisone by P450s expressed by *Rhizopus sp.*, which was commercialized by Pfizer [www.pfizer.com]. Additionally, the formation of dicarboxylic acids from alkanes, using endogenous P450 from an industrial *Candida tropicalis* strain, is reported with very high productivity (Picataggio et al., 1992; Jiao et al., 2001). In the future, this field will expand as soon as novel techniques will be applicable to ensure cost effective processes.

The research and application fields of the cytochrome P450s is broad and not only restricted to the chemical industry; P450 are applied in microbiology, plant science and medicine. P450s play an important role in biosynthesis of secondary metabolites (Imaishi and Ohkawa, 2002), where they are not only responsible for activation or biodegradation of xenobiotics, but also play a crucial role in biosynthetic pathways, such as metabolism of hormones, drugs, carcinogens, alkaloids, pesticides (Ingelman-Sundberg, 2004). P450s are also involved in physiological processes, such as steroidal hormones, vitamin D and bile acid biosynthesis. Without these physiological processes humans and most mammals are not viable (Montellano, 2005). Additionally, therapeutical applications of P450s gain in significance as well as the use in biomonitoring techniques. On the other hand, defects in P450 could lead to metabolic conditions, like the Antley Bixler syndrome (Iijima et al., 2009).

Despite their many uses, the activity of P450 monooxygenases towards non-natural substrates is usually very low. P450s reach only a few thousand conversions per minute for artificial substrates. In contrast to enzymes involved in industrial applications, which reach thousands per second (for example phytases, proteases). This limits the commercial applications. (Urlacher et al., 2004). Additionally, P450s cannot tolerate common bioprocess conditions, such as the presence of organic cosolvents, and depend on an equimolar amount of NAD(P)H for each reaction cycle. This increases the costs of the processes (Urlacher and Eiben, 2006).

The use of directed evolution to improve biocatalysts has been reported to successfully generate tailored P450 monooxygenase variants for specific applications. Engineered monooxygenases with increased activity in DMSO (Roccatano et al., 2005), increased organic solvent resistance (Montellano, 2005) (Wong et al., 2004a) or increased activity towards saturated hydrocarbon (octane) (Farinas et al., 2001) and gaseous alkane (propane) (Glieder et al., 2002) are reported. The affinity of P450 for non-natural substrates also has been increased, where the substrate specificity of P450 BM3 was shifted from C12 fatty acids to C10 and C8 (Fasan et al., 2008; Weber et al., 2011) or even to C3 (Glieder et al., 2002). Additionally, variants capable to hydroxylate inole (Appel et al., 2001) or oxidize substrates

as naphthalene, n-octane, and the oxidation of polycyclic aromatic hydrocarbons (PAHs) were generated (Carmichael and Wong, 2001; Li et al., 2001a, 2001b).

Currently, an extended research field focused on the optimization of P450 monooxygenase to improve the industrial use of P450s. The reaction and substrate spectrum is extended, the regio- and stereo- specificity is controlled, the enhancement of thermal and process stability and the cofactor regeneration is developing (Urlacher and Eiben, 2006). Among these research foci, the substitution of the costly NADPH cofactor is of special interest. These is also the main focus of the P450 BM3 evolution performed in this thesis.

1.1.3 Alternative cofactor systems for P450 BM3

Besides the functional complexity, low activity and limited stability, the requirement of expensive (10 g/1500 Euro) NADPH as cofactor in equimolar amounts restricts the industrial use of P450 BM3 (Wong and Schwaneberg, 2003). In consequence, to allow the application of P450s in cell free systems, the regeneration (re-use) or substitution of NADPH is of high industrial relevance. In order to decrease processes costs due to NADPH, whole-cell systems for cofactor regeneration, enzyme-coupled and electrochemical cofactor regeneration systems have been developed. Electrochemical cofactor regeneration has been taken into account, however, the non-biological conditions (alkaline pH, alcohol solvents) make challenging for most enzymes (Urlacher and Eiben, 2006).

Several proposed systems to substitute the NADPH are reported, such as mediated electron transfer (Nazor and Schwaneberg, 2006), light induced systems (Schröder et al., 1999), the “peroxide shunt pathway” (Joo et al., 1999) and electrochemically driven enzymes (Estabrook et al., 1996; Holtmann et al., 2009). Furthermore, NADPH regeneration systems have already been developed (Chefson and Auclair, 2006). The most used system in industrial processes is the enzyme-coupled NAD(P)H recycling, consisting of the addition of a dehydrogenase and a substrate that is oxidized to the system (for example formate dehydrogenase for the oxidation of formic acid to CO₂), resulting in the regeneration of NAD(P)H from NAD(P)⁺ (Mouri et al., 2006). Limitation of this system is, besides the presence of two enzymes in the reaction, that most dehydrogenases use NAD⁺ contrary to NAD(P)H used by most P450s. To tackle this, P450 monooxygenases have been engineered to use NADH as cofactor instead of NADPH (Neeli et al., 2005). NADH has the advantage to be 10 times less expensive, more stable and can better be regenerated than NADPH. Switching from NADPH to NADH as cofactor facilitated also the application for whole cell approaches, because there is a higher amount of internal dehydrogenases and NADH, compared to NADPH in *E.coli* cells

(Hollmann et al., 2011). The regeneration of NADH or NADPH in whole cell systems was applied to camphor hydroxylation in aqueous solution in addition to a two-phase system with isooctane (Mouri et al., 2006). Whole-cell systems delivered the necessary cofactors, but presented other challenges such as limited substrate uptake and toxicity of the substrate and/or products (Urlacher and Eiben, 2006).

Additional economical NADPH substitution systems have been developed. The “peroxide shunt pathway” was designed to exploit the natural ability of P450 to use peroxides, like H_2O_2 , as an electron source. However, P450s (as most enzymes) are very sensitive to peroxides and are inactivated at higher concentrations (Joo et al., 1999; Cirino and Arnold, 2002). In the recently reported light induced systems, the catalytic enzyme complex is directly reduced by light. A flavin-nucleotide, which is covalently bound to the enzyme, is photo-activated. The activated riboflavin channels the electrons directly to the heme-domain, where the heme-iron complex is reduced (Schröder et al., 1999).

Research in the development of electrically driven enzymes by immobilization on an electrode in order to replace NADPH by electrical sources has lately been increased to tackle the question of cofactor regeneration (Kazlauskaitė et al., 1996). In addition to the direct coupling of enzymes to electrodes, systems integrating mediators became increasingly attractive. Both approaches have the advantage of using cost-effective and renewable energy sources, however, low Total Turnover Numbers (TTN) are reported for the system, thus limiting its industrial application (Wong and Schwaneberg, 2003).

Mediated electron transfer (Schwaneberg et al., 2000; Nazor and Schwaneberg, 2006) and directed electron transfer (Nazor, 2007) have been proposed as alternative cofactor systems for NADPH. Common to both alternative cofactor systems, investigated in detail in this thesis and described below, is the replacement of NADPH by an artificial electron donor in solution. In the case of the mediated electron transfer approach, the artificial electron donor is zinc dust, and a mediator is needed to shuttle the electrons from the Zn-dust to the heme domain of the protein. The direct electron transfer approach is based on the direct interaction between a conductive polymer and the P450 monooxygenase.

1.1.3.1 Mediated electron transfer system

The mediated electron transfer was first reported by Estabrook et al. with Pt-electrodes (Estabrook et al., 1996) and applied for P450 BM3 by Schwaneberg et al. (Schwaneberg et al., 2000). In this system, Zn-dust is used as electron source and Cobalt (III)-sepulchrate (Co-

sep) as mediator allowing the electron transfer from the Zn-dust to the protein. Fig. 3 shows the reaction scheme of the mediated electron transfer with the substrate *p*-nitrophenoxycarboxylic acid (*p*NCA) and the Zinc/Co-sep-complex. The reaction takes place in solution, Zn^{2+} gets oxidized and the electrons are transferred *via* Co(II)-sep to the protein. Chloride ions (Cl^-) are essential for the system, establishing a water-soluble complex with Zinc (ZnCl_4^{2-}). The zinc ions are removed from the equilibrium and sufficient Zinc-dust can be dissolved (Schwaneberg et al., 2000). The Zinc-dust reduces the Co(III)-sep to Co(II)-sep. This promotes one electron to the P450 BM3 protein and can be used to reduce the substrate, in this case 12-*p*NCA to *p*-Nitrophenolate.

In comparison to other electrochemical methods, the relative activity of P450 BM3 with this mediator is 77 % higher and up to 1000 times less expensive than NADPH. The turnover rate of the Zinc/Co(III)-sep system reaches 20 % of the NADPH activity (Nazor and Schwaneberg, 2006). Unfavorable are the possible side reactions, which occur due to the high electric potential (-0.75V) too. In this cases, reactive oxygen species (ROS) are generated, which limit the NADPH-regeneration and damage the enzyme.

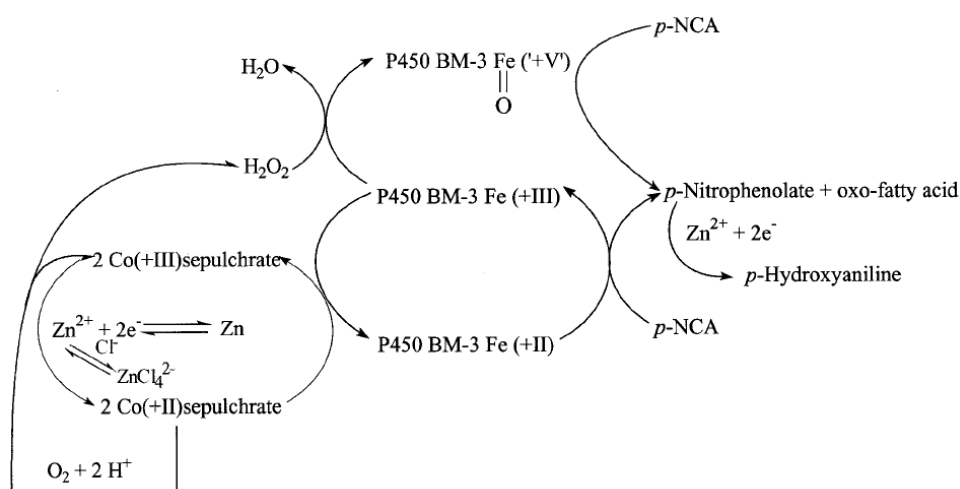


Fig. 3: Reaction scheme of mediated electron transfer with the substrate *p*NCA, the mediator Co(III)-sep and Zinc-dust as alternative electron donor (Schwaneberg et al., 2000).

Screening systems in 96 well format, based on this alternative electron sources, were established (Nazor and Schwaneberg, 2006) allowing the directed evolution of the catalyst resulting in a variant showing a three-fold increase in catalytic efficiency (P450 BM3 M3: $58 \mu\text{m}^{-1} \text{min}^{-1}$) (Nazor et al., 2008). Furthermore, recent studies report the first steps towards a Zn/Co-sep driven P450 BM3 reactor in which, after immobilization of P450 BM3 together with Zinc dust as electron source on DEAE-650S (diethylaminoethanol) sepharose and entrapped with K-carrageenan, the activity remained (Zhao et al., 2011).

1.1.3.2 Direct electron transfer using conductive polymers

Direct electron transfer was first reported for determining initial activities of BM3 with the conducting polymer Baytron in buffer and absence of electrodes (Nazor, 2007). The conductive polymer acts as electron donating source and electrons are transferred directly from the charged conductive polymer into BM3. The electron transfer between conducting polymer and BM3 is not understood on the molecular level despite that a few amino acids were identified, which modulate BM3 activities in presence of conducting polymers (Nazor, 2007).

The reported conductive polymers are commercial available formulations, named Clevios or Baytron (H.C. Starck [www.baytron.com]) and contain as monomer often 3,4-ethylenedioxythiophene (EDT or EDOT). The conductive polymer Poly(3,4-ethylenedioxythiophene (PEDOT)-Poly(styrene sulfonic acid (PSS)) was discovered and produced by H. Shirakawa, A.G. MacDiarmid und A.J. Heeger (Groenendaal, 2000). The selected polymer is attractive for potential application as alternative cofactor system of BM3. PEDOT-PSS consists of PEDOT-segments (1-2.5 kDa), which bind to PSS-chains (Luo et al., 2008)). PSS functions as counter-ion to balance charge, potential and solubility of PEDOT-PSS and to prevent oxidation of the PEDOT component. Furthermore, it enables an equal repartition of the otherwise water-insoluble PEDOT. This structure builds among each other loose cross linkage. Conductivity level of doped PEDOT-PSS ranges between semiconductors and metals (around 10 S/cm), with up to 10^2 - 10^3 S/cm and an absorbance maxima around at 610 nm [www.baytron.com]. The ratio of PSS to PEDOT and the PSS-chain length can be used to adjust conductivity of PEDOT-PSS, which decreases with reduced PSS chain length or increased PSS-PEDOT ratio (Groenendaal, 2000). Clevios P allows coating of glass or plastics surfaces with a conductive and durable PEDOT film employing micrometer sized gel particles (de Saint-Aubin et al., 2012). The polymer exhibits high conductivity, high transparency, high stability and an easy processing. Conductivity of Clevios coatings can be increased by supplementing polar compounds (ex. DMSO, glycerin, ethylen glycol) with high boiling points. Clevios is used for electrodes and for electrolytic capacitors (Zhi-Hui et al., 2010), LED lamps and coatings on surfaces of lamps or photographic films (Groenendaal, 2000).

Figure 4 shows the chemical composition of PEDOT-PSS and for BM3 biocatalysis, Clevios P was employed in solution (solid particle content 1.3 %). The ratio between PEDOT and PSS in Clevios P is 1:2.5 and the Clevios P suspension is dark blue [www.baytron.com].

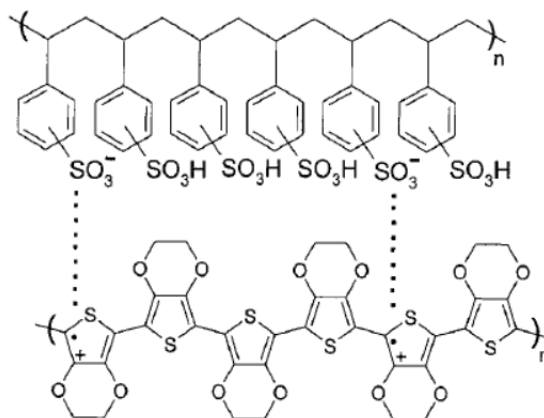


Fig. 4a: Chemical composition of the conductive polymer Clevios P [taken from www.baytron.com]. Clevios P was investigated as alternative electron source to the natural cofactor (NADPH), which transfers hydrides in P450 BM3 catalyzed reactions.

Conductive polymers would open novel opportunities for fine chemical production if activity and stability changes of electroenzymes could be overcome by tailoring enzyme properties through protein reengineering to application demands (Holtmann et al., 2009; Wong et al., 2003).

Protein engineering by directed evolution to improve electron transfer rates is the favored protein engineering strategy since it is rationally not understood how P450 BM3 has to be mutated to be driven more efficiently via conductive polymers. P450 BM3 variant (Y51F T577G) catalyzes the conversion of the substrate 3-phenoxytoluene to hydroxylated 3-phenoxytoluene with 568 min^{-1} in presence of Baytron P and in absence of NADPH (Nazor, 2007). A key for high conversions are matching redox potential of conductive polymer and monooxygenase and in a reduced state the conducting polymer can function as battery and can deliver a sufficient amount of electrons to the monooxygenase to determine initial activities. An important prerequisite for application is that the selected conductive polymers can be recharged by an electric potential to continuously provide electrons for the enzymatic reaction.

The PEDOT/PSS polymer is generated through oxidative polymerization with Fe-salts and synthesized in its oxidized state, which would not be suitable to drive P450 BM3. The reductase of P450 BM3 has a formal redox potential of -388 mV . An efficient electron donor for P450 BM3 requires a redox potential, which is more negative than the P450 BM3's redox

potential (< -400 mV). The formal redox potential of a PEDOT/PSS (Baytron P) solution is reported to be around -400 mV and because of existing reaction over potentials it is not suitable to function as electron donating “battery”.

In case that PEDOT/PSS is generated by electrochemical polymerization under reducing conditions an insoluble and dark blue film is precipitating on the electrode. PEDOT/PSS can act as redox polymer and function as electron shuttle to an enzyme, when “actively” reduced on the electrode surface by an applied potential below the redox potential of the PEDOT/PSS (e.g. -750 mV).

Promising conversions on electrode surfaces with in PEDOT/PSS films immobilized P450 BM3 are reported (Holtmann et al., 2009; Güven, 2011), as well as electrochemical driven conversions of model substrates in presence of CoSep as mediator (Ley et al., 2012).

Figure 4b shows the reaction scheme of mediated electron transfer setup from the electrode to CoSep and finally to P450 BM3, which drives the 12-pNCA conversion. The P450 BM3 model reaction generates a yellow *p*-nitrophenolate product. The performed reaction with PEDOT/PSS is similar to the direct electron transfer system (Fig. 4a.) in which PEDOT/PSS would be used instead of CoSep to directly transfer electrons from the electrode over PEDOT/PSS to P450 BM3, which is immobilized in PEDOT/PSS.



Fig. 4b: Reaction scheme of the electrochemical driven conversion of pNCA by P450 BM3 with CoSep as mediator.

Reports on direct electron transfers via conducting polymers encouraged us to perform direct P450 BM3 evolution experiments to increase direct electron transfer of P450 BM3 using PEDOT/PSS mixtures as conductive polymers.

1.2 Directed evolution and generation of high quality mutant libraries

Evolution was described by Charles Darwin in the 17th century. In nature, the evolution of organism occurs naturally in order to adapt populations to changing environmental conditions. Evolution is based on the principle, that randomly occurring DNA mutations generate organisms, which are “fitter”, more suitable and therefore survive to a selection pressure and provide the genetic constitution for the next generations. The procedure takes up to thousands of years (Campbell and Reece, 2009). Based in the same concept, the accelerated evolution of enzymes *in vitro* was described as directed protein evolution. Independent from the structural information, directed evolution can steer proteins properties artificially as it would occur naturally, except in very short time scales (~1 month to 1 year). Directed evolution comprises three main steps performed in iterative cycles to efficiently engineer proteins (Fig. 5). In Step I, the diversity is generated on the DNA level which is screened in the next step (Step II) for improved variants on the protein level. Finally, in the last step (Step III) the gene, encoding for the improved variants, is isolated and used for the next round of evolution (starting Step 1 in the cycle) (Arnold and Volkov, 1999; Tee and Schwaneberg, 2007; Güven et al., 2010).

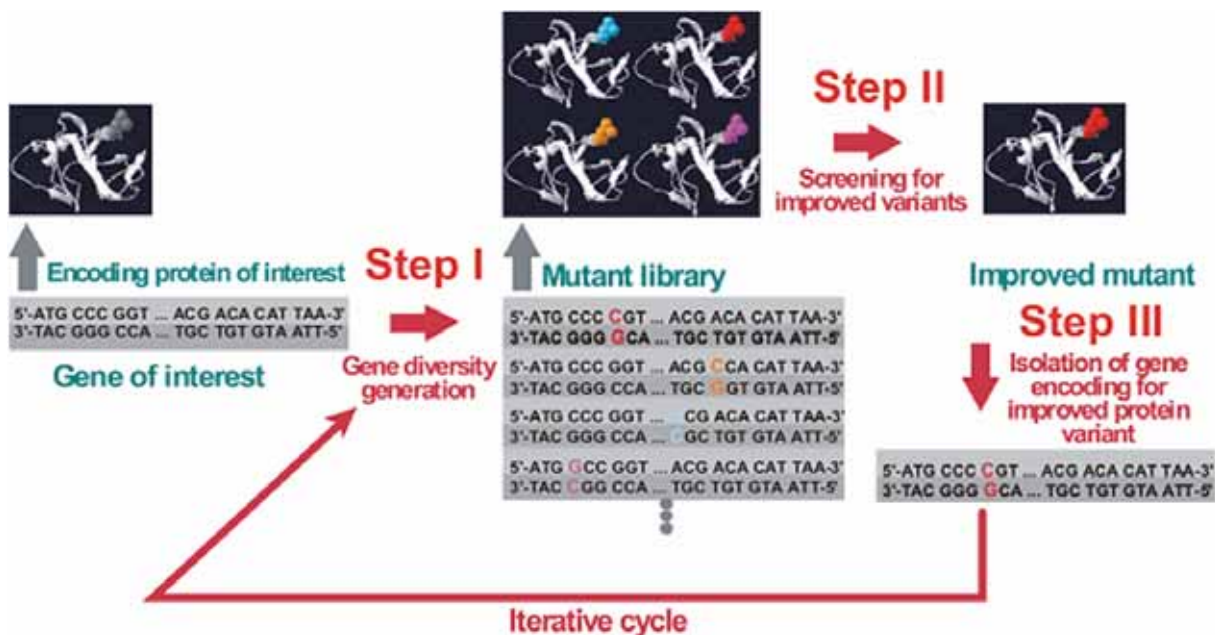


Fig. 5: Directed evolution scheme. Step I: Diversity generation on DNA level. Step II: Screening for improved variants on protein level. Step III: The gene, encoding for the improved variants, is isolated and used for the next round of evolution, starting with Step I (Güven et al., 2010).

Key challenges in directed evolution are the generation of diverse mutant libraries and development of high-throughput screening systems to identify improved variants (Lutz and Patrick, 2004; Wong et al., 2006b). Numerous success stories were reported, demonstrating

that directed evolution is a powerful method for improving enzymes properties such as specificity, activity, enantioselectivity, pH and thermal resistance (Yuan et al., 2005; Kaur and Sharma, 2006; Tee and Schwaneberg, 2007).

Advances in high throughput screening technologies are impressive as reports on flow cytometry (Bershtein and Tawfik, 2008; Yang and Withers, 2009; Prodanovic et al., 2011; Tu et al., 2011) or microfluidic screening devices (Agresti et al., 2010) prove. Despite achievable throughputs of ($\sim 10^8$ /day), it is impossible to sample through the combinatorial protein sequence space, since already 1.024×10^{13} different variants can be generated with a peptide of 10 amino acids (Wong et al., 2007b; Shivange et al., 2009). Therefore, the quality of mutant libraries should be increased by generating functionally enriched mutant libraries to reduce screening efforts for identifying improved variants. For instance, a mutational bias elevating the number of charged residues can increase solubility of water insoluble proteins (Shivange et al., 2009). Computational algorithms, such as the Mutagenesis Assistant Program (MAP) (Wong et al., 2006a, 2007c), GLUE-IT and PEDEL-AA (Firth and Patrick, 2008), are helpful tools to analyze the amino acid substitution patterns of random mutagenesis methods (MAP) and to develop promising strategies for high quality mutant library generation. The later can further be correlated to experimental setups by taking the coverage of explored protein sequence space into account (GLUE-IT/PEDEL-AA) (Volles and Lansbury, 2005; Firth and Patrick, 2008). Methods to generate focused mutant libraries target specific residues and are mainly employed to improve “localized” properties such as activity, specificity or selectivity. Focused mutant library generation requires often detailed structural information (Shivange et al., 2009). Properties which are rationally not understood or for which insufficient structural information is available are subjected to random mutagenesis. The subsequent analysis of obtained substitutions enables broadening our rational understanding and to find novel protein reengineering principles.

Options to generate genetic diversity comprise enzymatic (Yuan et al., 2005), chemical (Singer and Kuśmierk, 1982) and whole cell methods (Neylon, 2004; Matsumura and Rowe, 2005; Rasila et al., 2009) . The methods were summarized and classified by Wong at al. (Fig. 6) (Wong et al., 2006b).

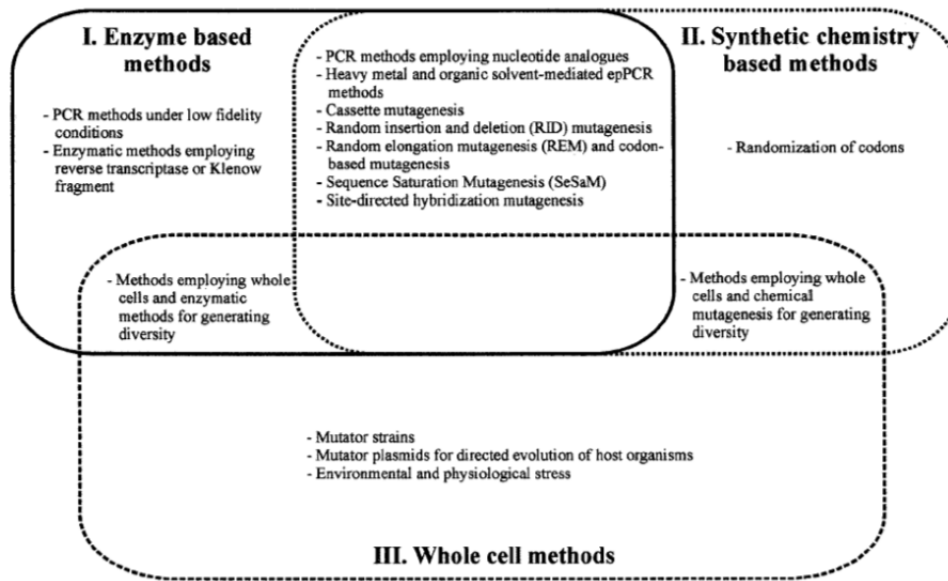


Fig. 6: Classification of current random mutagenesis methods in the three main classes. I: Enzyme based methods. II: Synthetic chemistry based methods and III: Whole cell methods (Wong et al., 2006b).

Chemical mutagenesis methods target one random nucleotide as point or as frameshift, deletion or insertion mutation. Chemical modification was used *in vivo* mutagenesis, a variety of reagents have been applied, including ethyl methane sulfonate (EMS), methylnitrosoguanidine (MNNG) and ethylnitrosourea (ENU). Only a few like EMS or hydroxylamine hydrochloride were reported as successfully used for *in vitro* mutagenesis. Depending on the application field and the properties of mutagenic substance, the effects were diverse, but the important role of tautomerism and rotation about the glycosyl bond of base has been reported (Singer and Kuśmierk, 1982).

Error-prone polymerase chain reaction (epPCR) derived protocols are the most commonly used enzymatic methods for random mutagenesis (Cadwell and Joyce, 1992; Neylon, 2004). The performance criteria to improve the quality of a random mutant library (Vanhercke et al., 2005) include an increase in the ratio of transversions to transitions mutations. The pattern and frequency of obtainable mutations by epPCR can be adjusted by varying the reaction conditions (e.g. unbalanced dNTPs, employed error-prone polymerases (Cline et al., 1996; Biles and Connolly, 2004), varied MnCl₂ concentration (Cirino et al., 2003) or alternatively by supplementing nucleotide analogs (Spee et al., 1993; Zacco et al., 1996). The triphosphate derivatives of analog 8-hydroxy-dGTP (Zacco et al., 1996), dITP (Spee et al., 1993), and dPTP (Zacco et al., 1996) are efficiently incorporated in PCRs, enabling high frequencies of nucleotide exchanges with predefined ratios between transitions and transversions at single positions in a codon. Other sequences dependent enzymatic random methods are transposon based (Kim et al., 2009), Staggered Extension Process (StEP) (Zhao

et al., 1998), Megaprimer PCR of Whole Plasmid (MEGAWHOP) (Miyazaki, 2003) or DNA-shuffling (Stemmer, 1994; Abécassis et al., 2000). But methods to generate random mutant libraries in directed evolution are limited in diversity generation (Arnold and Volkov, 1999; Wong et al., 2007a; Rasila et al., 2009). In the case of epPCR this is due to a polymerase bias leading to 63 % transitions with A to G and T to C, going with a low transversion probability, in this method the mutation of only one nucleotide per codon can be reached. Subsequently, only 150 of 380 possible amino acid exchanges are accessible. A method that would allow the exchange of each of the 20 amino acids replaced by its respective 19 counterparts would deliver 380 possibilities (Wong et al., 2006a; Shivange et al., 2009).

DNA polymerases display strong mutational preferences favoring the substitution of certain nucleotides over others. The result is a biased and reduced functional diversity in the generated mutant library. Along the different DNA polymerases classes and families, the conformation of the template binding domain, the catalytic center and the processivity is different. Polymerases having the ability to read over several mismatches have been reported, and used in the amplification of ancient DNA, which is highly degraded (d'Abbadie et al., 2007). DNA polymerases have been genetically engineered to have a decreased 3'-5' proofreading exonuclease activity, making them suitable for difficult templates such as those including non-standard nucleotides (Biles and Connolly, 2004). DNA polymerases resulting from the fusion of *Pyrococcus*-like enzyme with a processivity enhancing domain resulted in a variant (example Phusion polymerase from NEB) showing a high fidelity and processivity with a 50 fold lower error rate compared to the *Thermus aquaticus* DNA polymerase (Taq-polymerase) (Cline et al., 1996). These polymerases are suitable for difficult and long templates like it occurs when GC rich regions are present. To point out one well established engineered DNA polymerase, Mutazyme is used in an epPCR-based method and often included in comparison of amino acid substitution pattern analysis (Cline et al., 1996). The method produces all possible transition and transversion mutations with minimal bias and its mutational spectrum is distinct from that of Taq DNA polymerase.

Many methods are reported to improve the performance criteria of random mutant libraries, tunable mutation frequency, increased diversity and less biased libraries with an enriched transversion mutation spectrum were achieved (Vanhercke et al., 2005; Rasila et al., 2009). Still, a more or less strong bias towards transitions remains due to inherent DNA polymerase limitations. Therefore, the advancement of the diversity generation methods remains as a valuable research field.

1.3 Sequence Saturation Mutagenesis method (SeSaM)

The Sequence Saturation Mutagenesis (SeSaM) method was reported as a four step random mutagenesis method designed to overcome the limitations of epPCR based random mutagenesis methods (Wong et al., 2004b). SeSaM targets in contrast to epPCR each nucleotide “equally” avoiding mutagenic hot spots, achieving subsequent mutations in a codon (up to 37 %) (Mundhada et al., 2011), and allowing to adjust mutational biases through employed universal bases (Wong et al., 2004b, 2005a; Mundhada et al., 2011).

The method comprises four steps: In Step 1, a DNA fragment pool with random length is generated by the incorporation of nucleotides with phosphorothiolated cleavable bonds. In Step 2, the enzymatic elongation of the single stranded DNA fragments with the universal base occurs. In Step 3, the DNA fragments were elongated to full length gene and in Step 4, the universal base is replaced by unmodified nucleotides. The four steps are described below and summarized in Fig. 7-10 on the example of the universal P-base (Wong et al., 2004b).

Step 1: Generation of ssDNA fragment pool with random length distribution.

In the first step, a PCR amplification of the gene of interest is performed using a biotinylated primer and phosphorothiolated nucleotides to randomly incorporate cleavable bonds (Fig. 7, (Ruff et al., 2012a)). The phosphorothiolated bond can be cleaved by iodine treatment in alkaline solution generating a DNA fragment pool with random length. Based on the used biotinylated primer, the library is named forward or reverse library with the according base, which was targeted (for example: Fwd-A library). The cleaved single stranded fragments are separated and purified from the reaction mixture by the use of magnetic particles with a streptavidin-coated surface in a DNA melting solution reacting with the biotinylated primer.

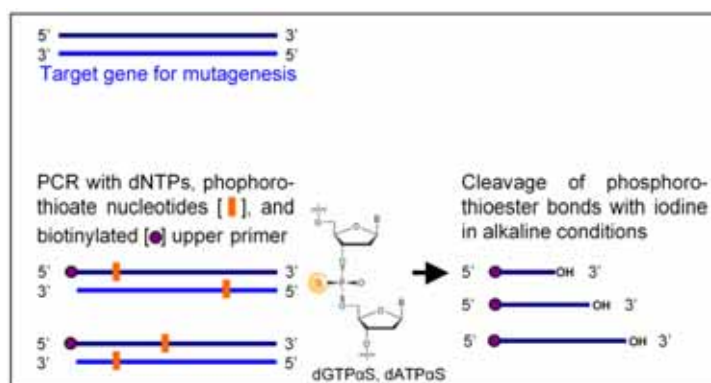


Fig. 7: SeSaM Step 1: Generation of ssDNA fragment pool with random length distribution.

Step 2: Enzymatic elongation of single stranded DNA with universal base

The single stranded DNA fragments generated in Step 1 are elongated with universal bases in a TdT (Terminal Transferase) catalyzed reaction (Fig. 8, (Ruff et al., 2012a)). The reported and employed universal bases are mentioned in the next paragraph.

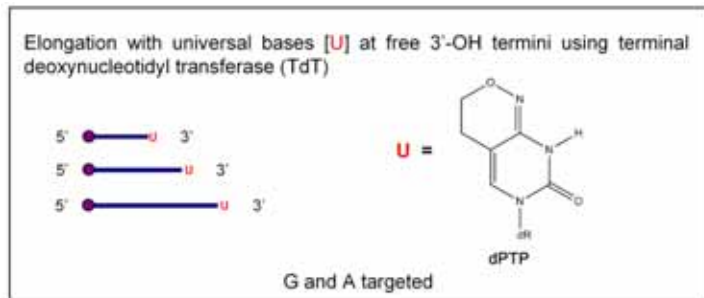


Fig. 8: SeSaM Step 2: Enzymatic elongation of single stranded DNA with universal base.

Step 3: Synthesis of the full length gene

The single stranded DNA fragments (from Step 2) are elongated to full length gene, using a template generated in a preliminary step (Fig. 9, (Ruff et al., 2012a)).

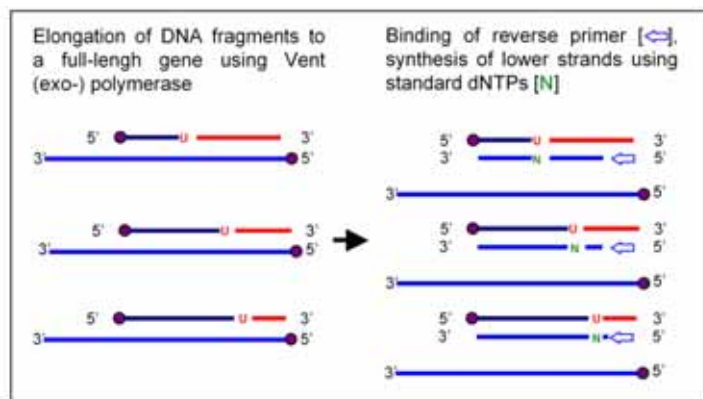


Fig. 9: SeSaM Step 3: Synthesis of the full length gene.

Step 4: Replacement of universal bases

The universal base is replaced by unmodified nucleotides by PCR amplification (Fig. 10, (Ruff et al., 2012a)). Based on the promiscuous base-pairing property of the employed universal bases, mutations are created. This number of cycles in the last step determines the number of transversion or transition per gene.

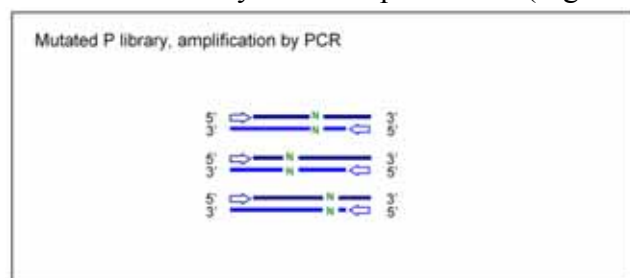


Fig. 10: SeSaM Step 4: Replacement of universal bases.

The SeSaM method is at the current development stage designed to generate amino acid substitution patterns that are complementary to those of epPCR. Three degenerate bases P (6-(2-deoxy-β-D-ribofuranosyl)-3,4-dihydro-8H-pyrimido-[4,5-C][1,2]oxazin-7-one), K (N⁶-methoxy-2,6-diaminopurine), I (2'-deoxyinosine) (Wong et al., 2005a) were reported to control mutational ratios of transitions to transversions in SeSaM libraries. The P base was

employed at A and G positions and yielded a ratio of six to four for T and C mutations and is well suited to introduce transversions at A and G positions. The bases K and I failed to complement the P base to maximize diversity at T and C positions (I yielded exclusive G mutations // K yielded an A to G ratio of 9 to 1) (Wong et al., 2008).

The SeSaM method relies on the promiscuous base pairing ability and coding bias of the employed universal bases, which are purine or pyrimidine analogues to achieve mutations with tunable mutational bias. Fig. 11 shows for the A-base as example the principle, why the P-base is only used at A and G positions to introduce a transversion bias (part 1) and how the transition bias is obtained at T and C positions on the example of T-base (part 2).

1) When the P base is introduced randomly at A or G position, the opposite base would be incorporated according to the base pairing properties of the P-base, pairing with G or A, and not with T as it occurs naturally opposite an A base. Opposite of the P base As and Gs are therefore introduced in the PCR amplification of the opposite strand. When in the last step the artificial base gets replaced by a natural base, the P is replaced by C and T bases (which pair with G and A). This principle allows obtaining transversion from A to C or T in the mutated gene. Step 2 is not displayed, as this step is the attachment of the artificial base to the single stranded fragments and doesn't have an impact on the occurring mutagenesis.

2) When P would be introduced at the T positions, only transversions from T to T or C would occur (see Fig. 11, part (2) below).

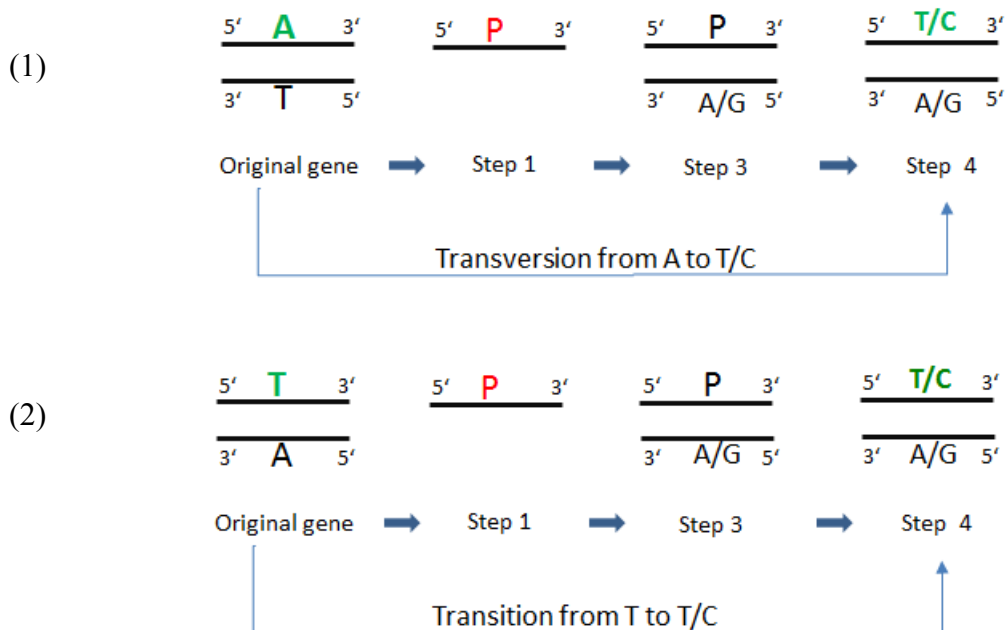


Fig. 11: Mutational bias obtained when the P-base is used at A position (1) or T position (2).

The nucleoside ribavirin (1- β -D-ribofuranosyl-1,2,4-triazole-3-carboxamide; in short R-base) is a well-known antiviral drug for hepatitis C (Crotty et al., 2000). R-base functions chemically as a purine analog pairing with T and C in a ratio of 1:1 (Crotty et al., 2000; Maag et al., 2001; Vo et al., 2003). The small size of the R-base and 1:1 ratio of T and C makes the respective nucleotide dRTP attractive for application in SeSaM and for complementing the P base. Combining P- and R-base would in SeSaM experiments generate at all four nucleotides transversions in a given sequence with an unmatched chemical diversity.

Previous studies demonstrate that HCV RNA polymerase can incorporate ribavirin triphosphate as a nucleotide analog of either ATP or GTP and ribavirin itself can serve as a template base for incorporation of cytidine and uridine with equal efficiency (Vo et al., 2003). Once ribavirin is in the RNA, it is presumably trapped in the „anti“ conformation and readily forms base pairs with incoming pyrimidines. This indicates, that incorporation of ribavirin into RNA should be mutagenic to viral RNA, promoting transitions of A to G and G to A (Crotty et al., 2000). The pseudo base (1,2,4-triazole-3-carboxamide) of ribavirin (R) pairs equally with cytosine and uracil and was proved not to be a chain terminator. Across from R, CTP and UTP could be incorporated, with CTP being more efficient than UTP. Neither GTP nor RTP could be incorporated. ATP was incorporated across from R even in the absence of template (Maag et al., 2001).

In the SeSaM method the R-base would be incorporated exclusively at T and C position to insure a transversion bias. If R would have been introduced at all 4 nucleotides, a transition and transversion bias would have been generated at A and G positions. For a transversion bias at A and G positions, the P-base was introduced in previous SeSaM developments. The figure below (Fig. 12) shows for the T-base as example the principle, why the R-base is only introduced at C and T positions to introduce a transversion bias (part 1) and on the example of the A-base how a transition bias is obtained at A and G positions (part 2).

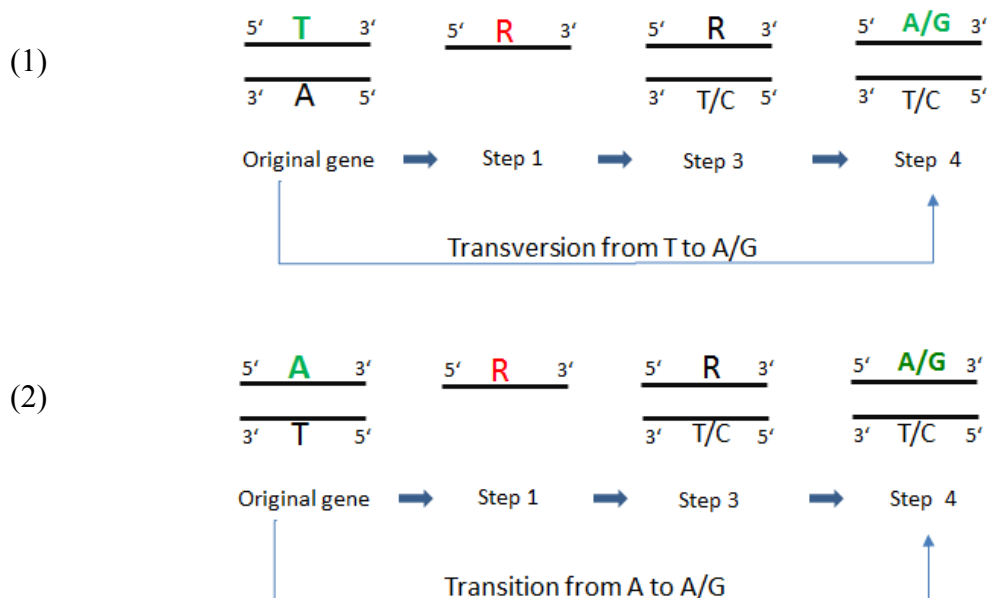


Fig. 12: Mutational bias obtained when the R-base is used at T position (1) or A position (2).

1.4 High throughput screening systems

Enzymes provide a broad variation of catalytic activities enabling reactions that are highly desirable for organic chemists such as regio- and stereoselective hydroxylation of non-activated carbon atoms, which are for instance catalyzed by cytochrome P450 monooxygenases (Hollmann et al., 2011). Tailoring catalyst properties by directed evolution to specific application demands in terms of stability, enantioselectivity or stereoselectivity, became a standard approach in biocatalysis, medical science as well as in synthetic biology (Kaur and Sharma, 2006; Wong et al., 2006b; Shivange et al., 2009). Rational and evolutive protein engineering strategies employ focused mutant (OmniChange (Dennig et al., 2011), CASTing (Reetz et al., 2006)) or random mutant libraries (Bornscheuer and Pohl, 2001; Shivange et al., 2009). The theoretically generated diversity exceeds the possible throughput of high throughput screening platforms in respect to the number of variants that can be screened (Shivange et al., 2009). For instance, in focused mutant libraries with five simultaneously NNK-randomized codons 10^8 clones have to be sampled for 99 % coverage (PEDEL AA & GLUE-IT (Volles and Lansbury, 2005; Firth and Patrick, 2008), OmniChange (Dennig et al., 2011)). Compared to the few thousand clones screened usually in microtiter plates (Wong et al., 2007a) not only the throughput is significantly increased, but also the costs and time requirements are reduced dramatically (Agresti et al., 2010). The availability of reliable and efficient pre-screening systems ($>10^4$ clones per day) is the main limitation to identify beneficial variants in diverse mutant libraries (Tee and Schwaneberg, 2006).

In the past decade innovative ultra-high throughput screening platforms based on flow cytometry (Griffiths and Tawfik, 2006; Bershtein and Tawfik, 2008; Yang and Withers, 2009) or microfluidic devices (Agresti et al., 2010) have been developed. Flow cytometer-based screening systems enable to sample more than 10^8 clones per day with excellent accuracy (Griffiths and Tawfik, 2006). The throughput is commonly 4 orders of magnitude higher than commonly employed microtiter plate based screening platforms and accuracy is usually higher than agar plate based pre-screening systems (Bernath et al., 2004a; Turner, 2006; Link et al., 2007). Fluorescent screening systems have in general a high sensitivity which ensures that active and inactive clones can reliably be separated even in very small reaction volumes (femto liter droplets) (Bernath et al., 2004b). A key requirement in every directed evolution campaign is to keep the link between phenotype and genotype, which is usually ensured by compartmentalization of mutant libraries, for instance in emulsions or whole cells (Olsen et al., 2000; Bernath et al., 2004b; Griffiths and Tawfik, 2006). In case of whole cell screening systems a main challenge lies in entrapping the product within the cell and thereby avoiding cross contamination (Bernath et al., 2004a). In case of emulsion systems a main limitation often lies in the requirement to generate double emulsions (water/oil/water), so that sorting in aqueous solution with a flow cytometer is possible. In double emulsions often more than one single emulsion droplet is entrapped reducing the fraction of active variants, that are sorted out. Nevertheless, flow cytometry based screening systems have successfully been used to enrich the active population in mutant libraries (Bernath et al., 2004a; Griffiths and Tawfik, 2006; Stapleton and Swartz, 2010) and to identify in successive rounds of sorting and/or diversity generation improved variants, for instance improving specificity (Santoro et al., 2002), inhibitor resistance (Tu et al., 2011) and activity (Aharoni et al., 2005a) of enzymes. For P450 monooxygenases (CYPs) (>5000 cloned members (Bernhardt, 2006)) colorimetric and fluorescence-based high throughput screening platforms based on microtiter plates (MTP) are available with a reported throughput of 10^3 - 10^5 clones per day (Wong et al., 2005b; Tee and Schwaneberg, 2007). Fluorescence based screening systems in MTP format were reported for monooxygenase with excellent sensitivities (900 fold increased activity; detection limit in nM-range) (Lussenburg et al., 2005). Among the fluorescence based screening systems for P450 monooxygenases, coumarin-derivates are used preferentially (Cheng et al., 2009; Park et al., 2010; Reinen et al., 2011). Coumarin-derivates have furthermore been employed successfully in directed evolution campaigns of cellulases, lipases and phosphatases (Wu et al., 2010).

1.5 Objectives

In this thesis entitled “Advances in directed monooxygenase evolution: From diversity generation and flow cytometry screening to tailor-made monooxygenases”, the main focus was the development of novel methods for increasing diversity (SeSaM-R base, Chapter I) and throughput screening (flow cytometry based screening system, Chapter II), which were validated for P450 BM3. Along with the main focus on methodological advancements in the two key steps of the directed evolution, the directed protein evolution of P450 BM3 for improved activity towards alternative cofactor systems was performed.

Directed evolution comprises three main steps and is performed in iterative cycles to efficiently reengineer proteins. In Step I, the diversity is generated on the DNA level, which is screened in the next step (Step II) for improved variants on the protein level and finally, in the last step (Step III), the gene encoding for the improved variants is isolated and used for the next round of evolution. Not only the evolution of P450 BM3 for alternative cofactor systems was performed, but each step of the directed evolution method was advanced and is considered in one chapter. Step 1, consisting of generation of high quality mutant library, was advanced by developing an advanced SeSaM protocol, in which a universal base, complementary to the P-base, was employed to generate more diverse libraries. Step 2 was advanced by generating a whole cell high throughput screening assay for monooxygenases allowing efficiently sampling of the diversity generated in Step 1. Subsequently, the advanced protocols suitable for the directed evolution methods were applied to evolve P450 BM3 for alternative cofactor systems in iterative rounds (Step 3).

The thesis was sub-divided in three main chapters tackling each step of directed protein evolution.

In Chapter I of the thesis, the application of the R-base as universal base complementary to P to further increase fraction of the theoretical amino acid sequence space, that can be covered by the SeSaM method, is reported. An advanced SeSaM method, in which a protocol for implementing the R base in a SeSaM experiment was developed and optimized. Optimized steps comprise Step 2 (incorporation of dRTP), Step 3 (polymerase for R-base elongation), and Step 4 (polymerase for amplification) of the SeSaM method. SeSaM libraries with R-base of the Enhanced Green Fluorescent Protein (EGFP) were generated and the transversion preference and the AS substitution pattern was determined. The R-base protocol was

subsequently combined with the P-base for generating for the first time transversions at all four nucleotides in a combined protocol.

In Chapter II of the thesis, a flow cytometer based whole cell high throughput screening system for P450 BM3 was developed using as substrate a coumarin derivative (7-Benzoxy-3-Carboxy-Coumarin Ethyl ester (BCCE)). In the first step the P450 BM3 variant F87A was employed in investigating the signal to noise ratio in crude cell extracts and in a whole cell flow cytometry setup. In the second step the mutant P450 BM3 M3 (R47F F87A M354S D363H), previously evolved for improved electron transfer *via* mediators^{38,39}, was randomly mutated (epPCR) and populations were sorted to identify more active variants. The flow cytometry based BCCE screening system was used as pre-screen to recover the population containing the most active variants in order to enrich the population of active P450 BM3 variants. The sorted variants were subsequently screened in 96 well microtiter plates to identify P450 BM3 variants improved in BCCE conversion and to validate the developed BCCE-flow cytometer screening system.

In Chapter III, the advanced methods developed in Chapter I and II were employed to generate P450 BM3 libraries to evolve the catalyst towards alternative cofactor systems. Random mutant libraries were generated using SeSaM and epPCR, enriched with the BCCE flow cytometer assay and screened with the BCCE as fluorescent substrate in MTP for improved mediated electron transfer. P450 BM3 was also evolved for a second alternative cofactor system, the direct electron transfer. Focused as well as random mutagenesis libraries of P450 BM3 were generated and screened for improved activity in the presence of a conductive polymer (Clevios P).

Additionally, in the Appendix Chapter the collaborative P450 BM3 projects are summarized in which the PhD candidate was involved. These projects were part of the 7 framework funded by the European union project Oxygreen focused on the effective redesign of oxidative enzymes for green chemistry. Within Oxygreen the monooxygenase mutein database (muteinDB) was supported in which muteins altering substrate specificity are collected, the evolution of P450 BM3 for substrate specificity was contributed and P450 BM3 muteins with surface modifications for electrochemical characterization were generated.

2. Material and Methods

Materials were used according to supplier's recommendation. Molecular biological methods were performed according to the protocols reported in Molecular Cloning (Sambrook and Russell, 2001). Directed Evolution methods were applied with small changes according to the protocols reported in Directed Enzyme Evolution and Directed Evolution Library Creation (Arnold and Georgiou, 2003).

2.1 Chemicals

All chemicals were of analytical grade or higher quality and purchased from Sigma-Aldrich Chemie (Steinheim, Germany), AppliChem (Darmstadt, Germany) and Carl Roth (Karlsruhe, Germany). Chemicals purchased from other suppliers or restricted to this use are mentioned.

ABIL EM 90	Evonik, Marl, Germany
Aminolevulinic acid (ALA)	Sigma Aldrich, Saint-Louis, USA
BCCE	Home made (section 2.14.2)
BCC-acid	Home made (section 2.14.2)
Catalase	Merck, Darmstadt, Germany
Carboxymethylcellulose (CMC)	Sigma Aldrich, Saint-Louis, USA
Cobalt(III)sepulchrate (Co(III)-sep)	Sigma Aldrich, Saint-Louis, USA
Jod	Sigma Aldrich, Saint-Louis, USA
Light Mineral Oil (LMO)	Sigma Aldrich, Saint-Louis, USA
Sodium hydrosulfite	Sigma Aldrich, Saint-Louis, USA
Zinc-dust	Carl Roth, Karlsruhe, Germany

2.2 Devices

Centrifuges 5810R	Eppendorf, Hamburg, Germany
CyFlow Space flow cytometer	Partec, Münster, Germany
Fluoreszent microscope, Orthoplan	Leitz Wetzlar, Wetzlar, Germany
Microplatereader Infinite M1000	Tecan Group, Männedorf, Switzerland
Microplatereader Sunrise	Tecan Group, Männedorf, Switzerland
Microtiter plate shaker Microtron	INFORS, Heinsbach, Germany
NanoDrop ND-1000	Thermo Fischer Scientifics, Willmington, USA
PCR-Cycler Mastercycler pro S	Eppendorf, Hamburg, Germany

Spectrophotometer Varian Cary 50 UV	Agilent, Waldbronn, Germany
Shaker CERTOMAT S-II	Sartorius, Göttingen, Germany
Shaker TIMIX 5	Edmund Bühler, Hechingen, Germany
Lyophilizer ALPHA 1-2 LDplus	CHRIST, Osterode am Harz, Germany
Sonotrode Sonoplus HD200	Bandelin, Berlin, Germany
Sorvall RC-6 Superspeed Centrifuge	Thermo Fischer Scientific, Bonn, Germany
Ultra Thurax – Disperser T10 basic	IKA®-Werke, Staufen, Germany
Resin Dispenser 48 Position	Mettler-Toledo, Columbus OH, USA
High Pressure Homogenizer	Avestin, Ottawa ON, Canada
Äktaprime plus	GE Healthcare, Uppsala, Sweden
GC-2010-plus	Shimadzu, Duisburg, Germany
GCMS-QP2010S	Shimadzu, Duisburg, Germany
Rotavapor-IKA HB10 basic	VWR, Darmstadt, Germany
Camera DC50	Nikon, Düsseldorf, Germany
Geldocumentation U:Genius	Syngene, Cambridge, UK

2.3 Other materials

Emulsion tubes (PS, 16 x 65 mm)	Nerbe plus, Winsen/Luhe, Germany
Analyzer cups – CyFlow (PS, 55 x12 mm)	Sarstedt, Nümbrecht, Germany
Microtiter plates, 96 deepwell 2.2 ml	Eppendorf, Hamburg, Germany
Microplates, 96 well, MICROLON 200	Greiner Bio-one, Frickenhausen, Germany
Microplates, 96 well, black, Fluotrac 200	Greiner Bio-one, Frickenhausen, Germany

2.4 Enzymes

Restriction enzymes were purchased from Fermentas (St. Leon-Rot, Germany), polymerases and terminal deoxynucleotidyl transferase (TdT) from New England Biolabs (Frankfurt, Germany). PhuS-Polymerase (derived from the Pfu-Polymerase), 3D1-polymerase (d'Abbadie et al., 2007), and Taq-polymerase were home made in the Institute.

2.5 Kits

QIAprep Spin Miniprep kit	Qiagen, Hilden, Germany
QIAquick PCR Purification kit	Qiagen, Hilden, Germany
QIAquick Gel Extraction kit	Qiagen, Hilden, Germany

Rapid DNA Dephos & Ligation kit	Roche, Mannheim, Germany
NucleoSpin Plasmid kit	Macherey Nagel, Düren, Germany
NucleoSpin Gel and PCR Clean-up kit	Macherey Nagel, Düren, Germany
NucleoSpin Extract II kit	Macherey Nagel, Düren, Germany
Experion RNA HighSens Analysis kit	BioRad, München, Germany
Experion Pro260 Analysis kit	BioRad, München, Germany
BCA Protein Assay kit	Thermo Fischer Scientific, Bonn, Germany

2.6 Media

LB Medium: Peptone 1%, Yeast Extract 0.5%, NaCl 1% in deionized H₂O.

TB Medium: Solutions A and B were autoclaved separately and mixed under sterile conditions to prepare 1L of TB media. *Solution A:* Peptone 12 g, Yeast Extract 24 g, and Glycerol 4 g were dissolved in 800 ml deionized H₂O. *Solution B:* KH₂PO₄ 2.31 g, and K₂HPO₄ 12.54 g were dissolved in 200 ml deionized H₂O.

SOB Medium: Peptone 2%, Yeast Extract 0.5%, NaCl 0.05% in deionized H₂O + 1% (V/V) KCl (1 M, pH=7 with NaOH) + addition of 0.5 % (V/V) MgCl₂ (2 M) after autoclaving.

SOC Medium: SOB medium + 2% (V/V) Glucose (1M).

2.7 Media additives

Trace Elements Solution (SEL) (Stock 1000X): CaCl₂ · 2H₂O 0.5 g, ZnSO₄ · 7H₂O 0.18 g, MnSO₄ · H₂O 0.10 g, Na₂-EDTA 20.10 g, FeCl₃ · 6H₂O 16.70 g, CuSO₄ · 5H₂O 0.16 g, CoCl₂ · 6H₂O 0.18 g were dissolved in 1000 ml deionized H₂O, filtered sterile through a 0.22 µm filter, and stored at 4°C.

ALA (Aminolevulinic acid) Stock-solution (1000X): 0.5 M ALA in deionized H₂O, filtered sterile through a 0.22 µm filter, and stored at -20°C.

IPTG (Isopropyl-β-D thiogalactopyranoside) Stock-solution (1000X): 0.1 M in deionized H₂O, filtered sterile through a 0.22 µm filter, and stored at -20°C.

Kanamycin Stock-solution (1000X): 50 mg/mL in deionized H₂O, filtered sterile through a 0.22 µm filter, and stored at -20°C.

Thiamine Stock-solution (1000X): 100 g/L in deionized H₂O, filtered sterile through a 0.22 µm filter, and stored at -20°C.

2.8 Nucleotides

Nucleotide analogs (dRTP, 3'-I-dATP, 3'-ac-2'dRTP, MANT-dATP, 3'-O-NH₂-2'-dATP) and phosphorothioated nucleotides (dATPαS, dCTPαS, dTTPαS, dGTPαS) were generously provided by BIOLOG Life Sciences Institute (Bremen, Germany). The dNTP mix was purchased from Fermentas (St. Leon-Rot, Germany).

2.9 Primers

Unmodified and biotinylated oligonucleotides were purchased from Eurofins MWG Operon (Ebersberg, Germany) in salt-free form and diluted in milli-Q water to a final concentration of 100 µM. Oligonucleotides containing dRTP were synthesized by Biomers (Ulm, Germany). Synthetic constructs (S1-S6) differing in 3 nucleotides were purchased from Eurofins MWG Operon (Ebersberg, Germany), and used for generating short template-DNAs. All primers and synthetic constructs used are summarized in Table S1 (see Appendix 6.1). PCRs were performed in 0.2 ml thin-walled PCR tubes from Sarstedt (Nümbrecht, Germany) employing a Mastercycler Gradient PCR-machine from Eppendorf (Hamburg, Germany). DNA was quantified by a NanoDrop photometer from NanoDrop Technologies (Wilmington, USA DE).

2.10 Vectors and strains

The commercial available vector pET28a(+) from Merck (Darmstadt, Germany) as well as the vector pCWori(+) (Barnes, 1996) and pALXtreme-1a (home made in the institute) were used as expression vector. pALXtreme-1a is a shortened pET28a(+) derivative which lacks the LacI^{Q1} gene. The vector maps are enclosed in the Appendix 6.3.

The strain *E. coli* BL21(DE3) Gold was used to express genes cloned in the pET vector system, and the strain *E. coli* BL21(DE3) Gold LacI^{Q1} was used for pALXtreme-1a. The strain *E. coli* DH5α was used for expression of the pCWori(+) vector as well as for intermediated cloning steps.

All strains and plasmids employed in this thesis and their characteristics are summarized in Table S2 (Appendix 6.1).

2.11 Microbiological methods

2.11.1 *E. coli* cultivation and P450 BM3 expression

P450 BM3 mutein expression in flasks and in deep-well microtiter plates was performed as described previously by Nazor (Nazor and Schwaneberg, 2006). For MTP expression, a master plate and overnight culture was prepared prior to expression. The master plate was prepared by picking single freshly transformed colonies into 96 well flat bottom microtiter plates (Greiner Bio-One, Frickenhausen, Germany), containing 150 μ l LB_{Kan} (50 μ g/ml). The plate was covered with a lid and was sealed with parafilm. The cells were cultivated at 900 rpm, 37°C, 14 – 16 hrs and 70% humidity with Microtrone shaker (INFORS, Heinsbach, Germany). After addition of 100 μ l autoclaved 50% glycerol solution (v/v) to the overnight culture, the plate was stored at –80°C. For overnight culture, the master plate, after thawing at room temperature for 20 minutes, was replicated using a 96-pin replicator into a 96-well flat bottom microtiter plate containing 150 μ l LB/Kan. The plate was sealed with a lid and parafilm. The overnight culture was incubated at 900 rpm, 37°C and 70% humidity overnight (14 – 16 hrs). Protein was expressed in sterile 2 ml 96 deepwell microtiter plates (Eppendorf, Hamburg, Germany). Each well of a deep well plate was filled with 600 μ L of TB-medium containing Kan (50 μ g/ml), 1 x trace elements solution, ALA (0.5 mM), IPTG (0.1mM), thiamine (0.3 μ M). The overnight saturated culture was replicated in the prepared deep well plate by pipetting 6 μ L of the overnight culture into each well of the deep well plate using a transfer pipette. The plates were covered with a lid cleaned with 70% EtOH and sealed with parafilm tightly. Protein was expressed at 700 RPM, 30°C and 70% humidity for 20 hours in Microtrone shaker (INFORS, Heinsbach, Germany). For flask expression, the preculture 5 mL LB_{kan} (50 μ g/ml) was inoculated with a single colony from agar plate and incubated overnight at 37°C, 250 rpm. The expression culture in flasks, TB-medium supplemented with respective antibiotics (kanamycin (50 μ g/ml)) and 1 x trace elements solution was inoculated with 2% of the overnight culture and incubated at 30°C, 250 RPM until OD₆₀₀ reaches 0.8-1.0. The culture was supplemented with Aminolevulinic acid (ALA) (0.5 mM) and thiamine (0.3 μ M) and expression was induced by the addition of IPTG (0.1 mM). Cells were expressed for 20 h at 30°C, 250 rpm on CERTOMAT S-II shaker (Sartorius, Göttingen, Germany) and harvested by centrifugation (4°C, 4000 rpm, 20 min, Eppendorf, Hamburg, Germany).

2.11.2 Fluorescence microscopy

Fluorescence microscopy analysis was performed with the microscope ORTHOPLAN (Leitz, Wetzlar, Germany). The cell culture (~10 μ l) was evenly spread on a microscope slide which was covered with a glass slide. A droplet of oil was applied and the sample was analyzed under UV-light at λ_{ex} of 350 nm or 405 nm (objective: 100/1.30). The images were recorded with the camera DC50 (Nikon, Düsseldorf, Germany).

2.11.3 Cryocultures

Escherichia coli overnight culture (37°C, 250 rpm, 14h) was supplemented in a ration of 1:1 with sterile glycerol (50% w/v in H₂O) and stored at -80°C. Cryocultures in MTP consist of 150 μ l overnight culture (14h, 900 rpm, 37°C, 70% humidity) supplemented with 100 μ l sterile glycerol solution (50% w/v in H₂O).

2.12 Molecular biological methods

2.12.1 Validation of dRTP as universal base for SeSaM method

SeSaM Step 2: Acceptance and optimization of the dRTP incorporation by terminal deoxynucleotidyl transferase (TdT).

The optimization of TdT catalyzed incorporation of deoxyribonucleotides dRTP to 3'-OH of a fluorescent labeled oligonucleotide (P15) was performed by varying the reaction conditions. The incubation times (15, 30, 60, 120 min), the amount of TdT (10-20 U), concentration of CoCl₂ (0 mM-2.5 mM), concentration of ZnCl₂ (10 μ M, 100 μ M), and the molar ratio of template-DNA to dRTP (1:5, 1:10, 1:20, 1:40) were varied. The R-tailed fluorescent labeled oligonucleotides were separated on a 36% TBE-acrylamid gel (150 V, 13 h) in 1 x TBE buffer (89 mM tris, pH 8, 89 mM boric acid, 2 mM EDTA) running in Mini-Protean Tetra Cell system from Bio-Rad (München, Germany). The gel was visualized on a FLA-3000 phosphorimager (excitation 494 nm; emission 518 nm) from Fujifilm (Düsseldorf, Germany) and DNA fragments were quantified using the AIDA 4.0 gel analysis software. In Step 2 up to 3 R-bases were incorporated (molar ratio of 1:5 (template-DNA to dRTP), TdT (10 U), CoCl₂ (0.25 mM); 37°C; 15 min) followed by heat inactivation (30 min; 75 °C).

SeSaM Step 3 and Step 4: selection of suitable polymerases through the “read” and “write” activity assays

The R-“read” activity assay was performed similarly as reported for the P-base (Wong et al., 2008) with the following differences: Primers were designed to yield PCR-products that can be distinguished through size from each template-DNA and further PCR products. Differences occurred since in contrast to the P-base (Wong et al., 2008) write and read activities assays two different templates-DNA had to be generated (Template-600 and Template-600-2). The Template-600 (Fig. 13; 1) was used in the read activity assay (Fig. 13; 2) and analyzed by gel electrophoresis. The latter analysis could be performed without a cloning step. For the write activity assay (Fig. 13; 4) a single stranded template-DNA had to be generated (Fig. 13; 3) and subsequently be used as template-DNA (Fig. 13; 4). Prerequisite to perform the write activity assay is the removal of the Template-600-2 (see Fig. 13; 3). For removal via DpnI digest the Template-600-2 has to be methylated. To obtain methylated DNA, the plasmid pALXtreme-1a was amplified in vivo. pALXtreme1a was isolated from a 5 ml cell culture (LB_{kan}, 14h, 37°C, 250 rpm) using the Nucleospin Extract II kit (Macherey Nagel, Düren, Germany). The methylated Template-DNA generation was achieved by isolation from the plasmid pALXtreme-1a of the double stranded Template-600-2 through restriction enzyme digest with *XmnI/HaeII* (Fig. 13; 1). The complementary strand to Template-600-2 is not shown in Fig. 13 and did not cause detectable interference with the write activity assay. The detailed experimental procedures for step one to five are described in the following paragraphs (represented graphically in Fig. 13; 1-5).

Preliminary template-DNA generation

Preliminary plasmids were constructed by PCR amplification of six synthetic primers (P16, Table S1, Appendix 6.1) of equal sequence and differing by 3 nucleotides CCC, TTT, AGA, GAG, AAA, GGG (shown with “XXX” in Fig. 13; 1). The PCR products were column purified by Nucleospin Extract II kit (Macherey Nagel) and hybridized in pALXtreme-1a vector by PLICing (Blanusa et al., 2010b). PCRs (50µl) contained: 2 U Phusion High-Fidelity DNA polymerase, 1 x Phusion HF buffer, 0.5 µM of each primer (P6, P7), template-DNA 50 ng, 0.2 mM of each dNTP. PCR protocol: 98°C for 30 sec (1 cycle); (98°C for 10 sec, 55 °C for 30 sec, 72 °C for 30sec) (15 cycles); 72°C for 5 min (1 cycle). This preliminary plasmids were used to generated the two starting templates-DNA Template-600 and Template-600-2. Template-600 was amplified by PCR using Primer P8 and P9 (Table S1, Appendix 6.1), DpnI digested (10 U DpnI, 120 min at 37°C) and purified (Nucleospin Extract II kit).

Read activity assay: Elongation of R-tailed oligonucleotides by a polymerase catalyzed reaction.

Read activity assay aim to test ability of various polymerases to elongated R, RR or RRR-tailed oligonucleotides pairing with a template-DNA containing match CCC or TTT as well as mismatch AGA, GAG, AAA or GGG. Six PCRs were performed in parallel, each with one template-DNA (CCC, TTT, or AGA, GAG, AAA, GGG) and a one R tailed primer (P12). A negative control was prepared with same PCR-setup without addition of any DNA polymerase. This read activity assay was performed for every polymerase listed using RR-(P13) or RRR-(P14) tailed primers (Table S1, Appendix 6.1). PCR-products were analyzed by gel electrophoresis. Elongated primers generated 460 bp fragments, which could easily be distinguished from the template-DNA (600 bp). (Fig. 13; 2). DNA polymerases were classified as having a “good” or “poor” read capability, depending on PCR efficiencies. Following DNA polymerases were tested with read activity assay: Taq, Deep Vent (exo-), Vent, Vent(exo-), DyNAzyme EXT, 9°NM, Phusion High-Fidelity from New England Biolabs (NEB) (Frankfurt, Germany), AmpliTaq, AmpliTaq Stoffel Fragment from Applied Biosystems (Darmstadt, Germany), 3D1 (d’Abbadie et al., 2007). PCRs were done in suppliers buffer according to suppliers recommendations. PCRs (12.5 µl) contained: 40 ng Template-600 (CCC, TTT, or AGA, GAG, AAA, GGG), 0.5 µM R-tailed primer, 1 x buffer, 2-5 U polymerase, 0.2 mM of each dNTP. PCR conditions: Vent, Vent (exo-): 95°C for 2 min (1 cycle); (95°C for 30 sec, 55°C for 30 sec, 72°C for 30 sec) (40 cycles); 72°C for 10 min (1 cycle); 3D1: 94°C for 2 min (1 cycle); (94°C for 30 sec, 52°C for 30 sec, 72°C for 1 min) (40 cycles); 72°C for 10 min (1 cycle); DyNAzyme EXT and AmpliTaq, Deep Vent (exo-), 9°NM, Phusion High-Fidelity, Taq: 94°C for 2 min (1 cycle); (94°C for 30 sec, 55°C for 30 sec, 72°C for 1 min) (40 cycles); 72°C for 10 min (1 cycle); AmpliTaq Stoffel Fragment: 95°C for 2 min (1 cycle); (95°C for 1min , 55°C for 1 min, 72°C for 1 min) (40 cycles); 72°C for 7 min (1 cycle).

Template-DNA generation for write activity assay.

As template-DNA for the write activity assay, a ssDNA PCR-product generated by the read activity assay is needed. To generate this template-DNA the read activity assay was performed as described above but using Template 600-2. The PCR-products of read activity assay were DpnI digested (20 U DpnI, 37 °C, overnight) and purified (QIAquick PCR purification kit Qiagen). This procedure assured that no starting plasmid remained in the

mixture, so only elongated R-tailed oligonucleotides are present in the PCR-setup for the write activity (Fig. 13; 3).

Write activity assay: Replacement of R-base by standard nucleotides.

Aim of the write activity assay was to test if polymerases possess the ability to replace incorporated R-bases by standard nucleotides. The write activity assay was performed for each polymerase listed above. PCR products were analyzed by gel electrophoresis. Amplified oligonucleotides generated a 250 bp fragments, which could easily be distinguished from template-DNA (= PCR-product of Step 3-template-DNA (460 bp)) (Fig. 13; 4). PCRs (12.5 μ l) contained: 30 ng purified ssDNA (from Step 3), 0.5 μ M primer (P10) 1 x buffer, 2-5 U polymerase, 0.2 mM of each dNTP, 1 x buffer. PCR conditions: Vent, Vent (exo-): 95°C for 2 min (1 cycle); (95°C for 30 sec, 55°C for 30 sec, 72°C for 30 sec) (25 cycles); 72°C for 10 min (1 cycle); DyNAzyme EXT and AmpliTaq, Deep Vent (exo-), 9°NM, Phusion High-Fidelity, Taq, 3D1: 94°C for 2 min (1 cycle); (94°C for 30 sec, 55°C for 30 sec, 72°C for 1 min) (25 cycles); 72°C for 10 min (1 cycle); AmpliTaq Stoffel Fragment: 95°C for 2 min (1 cycle); (95°C for 1 min , 55°C for 1 min, 72°C for 1 min) (30 cycles); 72°C for 7 min (1 cycle).

Cloning of PCR-products from write activity assay.

Write activity assay was repeated with a modified PCR protocol to generate the PCR-products for cloning. First the PCR-products from read activity assay (Template-600-2) were linearly amplified by Taq polymerase using the primer P10 for 15 cycles, followed by an exponential amplification for 10 cycles after addition of reverse primer P11 (Table S1, Appendix 6.1). Primer design allowed the direct hybridization of the PCR-products after purification by QIAquick PCR Purification kit (Qiagen) in adequately prepared pALXtreme-1a vector by PLICing (Blanusa et al., 2010b). Hybridization mixture was transformed in chemical competent *E. coli* BL21 Gold (DE3) cells and grown on LB kanamycin agar-plates. Thirty clones were randomly picked, grown in 5 ml LB kanamycin overnight and send for sequencing after plasmid isolation (Nucleo Plasmid kit from Macherey Nagel (Düren, Germany) (Fig. 13;5).

Scheme of the “read” and “write” activity assay used for the advancement of the SeSaM method:

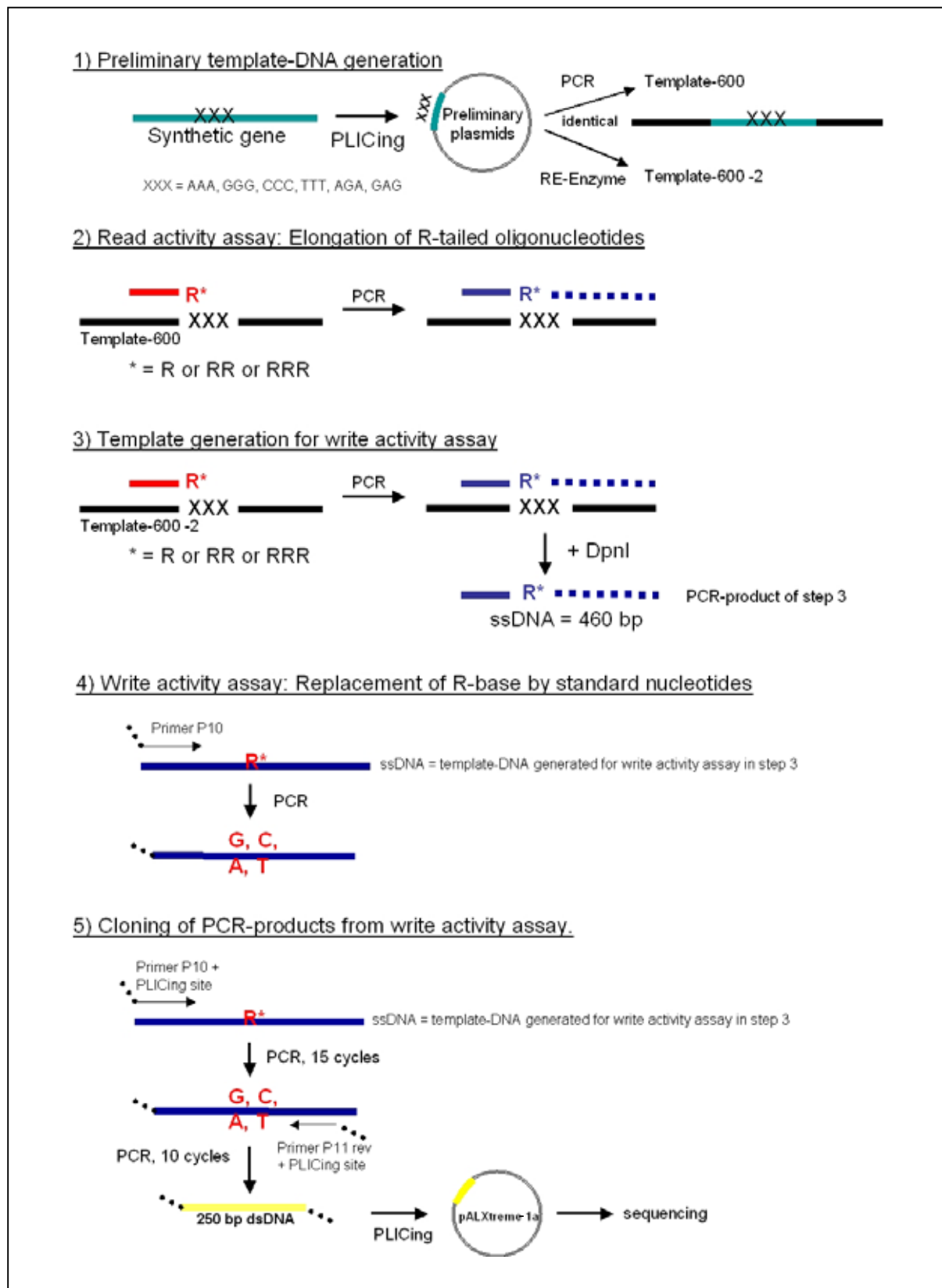


Fig. 13: Step one to five of the “read” and “write” activity assay.

2.12.2 SeSaM-R method

Preliminary step: Preparation of double stranded template-DNA for Step 1 and Step 3.

PCRs (50 μ l) contained: 1 x Phusion HF buffer, 0.2 mM of each dNTP, 0.5 μ M of each primer (P2 and P1 for Step 1 template-DNA, and P3 and P5 for Step 3 template-DNA), 0.5 U Phusion High-Fidelity DNA polymerase (New England Biolabs, Frankfurt, Germany) and 50 ng pEGFP plasmid (Clontech, Mountain View, CA, USA). PCR protocol: 98°C for 30 sec (1 cycle); 98°C for 10 sec, 55°C for 30 sec, 72°C for 30 sec/kb of the SeSaM template-DNA (15 cycles); 72°C for 5 min (1 cycle). The PCR products were digested with *DpnI* (20 U, 37°C, 3 h) and gel-purified (Nucleospin Extract II kit from Macherey Nagel, Düren, Germany).

Step 1: Generation of ssDNA fragment pool with random length distribution.

The preliminary generated EGFP-SeSaM Step 1 template-DNA was amplified by PCR in presence of dCTP α S and dTTP α S to randomly incorporate chemical cleavable phosphorothioate bonds (Wong et al., 2004b). PCRs (50 μ l) contained: 1 x ThermoPol buffer, 0.5 μ M of each primer (P1 and P4), 5 U Taq DNA polymerase, 360 ng/kb of the SeSaM template-DNA (preliminary prepared in Step 1). According to the desired library the following nucleotide combinations were used: C-libraries: 0.2 mM of each dATP, dGTP, dTTP, and 0.07 mM dCTP α S, and 0.13 mM dCTP; T-libraries: 0.2 mM of each dATP, dGTP, dCTP, and 0.08 mM dTTP α S, and 0.14 mM dTTP. For both setups the same PCR protocol was performed: 94°C for 2 min (1 cycle); 94°C for 15 sec, 65°C for 30 sec, 72°C for 30 sec/kb of the SeSaM template-DNA (15 cycles); 72°C for 3 min (1 cycle). PCR products were purified (Nucleo Extract II kit) and eluted (80 μ l NE-buffer). The cleavage of phosphorothiodiester bonds was performed in ThermoPol buffer (1x), supplemented with iodine (10 μ l, 20 mM in EtOH) and incubated (30 min, 70°C). Cleaved biotinylated DNA fragments were isolated by magnetic streptavidin beads (M-PVA SAV1, Chemagen, Baesweiler, Germany) and ssDNA was purified employing the NTC binding buffer (Nucleospin Extract II kit).

Step 2: Enzymatic elongation of single stranded DNA with dRTP.

Single-stranded DNA fragments generated in Step 1a and 1b were elongated by TdT catalyzed incorporation of dRTP (37°C, 15 min) and terminated by heat inactivation (30 min, 75°C). Reaction mixtures (25 μ l) contained: 1 x TdT buffer, 0.25 mM CoCl₂, 1 pmol of

ssDNA fragment (from Step 1b), 5 pmol dRTP and 10 U TdT. The ssDNA was purified with Nucleo Trap Extract II kit using the NTC buffer.

Step 3: Synthesis of the full length gene.

Full length *EGFP* were generated by PCR using the dRTP-elongated DNA fragments of Step 2 as primers and the preliminary generated Step 3 template-DNA. The PCRs (50 μ l) contained: 50 ng/kb of the ssDNA of Step 2, 50 ng/kb of the preliminary generated dsDNA SeSaM Step 3 template-DNA, 1 x Termopol buffer, 0.2 mM of each dNTP, 2 U Vent (exo-) DNA polymerase. PCR protocol: 94°C for 2 min (1 cycle); 94°C for 10 sec, 55°C for 30 sec, 72°C for 2 min/kb SeSaM template-DNA (30 cycles). PCR products were purified (NucleoTrap Extract II kit). The SeSaM-R-3D1 protocol was identical to the SeSaM-R protocol described above, except that 3D1 (d'Abbadie et al., 2007) DNA polymerase (5 U) and the respective 3D1-buffer were used.

Step 4: Replacement of universal bases.

Universal bases were replaced by standard nucleotides during PCR amplification. The PCRs (50 μ l) contained: 0.5 U Phusion High-Fidelity DNA polymerase, 0.5 μ M of each primer (P2 and P3), 50 ng full-gene length DNA from Step 3, 0.2 mM of each dNTP, 1 x Phusion HF buffer. The following PCR protocol was employed: 98°C for 30 sec (1 cycle); 98°C for 10 sec, 58°C for 15 sec, 72°C for 30 sec/kb of the SeSaM template-DNA (30 cycles); 72°C for 10 min (1 cycle). The PCR products were gel purified with QIAquick Gel Extraction kit (Qiagen, Hilden, Germany) to eliminate the “non-mutated” template-DNA supplemented in Step 3.

Cloning of EGFP-SeSaM libraries

PCR products (from Step 4) were digested with EcoRI/HindIII (10 U of each in 1 x FastDigest buffer (Fermentas, St. Leon-Rot, Germany)), purified (QIAquick PCR purification kit; Qiagen), and cloned into EcoRI/HindIII-digested and dephosphorylated pEGFP vector (Rapid DNA Dephos & Ligation kit; Roche, Mannheim, Germany). Subsequently, the ligation mixtures were transformed into chemical competent *E. coli* DH5 α cells and plated on LB agar plates containing ampicillin (100 μ g/ml). Thirty clones were randomly picked and sequenced.

2.12.3 SeSaM-P/R method

The SeSaM-P/R protocol allows recombination of SeSaM forward R-libraries with the SeSaM reverse P-libraries or vice versa. SeSaM Step 2 fragments with dPTP were prepared as described in the SeSaM-Tv⁺ protocol (Wong et al., 2008). SeSaM Step 2 fragments with dRTP were generated according to the above described SeSaM-R protocol.

Step 3: Recombination of R- or P-tailed SeSaM Step 2 fragments by PCR.

Step 2 fragments of forward R- and reverse P-libraries were hybridized and elongated to full length gene fragments by PCR. PCR conditions: Step 2 templates-DNA of each 50 ng (Step 2: R or P fragments), 1 x ThermoPol buffer, 0.2 mM dNTP, 2 U Vent(exo-) DNA polymerase. PCR protocol: 94°C for 2 min (1 cycle); 94°C for 1 min, 55°C for 1 min, 72°C for 2 min/kb of the targeted gene length (15 cycles); 94°C for 1 min, 65°C for 1 min, 72°C for 3 min/kb of the targeted gene length (15 cycles); 72°C for 5 min (1 cycle). PCR products were purified by QIAquick PCR purification kit (Qiagen).

Step 4: Replacement of universal bases.

In the SeSaM-P/R protocol the PCRs in Step 4 were performed as described in Step 4 of the SeSaM-R method. Gel purification could be omitted and was replaced by employing the QIAquick PCR Purification kit since no *EGFP* DNA was required to serve as template-DNA in Step 3. Cloning of SeSaM libraries was performed as described in the SeSaM-R protocol.

2.12.4 Agarose gel electrophoresis

DNA-fragments were separated by agarose gel electrophoresis running in 1x TAE-buffer (TAE-Puffer (50x): 2 M Tris 100 mM EDTA in H₂O pH=8,0 adjusted with HCl) for 30-60 min at 60-120V depending on fragment size and gel concentration (0.8-3%). Samples (50-100 ng DNA) were mixed with 1x loading dye (Loading dye (stock 6x): 6,7 ml glycerin, 10 mg bromphenolblau, 1 ml 10x TAE-puffer filled up to 10 ml with H₂O) and were applied on a 1% agarose gel (1% agarose in 1x TAE-buffer) with the DNA ladder (GeneRuler 1kb DNA Ladder, Fermentas, St. Leon-Rot, Germany) as reference for fragments between 250-10000 bp and the GeneRuler 50bp Ladder (Fermentas, St. Leon-Rot, Germany) on a 2% agarose gel for fragments between 50-1000 bp. Gel staining occurred with ethidiumbromid staining after separation (40 µl EtBr-Stock solution in 1000 ml H₂O) or by Gelred staining during the run 0.01% GelRed-solution (Stock dilute 1:3, Biotium, Hayward, CA USA) was added to the

agarose solution before casting. In both cases the gel was analyzed and documented on a UV-lamp with the geldocumentation device (U:Genius, Syngene, Cambridge, UK).

2.12.5 Polymerase Chain Reaction (PCR)

PCRs were performed in 0.2 ml thin-walled PCR tubes from Sarstedt (Nümbrecht, Germany) employing a Mastercycler Gradient PCR-machine from Eppendorf (Hamburg, Germany). DNA was quantified by a NanoDrop photometer from NanoDrop Technologies (Wilmington, USA DE). As negative control the PCR reaction mixture without template-DNA was carried along. If not mentioned otherwise, standard PCR was used.

2.12.5.1 Standard PCR

PCR contained (50 μ l: template DNA 50 ng, Taq-buffer 1 x, dNTPs 0.2 mM, Taq-polymerase 5 U, each primer 0.5 pmol/ μ l.

PCR protocol: 94°C for 1 min (1 cycle), 94°C for 30 sec, 55°C for 30 sec, 68°C for 1 min/kb (25 cycles), 68°C for 10 min (1 cycle).

2.12.5.2 Colony PCR

Colony-PCR was used to check if after transformation *E. coli* colonies carried the plasmids with desired insert. As template 10 μ l overnight culture was mixed with 40 μ l ddH₂O and incubated for 15 min at 95°C. To amplify the whole P450 BM3 gene the primer PP1 and PP2 were used or the P87/P88 to amplify the multiple cloning site of the vector pET28a(+) (see supplementary Table S1 in Appendix 6.1).

Colony-PCR (12.5 μ l) contained: template DNA 2.5 μ l, Taq-buffer 1 x, dNTPs 0.2 mM, Taq-polymerase 5 U, each primer 0.5 pmol/ μ l.

PCR protocol: 94°C for 1 min (1 cycle), 94°C for 30 sec, 58°C for 30 sec, 72°C for 1 min/kb (30 cycles), 72°C for 10 min (1 cycle).

2.12.5.3 Overlap extension PCR

The overlap extension PCR was used to generate the simultaneous SSM at 2 positions (Ho et al., 1989; An et al., 2005). Three fragments were generated by standard PCR and annealed by an additional PCR amplification step.

PCR contained (50 μ l): Template DNA 100 ng (each fragment 30 ng), PfuS-buffer 1 x, dNTPs 0.2 mM, PfuS-polymerase 5 U, each primer 0.5 pmol/ μ l.

PCR protocol: 94°C for 1 min (1 cycle), 94°C for 30 sec, 58°C for 30 sec, 72°C for 1 min/kb (30 cycles), 72°C for 10 min (1 cycle).

2.12.5.4 EpPCR library generation

EpPCR-libraries of P450 BM3 were constructed according to protocols from Cirino and Arnold (Arnold and Georgiou, 2003; Cirino et al., 2003) with variable MnCl₂ concentrations 0.05 mM, 0.1 mM, 0.2 mM. Gene specific primers PP1 and PP2 (see supplementary Table S1 in Appendix 6.1) were used for insert amplification. A standard epPCR master mix of 50 µl contained: Template plasmid DNA 1 ng/µl, Taq-buffer 1x, dNTPs 0.2 mM, Taq-polymerase 5 U, each primer 0.3 pmol/µl, MnCl₂ 0.05-0.4 mM. EpPCR protocol: 94°C for 30 sec (1 cycle); 94°C for 30 sec, 60°C for 1 min, 72°C for 1 min/kb (30 cycles); 72°C for 10 min (1 cycle). For vector amplification the primers P3 and P4 (see supplementary Table S1, Appendix 6.1) were used. The PCR products were DpnI digested (20 U; 37°C, 3 h) and purified using the Nucleospin Extract II kit (Macherey Nagel, Düren, Germany). Vector-PCR (50 µl) contained: Template DNA 50 ng/µl, HF-Buffer 1x, dNTPs 0.2 mM, Phusion High-Fidelity DNA Polymerase (NEB) 5 U, each primer 0.5 pmol/µl. PCR protocol: 98°C for 30 sec (1 cycle); 98°C for 10 sec, 55°C for 30 sec, 72°C for 1 min/kb (25 cycles); 72°C for 5 min (1 cycle). PCR products were hybridized by using the PLICing cloning method (Blanusa et al., 2010b).

2.12.5.5 Site directed (SDM) and site saturation mutagenesis (SSM) - PCR

Site directed and site saturation mutagenesis were done according to a modified QuickChange Mutagenesis (QCM) protocol (Hogrefe et al., 2002). The procedure consists of two steps. In the first step, two extension reactions are performed in separate tubes, containing either the forward or the reverse primer. Subsequently, the two reactions are mixed and the standard QCM procedure was carried out. PCR (50 µl) in step 1 contained: Pfu buffer 1x, dNTP mix 0.2 mM, Pfu DNA polymerase 1 U, primer (forward or reverse) 0.2 µM. PCR protocol for step 1: 95°C for 30 sec (1 cycle), 95°C for 30 sec, 55°C for 1 min, 68°C for 2 min/kb (3 cycles). Equal amounts of Step 1 were mixed and 1 U Pfu DNA polymerase was added before next PCR-reaction was started. PCR protocol for step 2: 95°C for 30 sec (1 cycle), 95°C for 30 sec, 55°C for 1 min, 68°C for 2 min/kb (15 cycles), 68°C for 60 min (1 cycle). PCR products were DpnI digested overnight at 37°C (10 U DpnI/50 µl PCR mixture) and purified with PCR-Purification Kit before transformation. Primer used for SDM and SSM are listed in supplementary Table S1 (Appendix 6.1).

2.12.6 Cloning

2.12.6.1 Preparation of chemical competent cells

Chemical competent cells were prepared by inoculation of 5 ml overnight culture in LB-media (at 37°C, 250 rpm, 14h). Main culture of 200 ml LB-media in 1 L flask was inoculated with 2% of the preculture and incubated at 37°C, 250 rpm until reach of $OD_{600} = 0.4$. The culture was cooled down on ice and centrifuged at 4°C, 3000 rpm, for 10 min (Eppendorf, Hamburg, Germany). All following steps were carried out on ice. The pellet was resuspended in 15 ml sterile filtered cooled TFB1-solution (30 mM K-Acetate, 50 mM $MnCl_2$, 100 mM $RuCl_2$, 10 mM $CaCl_2$, 15% glycerin in H_2O , pH=6.8 adjusted with KOH/HCl) and incubated for 10 min. Cells were centrifuged at 4°C, 3000 rpm, 10 min (Eppendorf, Hamburg, Germany) and pellet was resuspended in 2 ml sterile filtered cooled TFBII-solution (10 mM MOPS, 75 mM $CaCl_2$, 10 mM $RuCl_2$, 15% glycerin in A.dest, pH=6.8 adjusted with KOH/HCl). Competent cells were divided in 100 μ l aliquots and stored at -80°C.

2.12.6.2 Digestion with restriction enzymes

Restriction enzyme digestion was used for cloning purpose or to check integrity of genetic constructs. Reaction mixtures contained 1 μ g DNA, 5 U of each enzyme, 1 x restriction buffer. Digestion was performed following suppliers recommendation at 37°C for 2 h (NEB) or at 37°C for 10 min (Fermentas) followed by heat inactivation (20 min at 65 °C) or by purification with PCR Purification kits. The digestion mixture was separated and visualized by agarose gel electrophoresis.

2.12.6.3 PLICing

The PLICing method (Blanusa et al., 2010b) was used as alternative cloning method to hybridized DNA constructs in adequately prepared vector. For hybridization of P450 BM3 in pET28a(+) or pALXtreme-1a, the vectors were amplified with the primers PP3 and PP4 and the insert with the primers PP1/PP2 (see supplementary Table S1 in Appendix 6.1). The PCR products were digested with DpnI (20 U; 37°C, 3 h) and purified (Nucleospin Extract II kit from Macherey Nagel, Düren, Germany). PCR (50 μ l) contained: Template DNA 50 ng/ μ l, Taq-buffer 1x, dNTPs 0.2 mM, Taq-polymerase 5 U, each primer 0.5 pmol/ μ l. PCR protocol: 98°C for 30 sec (1 cycle), 98°C for 10 sec, 55°C for 30 sec, 72°C for 1 min/kb (25 cycles), 72°C for 5 min (1 cycle). For the iodine cleavage step, the vector-DNA was diluted to 0.03

pmol/ μ l and the insert-DNA to 0.05 pmol/ μ l. The iodine-cleavage reaction contained 4 μ l of the sample and 1 μ l of the iodine cleavage master-mix (5 μ l 10x iodine cleavage buffer (500 mM Tris, pH 9.0) and 3 μ l 100 mM iodine were dissolved in 99% ethanol and 2 μ l ddH₂O) and was incubated for 5 min at 70°C. DNA-hybridization was carried out by mixing 5 μ l of the cleaved vector and 5 μ l of the cleaved insert and incubation for 5 min at RT.

2.12.6.4 Transformation

Before transformation competent *E. coli* cells were thaw on ice. 100 μ l chemical competent *E. coli* cells were mixed with 50 ng plasmid DNA or 200 ng ligation mixture and incubated 20 min on ice. The heat-shock was carried out at 42°C for 45-60 s. Samples were immediately cooled down on ice 1 min, for regeneration filled up to 1 ml with pre-tempered LB-media and incubated for 45 min at 37°C, 250 rpm. The cells were plated on LB agar plates with corresponding antibiotics and incubated over night at 37°C. For validation a negative control consisting of H₂O and a positive control consisting of plasmid DNA were carried along.

2.12.6.5 Sequencing

DNA-sequencing was done at GATC Biotech (Konstanz, Germany) and Eurofins MWG-Operon (Ebersberg, Germany) and analysis of the resulting sequencing data was performed with the Clone Manager 9 Professional Edition Software (Scientific & Educational Software, Cary, NC, USA).

2.13 Biochemical methods

2.13.1 Activity assay in MTP format

2.13.1.1 NADPH consumption assay

Crude extracts prepared by Lysozyme digestion from cells expressed in flasks or MTP were used for NADPH consumption assay. In a flat bottom MTP plate following sample and control was setup and mixed well. Sample contained 25 μ l DMSO with substrate concentration of 2 mM-10mM, 75 μ l KPi buffer (0.1 M, pH 7.5), 100 μ l crude extract. Control was setup identically without the addition of substrate. After 5 min incubation, conversion was started by addition of 50 μ l NADPH (0.8 mM) and immediately the absorption was measured at 340 nm over 15 min with 30 sec interval in a microtiter plate spectrophotometer. NADPH consumption assay was also performed with purified protein, in

this case the amount of buffer and enzyme solution was adjusted to have between 0.5 μ M and 10 μ M P450 BM3 in the reaction.

2.13.1.2 4-Aminoantipirin activity assay (4- AAP assay)

The frozen cell pellets expressed in MTP were thawed. Cell lyse was done by addition of 140 μ l lysomix (1g lysozym /200 ml KPI pH 7.5) to each well and incubate at 900 rpm, 37°C, 70% humidity for 60 min in microtiter plate shaker Microtrone (INFORS, Heinsbach, Germany). The assay was carried out by adding: 340 μ l of 50 mM phosphate buffer pH = 7.5, 25 μ l substrate (50 mM 11-phenoxyundecanoic acid in DMSO or 5 μ l 3-phenoxytoluene (90 mM in DMSO)) and 5 μ l catalase-solution (46 mg/ml catalase from bovine liver 1558 U/mg dissolved in H₂O) and incubated under shaking (800 rpm) at room temperature for 5 min. The conversion was started by the addition of 5 μ l Clevios P or 50 μ l (1 mM NADPH) and incubated at room temperature for 60 min at 800 rpm. After incubation, the plates were centrifuged (Eppendorf Centrifuge 5810 R, Hamburg, Germany) at 4000 rpm, 4°C for 15 min and 180 μ l of the reaction mixture were transferred to a flat bottom microtiter plate. The reaction was stopped by adding 35 μ l quenching buffer (4M urea in 0.1M NaOH), followed by intensive mixing. The 4-AAP assay (colorimetric reaction) was proceeded by adding in this order: 20 μ l (10 mg/ml in H₂O) 4-AAP and 20 μ l (10 mg/ml in H₂O) potassium peroxodisulfate and incubated at room temperature for 35 min and 800 rpm. The bubbles were removed using a bunsen burner and the absorbance was measured at 509 nm and 600 nm using a microtiter plate reader.

When cell lysate prepared from protein expressed in flasks is used, after the enzymatic conversion and before centrifugation, 10 μ l of lysozyme (50 mg/ml) were added to the reaction mixture and incubated 5 min at 800 rpm RT to precipitate the conductive polymer in the reaction mixture.

The reaction mixture was centrifuged (Eppendorf Centrifuge 5810 R, Hamburg, Germany) at 4000 rpm for 5 min and 180 μ l were transferred to a flat bottom microtiter plate, filled with 35 μ l of the quenching buffer. The colorimetric reaction was proceeded like described above.

2.13.1.3 BCCE activity assay

The assay was performed analog to the MTP-assay described by Nazor and Blanusa (Nazor and Schwaneberg, 2006; Blanusa, 2010a) with minor modifications. The harvested cells in deepwell plates were resuspended in 300 μ l Tris/HCl-buffer (0.1 M, pH 8.2). After addition

of 5 μ l polymyxin B sulfate (3.6 mM), the 96well plates were incubated for 15 min at RT at 1000 rpm. 100 μ l of the lysate were pipetted into a black flat bottom 96 well MTP (Greiner Bio-one, Frickenhausen, Germany) and incubated for 5 min (700 rpm shaking) with 2 μ l of BCCE (2 mM in DMSO). The conversion of BCCE was initiated by addition of 50 μ l NADPH (1 mM). The remaining 200 μ l were used for the MET and supplemented with Cobalt(III)sepulchrates (8 μ l, 15 mM), the plate briefly mixed and incubated (RT, 1000 rpm, 15 min). The reaction was started by the addition of the electron donor, in case of the MET, 5 mg Zn was added in each well using the Resin Dispenser (Mettler-Toledo, Columbus OH, USA). The fluorescent signal was recorded for 20 min every 20 sec (λ_{Ex} 400 nm, λ_{Em} 440 nm) using a fluorescent microtiter plate reader.

2.13.1.4 pNCA activity assay

The pNCA activity assay (Schwaneberg et al., 1999a) was carried out in the same deepwell plates as used for the protein expression. The pellets were thaw and resuspended in 230 μ l pNCA-assay buffer (50 mM Tris-HCl / 50 mM phosphate buffer / 0.25 M KCl (1:1:1)). After addition of 5 μ l polymyxin B sulfate (3.6 mM), the plate was incubated for 20 min at RT, 1000 rpm (TIMIX 5 Shaker). The substrate pNCA (15 mM) 5 μ l and 5 μ l catalase (46 mg/ml) were added and the plate was incubated (RT, 1000 rpm, 5 min). The reaction was started by the addition of the electron donor, 50 μ l NADPH (1 mM) or in case of the MET, the mediator Cobalt(III)sepulchrates (8 μ l, 15 mM) was added, the plate briefly mixed and incubated (RT, 1000 rpm, 15 min) and then 5 mg Zn was added in each well using the Resin dispenser (Mettler-Toledo, Columbus OH, USA). The conversion was carried out at RT, 1000 rpm, for 60 min and stopped by adding 200 μ l NaOH (1 M). The plate was centrifuged (RT, 4000 rpm, 20 min) and 200 μ l of the supernatant was carefully transferred into a flat bottom MTP. The absorbance was measured at 405 nm with the MTP-spectrophotometer.

2.13.2 Flow cytometry screening systems

2.13.2.1 Whole cell flow cytometry screening system

Cell populations subjected to be analyzed by flow cytometry were expressed in flasks. Cells expressing the empty vector were used as negative control. After centrifugation of the culture (4000 rpm, 20 min, 4°C), cells were washed in PBS-buffer and the pellet was resuspended in sterile PBS-buffer (in 1/10 of the culture volume). Reaction mixture (300 μ l) contained 25 μ l

resuspended cells, 1 μl BCCE (200 mM in DMSO), PBS-buffer (0.03 M NaCl, 2.7 mM KCl, 0.01 M Na_2HPO_4 , 1.8 mM KH_2PO_4 , pH 7.4 adjusted with HCl) and was incubated 90 min. The reaction mixture was diluted 1:10 in PBS-buffer and filled in 3.5 ml analysis tubes (Sarstedt, Nümbrecht, Germany). The prepared cells were analyzed in a CyFlow Space flowcytometer (Partec, Münster, Germany) at a liquid flow-speed of 5 $\mu\text{l}/\text{min}$, using PBS-buffer as sheath fluid. Data of SSC, FSC and UV-laser emission (FL3: λ_{Ex} 350 nm and λ_{Em} 450 nm) were recorded. Sorting of desired populations occurred under size triggering and gating the UV-laser emission response with a trigger delay of 2, pulse of 10 and a sorting speed of 300-500 events/min. Sorted cells were collected, plated on LB_{kan} (50 $\mu\text{g}/\text{ml}$) agar plates and incubated overnight at 37°C. Enriching for active clones was achieved by washing the sorted and recovered colonies away from the agar plates and expressing the cells in flasks followed by another round of sorting.

2.13.2.2 Flow cytometry activity assay with w/o/w-emulsion

Cells subjected to analysis in water in oil in water emulsion (double emulsion) were prepared like described for flow cytometry assay with whole cells. The cell number was adjusted to $3 \times 10^8/\text{ml}$ by microscopic counting in a counting chamber. Emulsion mixture was prepared by mixing 80 μl of the cell suspension, 10 μl PMB (3.6 mM), 20 μl NADPH (10 mM) and 4 μl BCCE acid (200 mM), subsequent vortexing and keeping on ice. Instead of NADPH, 9 μl Co(III)-sep (15 mM) and 5 mg Zn-dust can be added. Optionally fluorescein (60 μM) or *EGFP* expressing cells can be added to primary emulsion mix as internal control dye to increase the analysis and sorting rate of true double emulsions (Blanusa, 2010a). 100 μl of the emulsion mixture were transferred in emulsion tubes (Nerbe plus, Luhe, Germany) and primary emulsions were prepared by addition of 1ml W1-emulsion solution (1.45 g ABIL EM 90 dissolved in 50 g LMO stored in the dark at RT) and emulsified 5 min at 10000 rpm with the Ultra Thurax on ice. The secondary emulsions were generated by addition directly on top of the primary emulsions of 1 ml W2-emulsion solution (0.6 g CMC and 0.8 ml tween 20 dissolved in 40 ml PBS, stored in the dark at RT) and the mixture was emulsified for 3 min at 8000 rpm on ice. Double emulsions were incubated 3 h in the dark. After 30 min, 1 h, 2 h and 3 h the emulsions were diluted 1:1000 with PBS buffer in analyzer tubes and were analyzed in a CyFlow Space flowcytometer (Partec, Münster, Germany) at a liquid flow-speed of 5 $\mu\text{l}/\text{min}$, using PBS-buffer as sheath fluid. Data of SSC, FSC and UV-laser emission (FL3: λ_{Ex} 350 nm and λ_{Em} 450 nm) were recorded. Sorting of desired populations occurred under size triggering and gating the UV-laser emission response with a trigger delay of 2, pulse of 10

and a sorting speed of 300-500 events/min. Sorted cells were collected, plated on LB_{kan} (50 µg/ml) agar plates and incubated overnight at 37°C.

2.13.3 Protein purification

P450 BM3 variants were purified according to published protocol (Schwaneberg et al., 1999b) by anion-exchange-chromatography using an ÄKTAprime plus pumping system (GE Healthcare, München, Germany) with a Kronlab ECOplus TAC 15/125PE5-AB-2 column (YMC Europe, Dinslaken, Germany) packed with Toyo Pearl 650 S-DEAE Sepharose Matrix (Tosoh bioscience, Tokyo, Japan). The column was washed with 5 column volumen (CV) ddH₂O and equilibrated with 5 CV buffer A (0.1 M Tris/HCl, pH 7.8) before loading the cell lysate. A flow rate of 5 ml/min was applied and all employed solutions were filtered and degassed. The crude cell lysate was injected after filtration through 0.45 µm filter (Carl Roth, Karlsruhe, Germany) into the 5 ml loop and loaded twice onto the column. Unbound protein was washed out with buffer A until the baseline was reached. Protein elution was performed in a stepwise gradient. Unspecific binding proteins were eluted with 150 mM NaCl equal to 7% buffer B (0.1 M Tris/HCl and 2 M NaCl, pH 7.8). The desired P450 protein was eluted with 13% of elution buffer B (260 mM NaCl) and fraction were collected. After elution, residual proteins were eluted with 100% buffer B (2 M NaCl) and the column was washed with ddH₂O, NaOH (0.2 M) and 20% ethanol, 5 CV each before storage.

The collected fractions were analyzed by SDS-PAGE (10%) for protein purity. Fractions containing the highest amount of pure P450 BM3 monooxygenase were recombined and concentrated using an Amicon Centrifugal Filter Units (30 kDa cut-off membrane; Millipore, Billerica, USA). Desalting of the purified BM3 variants was carried out using a PD-10 Desalting Column (GE Healthcare, Uppsala, Sweden) equilibrated in Tris/HCl buffer (0.1 M, pH 7.8). Protein solutions were frozen in liquid nitrogen before lyophilization for 48 h in a Christ ALPHA 1-2LD plus lyophilisator (Christ, Osterode am Harz, Germany).

2.13.4 Polyacrylamide gel electrophoresis (SDS-page)

Proteins were separated on 10% sodium dodecyl sulphat (SDS) (Laemmli, 1970) – polyacrylamide gel (24 mA, 90 min) in 1 x SDS-buffer (0.3% Tris, 1.5% Glycin, 0.1% SDS in H₂O, no pH adjustment) running in Mini-Protean Tetra Cell system from Bio-Rad (München, Germany). Resolving gel (5 ml) contained 1.9 ml ddH₂O, 1.7 ml 40% acrylamide-mix, 1.3 ml 1.5 M tris (pH 8.8), 0.05 ml 10% SDS, 0.05 ml 10% APS and 0.002 ml TEMED.

The gel was covered with isopropanol and after polymerisation, the isopropanol was removed and the stacking gel (1 ml) 0.68 ml ddH₂O, 0.17 ml 40% acrylamide-mix, 0.13 ml 1.0 M tris (pH 6.8), 0.01 ml 10% SDS, 0.01 ml 10% APS and 0.001 ml TEMED was casted. Samples were prepared by mixing with 1 x Roti-Load and heating at 95°C for 5 min. In each slot 4-10 µl sample or 2 µl marker (PageRuler Prestained Protein Ladder, Fermentas, St. Leon-Rot, Germany) were pipetted. For protein visualization, the gel was stained 20 min in staining solution (0.25% Coomassie, 45.5% methanol, 9.2% acetic acid, in H₂O) afterwards destained 1h in destaining solution (30% methanol, 10% acetic acid in H₂O) and stored in storage solution (8% methanol, 10% acetic acid, in H₂O) until the background was decolored.

2.13.5 Determination of P450 concentration by CO-gassing

The P450 concentration in solution was determined by carbonmonoxide (CO)-gassing (Omura and Sato, 1964a). The protein solution was diluted in KPI-buffer (50 mM, pH 7.5). After addition of one spatula sodiumhydrosulfit, the tube was vortexed and the solution splitted in two equal volumen. One part served as reference, the other was bubbled with CO-gas for 30 sec with low volumetric flow. The absorption spectrum from 400 to 600 nm of the reference and the sample was recorded with the spectrophotometer Varian Cary 50 and the P450 concentration was calculated according to the following formula (3) (Omura and Sato, 1964a, 1964b).

$$\text{P450 concentration [mM]} = \frac{(A_{450\text{nm}} - A_{500\text{nm}}) \times \text{dilution factor}}{\epsilon} \quad (3)$$

ϵ = extinction coefficient (for P450 = 91 mM⁻¹cm⁻¹)

2.13.6 Kinetic characterization of P450 BM3 variants

Kinetic parameters for BCCE

For kinetic characterization with BCCE a reaction mixture in a black flat bottom MTP contained: 196 µl tris/HCl-buffer (0.1 M, pH 7.8, 60-160 nM purified enzyme, 2 µl of BCCE and 5 µl catalase (12000 U/ml). Estimation of k_m and V_{max} were achieved by varying BCCE concentrations from 0 to 20 mM. The MTP was incubated for 5 min at 800 rpm, before reaction was started by addition of 50 µl NADPH (1 mM). For MET, the reaction was supplemented with 8 µl Co(III)-sep and incubated for 15 min at 800 rpm before the reaction

was started by transferring 100 μl of the reaction mixture in a black MTP containing 5 mg Zn-dust in each well. The fluorescent signal (λ_{Ex} 400 nm, λ_{Em} 440 nm) was recorded using an Infinite M1000 microtiter plate reader (Tecan Group, Männedorf, Switzerland). All measurements were done in triplicates. Concentration of the product was calculated from a standard curve obtained for 7-Hydroxy-3-Carboxy Coumarin Ethyl ester (3-CCE). Fitting of kinetic parameters was achieved using Origin 7.0 software (OriginLab Corporation, Northampton, MA, USA).

Kinetic parameters for pNCA

For kinetic characterization with pNCA a reaction mixture in a flat bottom MTP contained: 125 μl assay buffer (50 mM Tris-HCl / 50 mM phosphate buffer / 0.25 M KCl (1:1:1)), 60-160 nM purified enzyme, 5 μl of pNCA (in DMSO) and 5 μl catalase (12000 U/ml). Estimation of k_m and V_{max} were achieved by varying pNCA concentrations from 0 to 5 mM. The MTP was incubated for 5 min at 800 rpm, before reaction was started by addition of 50 μl NADPH (1 mM). For MET, the reaction was supplemented with 6 μl Co(III)-sep and incubated for 20 min at 800 rpm before the reaction was started by addition of 5 mg Zn-dust in each well with the Resin Dispenser. The MTP was incubated for 30 min at 600 rpm and RT. To stop the reaction 100 μl of 1M NaOH were added and the MTP was centrifuged at 4000 rpm for 5 min at RT. Carefully, 200 μl of supernatant were aspirated, pipetted into a new, flat bottom MTP and the absorbance at 405 nm was recorded using a microtiter plate reader. All measurements were done in triplicates. Concentration of the product was calculated from a standard curve obtained for p-nitrophenol. Fitting of kinetic parameters was achieved using Origin 7.0 software (OriginLab Corporation, Northampton, MA, USA).

2.14 Analytic and chemical methods

2.14.1 GC and GC-MS

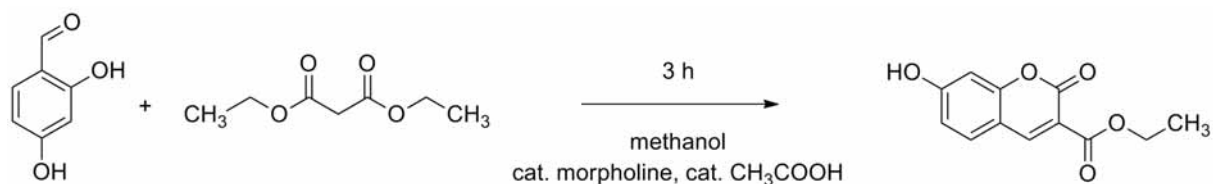
The enzymatic reaction mixture was extracted in 2 volumes chloroform and if necessary concentrated with rotavapor (IKA HB-10, VWR, Darmstadt, Germany) to obtain maximal 400 μl samples. Products were separated on GC-2010-plus (Shimadzu, Duisburg, Germany) and GCMS-QP2010S equipped with a Supreme 5 column (5% phenylpolysilphenylsiloxan) using hydrogen (GC-FID) and helium (GC-MS) as carrier gas at linear velocity of 30 cm/sec.

Column oven temperature program for separation of 3-phenoxytoluene products: 120°C for 1 min; 120°C to 250°C at 20°C min⁻¹; 250°C for 2 min. Peak identification occurred by comparison to pure standard and hydroxylation products were identified by their characteristic MS fragmentation patterns.

2.14.2 Substrate synthesis (Chilvers et al., 2001; Sun, 2008; Blanusa, 2010a)

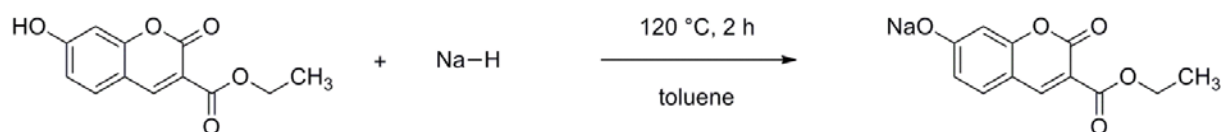
Step 1 – Synthesis of 3-carboxy-coumarin ethyl ester (3-CCE)

8.4 g (60.82 mmol) of 2,4-dihydroxybenzaldehyde was dissolved in 45 ml of anhydrous methanol. Solution was stirred and 8.7 g (54.32 mmol) of diethyl malonate was supplemented and refluxed. 450 mg (5.16 mmol) of morpholin and 150 mg (2.49 mmol) of acetic acid were supplemented to 2 ml of methanol and stirred until the precipitate fully dissolved. This solution was subsequently transferred to the refluxed reaction mixture and reflux was continued for another 3 hours. After cooling, the product was filtered and re-crystallized from boiling methanol (~300 ml).



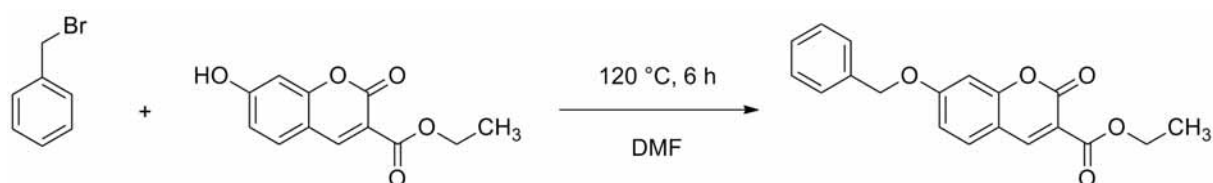
Step 2 – Preparation of sodium salt 3-carboxy-coumarin

For this step, 1.5 g (6.81 mmol) of 3-CC ethyl ester were dissolved in toluene (50 ml), stirred and heated (120°C) and concentrated by evaporation to 5 ml (30-60 min). After cooling the mixture to room temperature, 0.5 g (10.84 mmol) of NaH was supplemented. The mixture was heated to 120°C and stirred until toluene evaporated (1-2 hours). The obtained salt was dried in vacuum overnight.



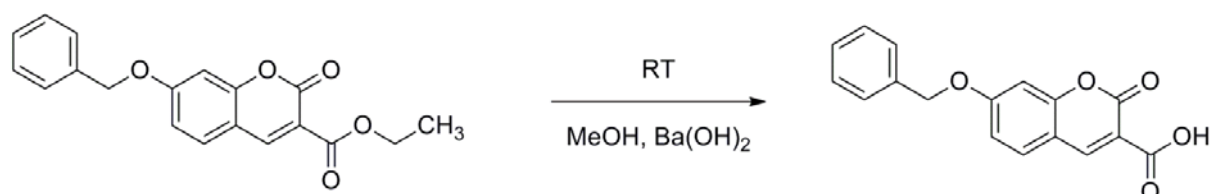
Step 3 – Attaching benzyl group to 3-CC ethyl ester

3 g (12.39 mmol) of prepared 3-CC methyl ester sodium salt was dissolved in 200 ml DMF (dried with molecular sieves). Mixture was heated to 120°C. During heating, 2.138 g (12.5 mmol) of benzyl bromide was supplemented. Mixture was stirred gently and kept at 120°C for 2 hours. One g of benzyl bromide (5.85 mmol) was supplemented and conversion continued at 120 °C for 4-6 hours and the same procedure was repeated once more (supplementing of 0.7 g, 4.09 mmol benzyl bromide; 1 h 120°C). Subsequently the reaction mixture was cooled to room temperature and poured into 400 ml of ice cold water. After precipitation (30-60 min), the suspension was filtered, rinsed with water, dried and re-dissolved in CH₂Cl₂. The organic phase was extracted twice with water, filtered, concentrated (Rotavap) and the precipitate was dried overnight in vacuum. The targeted compounds were purified by chromatography employing silica gel (DC60). Sample was dissolved in CH₂Cl₂ and elution was performed with an ethyl acetate : CH₂Cl₂ (1:20) mixture. Purity was monitored on TLC using same solvent system and main fractions were pooled according to TLC. ¹³C-NMR and ¹H-NMR spectra were recorded using a Bruker AV400 (Bruker, Madison, WI, USA).



Step 4 – Preparation of BCC-acid

A mixture of BCCE (18.2 mg, 58 μmol) and barium hydroxide octahydrate (powdered, 7.35g, 23.4 mmol) in MeOH (8 ml) was stirred at room temperature for 24 h. The heavy white suspension was diluted with brine (3ml) and acidified with 1M HCl to give a clear solution of pH 3-4. This aqueous solution was extracted with EtOAc (2x50 ml +1x20 ml) and the combined organic extracts washed with brine (10 ml) and three times with H₂O until no white precipitate was formed, dried (MgSO₄) and concentrated (Rotavap). (Inoue and Sakai, 1977; Paterson et al., 1995; Kociński, 2005)



7-Hydroxy-3-Carboxy-Coumarin Ethyl ester (3-CCE): $^1\text{H NMR}$ (400 MHz, DMSO) δ 1.29 (*t*, 3H, $J = 7.2$ Hz, CH_3); 4.26 (*q*, 2H, $J = 7.2$ Hz, CH_2); 6.73 (*s*, 1H, ArH); 6.84 (*d*, 1H, $J = 8.5$ Hz, ArH); 7.75 (*d*, 1H, $J = 8.8$ Hz, ArH); 8.67 (*s*, 1H, ArH) ppm. $^{13}\text{C NMR}$ (400 MHz, DMSO) δ 14.09, 60.76, 101.75, 110.39, 112.09, 113.95, 132.06, 149.38, 156.35, 157.06, 162.90, 164.01 ppm.

7-Benzoxy-3-Carboxy-Coumarin Ethyl ester (BCCE): $^1\text{H NMR}$ (400 MHz, CDCl_3) δ 1.32 (*t*, 3H, $J = 7.0$ Hz, CH_3); 4.31 (*q*, 2H, $J = 7.0$ Hz, CH_2); 5.07 (*s*, 2H, CH_2); 6.80 (*d*, 1H, $J = 8.7$ Hz, ArH); 7.38-7.17 (*m*, 5H, Ph-Ring); 7.42 (*d*, 1H, $J = 8.7$ Hz, ArH); 8.41 (*s*, 1H, ArH) ppm. $^{13}\text{C NMR}$ (400 MHz, CDCl_3) δ 13.26, 60.69, 69.75, 100.34, 110.77, 113.20, 113.22, 125.33, 126.45, 126.46, 127.54, 127.81, 129.72, 134.28, 147.89, 156.11, 156.42, 162.39, 163.13 ppm.

3. Results and Discussions

The results and discussions section is divided in three chapters. The main focus of this thesis was the methodological advancements in diversity generation (SeSaM method) and high throughput screening (flow cytometer based screening technology), which was complemented by the evolution of P450 BM3 for alternative cofactor systems. Directed protein evolution experiments consist of the three main steps performed in iterative cycles. Each step of the directed evolution method was advanced and is considered in one chapter. In Chapter I, the advancement of Step 1 consisting of generation of high quality mutant libraries is reported. Step 1 was advanced by developing an advanced SeSaM protocol, in which a universal base complementary to the P-base was employed to generate more diverse libraries. In Chapter II, Step 2 was advanced by generating a whole cell high throughput screening system for monooxygenases allowing efficiently to sample the diversity generated in Step 1. Subsequently, the advanced protocols suitable for the directed evolution methods were applied to evolve P450 BM3 for alternative cofactor systems in iterative rounds (Step 3), reported in Chapter III.

Chapter I: Advancement of SeSaM

Methods to generate random mutant libraries in directed evolution are limited in functional diversity generation. The Sequence Saturation Mutagenesis (SeSaM) method was reported as a four step random mutagenesis method overcoming the limitations of epPCR based random mutagenesis methods (Wong et al., 2004b). SeSaM targets in contrast to epPCR each nucleotide “equally” avoiding mutagenic hot spots, achieving subsequent mutations in a codon (up to 37%) (Mundhada et al., 2011), and allowing to adjust mutational biases through employed universal bases (Wong et al., 2004b, 2005a; Mundhada et al., 2011).

The advancement of the SeSaM method was investigated in two approaches. In section 2.1, an advanced SeSaM method is reported in which a protocol was developed and optimized for implementing the R (ribavirin) base in a SeSaM experiment. The R based protocol was afterwards combined with the original P base SeSaM protocol. Combining P and R base allows in SeSaM experiments to generate transversions at all four nucleotides of a given sequence with an unmatched chemical diversity. Subsequently, in section I.2, Step 2 should be further optimized by the use of a blocked base to allow the control of the number of added bases by the TDT.

I.1 dRTP and dPTP a complementary nucleotide couple for the Sequence Saturation Mutagenesis (SeSaM) method¹

In this chapter, an advanced SeSaM method in which a protocol for implementing the R base in a SeSaM experiment was developed and optimized is report (Fig. 14). The R-based protocol was subsequently combined with the P base for generating for the first time transversions at all four nucleotides in a combined protocol.

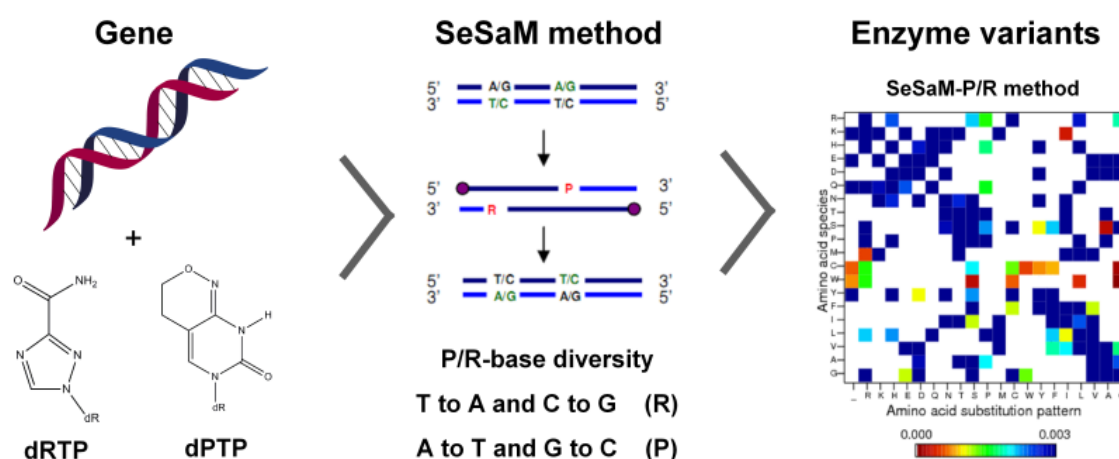


Fig. 14: Graphical abstract summarizing the work performed in Chapter II, section 2.1: IdRTP and dPTP a complementary nucleotide couple for the Sequence Saturation Mutagenesis (SeSaM) method.

The results section is divided into four parts. In the first part, preliminary experiments were performed to evaluate the applicability of dRTP in the SeSaM method. In Step 1 cleavage positions for subsequent chemical fragmentation are generated by PCR through incorporation of phosphorothioated bases. Optimized steps comprise Step 2 (incorporation of dRTP), Step 3 (polymerase for R-base elongation), and Step 4 (polymerase for amplification) of the SeSaM method. In the second part, an optimized dRTP-SeSaM protocol was validated by generating a GFP mutant library. In the third part the P- and R-libraries were combined in Step 3 to maximize transversions. In the fourth part, a MAP analysis for the diversity generated by SeSaM-R, SeSaM-P and SeSaM-P/R is performed (<http://map.jacobs-university.de> (Wong et al., 2006)).

¹ Results partially published: Anna Joëlle Ruff, Jan Marienhagen, Rajni Verma, Danilo Roccatano, Hans-Gottfried Genieser, Percy Niemann, Amol V. Shivange, Ulrich Schwaneberg, dRTP and dPTP a complementary nucleotide couple for the Sequence Saturation Mutagenesis (SeSaM) method, 2012, Journal of Molecular Catalysis B: Enzymatic

1.1 SeSaM Step 2 optimization of dRTP incorporation

Requirement for an application of ribavarin in the SeSaM method is the acceptance of the nucleotide dRTP by TdT. The TdT catalyzed incorporation of dRTP at 3'-OH of a 5'-FITC-labeled oligonucleotide served as model experiments to determine conditions leading an effective incorporation of dRTP by TdT into ssDNA fragments in libraries. The number of incorporated R-nucleotides can be visualized and quantified on an acrylamide gel analysis (see Experimental Procedures). The acrylamide gel (36%; Fig. 15) shows the 5'-FITC-oligonucleotide and each step in the ladder represents the addition of one R-nucleotide. The stepwise incorporation proves that TdT accepts dRTP well. Fig. 15 shows up to four distinct bands which represent the addition of up to four R bases.

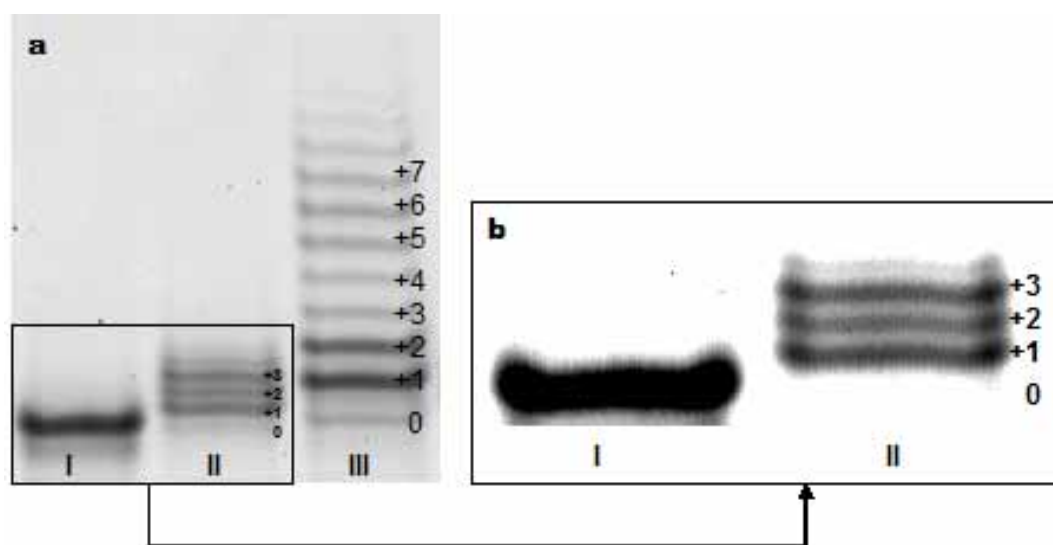


Fig. 15: a) Phosphorimager analysis of 3'-tailed FITC-oligonucleotides, separated on 36% polyacrylamide gels. Lane I, FITC only (control), lane II FITC with TdT catalyzed addition of dRTP (ratio of dRTP to template-DNA of 1:5), lane III FITC with TdT catalyzed addition of dPTP α S. b) Quantification of TdT catalyzed stepwise (+1, +2, +3) incorporation of dRTP in a fluorescent (FITC) labeled oligonucleotide. Panel B, shows an enlargement of Fig. 15 panel A Lane II, to allow better visualization of distinct bands. The incorporated nucleotides are marked with the corresponding number of stepwise addition (from 0 to +7).

The quantification of the bands was performed with the AIDA software for image analysis. dRTP is incorporated by TdT much faster compared to dPTP which shortens the incubation time from 120 min (dPTP) to 15 min (dRTP) (Fig. 15: lane III, indicates the dPTP incorporation under the suitable conditions). In addition, the CoCl₂ concentration was elevated from 0.05 mM to 0.25 mM and the TdT concentration was reduced from 1.6 U μ l⁻¹ to 0.4 U μ l⁻¹ (total volume 25 μ l). In contrast to other unnatural bases, the number of added R-bases can be adjusted by varying the molar ratio between template-DNA and dRTP (Fig. 15; lane II) For an efficient random mutagenesis, the dRTP incorporation conditions should be adjusted to up to three dRTP nucleotides to ensure efficient elongation in Step 3. Additionally polymerases were previously reported to elongate fragments with subsequent dPTP

inefficiently (Mundhada et al., 2011). Fig. 15 panel B, shows an enlargement of Fig. 15 Lane II, to allow better visualization of distinct bands. A template-DNA to dRTP ratio of 1:5 leads to the addition of two to three R-bases (Fig. 15; lane II) compared to the 5'-FITC-oligonucleotide without addition (Fig. 15; Lane I).

1.2 SeSaM Step 3 optimization: Polymerases for elongating R-tails

Fig. 13 (experiment 2 and 3) (see section 2.12.1) shows the detection system used to investigate the abilities of polymerases to elongate ssDNA fragments by dRTP incorporation. In total, ten polymerases (Taq, Vent, Deep Vent(exo-), Vent(exo-), DyNAzyme EXT, 9°NM, Phusion High-Fidelity, AmpliTaq, AmpliTaq Stoffel Fragment, 3D1) were selected based on proof-reading, amplification of “difficult” templates-DNA (GC rich) and experiences from dPTP amplification (Wong et al., 2008; Mundhada et al., 2011). Five polymerases (Taq, Deep Vent (exo-), Vent(exo-), DyNAzyme EXT, 3D1) could elongate oligonucleotides tailed with one R-base independently from the nucleotide in the opposite strand (Fig. 16, a) and Two polymerase were not able (Fig. 16, b). Three polymerases (Vent, 9°NM, Phusion High-Fidelity) were able to elongate the fragments tailed with three consecutive R-bases to a full length gene (Fig. 16, c). The elongation efficiency was high, but sequencing results showed that an A-base was incorporated at all three R positions. Incorporation of A at R-base positions has for instance been reported for RNA-polymerases (Vo et al., 2003).

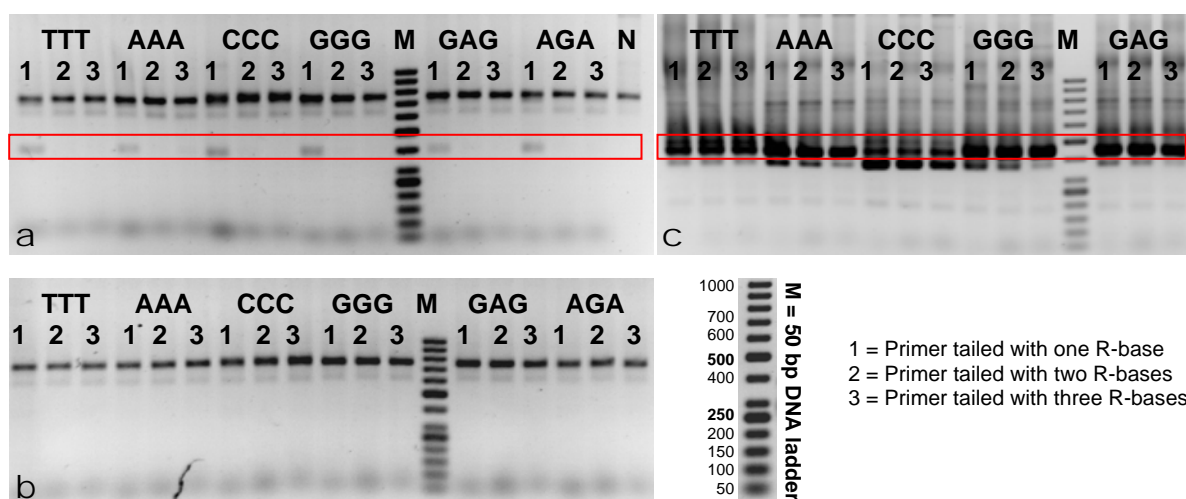


Fig. 16: Gel electrophoresis of the PCR Products generated in the Read activity assay (Fig. 13; in Material and Methods section 2.12.1). a) DyNAzyme EXT polymerase, b) AmpliTaq polymerase, c) Phusion High-Fidelity. DNA-templates (AAA, GGG, CCC, TTT, GAG, AGA) of 720 bp and generated PCR products of 460 bp (indicated by the red frame). N= negative control, PCR reactions without primers.

Exonuclease activity for R-tailed oligonucleotides was confirmed by incubating R-tailed oligonucleotides under PCR condition in absence of dNTPs. On acrylamid gels the truncation

of the primer could be observed (Fig. 17 b, lane 3). The R-tailed primers were monitored on acrylamide gels to verify the purity of the synthesized primers and to confirm the attachments of only one, two or the presence of three R-bases (Fig. 17 a). The two polymerases (3D1 and Vent (exo-)) were finally selected for Step 3 of the SeSaM-R method since both were able to elongate R-tailed oligonucleotides fragments to full length genes efficiently and lack an exonuclease activity.

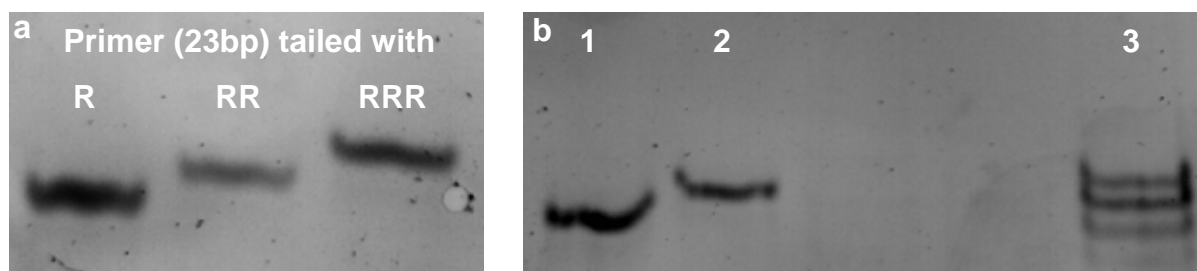


Fig. 17: Polyacrylamid gels of R-base tailed nucleotides. a) Primer of 23 bp tailed at the 3'-end with R, RR or RRR. b) Exonuclease activity check for R-tailed oligonucleotides, Lane 1: Primer tailed with one R-base, Lane 2: Primer tailed with two R-Bases, Lane 3: Primer tailed with three R-bases after treatment with Vent polymerase under PCR conditions (36% polyacrylamid gels stained with Ethidiumbromid).

1.3. SeSaM Step 4 optimization: Polymerases for nucleotide incorporation opposite of the R-base

In Step 4, the R-bases were replaced by a standard nucleotide in the complementary DNA strand during PCR amplification (Mundhada et al., 2011). The latter, as “write” termed polymerase activity (see 2.12.1 Material and Methods) enables through PCR a product formation which allows selecting polymerases capable of replacing R by a standard oligonucleotide. All employed polymerases, except AmpliTaq Stoffel Fragment, were able to efficiently replace the incorporated R-base by unmodified nucleotides and Taq polymerase was the most efficient one (Fig. 18). Deep Vent could also be used yielded a lower amount of PCR products than Taq. For Taq polymerases the ratio of incorporated T and C was determined to be ~1.5 to 1 after sequencing of 30 randomly selected clones.

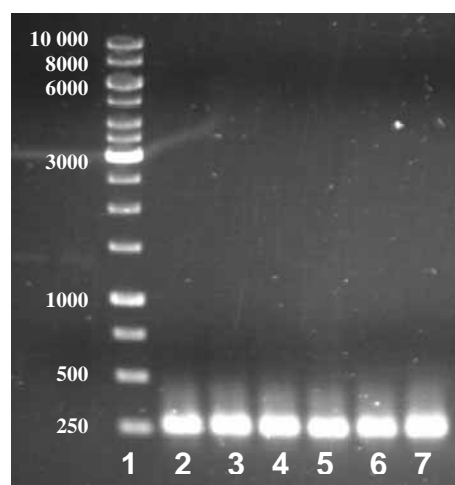


Fig. 18: PCR product of 250 bp generate in the write activity assay and used for cloning and sequencing analysis (see Fig. 13;5 in section 2.12.1). Lane 1: 1 kDa DNA Ladder in bp; Lane 2-7: templates used in the read activity assay to elongate primers tailed with one R-base, respectively: AAA, TTT, CCC, GGG, GAG, AGA.

1.4 SeSaM-R method of *EGFP*

Five SeSaM-R libraries of *EGFP* were generated by targeting T and C bases. The five *EGFP* libraries differ in the polymerase employed in Step 3, (Vent (exo-), three libraries; and 3D1, two libraries) and the molar ratio of template-DNA to dRTP (1:5, 1:10 and 1:20 Vent (exo-); 1:10 and 1:20 3D1). SeSaM libraries with 3D1-polymerase revealed a high fraction of unmodified template-DNA (45%; 20 sequenced clones), a notable number of deletions (15%; 20 sequenced clones) and transversions (31%). Statistical analysis on mutations generated by dRTP incorporation in Step 2 was performed by sequencing 29 clones of Vent (exo-) libraries with varied molar ratios of DNA *EGFP* fragment library to dRTP (1:5; 1:10; 1:20). The molar ratio of 1:5 (DNA *EGFP* fragment library to dRTP; 10 sequenced clones) yielded for random mutant library generation the preferred results in terms of transversions, deletions, and PCR yields. Table S3 (Appendix 6.2.) contains the sequencing results of the 29 clones and Fig. 19a shows the obtained amino acid substitution. Only 1 clone had a frameshift mutation and no deletion or subsequent mutation could be observed in any clone. The fraction of non-mutated *EGFP* was 27% (8 clones) and 45% of the mutations were transversions. The total number of mutations in 29 clones was 33 (1.13 mutations per gene; see Table S3 in Appendix 6.2.).

1.5 SeSaM-P/R method

In the SeSaM-P/R protocol, the P- and R-base libraries are combined in Step 3 to generate transversions at all four nucleotides for increasing chemical diversity. Out of 55 clones sequenced, only 3 (5.4%) were non-mutated and 12.7% (7 clones) contained frameshifts or deletions. Seven clones (12.7%) had consecutive nucleotide exchanges and 49.5% of all mutations were transversions. A total number of 113 mutations with an average of 2.05 mutations per gene was obtained (Table S3, Appendix 6.2.). 13.2% of the amino acid substitutions that are unobtainable by a standard epPCR-method (see Fig. 19b).

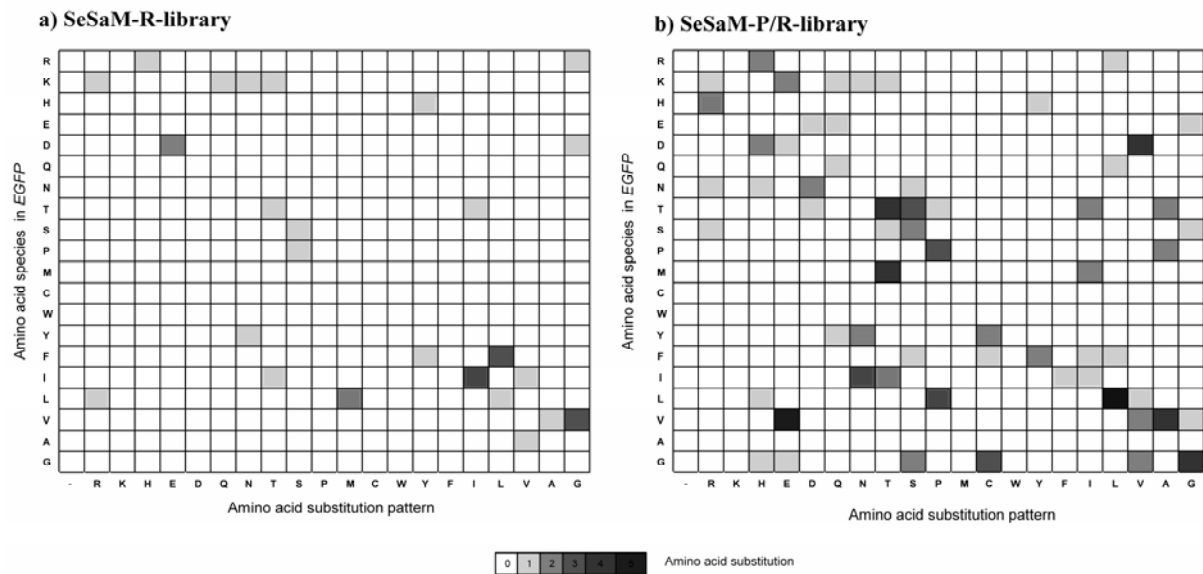


Fig. 19: a) Obtained amino acid substitution patterns of *EGFP*, generated by the SeSaM-R method (colored fields) calculated with MAP based on the mutational biased determined by sequencing of 29 randomly picked clones. b) Obtained amino acid substitution patterns of *EGFP*, generated by SeSaM-P/R method (colored fields) calculated with MAP based on the mutational biased determined by sequencing of 55 randomly picked clones. The Y-axis shows the original amino acid species and the X-axis shows the substitution patterns. The substitution patterns for 20 amino acid species is indicated from light gray (lowest probability) to dark gray (highest probability). Amino acid substitutions that do not occur are colored in white.

An additional important performance parameter of random mutagenesis methods is the distribution of mutations over the targeted gene. In contrast to the previously reported distribution (Wong et al., 2004b), a more homogenous distribution of the mutations could be achieved in the SeSaM-P/R method, especially at the last third of the EGFP gene (Fig. 20).

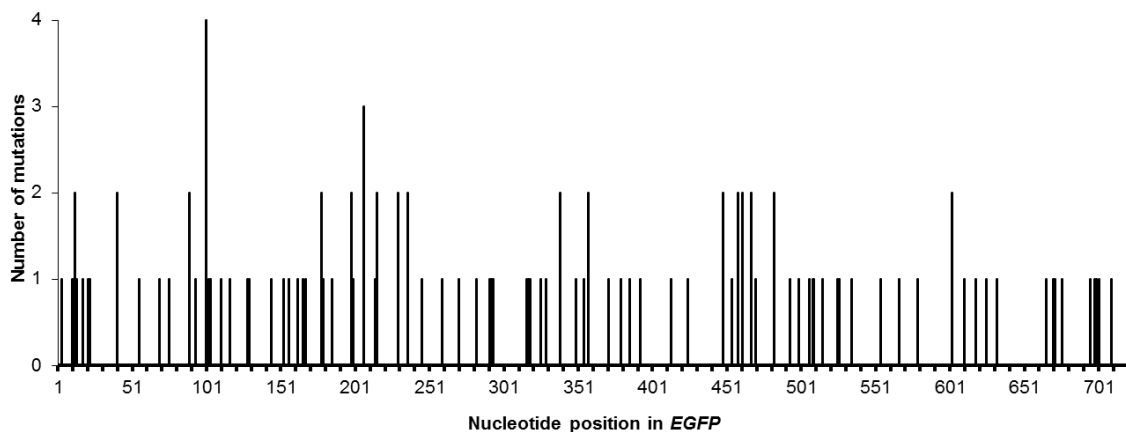


Fig. 20: Distribution of the mutations generated by the SeSaM-P/R method for *EGFP*.

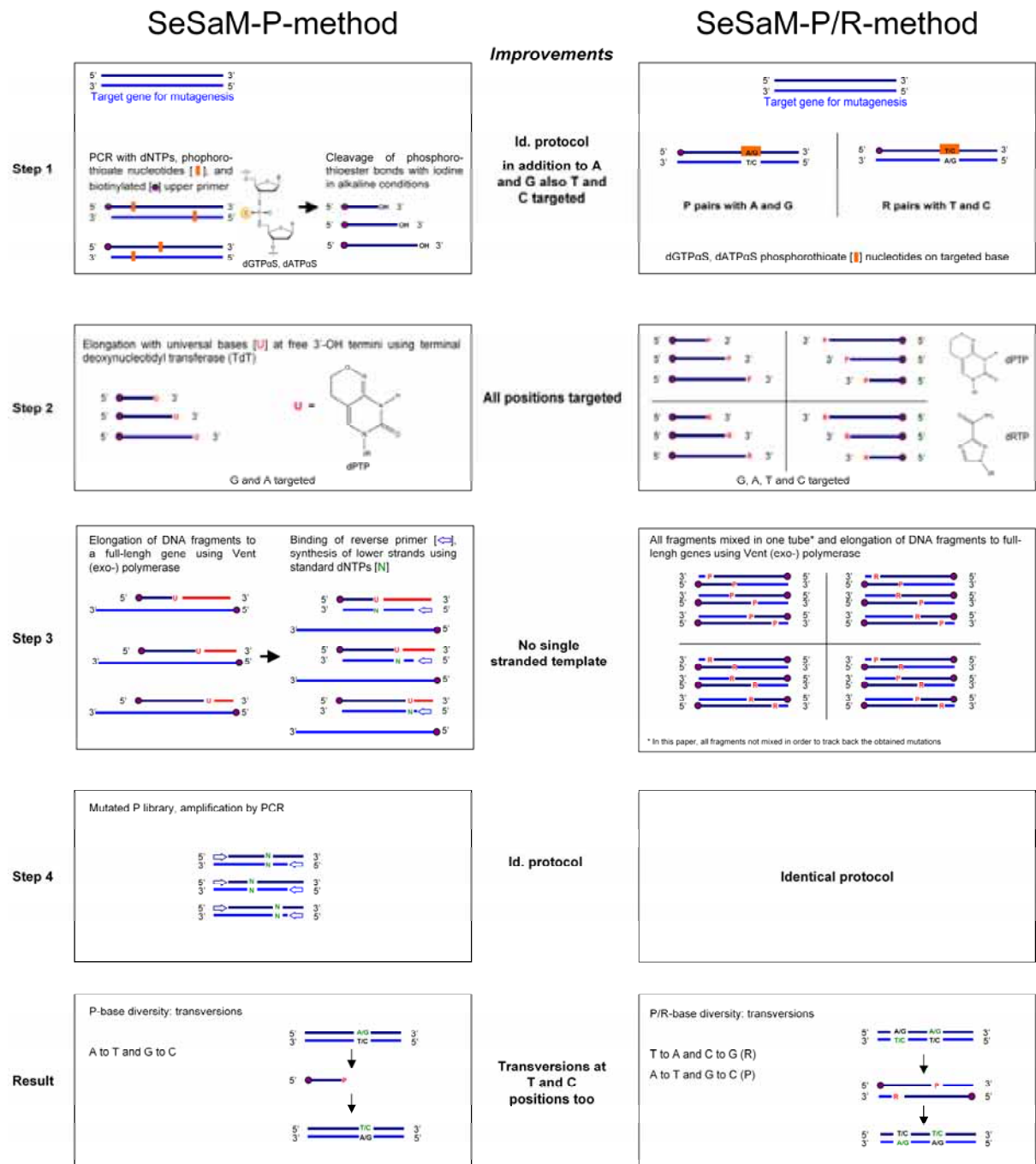


Fig. 21: Scheme of the SeSaM method. Underlying differences and advancements between previous protocols (left column) and the SeSaM-P/R method (right column). SeSaM includes 4 steps: Step 1: A ssDNA fragment pool with random length is generated by PCR-amplification with random incorporation of nucleotides with phosphorothioate cleavable bonds. Step 2: The ssDNA fragments are tailed by a terminal transferase catalyzed reaction with a universal base. Step 3: These tailed fragments are elongated by PCR amplification to full length genes. Step 4: Replacement of the universal bases by standard nucleotides through PCR leading to mutant libraries with randomly distributed mutations.

1.6 MAP analysis of amino acid substitution patterns for SeSaM-R and SeSaM-P/R

Fig. 22 shows the amino acid substitution patterns calculated by MAP for the mutation biased determined by sequencing of randomly selected clones in the mutant libraries of SeSaM-P (100 clones), SeSaM-R (29 clones) and SeSaM-P/R (55 clones). Fig. 22 shows on the Y-axis for all naturally occurring 20 amino acids in the *EGFP* wild-type and obtainable amino acid substitution patterns (X-axis). The deepening in color represents the probability of amino acid substitution which occurs in general at different amino acid positions. Amino acid substitution that do not occur are colored in white. Substitutions colored in orange or red are practically unobtainable in directed evolution experiments by screening a few thousands clones.

Comparison of Fig. 22a and Fig. 22b shows that both differ significantly in their amino acid substitution patterns. The SeSaM-P/R protocol in which both degenerated bases are employed represents from the determined mutational bias that P- and R-substitutions are balanced represented in the combined protocol despite a highly modified protocol (Fig. 21). Since as basis for calculation the determined mutational biases of randomly picked clones is used one could observe a few differences in the amino acid substitution patterns (R → P, E → V, N → Y, W → S, G → A).

Comparison of the mutational spectra obtained from random library (Fig. 22a, 22b, and 22c) pointed out that the amino acid exchange from hydrophobic to charged and charged to charged amino acid is higher in the SeSaM-R method compared to SeSaM-P method.

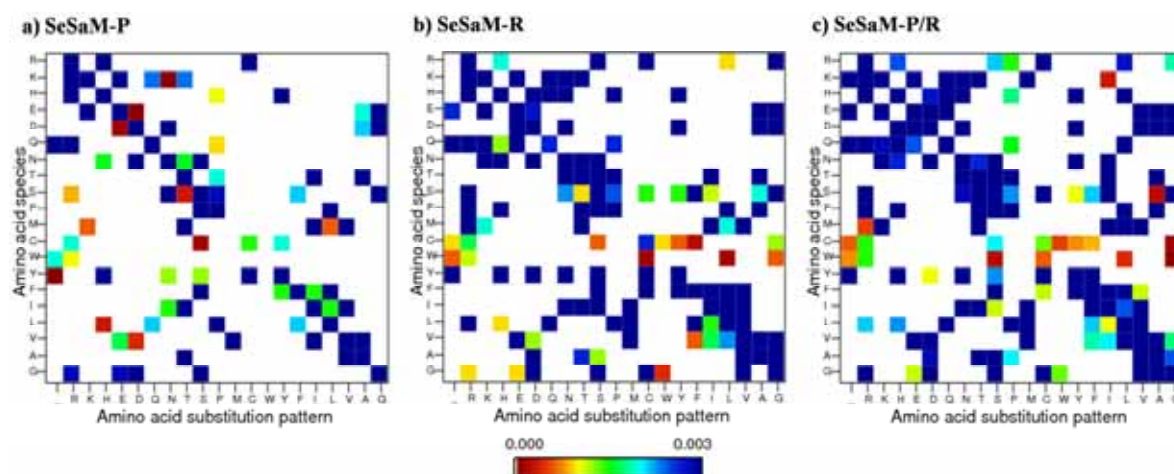


Fig. 22²: Amino acid substitution patterns for *EGFP* calculated by MAP server. a) SeSaM-P method, b) SeSaM-R method and c) SeSaM-P/R method. Y-axis shows 20 amino acids that occur in the *EGFP* wild-type. For the MAP-calculation the experimental determined bias from 55 sequenced clones (SeSaM-P/R) and 29 sequenced clones (SeSaM-R) of *EGFP* was employed. Each of the 20 amino acids is shown as one “specie” which takes into account all codons encoding the same amino acid. These codons are subjected to three random mutagenesis method (SeSaM-P, SeSaM-R and SeSaM-P/R) and the X-axis shows the obtainable substitution patterns for each amino acid “specie”. It should be noted that on a single codon level not all shown substitutions are obtainable since an average each amino acid specie is encoded by ~3 different codons. Amino acid substitutions that do not occur are colored in white.

² MAP analysis generated by Prof. Dr. D. Roccatano and Rajni Verma (Jacobs University Bremen)

Substitutions from charged to hydrophobic amino acid are not possible or occur with low probability in even the R or P method but occurs with high probability in the SeSaM-P/R method. Additionally, substitution from aliphatic to aromatic (I → F) was possible with SeSaM-P/R method suggesting the mutational spectra obtained using both bases (P/R) is more diverse compared to using a single universal base in the SeSaM method.

1.7 Discussion

The SeSaM random mutagenesis method was developed to overcome the main three limitations of PCR based random mutagenesis methods which are commonly employed in directed evolution experiments. EpPCR based methods produce mainly transitions (A → G and T → C) and few transversions (Cadwell and Joyce, 1992). A transition bias has a significantly lower chemical diversity on the protein level than a transversion bias (Wong et al., 2007b). Additionally, epPCR based methods lack subsequent mutations due to low mutation frequencies mutating therefore statistically only one nucleotide of a codon. The latter reduces the obtainable amino acid substitutions dramatically (Tee and Schwaneberg, 2007). SeSaM targets each nucleotide “equally” and therefore avoids mutagenic hot spots. The diversity generation is independent from employed DNA-polymerases (Wong et al., 2004b) and control over mutational bias is achieved in the SeSaM method through application of universal bases (Wong et al., 2005a). Increasing the fraction of transversions was identified as an attractive goal to improve the chemical diversity of random mutant libraries (Wong et al., 2008; Mundhada et al., 2011) and to produce amino acid substitution patterns which are complementary to those of epPCR methods. The P-base offered to introduce a transversion bias at A and G bases of a gene and the reported R-base complements the transversion bias of the P-base by introducing transversions exclusively at T and C bases (see Introduction section 1.3.). EpPCR methods are often transition biased which limits the chemical diversity on the protein level due to the organization of the genetic code and single mutations of epPCR methods in a codon substitute for instance hydrophobic amino acids preferentially by hydrophobic amino acids (Wong et al., 2007a). SeSaM-Tv-II (Mundhada et al., 2011), in the current manuscript referred to SeSaM-P, incorporates transversions (66.2% of transversions at A- and G-nucleotide positions (Mundhada et al., 2011)). Fig. 21 (right) shows the advancements obtained by employing the universal base R to introduce transversions at T and C positions and to incorporate the SeSaM-R protocol to a novel SeSaM-P/R protocol. Advancements in Step 1 and 2 led to more diverse fragmentations patterns, in Step 3 the single stranded template-DNA is omitted and diversity is increased due to parallel

employment of the P- and R-base. *EGFP* was used as model gene to ensure that the results of the developed advanced SeSaM protocols were comparable to previous reports (Wong et al., 2004b; Mundhada et al., 2011).

In detail, in Step 1 the SeSaM-P/R method is improved compared to SeSaM-P by addressing all four nucleotides and not only A and G nucleotides (Fig. 21). As a consequence the fragment library should ideally contain all possible fragment sizes of *EGFP* and not only cleaved fragments at A and G positions. In Step 3, the preparatory step of a single stranded template-DNA, to elongate the fragment library of Step 2 to the full length gene, could be omitted. The latter is achieved through generation of a forward and reverse library with complementary strands. Being able to generate fragments from the 5-prime end and the 3-prime end doubles the mutation frequency (1.1 SeSaM-R; 2.1 SeSaM-P/R) which can further be adjusted within the purification steps (Wong et al., 2008). This can be attributed to annealing of complementary forward and reverse strands both harboring for instance a universal base (Step 3). The latter can be observed for example at nucleotide position 34, which is replaced by different nucleotides in the clones numbered 5, 13, 15, and 22 (Table S3, Appendix 6.2.). Exchange of the same nucleotide position to different nucleotides was not observed in SeSaM-P or SeSaM-R mutant libraries. Notably, the distribution of the mutations within *EGFP* remained homogenous in the SeSaM-P/R method (Fig. 20).

Comparison of key performance parameters of SeSaM-P, SeSaM-R and SeSaM-P/R

Table 1 summarizes the key performance parameters of SeSaM-P, SeSaM-R and SeSaM-P/R. A comparison of the SeSaM-P (targeting A- and G-nt) to the SeSaM-R (targeting T- and C-nt) shows that the employed Vent (exo-) can generate 27.7% subsequent mutations at P-base positions whereas no subsequent mutation could be obtained in the SeSaM-R library. Therefore, achieving subsequent mutations with the R-base represents a main target to increase the diversity in SeSaM-P/R further. In addition, the ratio of Ts to Tv is nearly doubled in the P-library when compared to the R-library (0.51 for SeSaM-P and 1.2 SeSaM-R; Table 1). Varying the R-base concentration, altering the number of PCR cycles in Step 3 and Step 4, and investigating two polymerases (3D1 & Vent (exo-)) did not reduce the Ts/Tv ratio below 1.2. SeSaM-P/R has a balanced transition to transversion ratio of 1.0 which is in between the ratios of SeSaM-R and SeSaM-P. Fig. 22 shows the main advantages of the SeSaM-P/R which lie in the complementary amino acid substitutions patterns of SeSaM-P and SeSaM-R. In the diverse SeSaM-P/R protocol (Table 1), the ratio of unmutated DNA is reduced compared to SeSaM-R and SeSaM-P, the mutation frequency is nearly doubled and

the ratio of unobtainable substitution by epPCR is increased. The fraction of transitions (50.5%) remains however significant in the SeSaM-P/R method. The latter can likely be attributed to the employed polymerases (3D1, Vent (exo-), Taq in Step 3 and 4) which lack or have a “low” proof reading activity.

Table 1: Key performance parameters of SeSaM-P, SeSaM-R and SeSaM-P/R

Aspect	SeSaM-P _a	SeSaM-R	SeSaM-P/R
Universal base	P	R	P and R
Fragment library generation at nucleotide positions	A/G	T/C	A/G/T/C
Universal base (bias)	1.6 : 1	1.5 : 1	-
Distribution of mutations	Homogeneous	Homogeneous	Homogeneous
Single stranded template required in Step 3	YES	YES	NO
Deletions(%) - frameshifts (%) - Unmutated DNA(%)	0 - 0 - 20	0 - 3.4 - 27	0 - 12.7 - 5.4
Fraction Ts to Tv _b (bias indicator)	0.51	1.2	1.0
Mutations frequency (substitution / base)	1.37×10^{-3}	1.57×10^{-3}	2.8×10^{-3}
Fraction of consecutive mutations in sequenced clones (%)	27.7	0	12.7
Unobtainable amino acid substitutions by epPCR _c	7.2	3.0	13.2

^a Ref.:(Mundhada et al., 2011)

^b Ts = transition, Tv = transversion

^c Does not take into account the probability of each mutations. In other words the stated fraction can be regarded as a “minimal” difference.

Decisive for researchers performing directed evolution experiments is the benefit that the SeSaM methods provide over epPCR methods. EpPCR methods have been very successful in improving enzyme properties despite their limited chemical diversity (Bershtein and Tawfik, 2008). Fig. 22 compares the amino acid substitutions that are obtainable by SeSaM-P, SeSaM-R and SeSaM-P/R. It is important to note that amino acid substitutions with low probability (orange; red) are included despite that they are practically not found in directed evolution experiments in which a few thousand variants are screened. Differences in the amino acid substitutions are therefore higher than the values shown in Table 1 for “unobtainable amino acid” substitutions. In addition, the SeSaM protocols allow in contrast to epPCR to generate subsets of mutations for instance by only targeting A positions with a bias that excludes stop codons or targets only GC positions to AT mutations to reduce the GC content in GC rich genes.

A transition biased method might especially be beneficial for enzyme properties that require subtle chemically changes in amino acid substitutions. The amino acid exchanges as a result of a transition biased random mutagenesis method are limited in their chemical diversity (e.g. hydrophobic to hydrophobic residues). The latter might be beneficial for improving

“localized” enzyme properties such as activity, selectivity, or specificity, which require often subtle changes. Enzyme properties like solubility, stability (thermal resistance or pH resistance) can however likely be improved more efficiently by transversions, which lead to chemically more diverse amino acid substitutions (e.g. hydrophobic to charged) (Wong et al., 2007a).

1.8 Conclusions

SeSaM-P/R allows for the first time to introduce at all four nucleotides transversion mutations which are homogeneously distributed over the targeted gene and which mutate in an ideal case each nucleotide of a gene. Advancements compared to SeSaM-P lie in the more diverse fragmentations patterns, omitting the use of template-DNA (Step 3), doubling the mutation frequency, and chemical diversity due to parallel employment of the P- and R-base.

The SeSaM-P/R method nearly doubles the number of by epPCR unobtainable amino acid substitutions (Table 1) when compared to previous SeSaM methods. Transversions cause amino acid substitutions that are naturally not or barely occurring leading to chemically diverse amino acids substitution patterns. The latter mutational bias might become beneficial for protein reengineering challenges such as improving solubility of proteins in water, increasing thermal resistance or stability in organic solvents.

I.2 Advancement of the SeSaM method including nucleotide analogs

In the SeSaM method, a crucial step is the elongation of single stranded DNA fragments by TdT (Terminal transferase) with a universal base in Step 2 (see section 1.3 and I.1 for description of the main steps of the SeSaM method). When more than one base is incorporated by TdT the polymerases in Step 3 are not anymore able to elongate the “tailed” fragments. This leads to a high ratio of non mutated template in the mutant libraries and reduces or prevents the introduction of consecutive mutations. Therefore, the application of modified bases by protection groups to control and limit the number of added bases in Step 2 of the SeSaM method was investigated.

2.1 Nucleotide analogs with chemical cleavable blocks

A blocked base is a deoxyribonucleotide modified at 3' position of the sugar backbone by attaching a chemically cleavable block (Vaghefi, 2005). Different modified bases were synthesized by BIOLOG and the enzymatic additions by TdT were investigated in this thesis. A key step is the selection a suitable protection group as functional “chemical block”, because the catalysis mechanisms of the TdT is highly conserved and restricted by the 3' end of the base (Beabealashvili et al., 1986; Delarue et al., 2002). If modification occurs at the base, the TdT might not be able to elongate the fragments anymore. In Fig. 23 an overview of the synthesized and tested bases is given. To simplify investigations BIOLOG synthesized blocked dATP (instead of blocked universal bases P or R), which can be used as model base and should make no difference in the experimental setup or in the evaluation of the TdT performance. In principle, the addition of only one base is expected, if the concept of the chemical cleavable block is successful. After the enzymatic elongation by TdT the reaction mixture is treated with a de-blocking solution ensuring removal of the chemical block under mild conditions without damaging of DNA. After purification these fragments should be elongated once more using TdT in a second reaction to generate fragments in which the number of bases can be determined by the number of repeated elongation cycles. The necessary purification after de-blocking allows the elongation by the polymerase in step 3 of the SeSaM method. The experimental setup is described in section 2.12.1, the same FITC-labeled oligonucleotide (P15, Table S1, Appendix 6.1) was used.

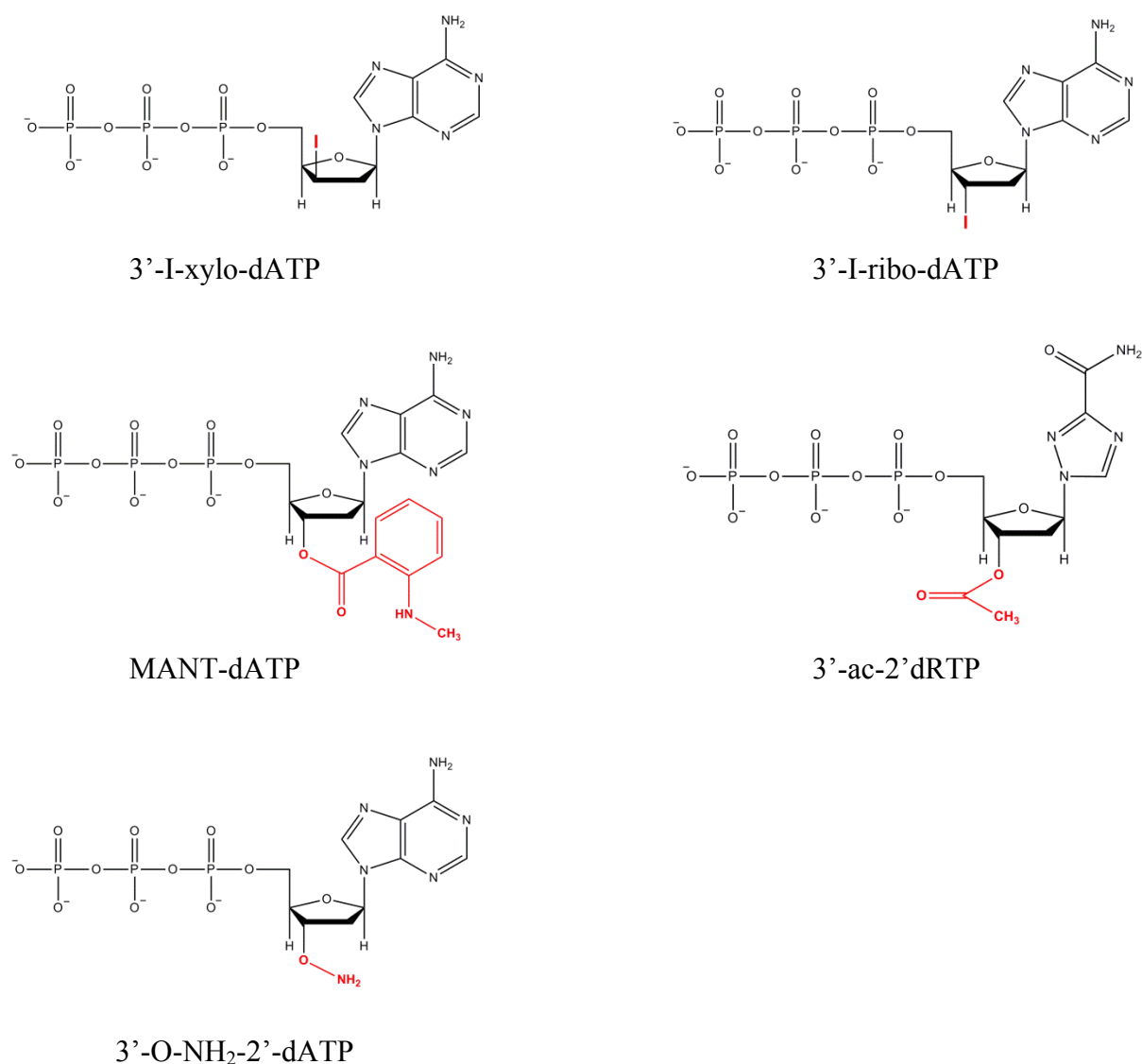


Fig. 23: Overview of the by BIOLOG synthesized blocked bases. Deoxyribonucleotides with chemically cleavable blocks attached on the 3' position.

2.1.1 MANT-dATP and 3'-ac-2'dRTP

Previously, the MANT-dATP and the 3'-ac-2'dRTP were investigated in several experimental setups. The attached chemical blocks were not a hindrance for the TdT and the fragments were elongated by several bases (see Fig. 26: lane 5, similar results were obtained). The condition to obtain the addition of only one base could not be achieved.

2.1.2 3'-I-dATP

In contrary, the third analyzed base 3'-I-dATP (2',3'-dideoxy-3'-iodo- β -D-xylofuranosyl-adenine-5'-O-triphosphate) could not be added (Fig. 24: lane 3-6) by TdT. The addition of the two possible conformations (3'-I-xylo and the 3'-I-ribo-dATP) by TdT was investigated, differing by the attachment of the iodine to the sugar backbone (Fig. 23). Several reaction parameters were modified, the concentration of TdT (0.4 U/ μ l to 1.6 U/ μ l), the CoCl₂ concentration (0-0.5 mM), the incubation time (increased from 15 min to 180 min), and finally the concentration of the base was varied between 2.4 μ M and 360 μ M. However, all attempts remained unsuccessful. Fig. 24 shows the obtained result of one of the analyzed conditions; all further results are similar (gels not shown). No band above the fluorescent labeled oligonucleotide could be observed, concluding that the TdT is not able to elongate fragments with the 3'-I blocked bases.

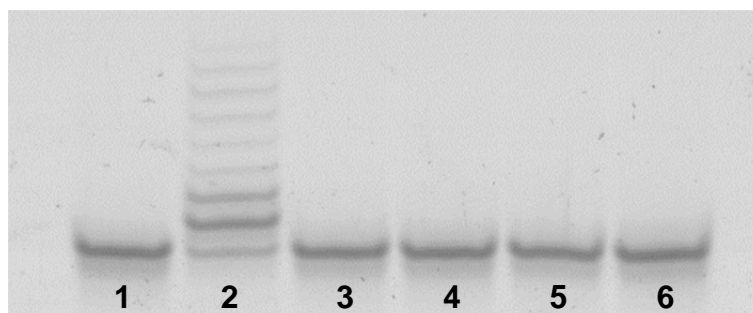


Fig. 24: Terminal transferase (TdT) catalyzed 3'-tailing with the blocked base 8-xylo-dATP. A 5'-fluorescein-labeled oligonucleotide served as model DNA fragment to visualize the 3'-tailing with a phosphoimager (lane 1). Reaction mixtures were separated on acrylamid gels (36%). Lane 2: dPTP α as positive control, lane 3-6: 8-xylo-dATP at different concentrations.

2.1.3 3'-O-NH₂-2'-dATP

The fourth investigated blocked base was 3'-O-NH₂-2'-dATP. In preliminary experiments the addition to a fluorescent labeled oligonucleotide by TdT was performed under the same condition as used for the R- and P-base. Fig. 25 shows the addition of the blocked base at different concentrations (12 to 96 μ M) on a 36 % acrylamide gel. At low concentrations (12 μ M) no addition could be observed, but with increasing concentration a narrow band appears with increasing intensity. This leads to the deduction that the base was added by the TdT, but the current conditions were not optimal.

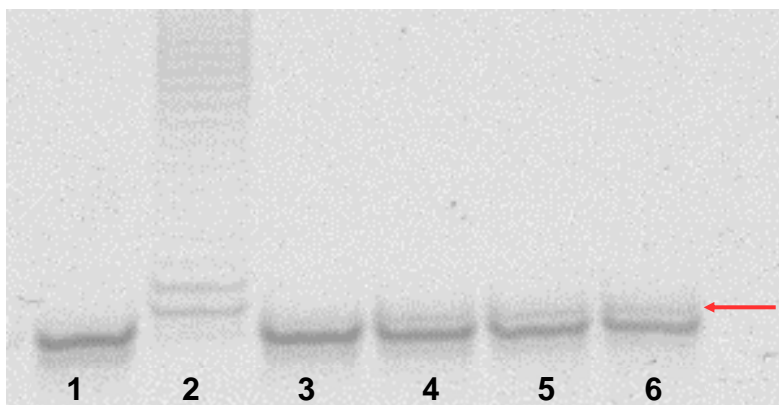


Fig. 25: Terminal transferase (TdT) catalyzed 3'-tailing with the blocked base 3'-O-NH₂-2'-dATP at different concentrations visualized on acrylamid gels (36 %). Lane 1: fluorescent labeled oligonucleotide, lane 2: dPTP α as positive control, lane 3 to 6: 3'-O-NH₂-2'-dATP at different concentrations, respectively 12 μ M, 24 μ M, 48 μ M, 96 μ M. The red arrow indicates the band which appears by addition of one base.

The experimental setup was repeated with addition of CoCl₂ (0.25 mM), increasing the amount of TdT (from 0.4 to 1.6 U/ μ l) and the elongation time (from 15 min to 180 min) (Fig. 26). Increasing the amount of TdT and the elongation time improved significantly the addition of more than one 3'-O-NH₂-2'-dATP. Fig. 26 shows several bands appearing above the FITC labeled oligonucleotide. Each stair of the ladder corresponds to the addition of one base. The amount of remaining template is still important. It might be that the base gets deblocked by the CoCl₂ and for this reason can be added by TdT. The efficiency of base addition can be estimated by the number of added bases under identical conditions. In Fig. 26 (lane 2, reaction with dPTP α S) single bands cannot be identified, a diffuse smear shows the addition of many bases under the modified reaction conditions (increased amount of TdT and incubation time), whereas the reaction condition were suitable for the blocked base. Thus, incorporation of dPTP α S is more efficient than of blocked bases. When comparing the elongation of dPTP α S to dATP, dATP incorporation is even more efficient, underlying the clear-cut inefficiency of the blocked base elongation.

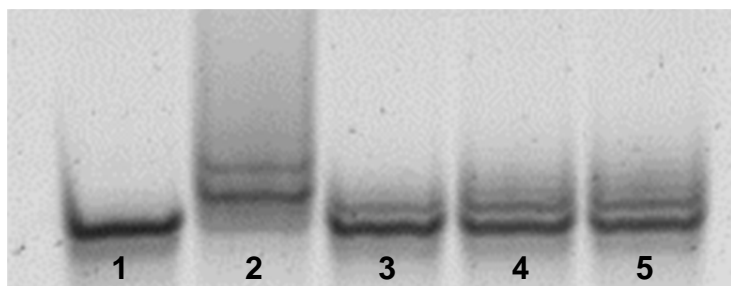


Fig. 26: Terminal transferase (TdT) catalyzed 3'-tailing with the blocked base 3'-O-NH₂-2'-dATP visualized on acrylamid gels (36 %). Lane 1: fluorescent labeled oligonucleotide, lane 2: dPTP α as positive control, lane 3 to 5: 3'-O-NH₂-2'-dATP at different concentrations, respectively 48 μ M, 144 μ M, and 240 μ M.

The same experimental setup was repeated without addition of CoCl_2 (Fig. 27: lane 2 and 5) and with addition of Na-acetate (Fig. 27: lane 3 and 4). Na-acetate and Na-nitrite solution (1 M Na-acetate and 0.7 M Na-nitrite) are used for de-blocking of the base. The processivity of the TdT was slightly reduced in the absence of CoCl_2 and drastically by the addition of 1 M Na-acetate. As control, the addition of unmodified dATP was performed. (Fig. 27: lane 4 with addition of Na-acetate, lane 2 without addition). Only after long incubation times (>120 min) fine bands appeared (similar to Fig. 27). Most likely, the long incubation time or due to buffer components of the TdT the base gets partially de-blocked and allows the addition by TdT. Another explanation might be that the TdT is able to elongate the base but very inefficiently compared to unblocked dATP and dRTP. Furthermore, the de-blocking method is not applicable since the inhibition of the TdT activity is problematic for later applications in the SeSaM method. A supplementary step to remove the de-blocking reagent is necessary. Under the same reaction conditions, dATP is easily elongated by TdT (Fig. 27: lane 2) but only few additions were observed after supplementing Na-acetate to the reaction (Fig. 27: lane 4). No dRTP elongation (Fig. 27: lane 3) could be observed in presence of Na-acetate compared to unmodified reaction parameters, at which 2-3 bases additions were obtained (Fig. 27: lane 5).

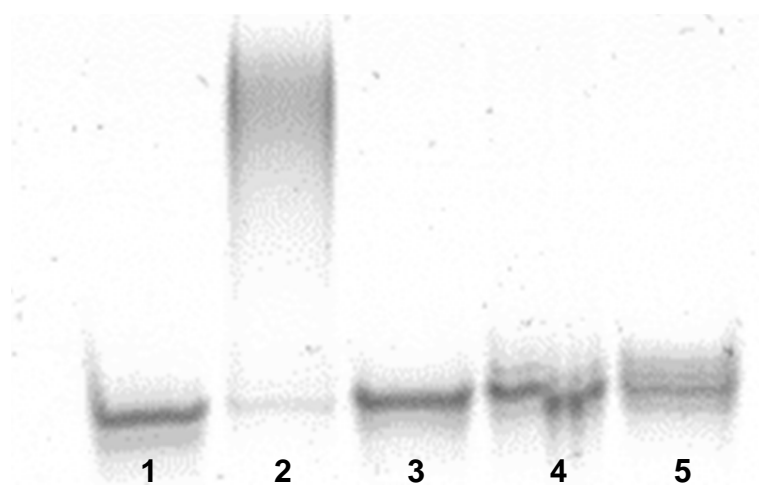


Fig. 27: Terminal transferase (TdT) catalyzed 3'-tailing with the blocked base 3'-O-NH₂-2'-dATP with addition of Na-acetate visualized on acrylamide gels (36 %). Lane 1: fluorescent labeled oligonucleotide, lane 2: dATP as positive control, lane 3: dRTP with addition of Na-acetate; lane 4: dATP with addition of Na-acetate; lane 5: dRTP.

Nevertheless, the de-blocking procedure was applied and the addition of a second base after purification was investigated. The experimental setup included several controls:

1. Addition of the base without modification of the reaction parameters and without addition.
2. Addition of the de-blocking solution.

3. Addition of the de-blocking solution before purification followed by a second elongation by TdT.
4. Addition of the de-blocking solution after purification followed by a second elongation by TdT.
5. Second elongation by TdT without any modification of the sample after first elongation.

In all samples, the elongation by TdT was not observed after addition of de-blocking solution. Even without treatment no second addition could be observed. The ratio in the purified sample of elongated fragments is very low compared to the amount of non-elongated. Additionally, the purification of the reaction mixture after TdT elongation had a very low yield after supplementing the de-blocking solution.

2.2 Discussion

The application of a blocked base in the SeSaM method was the basic concept to control and limit the number of added bases in Step 2. Four employed nucleotide analogs (3'-O-NH₂-2'-dATP, 3'-I-dATP, MANT-dATP and 3'-ac-2'dRTP) which were modified on the 3' position of the sugar backbone by the attachment of chemical cleavable blocks with different properties were probed for acceptance by the TdT.

The MANT and the acetyl modification on the base were not a hindrance for the TdT, several nucleotides could be added to the FITC-labeled oligonucleotide. The hydrogen bond formation which is crucial for the TdT reaction was present (Beabealashvili et al., 1986; Delarue et al., 2002).

The use of an iodine as cleavable block leads to no incorporation of the nucleotide analog. An explanation might be the impossibility of forming essential hydrogen bonds or the decreased flexibility in the binding site of the TdT. Looking at the structure of the TdT in presence of 3'-I-dATP, a sterical clash between the iodine on the 3' position of the sugar backbone and a α -helice of the TdT catalytic center was observed (Fig. 28).

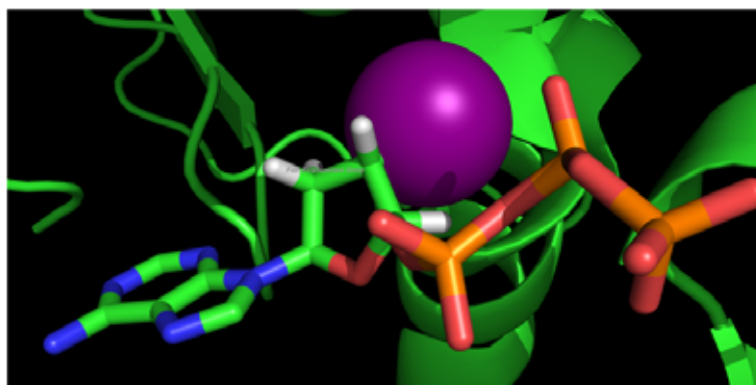


Fig. 28: Structure of TdT with I-dATP in the active center. Lila ball displays the I on the 3' position of the sugar backbone.

The incorporation of 3'-ac-2'dRTP was observed, but with very low efficiencies compared to the usually used bases dATP and dPTP. When CoCl_2 was present in the reaction, the addition of several bases was shown. In addition, only one base addition and no increase of the incorporated amount over time could be observed without the addition of CoCl_2 . Leading to the conclusion that CoCl_2 removed the cleavable block allowing the incorporation of the base (Chang and Bollum, 1990). Similar, the nucleotide analogs probably contains some impurities, as well as remaining unmodified dATP which can get incorporated and represents the band observed on the acrylamide gel. Nevertheless, the de-blocking procedure was tried and led to several problems, the recovery after purification was very low and the second enzymatic reaction could not be performed because remaining de-blocking solution was inhibiting the TdT. The recovered amount of elongated fragments after purification was too low for an application in SeSaM. The nucleotide amounts necessary to perform a qualitative SeSaM library are commonly 100 fold higher (200 ng).

2.3 Conclusions

The application in the SeSaM method of modified base on the 3' position of the sugar backbone through protection groups to control and limit the number of added bases in Step 2 was investigated. The concept of subsequently attached bases by adding one blocked base by TdT, followed by de-blocking and incorporation of a second base and a second de-blocking was not applicable for the SeSaM method. Further investigations on selected blocked base, de-blocking and purification of products from the TdT catalyzed elongation reaction are required to improve the yield and to proof a single base addition in each performed step.

Chapter II: Flow cytometry based screening system for P450 BM3

The availability of reliable and efficient pre-screening systems is the main limitation to identify beneficial variants in diverse mutant libraries. To accelerate the evolution of P450 BM3, a flow cytometry based screening system was developed. In this chapter, in the first part the whole cell assay based on the conversion of a coumarin derivative is described. Furthermore, to provide high throughput screening systems for the alternative cofactor systems, a flow cytometer assay based for mediated electron transfer was investigated in the second part.

II.1 High throughput screening system for accelerated directed evolution of P450 monooxygenases³

In this chapter, the first whole cell ultra-high throughput screening systems for P450 monooxygenases employing a flow cytometer allowing efficient sorting and enrichment of active variants from random mutant libraries with a throughput of 500 events per second is reported. The developed flow cytometry screening system does not require double emulsions for sorting since the converted fluorogenic substrate 7-Benzoyloxy-3-Carboxy-Coumarin Ethyl ester (BCCE) is retained within the *E. coli* BL21(DE3) Gold expression host. The ethyl ester is cleaved to the corresponding carboxylic acid in *E. coli* which cannot due to its negative charge penetrate easily by diffusion through *E. coli* membranes in contrast to the corresponding ester (Kanaya et al., 1998; Henne et al., 2000). The monooxygenase P450 BM3 (CYP102A1) (variant F87A) (Schwaneberg et al., 1999a) was selected for development of the screening system as model monooxygenase due to its industrial attractiveness and broad substrate profile (Appel et al., 2001; Tee and Schwaneberg, 2007; Whitehouse et al., 2012).

1.1 Assay development and proof of principle

BCCE was synthesized (see section 2.14.2 Material and Methods) and fluorescence was recorded upon hydroxylation (see Fig. 29) via O-dealkylation, as previously described for 7-benzoyloxy-trifluoromethyl coumarin by Cheng *et al.* using P450 3A4 (Cheng et al., 2009).

³ Reprinted (adapted) with permission from Anna Joëlle Ruff, Alexander Dennig, Georgette Wirtz, Milan Blanus, Ulrich Schwaneberg, Flow cytometer-based high throughput screening system for accelerated directed evolution of P450 monooxygenases, 2012, ACS-Catalysis 2, 2724-2728. Copyright 2012 American Chemical Society.

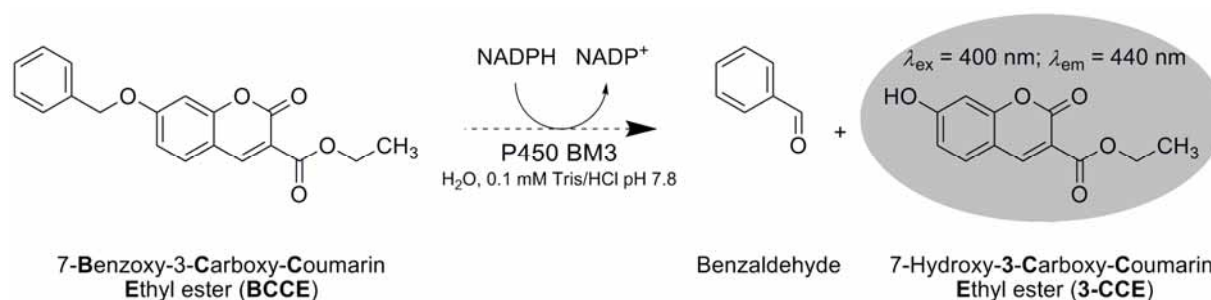


Fig. 29: Scheme of the 7-Benzoxo-3-Carboxy-Coumarin Ethyl ester (BCCE) conversion catalysed by P450 BM3 variants (Ruff et al., 2012b).

The flow cytometry screening system was developed in two steps. In the first step the variant P450 BM3 F87A was employed in investigating the signal to noise ratio in crude cell extracts and in a whole cell flow cytometry setup. In the second step the mutant P450 BM3 M3 DM (R47F F87A M354S D363H R471C N543S) was randomly mutated (epPCR) and sorted to identify more active variants. The mutant M3 DM was evolved for improved electron transfer via mediators starting from the reported variant P450 BM3 M3 (R47F F87A M354S D363H). (Nazor and Schwaneberg, 2006; Nazor et al., 2008). The flow cytometry based BCCE screening system was used as pre-screen to sort out the most active variants and enrich the population of active P450 BM3 variants. The sorted variants were subsequently screened in a 96-well microtiter plate to identify P450 BM3 variants with higher activity towards hydroxylation of BCCE (Tab. 2) and to validate the developed BCCE-flow cytometer screening system.

Table 2: Kinetic characterization of P450 variants converting 7-Benzoxo-3-Carboxy-Coumarin Ethyl ester. Novel substitutions in the parent P450 BM3 M3 DM are highlighted as bold letters.

Variant	k_{cat} ^[a]	K_m [μM]	K_{eff} ^[b]
P450 BM3 M3 DM (R471C N543S) ^[c]	0.07 ± 0.005	25.2 ± 4.2	0.17
P450 BM3 M3 DM-1 (R255H)	0.48 ± 0.05	25.3 ± 5.5	1.14
P450 BM3 M3 DM-2 (R203H I401V F423L)	0.24 ± 0.01	34.3 ± 3.4	0.42

[a] [mmol product s⁻¹ mmol⁻¹ P450]; [b] Catalytic efficiency in [min⁻¹ μM⁻¹]; [c] Starting variant P450 BM3 M3 DM = P450 BM3 M3 (Nazor et al., 2008) + N543S R471C

BCCE conversion of P450 BM3 variants displayed a detectable fluorescence (λ_{Ex} 400 nm and λ_{Em} 440 nm) and the control samples (pET28a(+)/lacking P450 BM3 gene) (Fig. 30A) revealed a low noise-to-signal ratio in MTP. No fluorescence could be detected for *E. coli* cells harboring the pET28a(+) vector without the P450 BM3 gene. Fig. 31 shows a control population lacking P450 BM3 F87A (left) and a population expressing P450 BM3 F87A in *E.*

coli (right). The flow cytometer analysis illustrates that both populations can clearly be distinguished (Fig. 31; fluorescence intensity and distribution) and yielded a final signal-to-noise ratio of ~10:1 (Fig. 31; λ_{Ex} 350 nm and λ_{Em} 450 nm).

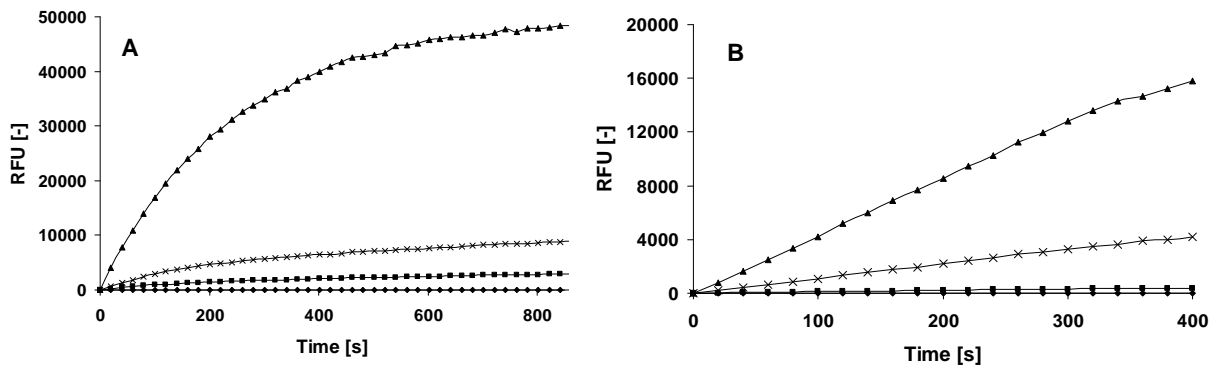


Fig. 30: Conversion over time of BCCE using cell free lysates with adjusted protein concentration by CO titration (Omura and Sato, 1964a, 1964b) (A) and whole cells (B). pET28a(+) (◆) as background signal, variant P450 BM3 M3 DM (R47F F87A M354S D363H R471C N543S) (■) and the obtained mutant P450 BM3 M3 DM-2 (x) (R47F F87A M354S D363H R471C N543S R203H I401V F423L) and P450 BM3 M3 DM-1 (▲) (R47F F87A M354S D363H R471C N543S R255H). Novel substitutions in bold and fluorescent signals were measured in a 96-well microtiter plate reader.

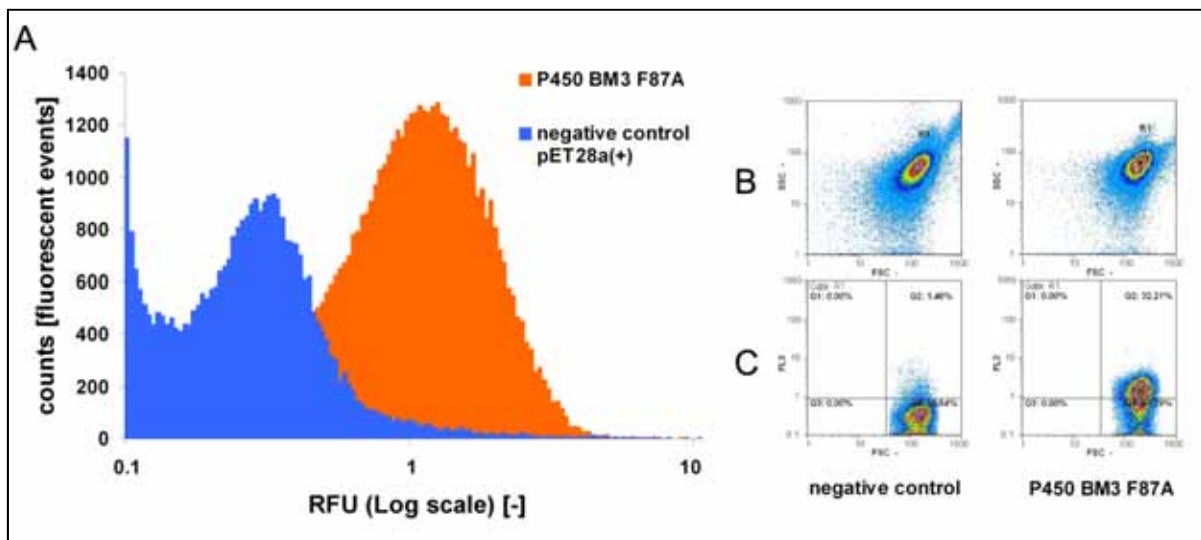


Fig. 31: Overlay of the emitted fluorescence from two different cell populations (A; flow cytometer analysis: blue cells representing the negative control (E. coli BL21 (DE3) Gold & empty vector pET28a(+)) and in orange: E. coli BL21 (DE3) Gold cells expressing active P450 BM3 F87A). B: flow cytometer analysis after conversion of BCCE with P450 BM3 F87A expressing E. coli BL21 (DE3) Gold cells and pET28a(+) harboring E. coli BL21 (DE3) Gold cells (as negative control). R1 (C) shows the gated population; Side scatter (SSC; log₃ scale), Forward scatter (FSC; log₃ scale) and UV-laser (FL3: λ_{Ex} 350 nm and λ_{Em} 450 nm; log₄ scale) were recorded. (Ruff et al., 2012b).

Additionally, a whole cell conversion of BCCE by P450 BM3 F87A in *E. coli* (5×10^6 cells/ μ l) was visualized and microscopic analysis proved entrapment of the coumarin derivate in *E. coli* (Fig. 32). Fig. 30A shows that conversion in crude cell extracts follows the same trend as in whole cells for the variants DM, DM-1 and DM-2 (Fig. 30B).

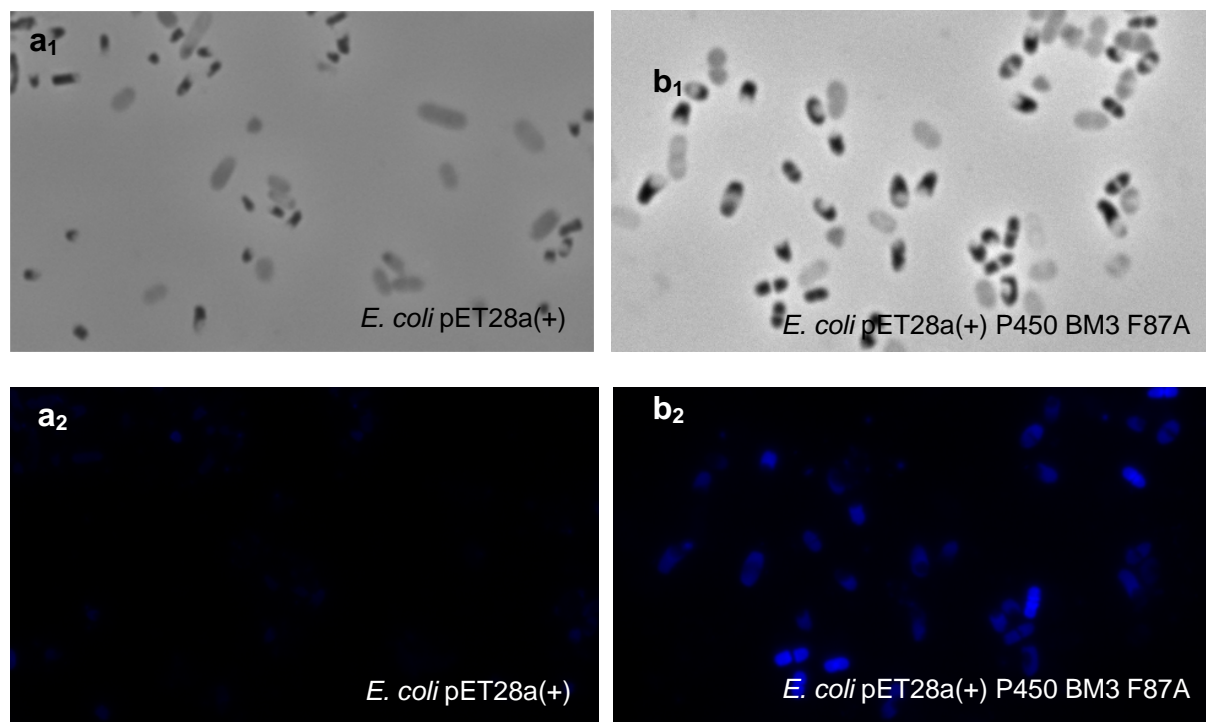


Fig. 32: Light microscopy (a1, b1) and fluorescence microscopy (a2, b2) of *E. coli* cells after incubation with BCCE. Figures show results using an empty pET28a(+) vector (a1, a2) and a pET28a(+) vector expressing P450 BM3 F87A (b1, b2). Fluorescence could be observed in P450 BM3 F87A expressing cells whereas in the negative control only a low background fluorescence was observed (Ruff et al., 2012b).

For further evaluation mixed populations consisting of varied ratios of active (P450 BM3 F87A) to inactive population (pET28a(+) without P450 gene) were merged (ratios of 9:1 and 1:1) and sorted (threshold >50-fold pET28a(+) RFU). After sorting of both mixed populations, cells were plated without further concentration on LB_{kan}-agar plates and incubated overnight (37°C). 60 clones were picked and investigated for BCCE conversion in 96 well microtiter plates. Ratio 9:1 yielded 100 % of active population and ratio 1:1 resulted in an increase from 50 to 82 % of active variants after only one round of sorting. This demonstrates that the BCCE based flow cytometry screening system can efficiently enrich the population of active variants and thereby fulfills requirements postulated for high throughput screening systems (Bernath et al., 2004a; Bershtein and Tawfik, 2008). As a final proof, error-prone PCR libraries (0.05 mM, 0.1 mM, 0.2 mM MnCl₂) were generated based on the P450 BM3 M3 DM variant (R47F F87A M354S D363H R471C N543S). The P450 M3 DM library ($\sim 10^4$ variants) was sorted and enriched three times. After each round of enrichment the percentage of active clones was determined by measuring the BCCE-activity of 90 clones in a

96 well MTP. After the third enrichment, 600 clones were picked, expressed and subjected to activity measurements in MTP employing BCCE as substrate. The “true” standard deviation of P450 BM3 activity in 96 well MTP format was determined to be 10 % ensuring a reliable detection of improved variants (Wong et al., 2005b). Around 8 % of the re-screened variants displayed increased P450 monooxygenase activity for BCCE when compared to the starting variant P450 BM3 M3 DM. The three most active variants were sequenced and two turned out to have identical substitutions (P450 BM3 M3 DM-1 & P450 BM3 M3 DM-3: R255H, P450 BM3 M3 DM-2: R203H I401V F423L). Variants P450 BM3 M3 DM-1 and P450 BM3 M3 DM-2 were purified and finally used for kinetic characterizations applying varying concentrations of BCCE as shown in Figure 33.

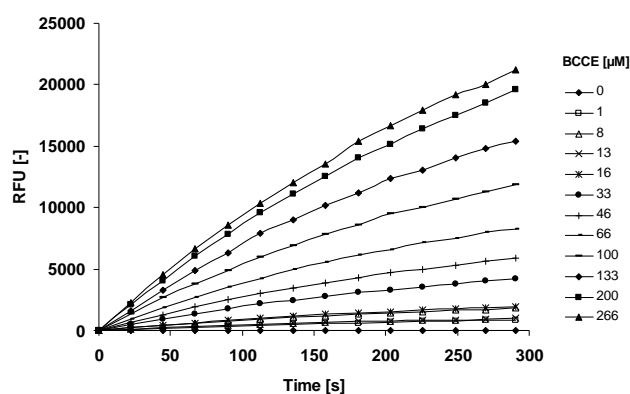


Fig. 33: BCCE conversion with purified P450 BM3 M3 DM-1 (R255H) with varied concentration (Ruff et al., 2012b).

Sequencing results revealed that all four identified substitutions in P450 BM3 M3 DM-1 & DM-2 are located in the heme domain of P450 BM3 (R255H & R203H I401V F423L) (Whitehouse et al., 2012). Out of four mutated positions, the positions R203H and F423L seems not have been reported to influence any P450 BM3 property. Position R255S improves alkane hydroxylation (Glieder et al., 2002), whereas position I401P influences electron transfer and coupling efficiency of P450 BM3 (Whitehouse et al., 2009). Remarkable improvements could be found in variant P450 BM3 M3 DM-1 (R47F F87A M354S D363H R471C N543S R255H) where k_{cat} was increased 7 fold and K_m remained unchanged (Table 2). Characterization of variant P450 BM3 M3 DM (R47F F87A M354S D363H R471C N543S), P450 BM3 M3 DM-1 (R47F F87A M354S D363H R471C N543S R255H) and P450 BM3 M3 DM-2 (R47F F87A M354S D363H R471C N543S R203H I401V F423L) demonstrates that the developed flow cytometer screening system is capable of identifying improved variants in random mutant libraries. A BCCE turnover of $>0.07 \text{ s}^{-1}$ can be regarded

as lower detection limit and therefore as a prerequisite for flow cytometer sorting of population with active and non-active monooxygenase variants. The library of sorted active variants can furthermore be used in standard microtiter plate screening systems for P450 BM3 monooxygenase properties such as organic solvent resistance (Wong et al., 2004a), improved selectivity (Tee and Schwaneberg, 2006) and/or activity towards non-natural substrates (Reinen et al., 2011).

1.2 Conclusions

In summary, the first flow cytometer based high throughput screening platform that can be applied in directed evolution campaigns of P450 monooxygenases was developed. All requirements for an efficient high throughput screening platform were fulfilled and optimized (reliable fluorescent reporter; compartmentalization in whole cells and therefore direct link of gene- and phenotype). Sorting and enrichment was possible at an excellent throughput of 500 events per second with an average sampling time of 4 min, corresponding to 1.2×10^5 screened events per run (theoretically 3.6×10^7 events per day). Variants with up to 7-fold increased activity (P450 BM3 DM-1) could be identified from a random mutant library. A main advantage of the reported BCCE screening system is the direct sorting of fluorescent whole cell (*E. coli*) omitting the preparation of double emulsions and thereby simplifying screening procedures. Furthermore, the presented screening platform is not only restricted to P450 monooxygenases, but also could find applications in metagenomic screenings, improving protein expression, screening of recombination libraries or electron transfer partners. Specifically, P450 monooxygenases that catalyze an *O*-dealkylation of coumarin derivatives (e.g. human CYP3A4) could be employed in the flow cytometer based BCCE screening system. Additionally, cellulases, lipases and phosphatases are also capable to hydrolase coumarin derivatives.

II.2 Flow cytometry assay based on w/o/w-emulsification for mediated electron transfer

In a flow cytometry screening system, compartmentalization is the essential prerequisite to ensure the link between genetic information (genotype) and activity (phenotype) as well as enrichment of fluorescent particles (cells) within a population (Griffiths and Tawfik, 2006; Bershtein and Tawfik, 2008). Three basic strategies have been developed in the past: 1. Phage display, 2. Emulsification (water-in-oil=w/o; water-oil-water=w/o/w) of a catalyst, substrate and genetic information and 3. Trapping the fluorescent product within a cell (whole cell assay) (Farinas, 2006; Hardiman et al., 2010). Besides handling and further experimental requirements, the major drawbacks of emulsification are: a) Encapsulation of multiple cells during emulsion preparation (false positive clones) and b) Difficulties in recovery of genetic information due to required permeabilization of bacterial membranes for substrate delivery (Aharoni et al., 2005b). Consequently, whole cell assays are generally preferred due to easy handling, homogeneous shape and volume of the reaction compartment as well as simple recovery of cells on agar plates (Griffiths and Tawfik, 2006). These advantages were used to develop the whole cell flow cytometry screening system for directed evolution of P450 monooxygenases (section II.1).

Emulsions (w/o and w/o/w) can be used to compartmentalize and screen large gene libraries for a specific property. The emulsification process (w/o) enables to entrap the protein and subsequent products for reporting enzymatic activity in aqueous solution. A second (re-) emulsification (w/o/w) generates droplets containing fluorescent markers, which can be isolated by fluorescence activated cell sorting (FACS) (Bernath et al., 2004a, 2004b). Successful directed evolution of several biocatalysts (e.g. protease, thiolactonase) employing emulsification and sorting by flow cytometry are reported (Aharoni et al., 2005a; Wu et al., 2010; Tu et al., 2011).

2.1 Emulsification of P450 BM3 in presence of Zinc-dust

The evolution of P450 BM3 for mediated electron transfer requires the compartmentalization of the protein in presence of the alternative cofactor (Zn/Co(III)-sep), which cannot be applied in whole cell screening systems. A flow cytometry assay based on w/o/w-emulsification for mediated electron transfer, would require not only a substrate staying in the water phase but potential products have to remain inside the compartment avoiding cross-contamination within a population of cells. Therefore, it was significant that the permeabilized P450 BM3

expressing cells allowed the conversion of the substrate in presence of Zn-dust and mediator, both remaining within the emulsion in the water phase together with the permeabilized cells. The substrate BCCE which was used in the whole cell assay could not fulfill this requirement as the substrate was hydroxylated by P450 BM3 but had a poor solubility in water. The modification of the coumarin derivatives by attaching a COOH group lead to more polar molecules (Kanaya et al., 1998; Henne et al., 2000). Therefore BCC-acid was synthesized and used as substrate in the emulsion as the charge substrate remains in the water phase (the synthesis is reported in the experimental section). P450 BM3 expressing cells permeabilized with polymixin B were able to convert the substrate with similar efficiency to the BCCE substrate in the MTP (Fig. 34).

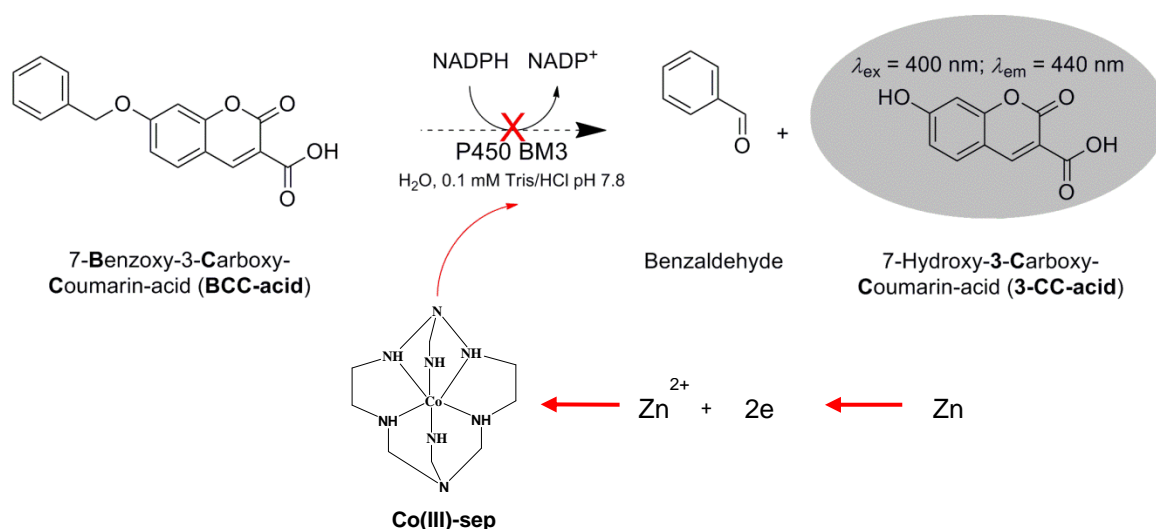


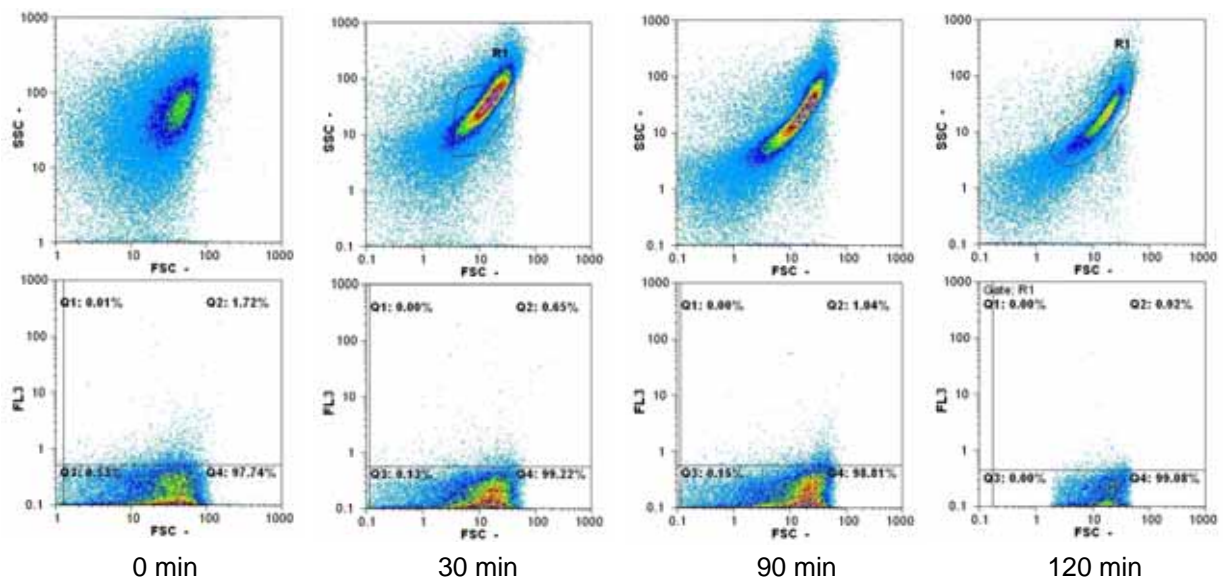
Fig. 34: Scheme of the BCC-acid conversion by P450 BM3 in presence of the alternative cofactor system Zn/Co(III)-sep instead of the natural cofactor NADPH.

The entrapment and the compartmentalization of *EGFP* expressing cells in w/o/w-emulsion and in presence of Zn-dust as well as the mediator served to identify the number of entrapped cells and evaluate the shape of the emulsion. The emulsification was performed according to a published protocol (Tu et al., 2011) and reported in Material and Methods (section 2.13.2.2). Microscopy analysis showed that an average of 1-2 cells was entrapped within the emulsions which were equally in roundness and with variable size of around 10-20 μm .

Finally, the entrapment of P450 BM3 expressing cells (permeabilized with polymixin B), the substrate BCC-acid, the water soluble mediator Co(III)-sep and Zn-dust in w/o/w-emulsion was performed. When Zn-dust (particle size $<63 \mu\text{m}$ obtained from Carl Roth (Karlsruhe, Germany)) applied in microtiter plates was used, the emulsions were sticky and inhomogeneous since a “S” shaped population in the flow cytometer is present (Fig. 35). Sticky means the emulsions were attached to each other by the oil phase laying around and

poorly mixed with the water phase. The “S” shape population can be observed in the plot of the FSC against the SSC (Fig. 35). The “S” shape appears after 30 min of incubation and increases over time, concluding that the emulsions were degraded during incubation. The activity is represented in the plot of the FL3 laser against the FSC, showing the fluorescence of the detected particles (Fig. 35). The gated population (Q2) is used to evaluate the increase in fluorescent events. But no activity increase over time could be observed as the percentage of fluorescent elements present in the gated population Q2 decreased from 1.7% to 0.92%.

a)



b)

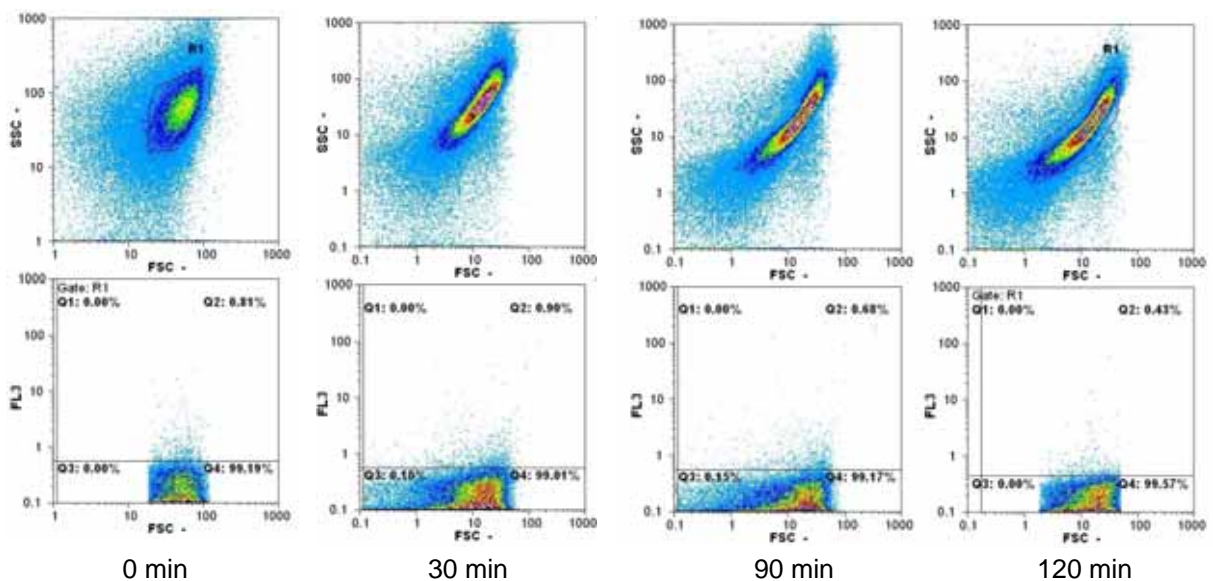


Fig. 35: FACS-plots of double emulsions, containing cells, BCC-acid and Zn/Co(III)-sep after 0 min, 30 min, 90 min and 120 min incubation. a) emulsion of cells lacking the P450 BM3 gene, b) emulsion containing P450 BM3 F87A expressing cells. R1 and Q2 show the gated population. Side Scatter (SSC), Forward Scatter (FSC) and UV-laser [RFU in Log scale] (FL3: λ_{Ex} 350 nm and λ_{Em} 450 nm) were recorded.

Reducing the size of the Zn-dust particles from $<63\ \mu\text{m}$ to $5\ \mu\text{m}$ (Zn-dust special 615 from Conmet) and $3.5\ \mu\text{m}$ (Zn-dust Superfine 620 from Conmet) in the reaction set up, a clear influence on the shape and distribution of the generated emulsion particles was visible. The emulsions had a homogenous size distribution but a dispersive SSC (shape) distribution (Fig. 36). The distribution of the particles in the FSC (size) was in a narrow range but the SSC (granulosity) was spreading. Using smaller Zn-dust particles only one major population was detected in the SSC and FSC plot, showing good stability over at least 120 min, but degradation happening after a 3 hours of incubation. The activity of P450 BM3 F87A in presence of the alternative cofactor (Zn/Co(III)-sep) was only slightly reduced in the MTP assay applying crude lysate within the reaction mixture.

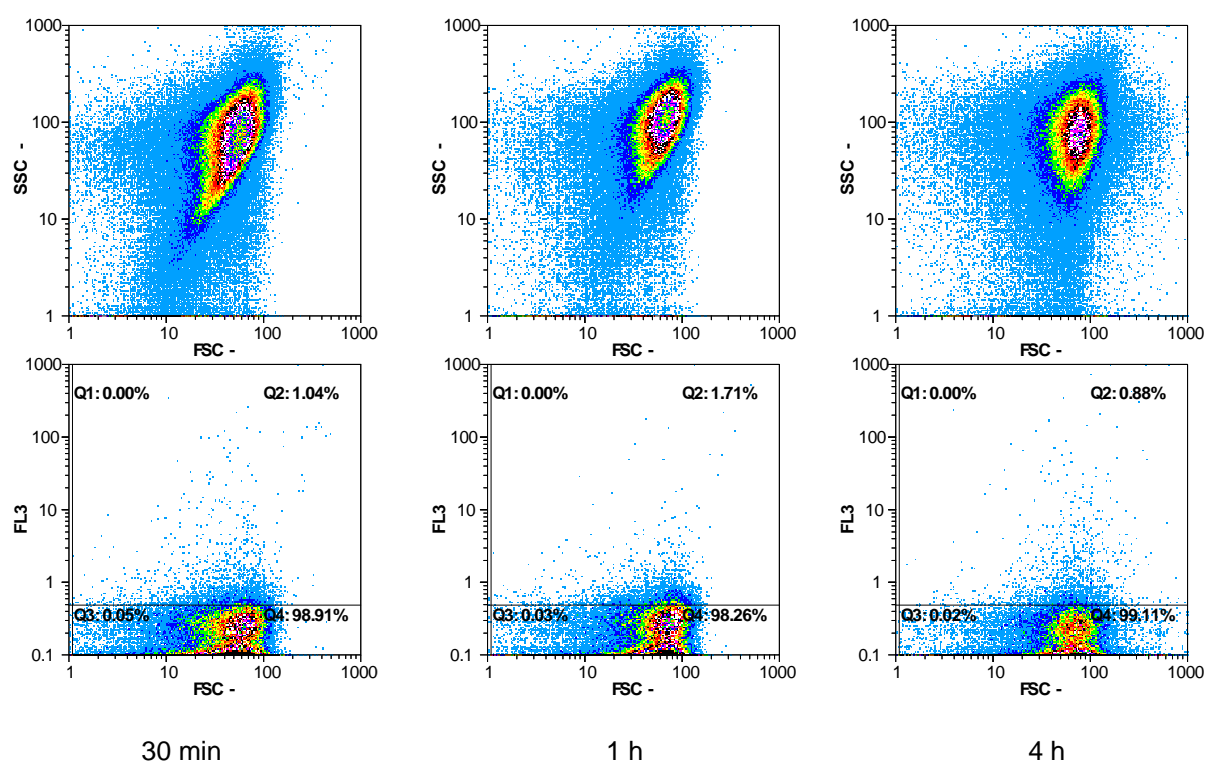


Fig. 36: FACS-plots of double emulsions, containing *E. coli* P450 BM3 M3 cells, BCC-acid and Zn/Co(III)-sep after 30 min, 1 h and 4.0 h incubation. FL3 [RFU in log scale] = UV-laser signal at λ_{Ex} 350 nm and λ_{Em} 450 nm.

In the flow cytometer analysis, the comparison of emulsions prepared with P450 BM3 expressing cells and lacking the P450 BM3 gene revealed no detectable activity (Fig. 36), that would have been displayed as an increasing fluorescence of the gated population Q2 (Fig. 36). To obtain not only stable and homogenous, but also an active signal within the emulsion, the compartmentalization was repeated varying the emulsification time, the cell concentration, the amount of Zn-dust and the temperature. None of these optimization steps led to an improvement of the fluorescent signal within the active population.

This results were confirmed by fluorescence microscopy and phase contrast analysis of the w/o/w-emulsion with P450 BM3, BCC-acid and Zn/Co(III)-sep. A fluorescent signal could not be detected. Although the emulsion can be regarded as equally shaped and the size distribution mainly homogenous (Fig. 37) more than one cell was encapsulated.

After sorting encapsulated cells expressing *EGFP* and P450 BM3 together with BCC-acid, Zinc-dust and NADPH, the emulsions were plated on agar plates and incubated overnight, but no colonies grew. Cells entrapped by emulsification as well as cells only incubated in presence of Zn-dust and without addition were grown overnight on agar plates. In the cases where Zn-dust was added, no colonies could be observed; only cells without treatment were growing.

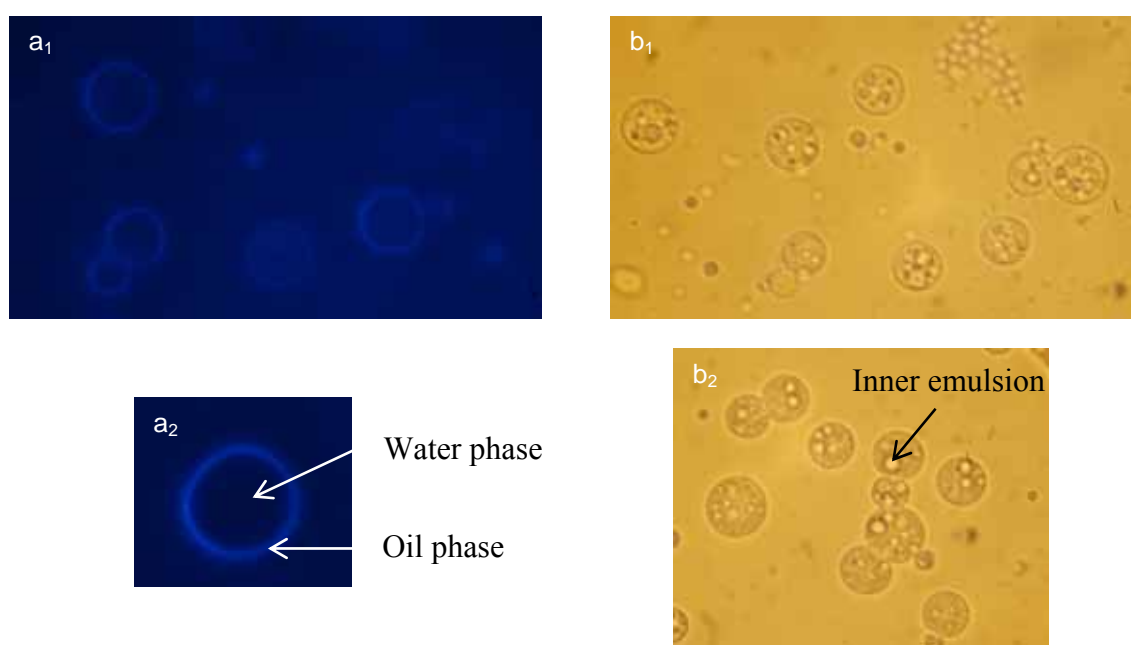


Fig. 37: Fluorescence microscopy (a₁, a₂) and phase contrast (b₁, b₂) of w/o/w-emulsion with P450 BM3, BCC-acid and Zn/Co(III)-sep.

2.2 Discussion

The entrapment of P450 BM3 expressing cells (permeabilized with polymixin B), the substrate BCC-acid, the water soluble mediator Co(III)-sep and Zn-dust in w/o/w-emulsion was performed after optimization of the emulsification process with *EGFP* cells. When Zn-dust of particle size <63 μm was used, the emulsion were inhomogeneous. Therefore, Zn-dust of smaller particle size was investigated (3.5 and 5 μm), the emulsions were more homogenous, but no activity could be detected, nor an increase of the fluorescent signal was recorded over time in the flow cytometry measurements. The very low conversion rate in presence of the alternative cofactor compared to NADPH could be the reason for the lacking

activity. Possible reason could also be due to the compartmentalization procedure that the Zn-dust particles get hardly accessible to the mediator and the protein or appearing quenching effects.

Besides the flow cytometry measurements the emulsion were analyzed by fluorescence microscopy. No fluorescent signal could be detected in the fluorescence microscopy of the w/o/w-emulsion with P450 BM3, BCC-acid and Zn/Co(III)-sep, because the background fluorescence from the oil phase was overlapping with the very low and hardly detectable fluorescent signals.

To exclude as reason for the lacking activity in the emulsified reaction mixture the changed Zn-dust brand and particle size, the activity of P450 BM3 F87A in presence of the alternative cofactor (Zn/Co(III)-sep) was investigated with crude cell lysate in MTP. Only slightly reduced activity was observed with the smaller particle sized Zn-dust (3.5 and 5 μm) compared to the usually employed Zn-dust (<63 μm) in the MTP. Nevertheless, the increase of the fluorescent signal over time could clearly be observed, showing that P450 BM3 can hydroxylate BCC-acid in presence of Zn/Co(III)-sep. In the reaction, 5 mg Zn-dust was supplemented with the resin dispenser, which has a decreased accuracy for powders with high densities (Zn-dust super fine = 7100 Kg/m³). Subsequently, the activity difference was related to the increased quenching caused by the mean density increase.

In addition to the activity measurements of the encapsulated cells expressing P450 BM3 together with BCC-acid and NADPH, the survival rate was analyzed. After sorting, the emulsions were plated on agar plates and incubated overnight, but no colonies grew. Cells entrapped by emulsification as well as cells only incubated in presence of Zn-dust were grown overnight on agar plates. In each case, no colonies could be observed indicating that a compound within the solution has an inhibitory effect on microbial growth. Zn-dust is widely applied as additive in dyes for industrial application to inhibit the microbial growth on surfaces exposed to extreme conditions as well as anti-corrosion systems in vehicles, vessels, bridges, containers, bulkheads, beams, flood-gates, wind turbines, tanks, screws and rivets (www.conmet.de). The inhibitory effect of Zn-dust on the microbial growth does not exclude the application as alternative cofactor in a cell free system or when cell recovery can be omitted.

2.3 Conclusions

In summary, a flow cytometer-based ultra-high throughput screening assay for directed evolution of P450 BM3 towards improved mediated electron transfer with Zn-dust could not be developed. On the one hand two requirements for an efficient ultra high throughput screening platform could be fulfilled. A fluorogenic compound (BCC-acid) that is hydroxylated by a P450 BM3 monooxygenase to a fluorescent reporter could be selected. As well as the compartmentalization of the catalyst, the genetic information and the fluorescent reporter in a w/o/w-emulsion was performed, but on the other hand two basic requirements had to be fulfilled. A reliable distinguishing between active and inactive variants and subsequently the enrichment of active clones within a population of cells could not be reached.

The entrapment of P450 BM3 expressing cells (permeabilized with polymixin B), the substrate BCC-acid, the water soluble mediator Co(III)-sep and Zn-dust in w/o/w-emulsion was successful. Stable emulsion could be generated, but no detectable activity was recorded. Neither the fluorescence increases over time nor the regeneration of the cells could be obtained. The inhibitory effect of the Zn-dust on the microbial grow was pre-dominant and excluded the use of the double emulsion technology for the generation of an assay for the evolution of P450 BM3 for mediated electron transfer.

Chapter III: Evolution of P450 BM3 for alternative cofactor systems

III.1 Evolution of P450 BM3 towards improved Mediated Electron Transfer (MET)

The alternative cofactor system using Zn-dust as electron donor and Co-sep as mediator for P450 BM3 which is described as mediated electron transfer was first reported by Schwaneberg et al. (Schwaneberg et al., 2000). Subsequently, protein engineering of P450 BM3 was performed and the best reported variant reached 40% of the turnover compared to the natural cofactor NADPH (Nazor and Schwaneberg, 2006). Increased activity in presence of the Zn/Co(III)-sep and turnover rates comparable to the natural cofactor NADPH would make this system synthetically attractive.

This chapter of the thesis aims to further engineer P450 BM3 towards improved Mediated Electron Transfer (MET) by directed evolution. Starting variant was the mutant M3 (R47F F87A M354S D363H) reported by Nazor et al. with a 2.3 fold improved K_{cat} for the MET (Nazor and Schwaneberg, 2006). In previously performed experiments this variant was engineered and another variant (N543S) with 1.3 fold improvement was selected from an epPCR library. The random library was screened with the pNCA assay (Schwaneberg et al., 1999a), already reported for successful identification of improved P450 BM3 variants for MET. However, the parent gene (M3) as well as the improved variant (N543S) had an additional mutation R471C.

In this thesis, the evolution of P450 BM3 M3 was started first by generating focused mutant libraries to investigate the impact of the single position (R471 and N543). Subsequently, the obtained best variant (P450 BM3 M3 R471C N543S) was evolved in the next round of directed evolution by random mutagenesis approaches. An epPCR and a SeSaM library were generated and enriched with the developed high throughput flow cytometer whole cell screening system before screening in the MTP for improved activity towards the MET (see section II.1). Finally, the positions identified in the random approaches were individually saturated and recombined to select the most beneficial amino acid combination for improved MET in P450 BM3.

1.1 Activity assays for P450 BM3 in presence of Zn-dust and protein purification

1.1.1 Fluorescent MTP assay in presence of Zn/Co(III)-sep

The pNCA assay was reported to be successful for the evolution of P450 BM3 towards improved MET (Nazor and Schwaneberg, 2006). To simplify the investigation and enhance the sensitivity of the assay the application of a fluorescent MTP assay was established. The MTP assay based on the conversion of BCCE (section II.1) could be adapted to determine the activity in presence of the alternative cofactor system Zn/Co(III)-sep, additionally to the natural cofactor NADPH. The assay could be used as endpoint assay or to perform continuous measurements of P450 BM3 activity. The coefficient of deviation was determined to be 13% if only one endpoint measurement was recorded after 30 min or 26% in continuous measurement mode with 20 sec intervals (Fig. 38).

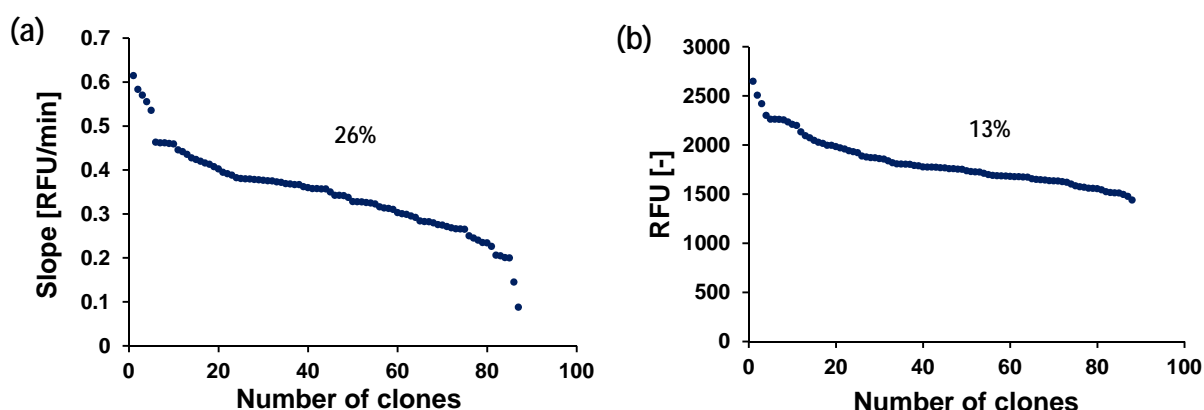


Fig. 38: Coefficient of variation of the fluorescent BCCE assay in continuous measurements (a) and as endpoint measurement (b).

1.1.2 Calibration curve of 7-Hydroxy-3-Carboxy-Coumarin Ethyl ester (3-CCE)

The calibration curve of 3-CCE, the obtained product after hydroxylation of BCCE by P450 BM3, was performed under the same condition as in the reaction mixture. The reaction scheme is shown in Fig. 39 and described in the assay development (section II.1)

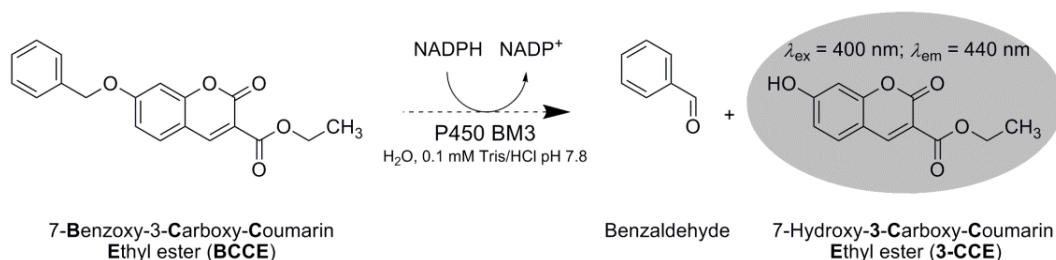


Fig. 39: Scheme of the BCCE conversion catalyzed by P450 BM3.

The linear fit of the calibration curve (Fig. 40) in presence of NADPH or the alternative cofactor system Zn/Co(III)-sep was used for calculation of the kinetic parameters in section III.1.2 and section III.1.3.

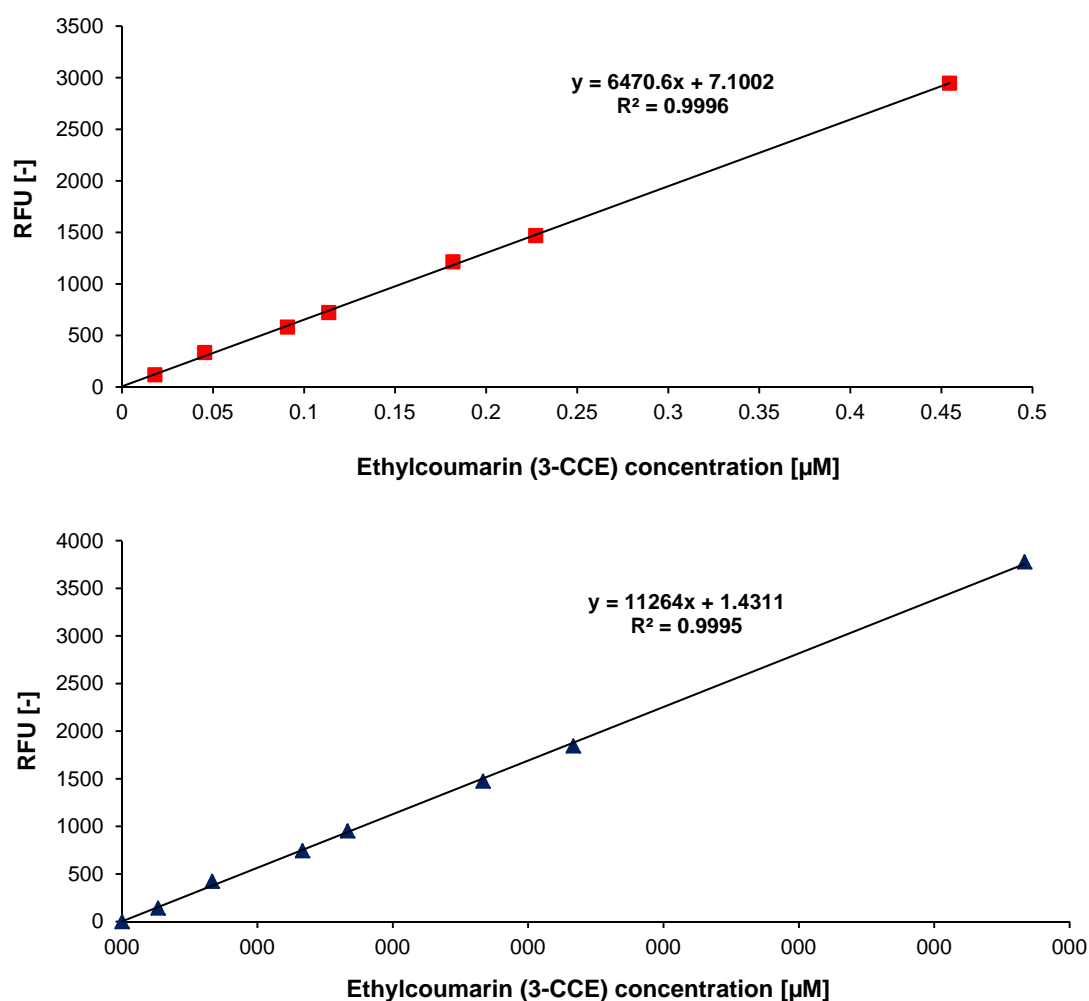


Fig. 40: Calibration curve of 3-CCE in presence of NADPH (a) or Zn/Co(III)-sep (b) in the reaction mixture monitored at λ_{ex} 400 nm, λ_{em} 440 nm.

1.1.3 Thin Layer Chromatography analysis of the BCCE conversion

In addition to the fluorescent measurements, the activity of the P450 variants was monitored by Thin Layer Chromatography (TLC) analysis. The reaction of the BCCE conversion by P450 BM3 was analyzed after extraction by TLC to visualize the product formation. The products were extracted from the reaction mixture using Dichlormethane (DCM), Ethyl acetate (EtAc) or Chloroform (CHCl_3) and spotted together with the reference 3-CCE (product of the BCCE hydroxylation) (Fig. 41). The upper spot corresponds to the BCCE hydroxylation product, the 3-CCE and the lower spot corresponds to the substrate BCCE according to the references spotted in line 5/6 and 7. The reaction mixtures extracted with the

different organic solvents have both spots indicating that the hydroxylation of the BCCE is occurring and the product can be visualized on the TLC.

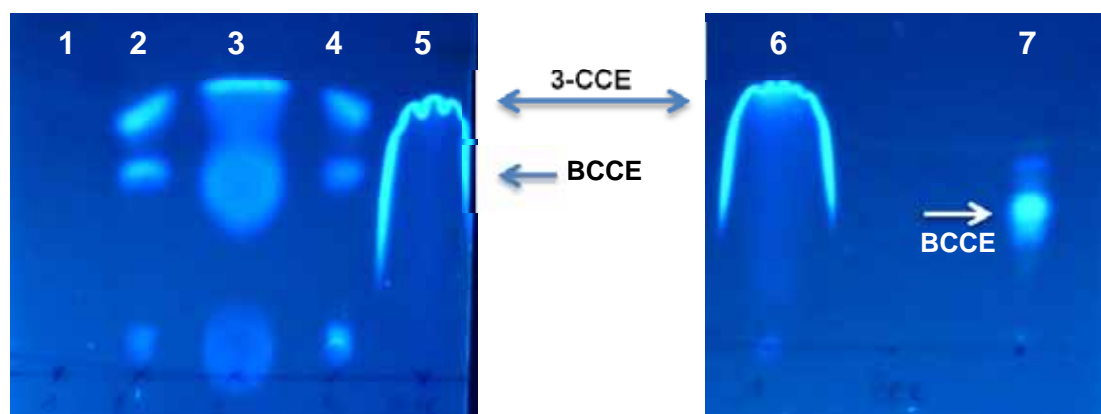


Fig. 41: TLC analysis of the BCCE conversion by P450 BM3 F87A, monitored under UV-light. Lane 1: Reaction mixture without substrate; Lane 2-4: Reaction mixture extracted respectively in DCM, EtAc or CHCl₃; Lane 5 and 6: BCCE hydroxylation product, 7-Hydroxy-3-Carboxy-Coumarin Ethyl ester (3-CCE); Lane 7: Substrate BCCE (7-Benzoxo-3-Carboxy-Coumarin Ethyl ester). Eluent DCM : EtAc in ratio 20:1, TLC-plates of Silica gel with fluorescence indicator UV₂₅₄ (Macherey-Nagel, Düren, Germany),

1.1.4 P450 BM3 purification and concentration determination

Kinetic characterization of selected variants was performed using purified P450 BM3 protein. Variants mentioned and selected in the evolution of P450 BM3 for improved DET and MET as well as in the flow cytometer assay development were purified. The purification of the analyzed P450 BM3 variants was achieved applying a well established purification protocol (Schwaneberg et al., 1999b). Exemplarily, the chromatogram of the anion exchange purification step and the SDS-page of one selected variant P450 BM3 WT is shown (Fig. 43). Peak 1 represents the flow through of the column, containing all proteins which cannot bind to the matrix. The proteins which were bound to the column and are eluted at low salt concentration (150 mM NaCl) were monitored when the concentration of the elution buffer was adjusted to 7% (Peak 2). The P450 BM3 monooxygenase was eluted when the salt concentration was elevated to 260 mM NaCl (13% of the elution buffer) and collected in the fractions 5-8 (Peak 3). All remaining proteins were eluted at concentration of 2 M NaCl (Peak 4) to separate from all particles.

The protein purity was monitored by SDS-page and calculated by determination of the P450 BM3 concentration at the ratio of the total protein amount determined by BCA-kit. In all cases the purity was above 85%. The fractions obtained during the protein elution are shown in Fig. 42. On the left side 1 μ l purified protein was loaded and on the right side the gel was overloaded with 4 μ l to monitor residual impurities.

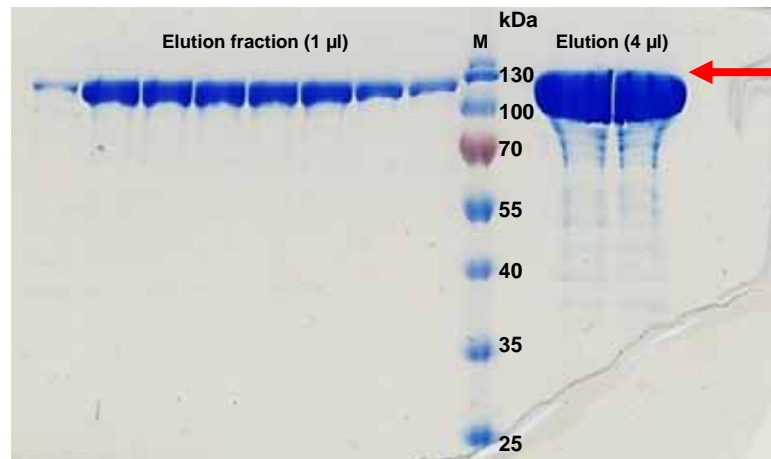


Fig. 42: Elution fraction of P450 BM3 purification separated on 10% acrylamide gel and stained with coomassie brilliant blue (3-5 ml per fraction). Red arrow indicates the P450 BM3 at 120 kDa; M: pre-stained protein ladder from NEB.

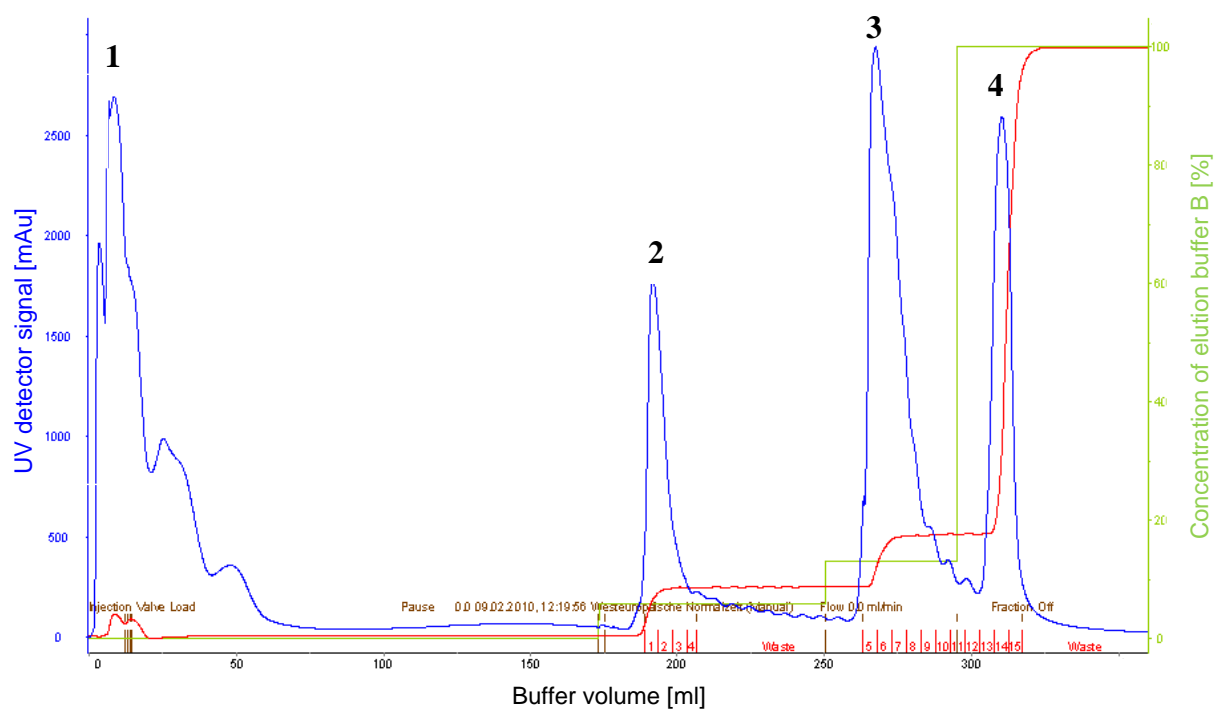


Fig. 43: Chromatogram monitored during the purification of P450 BM3 WT by anion exchange chromatography. Blue line: UV-detector at 280 nm; Red line: conductivity; Green line: concentration of elution buffer. Peak 1: flow through (unbound proteins); Peak 2: elution at 150 mM NaCl; Peak 3: elution at 260 mM NaCl; Peak 4: elution at 2 M NaCl.

The P450 concentration was determined by CO-normalization (Fig. 44) according to Omura et al. (Omura and Sato, 1964a) and calculated according to equation (2) (see 2. Material and Methods).

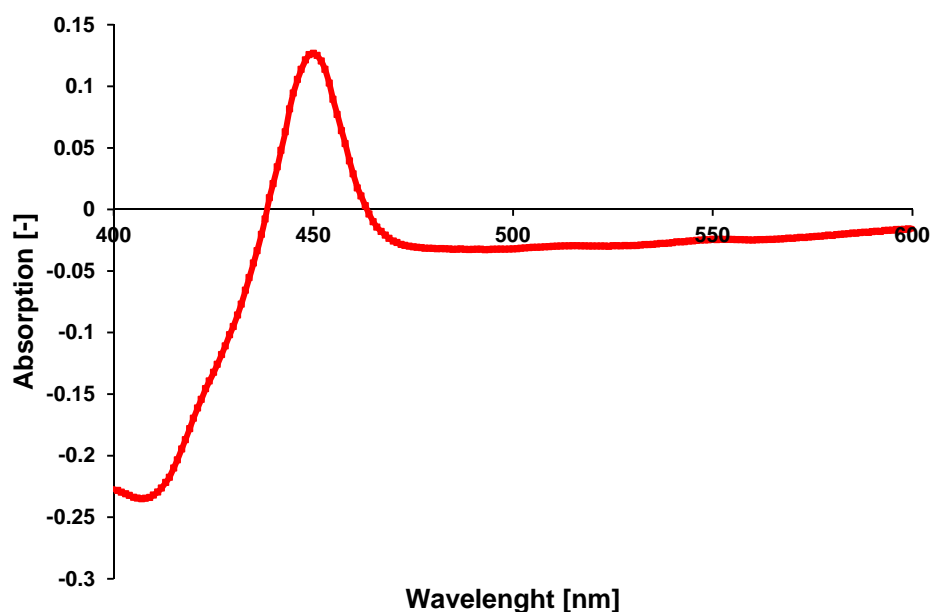


Fig. 44: Absorption spectra of P450 BM3 (dilution 1:8) after CO gassing and with subtracted background. Background consist of the sample with protein and without CO gassing. P450 concentration: $((0.126 - (-0.032)) * 8) / 91 = 0.014$ mM.

1.2 Saturation mutagenesis at positions N543 and R471

Starting from the reported variant P450 BM3 M3, which was engineered by random mutagenesis for improved MET, the position N543 and R471 selected in previous directed evolution rounds were saturated using a NNK degenerated codon (Reetz et al., 2008). From each library 400 clones were screened with the pNCA assay in presence of the alternative cofactor system Zn/Co(III)-sep. The screening of the site saturation library at position N543 did not lead to the identification of improved variants. At position R471, two improved variants could be identified and revealed after sequencing (the substitution R471T). In the previous directed evolution experiment the parent gene also posed the substitution R471C, increasing the complexity of the analyzed and compared variants. No improvement in the single mutant (M3+N543S) could be identified.

To investigate the impact of the position N543, the following variants M3 **N543S** (R47F F87A M354S D363H N543S); M3 **N543S R471C** (R47F F87A M354S D363H R471C N543S); M3 **R471C** (R47F F87A M354S D363H R471C); M3 **R471T** (R47F F87A M354S

D363H R471T) were generated by site directed mutagenesis (SDM) and after purification the kinetic parameters were compared to the variant M3 (R47F F87A M354S D363H) (Table 3). All variants showed activity with the natural cofactor NADPH. The single mutant N543S and the R471T have a lower K_m and R471C an unmodified K_m but no significant activity increase could be observed. Interestingly, a synergistic effect could be observed in the double mutant N543S R471C, the K_{cat} was 2 fold improved leading to 3 fold increased catalytic efficiency (Fig. 45).

Table 3: Kinetic characterization of P450 BM3 variants hydroxylating 12-pNCA in presence of Zn/Co(III)-sep. Novel substitutions in the parent P450 BM3 M3 are highlighted as bold letters.

Variant	k_{cat} ^[a]	K_m [mM]	K_{eff} ^[b]
P450 BM3 M3	3.46	0.68	5.0
P450 BM3 M3 R471C	4.1	0.60	6.8
P450 BM3 M3 R471T	2.48	0.44	5.6
P450 BM3 M3 R471C N543S	8.66	0.50	17
P450 BM3 M3 N543S	4.62	0.50	9.3

[a] [mmol product min⁻¹ mmol⁻¹ P450]; [b] [min⁻¹ mM⁻¹];

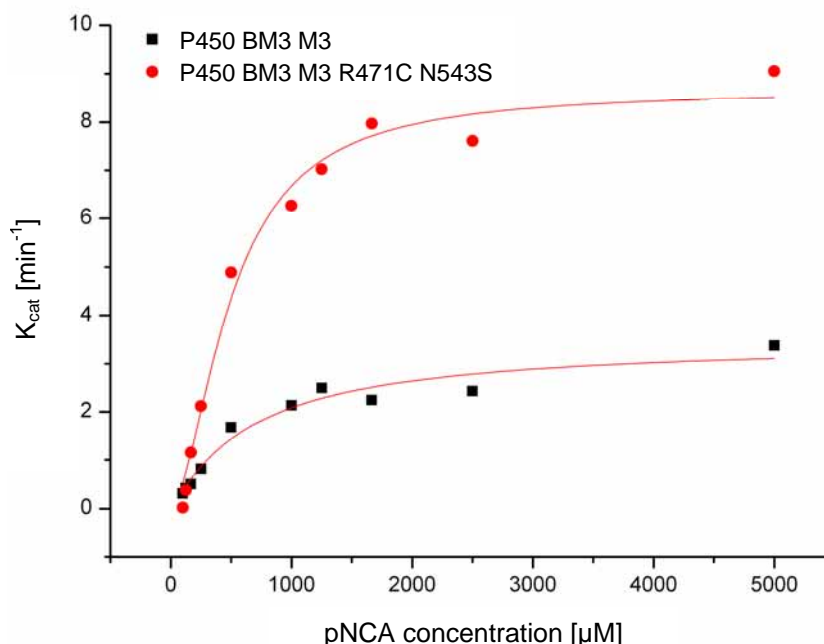


Fig. 45: Plot of the activity measurements used to determine the kinetic parameters of P450 BM3 M3 N543S R471C (R47F F87A M354S D363H R471C N543S) (●), and P450 BM3 M3 (R47F F87A M354S D363H) (■). Fitting according to the hill equation was performed.

1.3 Directed evolution towards improved MET

To identify new hot spots and improved P450 BM3 M3 variants for the MET, five epPCR- and four SeSaM-libraries were generated. The newly developed high throughput flow cytometer screening assay for P450 BM3 (section II.1) was applied to enrich and pre-screen active clones from the random mutant libraries. Sorted variants were re-screened in MTP using substrate BCCE (reported in section II.1).

1.3.1 Generation and screening of error-prone Polymerase Chain Reaction (epPCR) libraries

EpPCR libraries of M3 N543S R471C using 0.4, 0.2, 0.1, 0.05, 0.2 mM MnCl₂ were generated and enriched three times with the whole cell flow cytometer assay. Fig. 46 shows the vector backbone amplification and the generated epPCR products transformed in BL21 (DE3) Gold LaqI^{Q1} cells after hybridization by PLICing (Blanusa et al., 2010b) in the vector pALXtreme-1a. 10⁴ clones were expressed, sorted and enriched for active clone population.

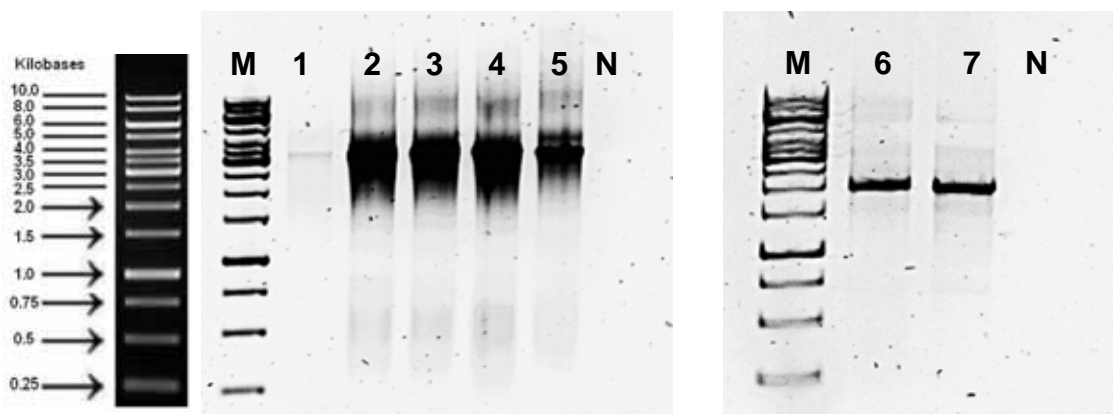


Fig. 46: PCR products separated by agarose gel electrophoresis and stained with GelRed. Lane M: 1 kb DNA Ladder; Lane 1-5 epPCR products of P450 BM3 (3150 bp) with respectively 0.4, 0.2, 0.1, 0.05, 0.2 mM MnCl₂; Lane N: negative control, PCR reaction mixture without template DNA; Lane 6 and 7: pALXtreme-1a vector backbone amplification (~2.5 kDa).

The flow cytometer plot (Fig. 47) shows the enrichment of the active population. Each plot indicates the percentage of fluorescent particles above the settled threshold (Q2). The threshold was adjusted prior to each measurement and sorting procedure by analyzing cells with the pET28a(+) vector lacking the P450 BM3 gene. The population Q2 indicates the amount of fluorescent particles in regard to all analyzed elements which are monitored in the by size gated population R1. The gated population R1 indicates the particles of similar size forming a homogenous population which is considered in the other plots and subtracted from the background. The fluorescent population Q2 increased from 2.5 % in the first enrichment

round to 5.5 % after the second sorting and to 7.8 % after the third enrichment round compared to 1.8 % fluorescent particles in gate Q2 when cells with the pET28a(+) vector lacking the P450 BM3 gene are analyzed. The increase of the population in the selected gate underlies the enrichment of the active variants.

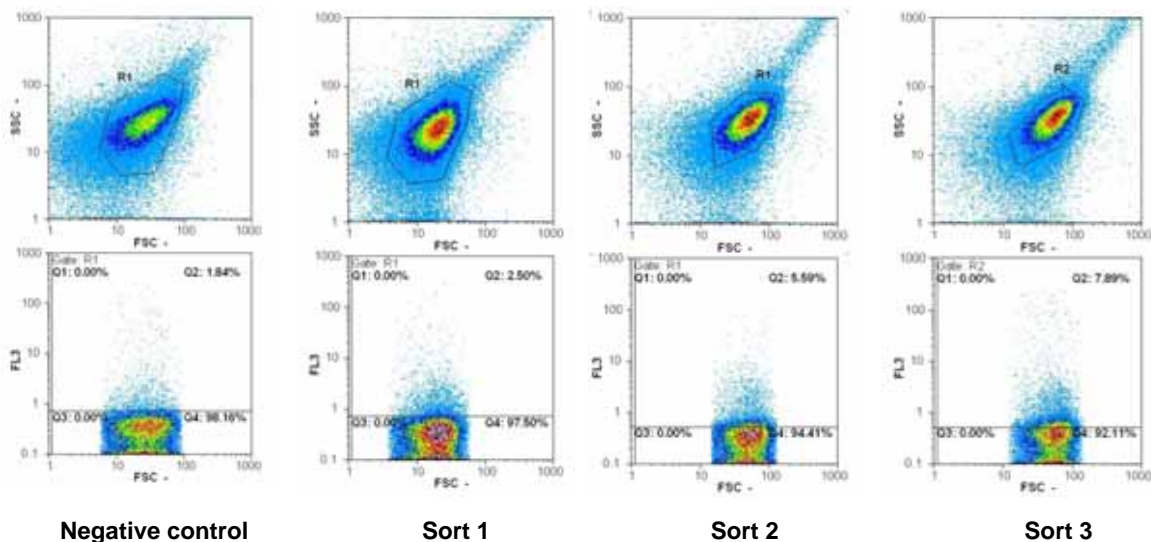


Fig. 47: Flow cytometry plot of the negative control, cells containing pET 28 a(+) lacking P450 BM3 gene; cells expressing P450 BM3 epPCR library after three rounds of enrichment.

Finally, the enriched library was re-screened with the fluorescent assay in MTP for improved activity in presence of the alternative cofactor system Zn/Co(III)-sep. The selected variants (**P450 M3 DM-1**: R47F F87A M354S D363H R471C N543S R255H; **P450 M3 DM-2**: R47F F87A M354S D363H R471C N543S R203H I401V F423L) for improved activity with NADPH and BCCE revealed also to be the most active ones with the alternative cofactor system Zn/Co(III)-sep. In addition to the characterization with NADPH, the kinetic parameters were determined for Zn/Co(III)-sep (Table 4).

Table 4: Kinetic characterization of P450 variants converting BCCE in presence of Zn/Co(III)-sep. Novel substitutions in the parent P450 BM3 M3 DM are highlighted as bold letters.

Variant	Zn/Co(III)-sep			NADPH		
	k_{cat} ^[a]	K_m [μ M]	K_{eff} ^[b]	k_{cat} ^[a]	K_m [μ M]	K_{eff} ^[b]
P450 BM3 M3 DM (R471C N543S) ^[c]	1.8	44	0.04	4.2	25.2	0.17
P450 BM3 M3 DM-1 (R255H)	3.0	62	0.05	28.8	25.3	1.14
P450 BM3 M3 DM-2 (R203H I401V F423L)	6.8	63.4	0.10	14.4	34.3	0.42

[a] [mmol product min⁻¹ mmol⁻¹ P450]; [b] [min⁻¹ μ M⁻¹]; [c] Starting variant P450BM3 M3 DM = P450BM3 M3 (Nazor et al., 2008) + N543S R471C

The K_m values for BCCE in presence of Zn/Co(III)-sep are increased and nearly doubled compared to the K_m values for BCCE with NADPH. The catalytic efficiency is reduced with

Zn/Co(III)-sep compared to NADPH. The NADPH improved variant P450 BM3 M3 DM-1 (**R255H**) is only slightly improved with Zn/Co(III)-sep and reaches 10 % of the conversion obtained with NADPH. In contrary, the variant P450 BM3 M3 DM-2 (R203H I401V F423L) which showed a 3 fold improved K_{cat} with NADPH reaches 50 % of the NADPH conversion with Zn/Co(III)-sep and remains 3 fold improved. This variant P450 BM3 M3 DM-2 (**R203H I401V F423L**) is more efficient than P450 BM3 M3 DM-1 (**R255H**) with Zn/Co(III)-sep in contrary to NADPH where it was found to be vice versa.

1.3.2 Generation and screening of SeSaM libraries

The next round of evolution was proceeded by the generation and screening of SeSaM mutant libraries (Mundhada et al., 2011; Ruff et al., 2012a). The advanced random mutagenesis method SeSaM-R reported in Chapter I of this thesis was applied to evolve P450 BM3 for MET. The libraries were treated similar to the epPCR libraries enriched by the reported whole cell flow cytometry assay and screened with the fluorescent assay in MTP.

SeSaM was reported to be efficient with genes up to 1500 bp sizes (Wong et al., 2004b). As P450 BM3 (3150 bp) exceeds this limitations, the gene was divided (2 times 1500 bp) and the two generated libraries were assembled after individual mutagenesis using the PLICing cloning technology (Blanusa et al., 2010b) (Fig. 48).

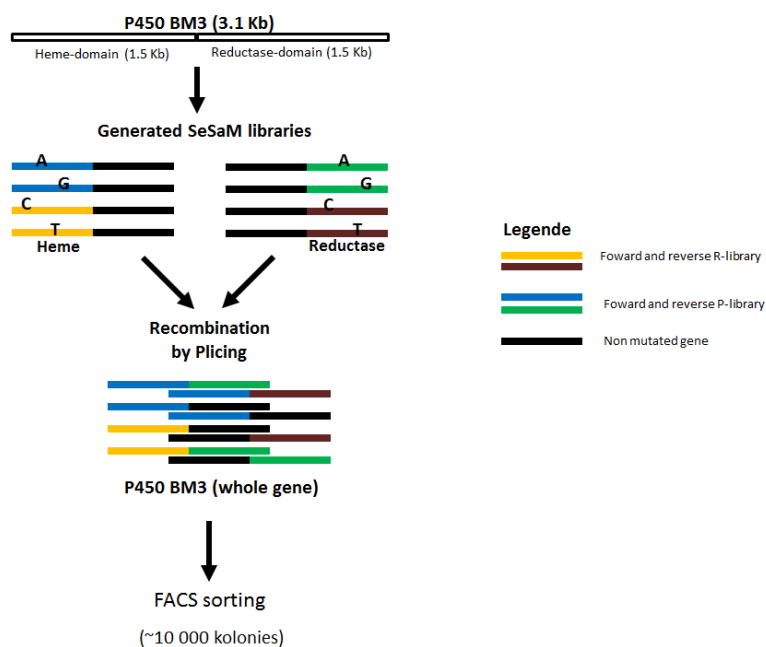


Fig. 48: Scheme of the generated SeSaM libraries.

Exemplarily, the different steps of the P450-HEME library generation with the SeSaM-R method are shown. SeSaM libraries generated with the published SeSaM Tv+ protocol (Mundhada et al., 2011) and biased by using the P-base as well as SeSaM libraries including the R base following the SeSaM-R protocol (Ruff et al., 2012a) of the P450 BM3 M3 (reported by Nazor et al. (Nazor et al., 2008)) were generated. The heme and the reductase domain were mutagenized individually and recombined by the PLICing method. In total, 16 individual libraries were generated: for the heme as well as the reductase domain each the following 8 combinations: forward and reverse P-library targeting the A and G base; forward and reverse R-library targeting the T and C base. In the end, due to the recombination by PLICing 9^2 combination were possible. For example, P-based library of the heme domain combined with non mutated reductase domain, or a R-based library of the reductase domain and vice versa (Fig. 48, summarized the applied mutagenesis scheme).

The agarose gels and the Experion data were recorded similar for the other libraries (P450-HEME with SeSaM-P method, P450-reductase with the SeSaM-P and SeSaM-R method).

Preliminary step – optimization of optimal phosphorothiolated nucleotides concentration:

The optimal ratio of phosphorothiolated nucleotides to unmodified nucleotides for the T and C base had to be determined preliminary to the library generation. The agarose gel shows the decreasing intensity of the 1.5 kb band and the increasing amount of cleaved smaller fragments with increasing concentration of phosphorothiolated nucleotides. The selected optimal phosphorothiolated nucleotide concentration was for T reverse 18%, for C reverse 25%, for T forward 20% and C forward library 30% (Fig. 49).

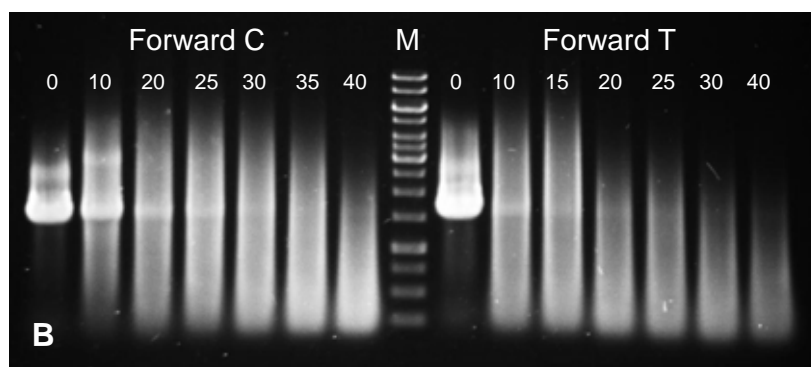
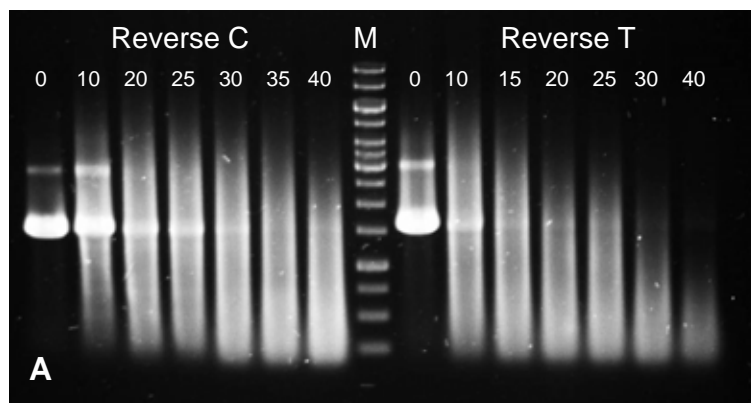


Fig. 49: Agarose gel of the optimal phosphorothiolated nucleotides concentration determination for C or T reverse- (A) and C or T forward-library (B). 0-40 indicates the ratio in % of phosphorothiolated nucleotides to unmodified nucleotides.

Preliminary step – Preparation of double stranded template-DNA for Step 1 and Step 3:

The second necessary preliminary step for the SeSaM library generation is the template generation for Step 1 and Step 3 of the gene of interest (2.12.2-3). The SeSaM specific sequence is attached by PCR to the gene (2.12.2). Fig. 50 shows the agarose gel of the PCR in which only one band corresponding to P450 BM3 at 1500 bp is appearing, no unspecific binding could be observed.

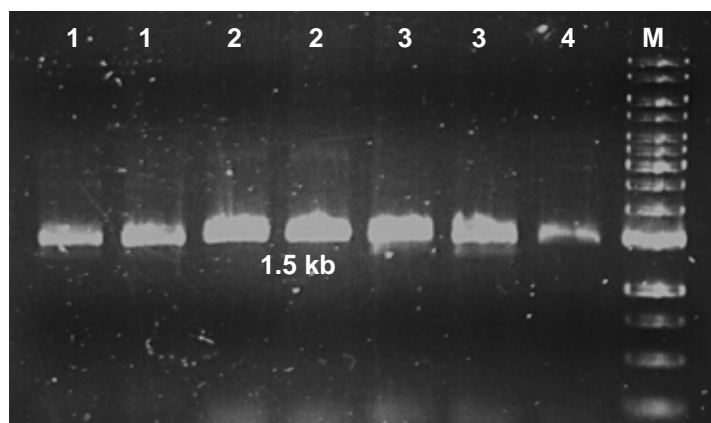


Fig. 50: Agarose gel stained with GelRed of the preliminary template generation for Step 1 and Step 3. Lane 1: forward template for Step 1; Lane 2: reverse template for Step 3; Lane 3: template up for Step 3; Lane 4: template down for Step 4. Size of the P450 BM3-Heme gene is 1.5 kb.

Step 1: Generation of ssDNA fragment pool with random length distribution:

The generated ssDNA fragment pool with random length distribution can be visualized on agarose gels or with the automated electrophoresis system. Fig. 51 indicates the fragments displayed with the Experion after cleavage of the phosphorothiolated nucleotides which were randomly incorporated by PCR. The band of the uncleaved fragment at 1.5 kb is decreased and the number of ssDNA fragments with random length is homogenously distributed. The ladder did not run appropriately, the upper band should have a size of 1.5 kb and not like stated by the marker on the level of 3 kb.

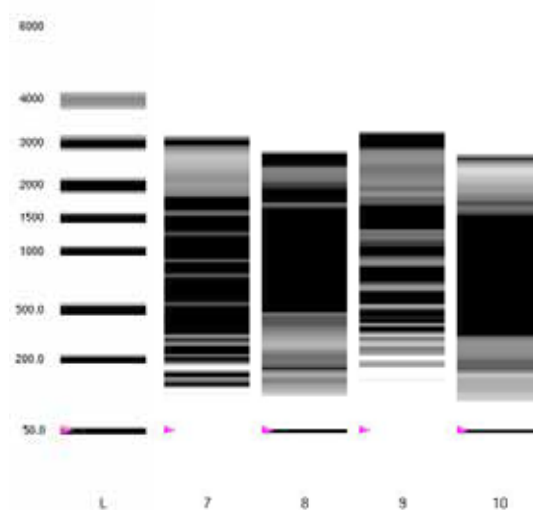


Fig. 51: Automated gel electrophoresis pictures of the ssDNA fragment pool with random length distribution analyzed with the RNA-chip-kit (BioRad). Lane L: RNA ladder misleading as it did not run appropriately the 3 kb band corresponds to the 1.5 kb band; Lane 7: Forward library targeting the C base; Lane 8: reverse library targeting the C base; Lane 9: Forward library targeting the T base; Lane 10: reverse library targeting the T base.

Step 2: Enzymatic elongation of single stranded DNA with dRTP and Step 3: Synthesis of the full length gene.

The results of both steps were not recorded. Due to very low yield (<10ng/kb SeSaM template) the PCR products could not be visualized on agarose gels.

Step 4: Replacement of universal bases.

In Step 4 the universal base is replaced by unmodified nucleotides and the PCR product is visualized on agarose gels. In a successful generated library the PCR product of step 4 remains in only one band according to the targeted gene size. In Fig. 52 the resulting library of P450 BM3-HEME (1.5 kb) separated by agarose gel electrophoresis is shown. The double stranded DNA fragments were used after purification for the hybridization in the expression vector.

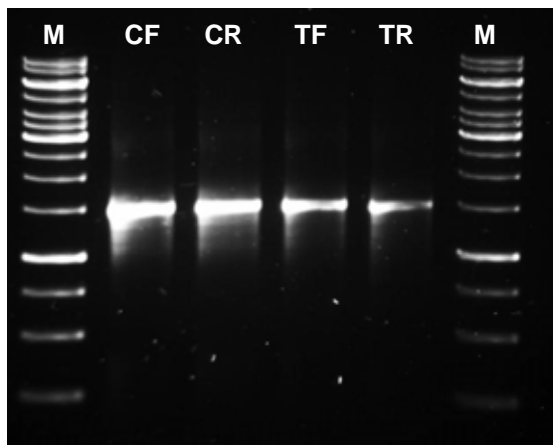


Fig. 52: Agarose gel of the generated PCR products in Step 4 of SeSaM mutagenesis method. CF: Forward library targeting the C base, CR: reverse library targeting the C base; TF: Forward library targeting the T base; TR: reverse library targeting the T base. of 1.5 kb. Size of the resulting P450 BM3-HEME library is 1.5 kb.

After hybridization into expression vector pALXtreme-1a and transformation into B121 (DE3) Gold $lacI^{Q1}$ cells, around 10^4 colonies were expressed and enriched two times with the whole cell flow cytometer screening system. The flow cytometer plots (Fig. 53) show size (FSC) and shape (SSC) distribution of the target population as well as activity (FL3). Identical criteria for screening and selection of active clones were used as for epPCR library. The sorted and targeted population Q2 decreased from 29.19% fluorescent particles to 3.73% during the enrichment rounds. Nevertheless, the positive and negative control could clearly be distinguished; the gated population Q2 includes only 0.36% fluorescent elements in the negative control compared to 44.3% with cells expressing P450 BM3 F87A, proving that the calibration was performed well and the lasers were operating. The effective enrichment of the population could not be reached due to technical problems with the flow cytometer device, which were unsolvable in a near time frame. The sorting chamber is required for enrichment and sorting of events but not for the analysis of population. For this reason the experiment was aborted after the second round of enrichment and 400 colonies after the first enrichment round as well as 400 colonies after the second round were randomly selected and screened with the fluorescent MTP assay.

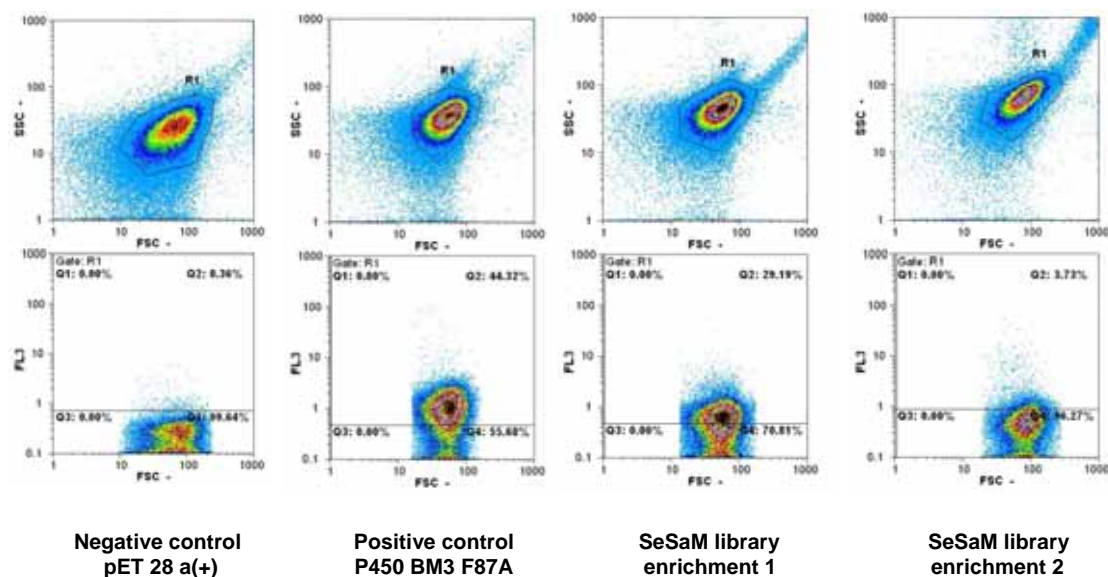


Fig. 53: Flow cytometry plot of the negative control, cells containing pET 28 a(+) lacking P450 BM3 gene; Positive control, cells expressing P450 BM3 F87A; SeSaM library of P450 BM3 M3 after two rounds of enrichment (sort 1 and sort 2).

Out of the 800 screened colonies in MTP, 3 % were re-screened and finally 5 with a 1.3-2.3 fold activity improvement were selected for sequencing (Fig. 54). An influence of the substrate concentration on the catalytic efficiency could be observed in the selected variants. At low substrate concentrations (25 μM) the variants were up to 2.3 fold improved compared to the variant M3, but with increasing BCCE concentration (50 μM) the activity accounts only 1.3 fold improvement.

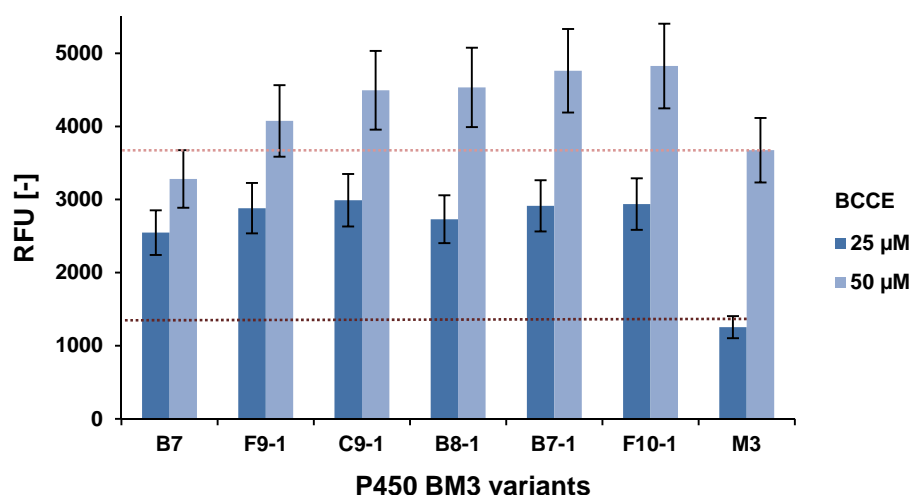


Fig. 54: Activity of P450 BM3 variants selected in the SeSaM library screening and re-screening. Conversion of BCCE (25 μM and 50 μM) in presence of Zn/Co(III)-sep monitored at λ_{ex} 400 nm, λ_{em} 440 nm. Measurements were done in triplicate. Error-bare indicate the error range of the assay.

Sequencing results revealed that all variants had only the substitution F87A, none of them had the parent gene configuration (P450 BM3 M3: R47F F87A M354S D363H).

In summary, the screening of random mutagenesis library generated with the SeSaM method could not identify new hot spots or variants with improved activity. Nevertheless, the selected variant (F87A) had a 2 fold improved activity for the MET compared to the reported variant P450 BM3 M3.

1.4 Saturation and iterative recombination of selected hot spots (R255, R203, I401, F423) for improved MET

The position (R255, R203, I401, F423) detected in the screening of the random mutagenesis library were saturated in the starting gene P450 BM M3 DM (R471C N543S) using the degenerated codon NNK. The NNK codon was selected instead of NNN to reduce the number of stop codons without reducing the number of obtainable amino acid. 200 clones from each library were screened with the fluorescent MTP assay in presence of the alternative cofactor Zn/Co(III)-sep. Additionally, the saturation of position R255 in the variant P450 BM3 M3 DM I401V was screened (Fig. 55).

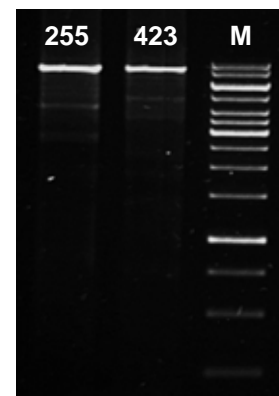


Fig. 55: PCR product of the site saturation mutagenesis at position R255 and F423 separated on 1 % agarose gel and stained with GelRed. Band at 8000 bp corresponding to the gene P450 BM3 (3150 bp) in the vector pET28a(+) (5000 bp).

In all libraries, except the saturation at position R255 in the variant P450 BM3 M3 DM I401V, improved variants compared to the variant P450 BM3 M3 could be detected, but none of them had an increased activity when compared to variant P450 BM3 M3 DM-2 (R203H I401V F423L). Sequencing results of the improved variants showed that on position F423 the amino acid substitution to a leucin was predominant, out of 2 sequenced clones both had the substitution F423L like in the triple mutant P450 BM3 M3 DM-2 (R203H I401V F423L). At position R203 out of 3 sequenced clones 2 had the amino acid substitution R203G and one the substitution R203V. At position R255 the substitution R255Q and like in the triple mutant P450 BM3 M3 DM-2 (R203H I401V F423L) the amino acid substitution R255H could be observed. At position I401, the amino acid substitution I401V could be noticed. The additional saturation of position R255 in variant P450 BM3 M3 I401V didn't lead to improved variants. Concluding, from the single site saturation experiments all detected positions are relevant for the MET, but substitution at position R255 in addition to I401V were not beneficial since variants with reduced activity were observed.

Since the single mutants were more active than the mutant P450 BM3 M3 DM-1 (R255H), the amino acid substitutions were iteratively introduced by SDM into P450 BM3 M3 DM

(R471C N543S). The variants were sequenced, expressed and after CO-normalization the activity with Zn/Co(III)-sep was compared. The generated variants as well as the selected variants in the epPCR-screening are summarized in Table 5.

Table 5: Generated and selected variants which were compared in the activity assay with Zn/Co(III)-sep.

	Name of the variants	Amino acid substitutions						
Variants selected in the individual SSM libraries	C4	M3	N543S	R471C	R203val	I401V		
	E5	M3	N543S	R471C		F423L	I401V	
	H2	M3	N543S	R471C			I401V	
	C6	M3	N543S	R471C				R255Q
Variants selected in the screening of the epPCR library	DM-1	M3	N543S	R471C				R255H
	DM-2	M3	N543S	R471C	R203H	F423L	I401V	
Variants generated by SDM - Iterative recombination	Re-1	M3	N543S	R471C		F423L	I401V	R255Q
	Re-2	M3	N543S	R471C		F423L	I401V	R255H
	Re-A	M3	N543S	R471C		F423L		R255H
	Re-B	M3	N543S	R471C		F423L		R255Q
	Re-3	M3	N543S	R471C	R203H	F423L	I401V	R255Q
	Re-4	M3	N543S	R471C	R203H	F423L	I401V	R255H
	Re-5	M3	N543S	R471C	R203Val	F423L	I401V	
	Re-6	M3	N543S	R471C	R203Val			R255Q
	Re-7	M3	N543S	R471C	R203Val			R255H
	Re-C	M3	N543S	R471C	R203Val	F423L	I401V	R255Q
	Re-D	M3	N543S	R471C	R203Val	F423L	I401V	R255H
	Re-E	M3	N543S	R471C	R203Val	F423L		R255Q
	Re-F	M3	N543S	R471C	R203Val	F423L		R255H

The activity of this generated variants was monitored by the BCCE conversion in the presence of the alternative cofactor and is summarized and compared to the improved variants detected in the first round of directed evolution (epPCR library) (Fig. 56).

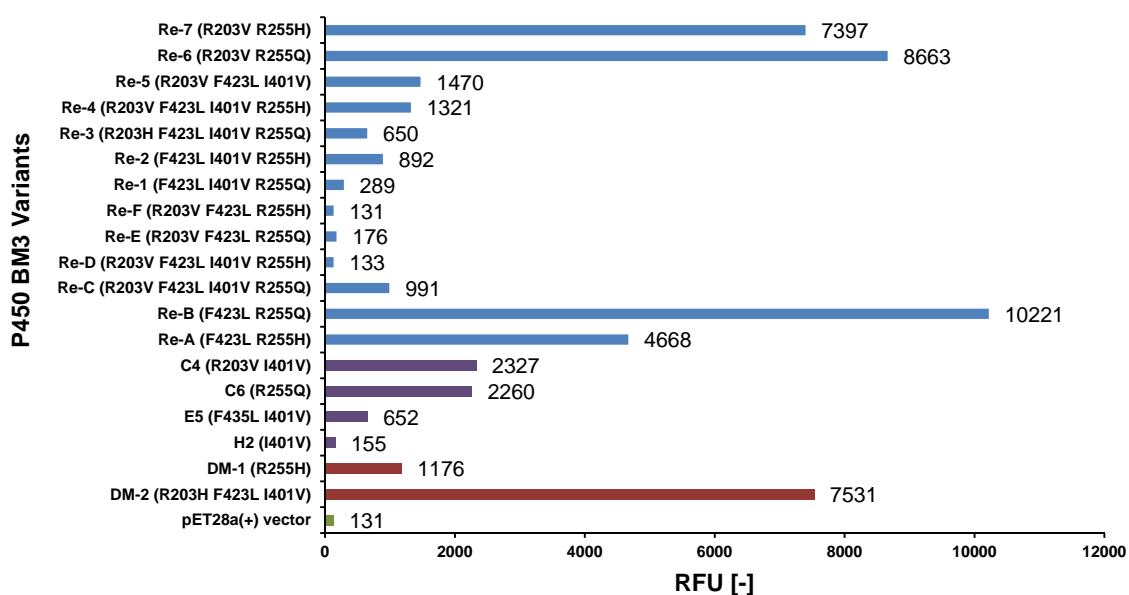


Fig. 56: Activity of the P450 BM3 variants generated in the iterative site saturation mutagenesis libraries (lila bar) or by site directed mutagenesis (blue bar) and compared to the improved variants selected in the first round of directed evolution (red bar). As reference the pET28a(+) vector lacking the P450 BM3 gene is included (green bar). Conversion of BCCE in presence of Zn/Co(III)-sep monitored at λ_{ex} : 400 nm, λ_{em} : 440 nm after protein normalization.

Concluding, position R255 and R203 as well as F423 are relevant for the improved MET. Out of the tested variants (Table 5), the variant Re-6 (R203V R255Q) and Re-B (F423L R255Q) were 1.4 fold respectively 1.15 fold improved compared to the selected variant in the first round of directed evolution (DM-2: R203H F423L I401V). Several combinations are beneficial, but the best showed to be P450 BM3 Re-6 (R203V R255Q). If the substitution I401V was included in addition to substitution at position 423 or 203 (Re-1 and Re-E), the activity dropped drastically under the values monitored for the variant P450 BM3 M3 DM-2. In addition, the combination of substitution I401V with amino acid substitution at position R255 did not lead to any further improvement.

The evolution pathway starting from the reported P450 BM M3 and leading to the variant P450 BM3 Re-6 (R203V R255Q) is summarized in Fig. 57.

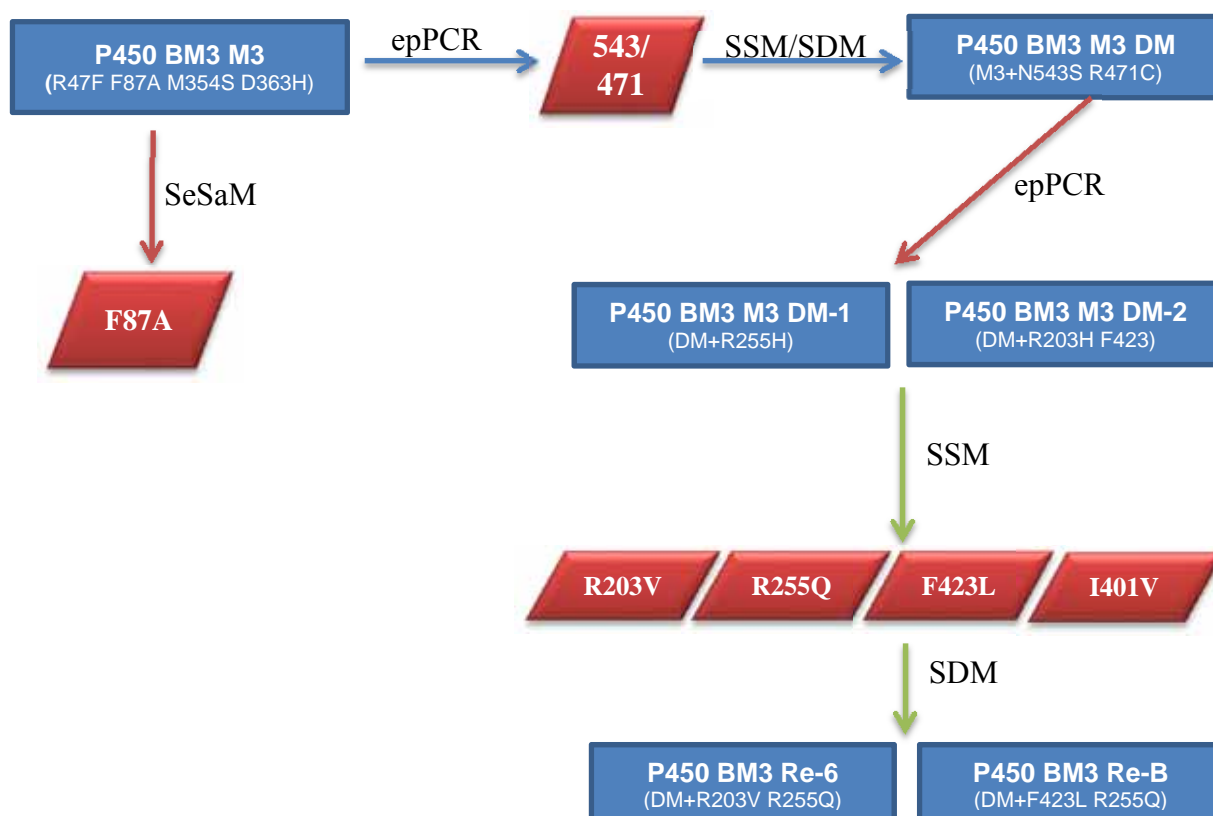


Fig. 57: Scheme of the evolution pathway starting from P450 BM3 M3 and summarizing the selected variants improved for MET. Red trapeze indicates identified positions; blue frames indicate the characterized variants.

1.5 Discussion

This chapter of the thesis describes the aim to further engineer P450 BM3 towards improved MET by directed evolution. Besides the preliminary experiments to setup a suitable screening system, the purification as well as the determination of the P450 concentration were settled according to published protocols (Omura and Sato, 1964a; Schwaneberg et al., 1999b).

The reported fluorescent MTP assay based on the conversion of BCCE (II.1 and III.1.1.1) could be adapted to determine the activity in presence of the alternative cofactor system, applying Zn/Co(III)-sep as electron source and mediator. The coefficient of deviation was determined to be around 13 % using a single endpoint measurement after 30 min which was in the range of applied assays for screening. Standard deviations of less than 15% were reported successful for application in directed evolution campaigns (Wong et al., 2005b). However, in continuous mode, the coefficient of deviation was nearly doubled (26%) and not suitable to be applied as single method to select improved variants in the screening. One reason could be the high deviation in the beginning (first 60 sec) of the kinetic measurement in which the equilibrium between Zn-dust and Zn^{2+} in solution is adjusted (Schwaneberg et al., 2000).

In addition to the fluorescent measurements, the product formation by the P450 variants catalyzed conversion of BCCE was analyzed by Thin Layer Chromatography (TLC) analysis. The reaction of the BCCE conversion by P450 BM3 was analyzed after extraction by TLC. The product formation could clearly be visualized allowing the use of this method as fast activity check. Furthermore, the product detection was confirmed by this TLC method excluding that not only a substrate depletion leading to the fluorescence increase was occurring.

The evolution of P450 BM3 M3 was undertaken by the screening of saturation mutagenesis libraries followed by the generation of focused mutagenesis at position N543 and R471 in which a variant P450 BM3 N543S R471C with a 3 fold improved catalytic efficiency as well as a 2 fold improved K_{cat} could be identified. Interestingly, a synergistic effect could be observed in the double mutant N543S R471C, the K_{cat} was improved whereas the single mutant P450 BM3 M3 N543S and P450 BM3 M3 R471C did not show any improvement. In Fig. 58 the interaction of the amino acid N543 is shown. Both positions are located at the FMN-Heme interface, but the amino acid substitution R471 cannot be displayed because lying in the non resolved crystal structure part. Therefore, the assumption why a synergetic effect between N543S and R471C was observed is difficult to predict. Nevertheless, one of the reasons could be that substitutions at position N543 would loss the hydrogen bonds to the

amino acid S489 lying in close proximity. Leading to the hypotheses that due to the possible weakening of the constitution of two loops a better access of the Co(III)-sep to the e-transport chain was reached.

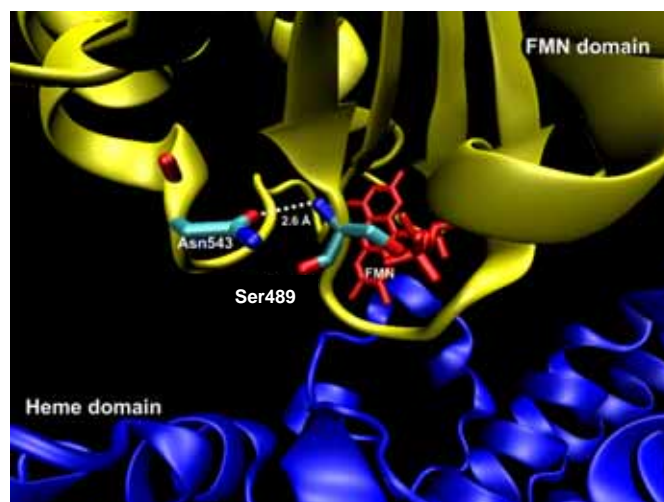


Fig. 58: Crystal structure of P450 BM3. The interaction between amino acid N543 and S489 are displayed.

To identify further improved P450 BM3 M3 variants for the MET, five epPCR as well as four SeSaM libraries were generated, enriched with the flow cytometer and screened in MTP with the fluorescent assay. The selected variants in the epPCR libraries (P450 M3 DM-1: R47F F87A M354S D363H R471C N543S R255H; P450 M3 DM-2: R47F F87A M354S D363H R471C N543S R203H I401V F423L) for improved activity with NADPH and BCCE revealed also to be the most active ones with the alternative cofactor system Zn/Co(III)-sep. A major difference could be observed compared to the obtained kinetic parameters with NADPH; the variant P450 BM3 M3 DM-2 (R203H I401V F423L) (3 fold improved K_{cat}) is more efficient than P450 BM3 M3 DM-1 (R255H) with Zn/Co(III)-sep. The best variant with NADPH was P450 BM3 M3 DM-1 (R255H). Demonstrating that for the MET the position R203, F423 and I401 play an important role. The inefficiency of the alternative cofactor system compared to the natural cofactor NADPH is underlined by the increased K_m values for BCCE and the decreased catalytic efficiency in presence of Zn/Co(III)-sep. In addition, the conversion obtainable with Zn/Co(III)-sep only reaches 10 % (P450 BM3 M3 DM-1 (R255H)) and 50% P450 BM3 M3 DM-2 (R203H I401V F423L) compared to NADPH.

The identified positions (R203, R255, F423, I401) were individually saturated and the beneficial amino acid substitutions were iteratively recombined (Fig. 59). The generated variants were compared and the variants Re-6 (R203V R255Q) and Re-B (F423L R255Q)

showed a 1.4 and 1.15 fold activity increase compared to P450 BM3 M3 DM-2 (R203H I401V F423L).

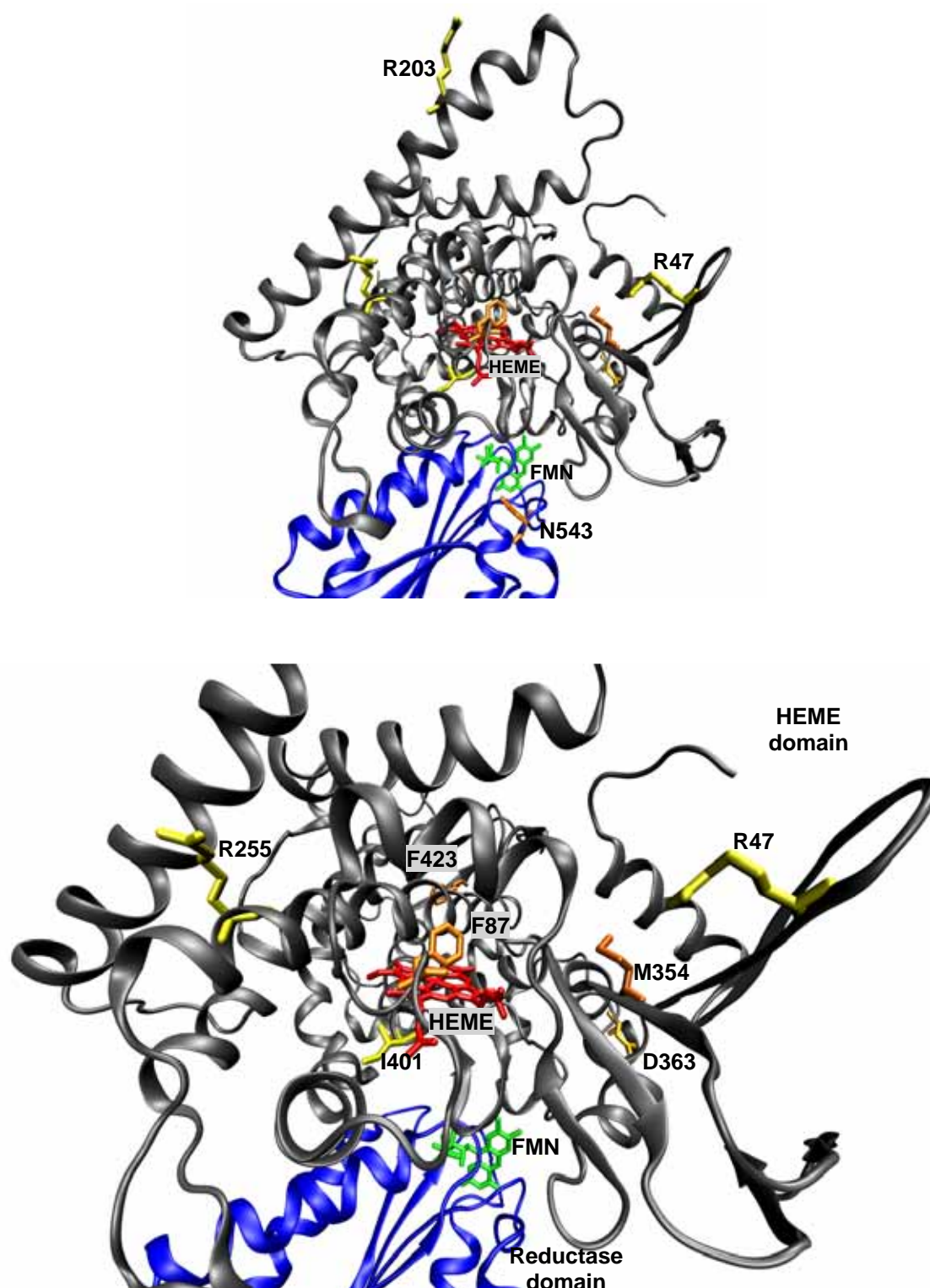


Fig. 59: Crystal structure of P450 BM3: Displayed are the amino acids beneficial for the MET. The upper picture shows the amino acid R203 and R47 and a general overview to localize the position mentioned in the lower picture. The amino acid R47, F87, R255, M354, D363, I401, F423 are displayed in the lower picture.

Position F423 is located around the heme, position I401 is placed beneath the heme in close proximity, position R255 and R203 on the surface whereas R255 is in proximity to the

position F87. Position I401 is located beneath the heme, which allows direct interaction. The amino acid substitution I401P is reported to influence conformations of the heme center, and most probably also the electron transfer. This would indicate that the electrons are transferred from this site to the oxygen in the active center (Whitehouse et al., 2009).

Amino acid substitution at position R255 are reported beneficial in a variant selected for the conversion of short chain alkanes (Glieder et al., 2002; Fasan et al., 2008), indicating that in the variants selected for improved MET, the position R255 lying in close proximity to the position F87A in the catalytic center is relevant for the substrate conversion and probably not influencing electron transfer properties.

In total, out of ten considered and mutated amino acids four arginine (R203, R255, R47, R471) and two phenylalanine residues (F423 and F87) were targeted for saturation mutagenesis. Thus, mainly amino acids (arginine) with electrically positively charged side chains were substituted. Indicating the relevance of positively charged amino acids which are beneficial for the transfer of the negatively charged electrons. At amino acids located in near proximity to the heme iron cluster or in the substrate entrance channel substitution to amino acids with hydrophobic side chains were observed (R47F, F87A, F423L). The amino acid located on the surface of the protein at position R203 and R255 were substituted by epPCR to amino acids with chemical similar properties, arginine substitute to a histidin in both cases. But the best variant in the site saturation library revealed a substitution to an amino acid with a hydrophobic side chain at position R203 (R203V), located on the surface of the protein and to an amino acid with a polar uncharged site chain at position R255 (R255Q). At position I401 and N543 the property of the amino acids remained unchanged.

Position R203 is located on the surface similar to the previously detected position M354 and D363 located in a surface region and reported as relevant for the MET (Nazor et al., 2008).

Up to now, P450 BM3 crystals soaked with the mediator could not be generated and solved. The binding of the mediator or the electron transfer way is not yet described. Two possible hypotheses for the interaction principle between the mediator Co(III)-sep and the protein P450 BM3 can be postulated. On the one hand the mediator is not entering the protein matrix but is shuttling the electron from the outside to the electron transfer chain within the protein (Nazor et al., 2008; Güven, 2011). This hypothesis is supported by the finding of hot spots located in surface region of the protein. On the other hand the mediator may bind in close proximity to the electron transfer chain or near the heme-FMN interface. The electron transfer

chain is not entirely described (Whitehouse et al., 2012) but several amino acids (I401, W1046) which play a crucial role were identified (Sevrioukova et al., 1999a, 1999b).

In contrast, the screening of random mutagenesis libraries generated with the SeSaM method could not identify any new hot spots. Despite the successful generation of the SeSaM library, which was confirmed by sequencing of randomly selected clones, the unsuccessful selection of improved variants after screening stays not understood. Additionally, the enrichment step using the flow cytometer was not successful to enrich the active population over 3 rounds of enrichment to reduce the screening efforts. The decrease of the active population during the enrichment rounds was due to technical problems operating the sorting device. Nevertheless, the screening of the SeSaM library was proceeded in MTP and variants with improved activity could be selected. Sequencing revealed only the substitution (F87A) in all five sequenced clones, none of them had the parent gene configuration (M3: R47F F87A M354S D363H). This was an unexpected result as F87A variant was not used as template DNA. A contamination by the template DNA used for the vector backbone amplification could be excluded as in the PCR reaction, pALXtreme-1a P450 BM3 M3, was used as template DNA.

Interestingly, the selected variant F87A had a 2 fold improved activity for the MET with BCCE as substrate compared to the reported variant M3 (Nazor et al., 2008). The K_{cat} of the selected variant depended on the employed substrate concentration. At low substrate concentration a 2.3 fold improvement compared to a 1.3 fold improvement at higher substrate concentration (BCCE) was observed. The results obtained in this Thesis with BCCE were contradictory to the results reported by Nazor. When the F87A variant was identified as improved variant for MET, the screening was performed with the pNCA assay and the variant M3 was reported as improved for MET compared to F87A variant. (Nazor and Schwaneberg, 2006). Considering that the kinetic data are dependent on the substrate used to determine the activity for MET, the kinetic data reported by Nazor, which were recorded for pNCA, can hardly be compared to the data obtained in this thesis for BCCE.

Nevertheless, the results obtained in this thesis are coherent to the measurements reported by Ley et al. (Ley et al. 2012, submitted). Several variants including the M3 and the F87A were compared to their catalytic performance in the eMTP. The enzyme in presence of the mediator Co(III)-sep was driven in solution by an electrical current, which replaced the Zn-dust as electron donor (Ley et al. 2012, submitted). In these experiments F87A was selected as the most efficient variant for the MET.

Altogether these presented data underline the importance to consider the performance defined in the electrochemical setup together with obtained kinetic data in solution to ensure that

selected variants were improved for the MET. In solution, using Zn/Co(III)-sep as alternative cofactor system instead of NADPH, only a statement about the activity and product formation rate can be formulated. This data doesn't allow an assertion about the electron transfer rate. Therefore an electrochemical characterization would be required.

Additionally considering the analysis of crystals soaked with the mediator Co(III)-sep and extensive modeling work would furthermore allow to verify the obtained experimental data and underline the formulated hypotheses which key amino acid has are responsible and important for MET.

1.6 Conclusions

The evolution of P450 BM3 M3 reported by Nazor et al. for improving the MET could further be extended towards increasing activity in presence of the alternative cofactor system Zn/Co(III)-sep. Subsequent random mutagenesis libraries were generated by epPCR and with the SeSaM method enriched with the flow cytometer assay and screened with the BCCE fluorescent assay in MTP. Variant P450 BM3 M3 DM (N543S R471C) with 3 fold improved catalytic efficiency ($K_{\text{eff}} = 17 \text{ min}^{-1} \text{ mM}^{-1}$) compared to the variant P450 BM3 M3 ($K_{\text{eff}} = 5 \text{ min}^{-1} \text{ mM}^{-1}$) and subsequently variant P450 BM3 DM-2 (R203H F423L I401V) which had a nearly 4 fold improved K_{cat} (P450 BM3 DM-2: $K_{\text{cat}} = 6.8 \text{ min}^{-1}$, P450 BM3 DM: $K_{\text{cat}} = 1.8 \text{ min}^{-1}$) were identified. Four new hot spots (R255, R203, F423, I401) could be identified, which were not reported before for the MET. These identified positions were individually saturated and the recombination of the beneficial amino acid substitution led to variants (Re-6 (R203V R255Q) and Re-B (F423L R255Q)) respectively 1.4 fold and 1.15 fold improved in activity compared to P450 BM3 M3 DM-2 (R203H F423L I401V). Summarizing, the selected improved variants give valuable information, which amino acid substitutions are relevant for the MET but further investigation through an electrochemical characterization would be necessary to confirm an improved electron transfer rate.

III.2 Evolution of P450 BM3 towards improved Direct Electron Transfer (DET)

The alternative cofactor system using a conductive polymer as electron donor for P450 BM3, which is described as direct electron transfer (DET) was reported first by Nazor et al. (Nazor, 2007). The evolution of P450 BM3 by screening of focused mutagenesis libraries with the 4-AAP assay was reported to improve P450 BM3 for DET. The best reported variant P450 BM3 Y51F T577G was 100 fold increased in activity in presence of Baytron P compared to the natural cofactor NADPH.

In this chapter of the thesis, the aim is to further engineer P450 BM3 towards improved DET by directed evolution. The PEDOT/PSS formulation is used as reduced polymer modeling the DET. Starting variant for the work performed in this thesis is the reported activity improved variant P450 BM3 Y51F T577G (Nazor, 2007).

The conductive polymer used in previous experiments was Baytron P (obtained from H.C. Starcks, Leverkusen, Germany). Baytron P is a conductive polymer containing mainly PSS and PEDOT in a ratio of 1 to 2.5. In 2009 the Baytron P formulation was renamed as Clevios P by H.C Starcks, but the composition remained similar and unchanged in the ratio of PSS to PEDOT, as stated by the company. In this thesis, only the new batch of conductive polymer (Clevios P) was available and could be used. Preliminary experiments showed that P450 BM3 could not hydroxylate the target substrate 3-phenoxytoluene in presence of Clevios P with the reported product formation rates for Baytron P. No product formation in presence of only the conductive polymer could be observed. Therefore the prerequisites for an efficient screening system had to be optimized prior to the mutagenesis and evolution of P450 BM3. The 4-aminoantipyrine (4-AAP) assay was optimized, the linear detection range was determined and the coefficient of deviation of a 96 well plate was calculated. Subsequently, the variant P450 BM3 was evolved first by focused mutagenesis approach and then by a random mutagenesis. Finally, the reaction performed with purified protein was analyzed in detail to elucidate if the obtained signal during the activity measurements correlated with product formation or was due to the deviation of the background signal.

2.1 Colorimetric screening assay for activity detection in presence of a conductive polymer as alternative cofactor

Prerequisite for a successful directed protein evolution is a medium or high throughput screening assay allowing to sample the diversity of the generated libraries in an efficient and reliable way (Tee and Schwaneberg, 2007). Various medium throughput microtiter plate

screening assays were reported for P450 BM3 (Whitehouse et al., 2012). Widespread assays are based on depletion of NADPH (Arnold and Georgiou, 2003) as well as others like indol hydroxylation (Li et al., 2000, 2008) or pNCA assay (Schwaneberg et al., 1999a). All these assays were reported to be very efficient and successfully applied in directed evolution campaigns to engineer P450 BM3 towards properties such as activity, stability as well as mediated electron transfer (Tee and Schwaneberg, 2007; Whitehouse et al., 2012).

The 4-AAP assay is a 60 years old detection system developed by Emerson and already used in the 1950 by Ettinger and coworkers to detect $\mu\text{g/L}$ levels of phenol in water (Powell et al., 1984). A phenol-4-aminoantipyrine dye complex is formed by an oxidative coupling reaction mechanism (Faust and Mikulewicz, 1967), leading to a p-quinoid species. The extended conjugated system causes the change in color from uncolored to purple-red. A screening assay based on this phenol detection principle was reported for successful evolution of P450 BM3 for hydroxylation of aromatic compounds to phenolic products (Wong et al., 2005b). Scheme in Fig. 60 describes the 4-AAP detection system reported by Wong et al. (Wong et al., 2005b).

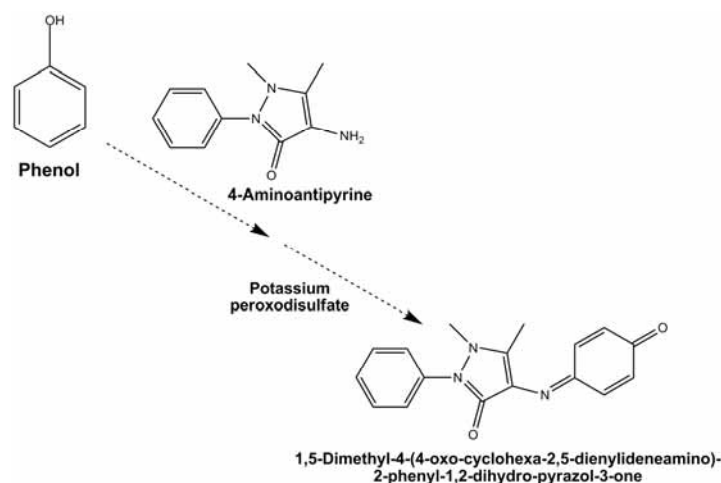


Fig. 60: Scheme of the 4-AAP detection system (Wong et al., 2005b).

In the present study the 4-AAP assay was selected, due to its high sensitivity (50 to 500 μM) and reliability to screen for improved P450 BM3 variants. This assay was reported as successfully applied to screen for activity improved P450 BM3 variants in presence of a conductive polymer (Baytron P) as alternative cofactor system. Fig. 61 shows the reaction scheme of the P450 BM3 catalyzed hydroxylation of 3-phenoxytoluene. The subsequently formed product, 3-phenoxytoluene, can be detected by the 4-AAP detection system (Wong et al., 2005b).

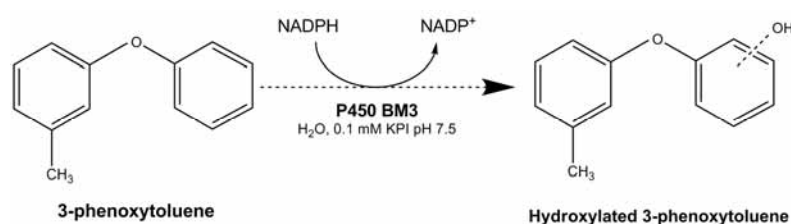


Fig. 61: Scheme of the P450 BM3 catalyzed reaction used in the screening assay to improve the catalyze for the direct electron transfer.

2.1.1 Optimization of 4-AAP assay

Screening systems with standard deviation less than 15 % have successfully been used in directed evolution experiments (Schwaneberg et al., 1999a; Wong et al., 2005b). Preliminary experiments showed that P450 BM3 could not hydroxylate the substrate 3-phenoxytoluene in presence of Clevios P with the reported product formation rates for Baytron P. The reported protocol for the 4-AAP screening system in presence of Baytron P could not be alienated to the use of Clevios P. Using this protocol, no activity in presence of Clevios P could be detected. This first experiments already indicated that most probably no direct electron is present and the previous reported data could not be confirmed. The addition of only the polymer without regeneration system, might limit the reaction.

The very low conversion rates and subsequently the only hardly detectable signal to background ratio lead to the addition of NADPH to the reaction mixture in supplementary to the presence of the conductive polymer. Just with a clearly detectable activity, the different assay parameters could be analyzed and optimized. The described 4-AAP screening assay had to be optimised to a 96- well plate format ensuring an easy to handle screening procedure with a low standard deviation in presence of the conductive polymer Clevios P.

Therefore, the amount of buffer (100-500 μ l), the buffer type (KPI, Tris/HCl), the buffer concentration (0.1-1 mM), the volume of crude lysate (20-300 μ l), the cell permeabilization method (lysozyme or polymixin B), the substrate concentration (2-10 mM 3-phenoxytoluene) and the volume of conductive polymer were varied. Neither the high buffer concentrations nor the type of buffer influenced the activity of the protein. The enzyme showed the highest activity in a pH range from 7 to 8.5 with an optimum at pH 7.8. Lysozyme lysed cells increased the activity compared to polymixin B permeabilized cells. Increased substrate concentration did not increase the activity, proving that the substrate was not a limiting or inhibiting factor. Similar, increased DMSO concentration did not increase the activity of the protein. On the contrary, the activity decreased with DMSO concentration higher than 5 %.

Analogue, no activity could be detected by increasing the volume of cell lysate or the concentration of conductive polymer. The conductive polymer Clevios P decreased pH within the reaction mixture. The Clevios P stock solution had a pH of around 4. Therefore, only 10 % clevios could be added to the reaction mixture without any drastic pH drop (pH of the reaction between 7.0 and 7.8), involving an enzyme inactivation at low pH range. Furthermore, the concentration of the colorimetric reaction compounds (4-aminoantipyrin (4-AAP) and peroxodisulfate solution) was varied to increase the difference between the detectable signal and the background reaction. The colorimetric reaction was reported to be efficient at pH > 9 by addition of 0.18 mg/ml of each compound. Due to the acidic pH of Clevios P the volume of supplemented quenching buffer (0.1 M NaOH, 4M Urea) was increased from 25 μ l (Wong et al., 2005b) to 35 μ l, when using in the deepwell format 180 μ l supernatant to efficiently elevate the pH above 9. By varying the amount of 4-AAP and peroxodisulfate solution from 0.075-0.4 mg/ml no increase in the detectable signals could be reached. Therefore, the addition of 0.2 mg/ml of 4-aminoantipyrine and potassium peroxodisulfate solution (Arnold and Georgiou, 2003) was maintained. In the experimental part the screening assay protocol with finally employed concentrations is described.

2.1.1.1 Removal of the conductive polymer

Besides the optimisation of the screening system parameters an important fact was the effective precipitation of the conductive polymer in the reaction mixture to perform the colorimetric detection. After enzymatic conversion with permeabilized cells expressing P450 BM3, the plates were centrifuged to obtain a clear supernatant which was analysed by the 4-AAP colorimetric reaction and the amount of phenolic products quantified. Since, Clevios P is a water soluble dispersion, it was not removable from the reaction mixture by centrifugation, the cell free supernatant stayed light gray to black, which disturbs the colorimetric detection (Fig. 62).

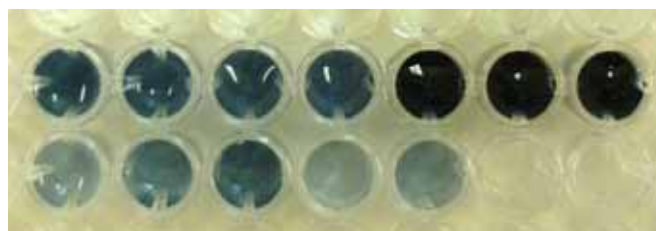


Fig. 62: Reaction mixture of the 3-phenoxytoluene conversion by P450 BM3 (cell free supernatant) with Clevios P, after centrifugation. Light gray: Clevios 1:10 dilution; dark black: Clevios P undiluted.

The employed conductive polymer Clevios P had an absorption maximum in the reduced state at 650 nm. Fig. 63 shows the adsorption spectrum of Clevios P under reduced and oxidized

condition. Even in a dilution of 1:10, corresponding to employed concentration in the enzymatic reaction, the absorption spectra was interfering with the detection wavelengths of the 4-AAP, measured at 509 nm and 600 nm. The obtained background of the conductive polymer was not negligible and was depending on the volume of lyzed protein. Absorption of ~ 0.35 was reached with a Clevios dilution of 1:10, which corresponds to the concentration used in the enzymatic reaction. Additionally, Fig 63 proves that Clevio P is in an oxidized state when added to the enzymatic reaction, which is contrast productive as reduced polymer with a redoxpotential > -400 mV is required reduction of the enzyme and effective enzymatic conversion.

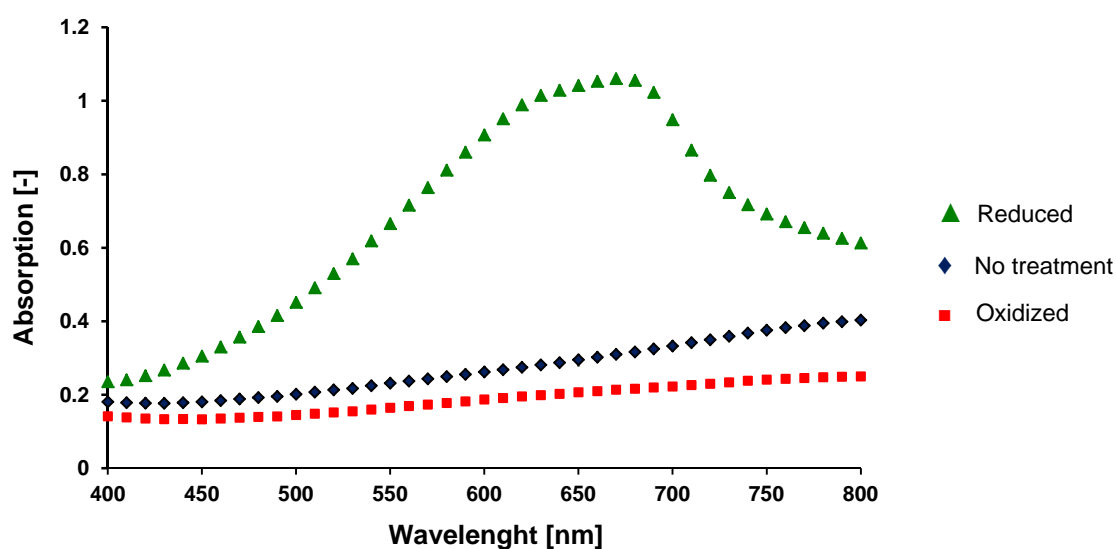


Fig. 63: Absorption spectrum of oxidized (■), reduced (▲) and non treated Clevios P (1:10 dilution) (◆). Clevios P was oxidized with potassium peroxodisulfate and reduced with Natriumdithionite.

With the aim to develop a screening assay for DET, the interference of the conductive polymer with the colorimetric detection had to be solved and was investigated by the addition of different additives, filtration and precipitation methods. All parameters mentioned in section 2.1.1 assay optimisation, did not solve the challenges applying Clevios P as alternative cofactor. Thus, first as simplest method reported effective for Baytron P, the precipitation of Clevios was tried by centrifugation. The reactions mixture was centrifuged from 1000 to 11000 g force as well as at different temperatures. In addition a pH shift and heating the reaction mixture up to 95°C was applied before centrifugation. No precipitation of Clevios in the reaction mixture could be achieved. Clevios P could only be partially removed from the reaction mixture in presence of lyzed cells, observed during the assay optimization. The hypothesis was postulated that Clevios P probably binds to an unidentified compound in the cell lysate. For this reason, cell debris from cells expressing the empty vector was prepared by

sonification and supplemented to the enzymatic reaction. Again, no precipitation could be obtained by this treatment. Furthermore, the addition of additives like agarose, SDS, alginat, gelatine, binding the polymer to anion, cation exchange and size exclusion matrix like used for the protein purification, addition of metal ions (Cu, Co, Zn), filtration through 22 μ M filters or membranes (cellulose, PVDF, nylon) were investigated without success. Finally, the reaction mixture was supplemented with BSA, polymixin B sulfat and lysozyme at high concentrations (100 mg/ml). Polymixin B had no effect, after centrifugation the polymer stayed in solution. In fact, only lysozyme had an effect. After addition of 5-50 mg/ml lysozyme, Clevios could effectively be precipitated by centrifugation and the supernatant remained as clear solution. Fig. 64 shows the supernatant of the enzymatic reaction after conversion and Clevios precipitation as pellet using lysozyme.

Concluding, the conductive polymer could efficiently be separated from the reaction mixture so that the color detection was not interfered. The observed correlation between the presence of lysed cells and the increasing Clevios P precipitation became explainable. As the lysozyme concentration was increased proportional to the amount of cells in the reaction mixture, the improved Clevios precipitation in fact was related to the increasing lysozyme concentration.

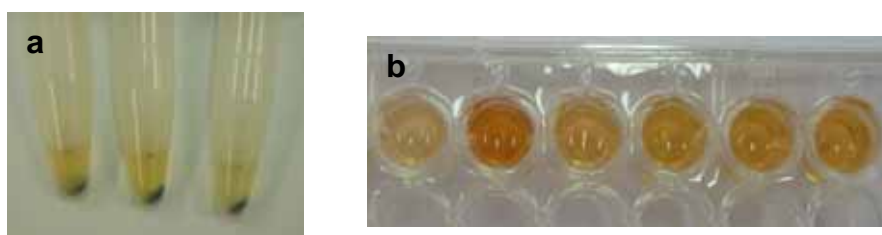








Fig. 64: Reaction mixture after Clevios P precipitation. a) Reaction mixture identical to the one in Fig. 62 with lysozyme treatment before centrifugation. b) Colorimetric assay performed with the supernatant from the 3-phenoxytoluene conversion with Clevios P.

2.1.1.2 Influence of the conductive polymer formulation

The detectable activity in presence of the conductive polymer remained very low, also after the described optimisation of the assay. To improve the enzymatic conversion rate several conductive polymer formulation similar to Clevios P were tested (Table 6). The formulation contained different ratios of PEDOT/PSS and additives like organic solvents and polymeric binders.

Table 6: Overview of the available Clevios formulations and the specifications (Quelle: H.C. Starcks).

	moderate conductivity —————→ high conductivity	PEDOT:PSS ratio	Viscosity at 100 s ⁻¹ [mPas]	Solid Content [%]
After addition of 5% Demethylsulfoxid				
Clevios P		1:2.5	60-100	1.2-1.4
Clevios PH		1:2.5	Max. 25	1.2-1.4
Clevios PH 510		1:2.5	20-100	1.5-1.9
Clevios S HT		1:2.5	3-5 dPas	Not specified
Clevios F CPP 105 DM		1:2.5	30-60	1.0-1.4
Clevios F E		1:2.5	40-80	2.2-2.6

The activities of the enzymatic conversion in presence of the conductive polymer formulation were determined and compared to the activity obtained with Clevios P, considering the addition of equal Clevios P volumes for the enzymatic reaction (Fig. 65).

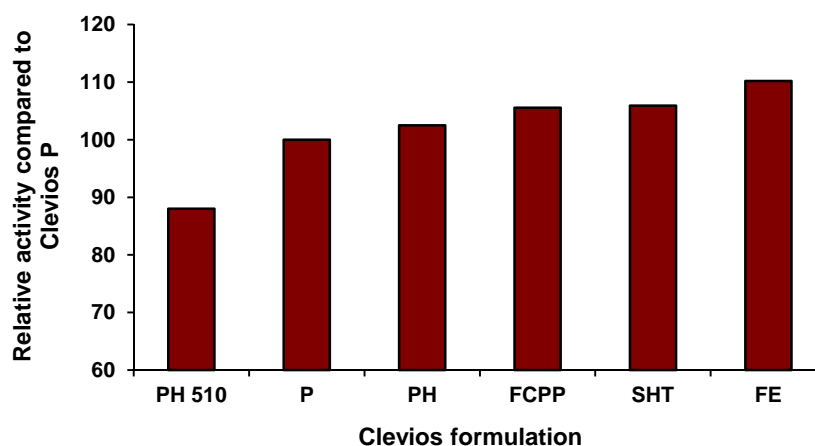


Fig. 65: Influence of Clevios P formulation on the enzymatic activity

With the assumption that the signal obtained in the activity assay can be considered as activity, Clevios FE showed the highest product formation rate. Nevertheless, the difference in activity was less than 12%, which is in the error range of the 4-AAP assay (Wong et al., 2005b). Clevios P was maintained for further experiments as the activity increased not more than 10%. More probable would be the conclusion that no product formation is obtained. Due to this observation and to keep data comparable to cooperation partners and previous measurements Clevios P was used for further investigations.

2.1.2 Linear detection range of the 4-AAP assay

The adapted assay allowed the detection of phenolic product in presence of the conductive polymer Clevios P in a range from 0.1–0.6 mM. Hydroxylated 3-phenoxytoluene was not commercially available, therefore phenol was selected as reference compound according to Wong et al. (Wong et al., 2005b). The calibration curves were established in triplicate maintaining the same conditions as in the assay procedure (Fig. 66). To avoid the influence of lysozyme or Clevios P on the phenol concentration in the samples, calibration curves were performed with and without addition, but no adsorption of phenolic compounds could be observed. Equation (1) and (2) were obtained by linear fitting of the calibration curve data and applied for calculation of generated product amounts.

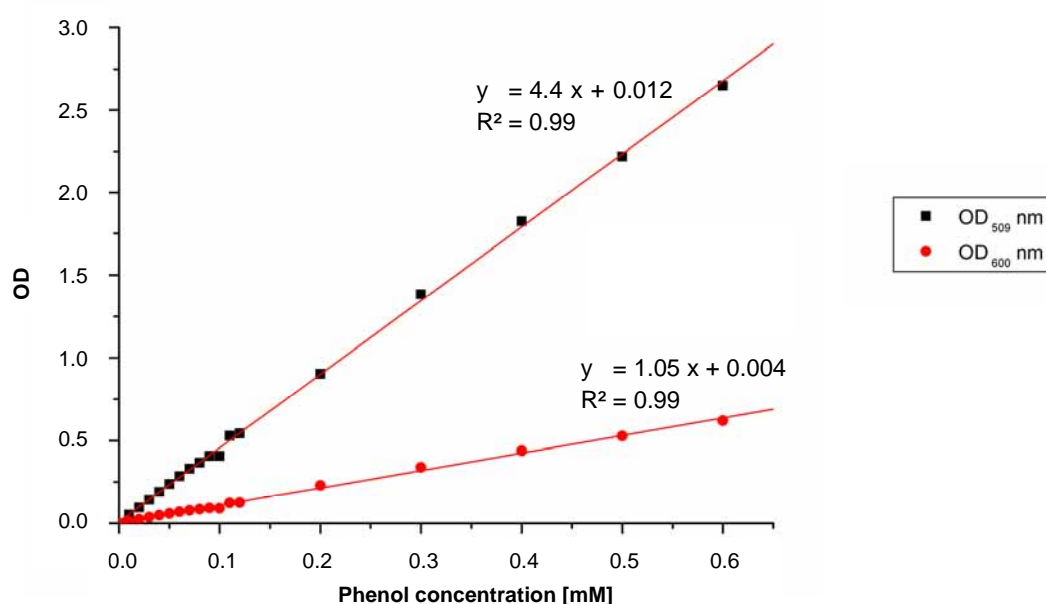


Fig. 66: Calibration curve of the 4-AAP assay for phenol detection.

2.1.3 Activity check and standard deviation in 96 well plate format

The detectable activity in presence of the conductive polymer remained very low, also after optimisation of the MTP screening assay. Commonly, the product formation rate was 10 fold lower with the alternative cofactor as with the natural cofactor NADPH. The detected OD_{509 nm} increase after 1h conversion was around 0.03 with Baytron P compared to 0.3-0.8 with NADPH, which was in case of Clevios P under the reported detection limit for the 4-AAP assay. Nevertheless, the standard deviations of 96 well plates were determined with Clevios P to be 7.4% for P450 BM3 WT, 3.7% for P450 BM3 Y51F and 4.8% for P450 BM3 Y51F T577G (Fig. 67). All assay optimization and activity check were performed with the assumption that the signal obtained in the activity assay can be considered as product

formation and is not due to deviation of the background signal. The absorbance values of the cells expressing empty vector were high compared to the expected active and improved variant P450 BM3 Y51F T577G. Concluding, the absorbance difference between the non mutated P450 BM3 WT, the reported improved variant Y51F T577G, and the empty vector was hardly detectable. Leading to the conclusion that no activity could be detected. This is only due to the lack of a suitable electron donor, Clevios P without applying a reducing potential and without regeneration system cannot deliver electrons to the enzyme. The 4-AAP assay itself is working because when NADPH is supplemented to the reaction, a clear activity increase and difference between the empty vector and the P450 BM3 variant can be measured.

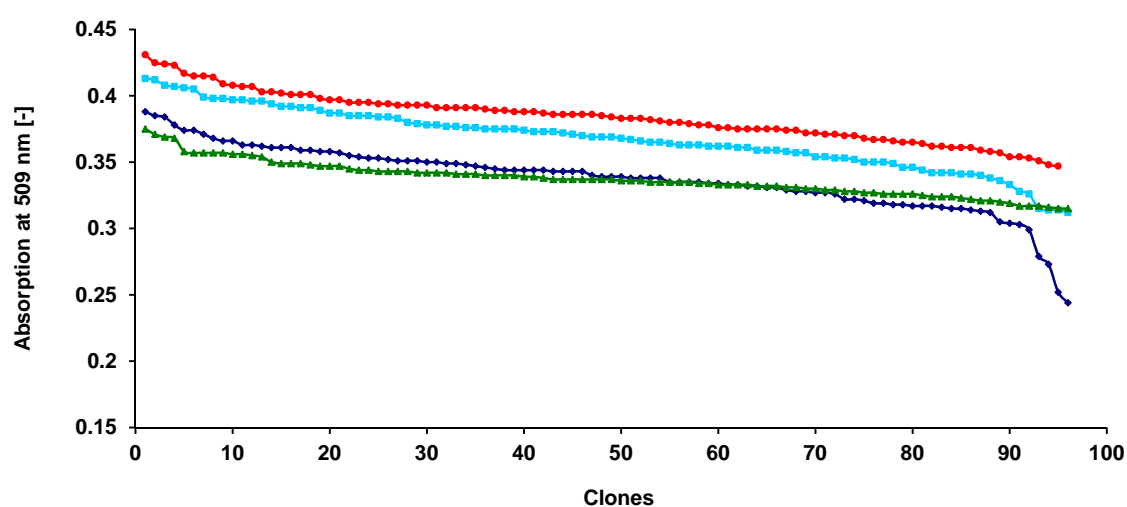


Fig. 67: Standard deviation in 96 well plates format of the 3-phenoxtoluene conversion in presence of the conductive polymer Clevios P as alternative cofactor system by P450 BM3-WT (◆), pET28a(+) empty vector (●), P450 BM3-Y51F (▲) and P450 BM3-Y51F T577G (●). Product detection with the 4-AAP assay.

Mutations inside the P450 BM3 genes were verified by sequencing and the activity measurements done in triplicate to ensure that a permute of the plasmids could be excluded. However, after solving the main problem which made measurements in 96 well formatted or with crude cell lysate impossible, the detectable activity stayed very low and was hardly to differentiate from the vector lacking the P450 gene (Fig. 67), the product formation rates of P450 BM3 WT were even lower. Only variant P450 BM3 Y51F T577G showed higher absorption values as pET28a(+) vector lacking the P450 BM3 gene.

Nevertheless, the optimised assay could be employed to evolve P450 BM3 for DET since the assay has a low standard deviation. The detection of variants with improved activity would be possible. As for proteins engineered and screened for new properties the starting gene does not or only very barely pose the ability of the targeted properties.

2.2 Protein engineering of P450 BM3 for improved direct electron transfer (DET)

The hypothesis formulated by Nazor et al. that mutations at the FMN interface could widen a water access channel for the polymer PEDOT/PSS to the FMN domain facilitating the electron transfer was traced for Clevios P. Additionally, screening of focussed mutant libraries at positions in proximity to the FMN binding site yielded a mutant bearing the amino acid exchange T577G with a significantly improved activity with the conducting polymer Baytron P (PEDOT/PSS) (Nazor, 2007). Therefore, based on crystal structure investigations, four amino acid positions were selected with the aim to bring the water-soluble conducting polymer PEDOT/PSS in close proximity to the electron transfer chain of P450 BM3. The structure guided approach was complemented by a random mutagenesis approach, in which epPCR libraries were generated to detect new hot spots and evolve the catalyst P450 BM3 for improved direct electron transfer (DET).

2.2.1 Role of the FMN in P450 BM3 Y51F T577G

Besides the evolution of P450 BM3 for improved DET, the understanding of the function relationship of the DET is of importance. Screening of a site-saturation library at amino acid position 577 close to the cofactor flavinmononukleotide (FMN) yielded a mutant bearing the amino acid exchange T577G with a significantly improved activity using a conducting polymer such as Baytron P (PEDOT/PSS) (Nazor, 2007). Nazor et al. proposed that the conductive polymer is binding in close proximity to the FMN binding site and could directly transmit electrons to the electron transfer chain. This raised up the question for the importance of the bound FMN cofactor. The T577G substitution might lead to breaking of hydrogen bonds to W574 or FMN (Nazor, 2007). Loss of either of them would allow more flexibility in the polypeptide backbone, leading to a destabilization of the FMN in its binding cavity (Nazor, 2007). The variant Y51F T577G was reported to show no activity with the natural cofactor NADPH, this postulated the hypotheses that the FMN is lost due to the mutation T577G and the FMN cavity is increased, which would allowed easier access of the conductive polymer to the electron transfer chain.

Hence, it was reasonable first to verify the fate of the cofactor FMN upon substitution at position T577 before choosing further amino acid positions for the construction of further structure guided mutant libraries of P450 BM3. FMN can be detected through his specific absorption or fluorescence spectrum. Absorption maxima at 370 nm and 450 nm as well as fluorescent properties (λ_{ex} 450 nm and λ_{em} 520 nm) (Viñas et al., 2004) are characteristic for

the unbound form of FMN. Since the cofactor flavinadeninucleotide (FAD) of the reductase-domain shows a very similar fluorescence spectra compared to FMN, reductase-deficient mutants were constructed. The truncated versions of P450 BM3 Y51F and P450 BM3 Y51F T577G were constructed by PCR amplification and cloned in pET28a(+) by the restriction enzymes NcoI/EcoRI and T4-ligase (Fig. 68).

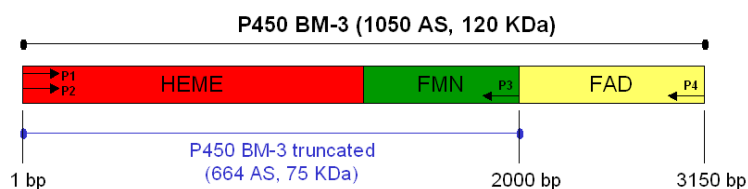


Fig. 68: Scheme of the generated FAD deficient P450 BM3 variant. P1-P4 indicates the primer used, sequences are given in the Table S1 (Appendix 6.1).

Both proteins were expressed and purified according to standard protocols (Schwaneberg et al., 1999b). The purity of both variants was checked on a SDS-gel (Fig. 69: Lane 2 and 3). The truncated protein has a size of around 75 kDa and purity with up to 90 % were generated.

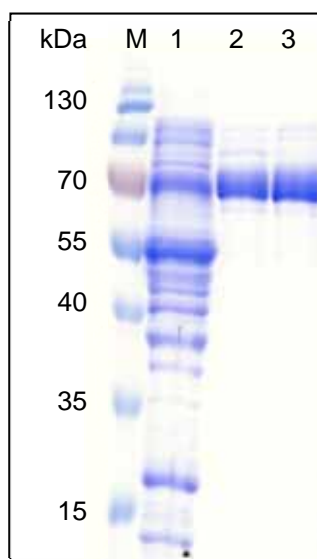


Fig. 69: SDS-page of the purified P450 BM3 Y51F T577G truncated protein. Lane M: PageRuler Prestained Protein Ladder (Fermentas), Lane 1: non bond protein washing fraction, Lane 2 and 3: purified P450 BM3 Y51F T577G truncated at the FMN domain.

To identify the presence of the FMN, absorption and fluorescence spectra were recorded and compared (Fig. 70). The obtained data for variant P450 BM3 Y51F T577G was compared to the truncated P450 BM3 Y51F to investigate the impact of the substitution T577G on the fate of the FMN.

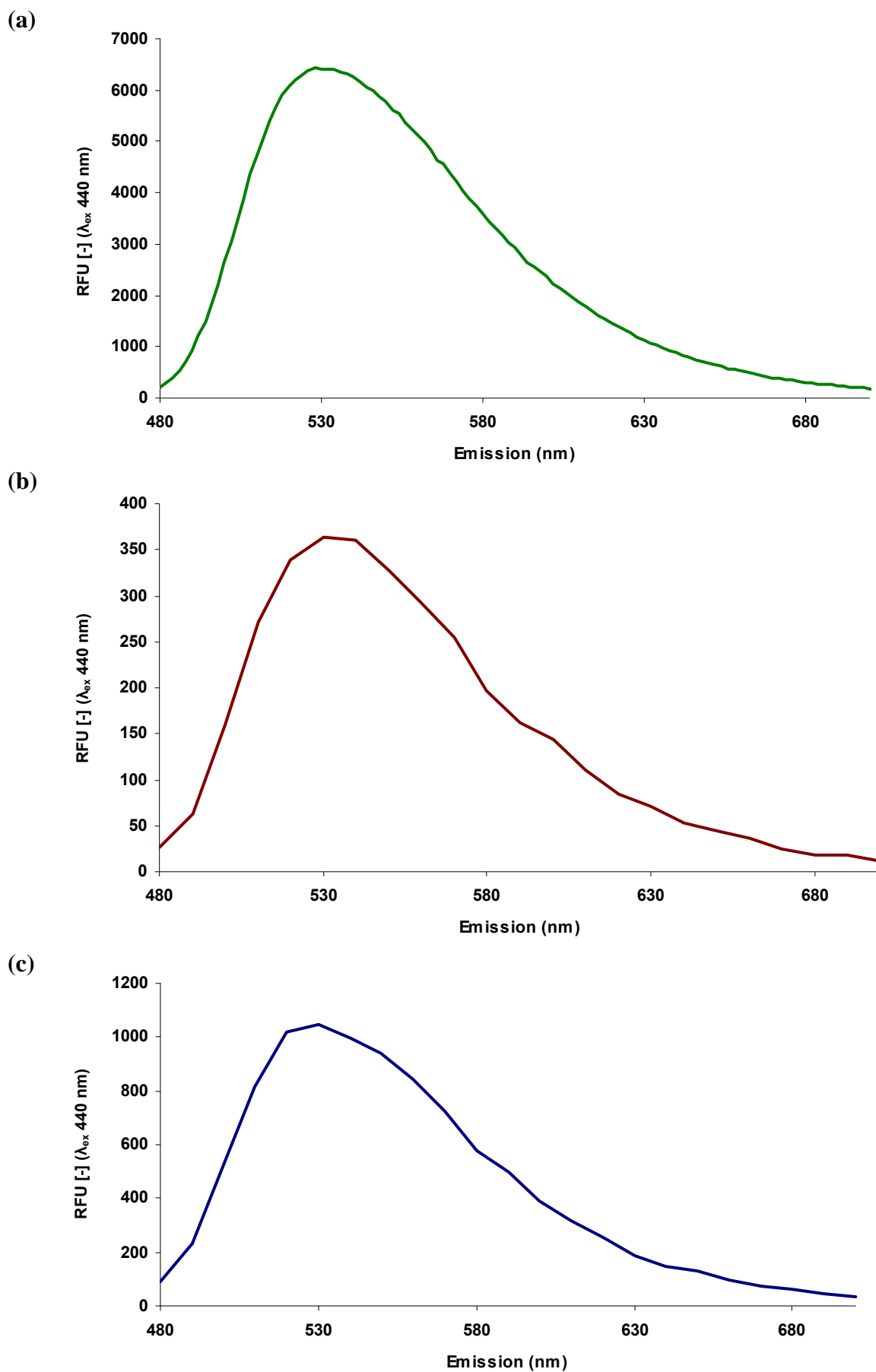


Fig. 70: Fluorescence emission spectra from 460 – 700 nm of (a) FMN, (b) purified Heme-FMN-domain of P450 BM3 Y51F and (c) purified Heme-FMN-domain of P450 BM3 Y51F T577G (λ_{ex} 440 nm).

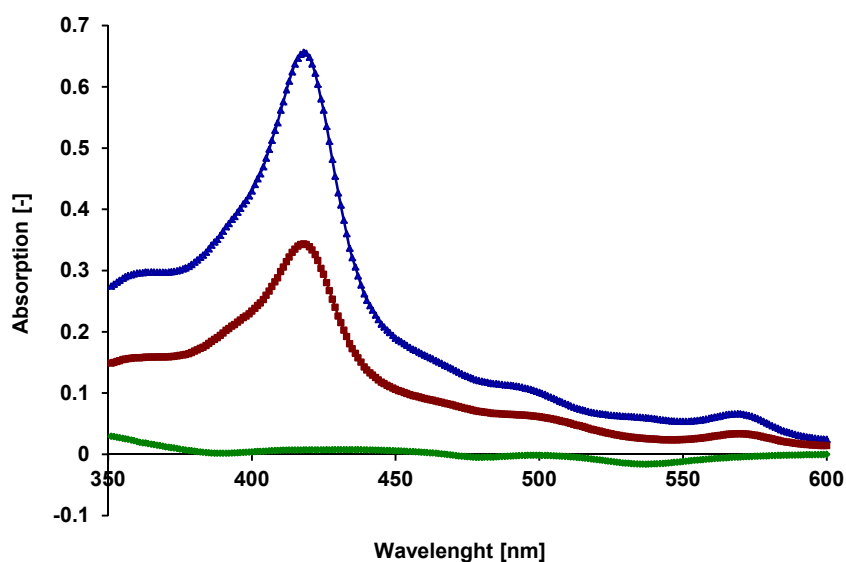


Fig. 71: Absorption spectra from 350–600 nm of Buffer (◆) (KPI 0.1M pH 7.5), purified Heme-FMN-domain of P450 BM3 Y51F (■) and purified Heme-FMN-domain of P450 BM3 Y51F T577G (▲).

Recorded fluorescence spectra indicated that the FMN is not lost after introducing amino acid substitution T577G (Fig. 71). The characteristic peak for FMN at 520 nm was observed in the absorption/fluorescence spectra as well as in the full sized P450 BM3 protein and the truncated variants (Y51F and Y51F T577G). The characteristic spectrum was not observed in fractions which were earlier eluted from the purification column and only contained very low P450 BM3 amounts. No differences in the absorption spectra could be observed. Each spectrum of the variants revealed an absorption maximum at 417 nm, corresponding to the heme iron cluster. This peak was overlaying the absorption maxima at signal 370 nm and 450 nm which are characteristic for the FMN. However, the FMN cannot clearly be distinguished within the absorption spectra. T577G compared to the non mutated variants, the FMN is not missing.

2.2.2 Structure guided mutant libraries

Accordingly to the results in section 2.1, five residues in the FMN-cavity of P450 BM3 were selected to enhance the activity of the monooxygenase with the conducting polymer Clevis P. Based on bioinformatics and structural analysis of P450 BM3 four structure-guided mutant libraries of P450 BM3 Y51F T577G at positions 488, 536, 537 and 574, which most likely interact with FMN through hydrogen bonds, were constructed (Fig. 72). Additionally, position 471 was selected, which was indicated as being essential for P450 BM3 activity in libraries generated for Mediated Electron Transfer (MET) (section III.1).

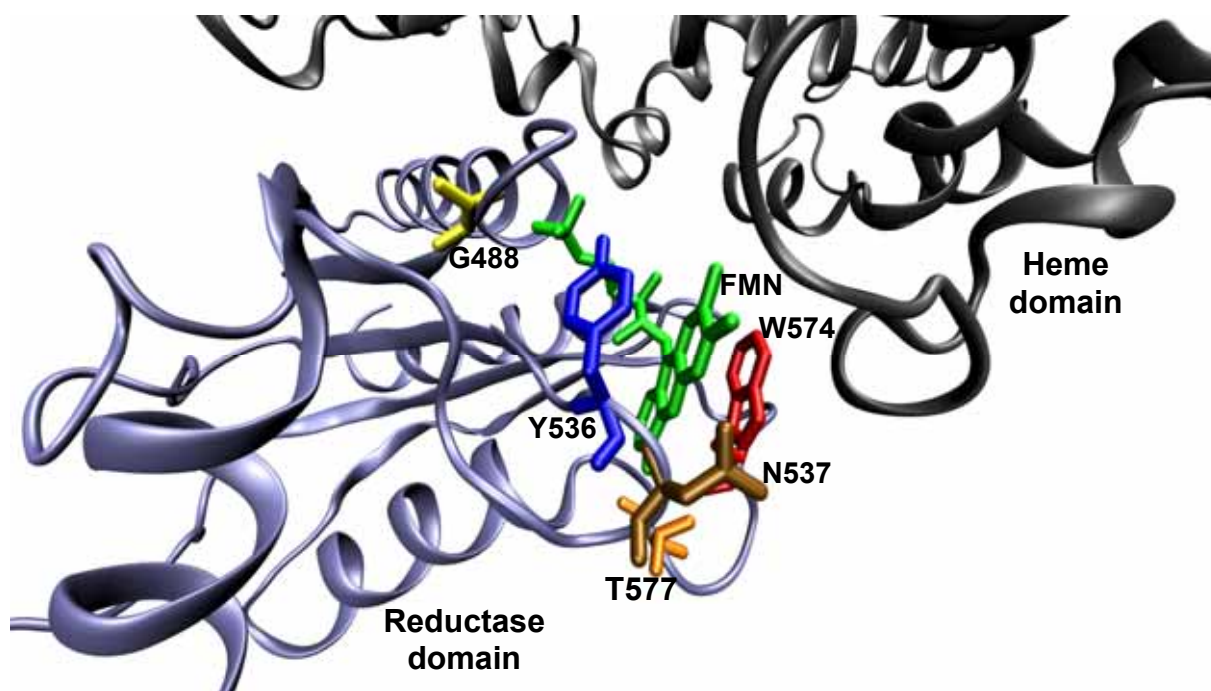


Fig. 72: Crystal structure of the P450 BM3 FMN-binding site. Displayed are the cofactor FMN (green), residue T577 (orange) and the four residues G488, Y536, N537 and W574 (yellow, blue, tan, orange) which were selected for site-saturation mutagenesis.

2.2.2.1 Screening of SSM libraries

All sites (R471, G488, Y536, N537, and W574) selected for the structure guided mutant libraries were NNK saturated using P450 BM3 variant Y51F T577G as template. Amino acid residue W574 was additionally saturated in the variant Y51F. 400 clones of each library (in total 1600 colonies) were screened with the 4-AAP assay and the substrate 3-phenoxytoluene for improved activity with the conducting polymer. The screening result of one plate is represented as example in Fig. 73. The activity increase of the improved variants compared to the starting variant P450 BM3 Y51F T577G stayed below 15 %.

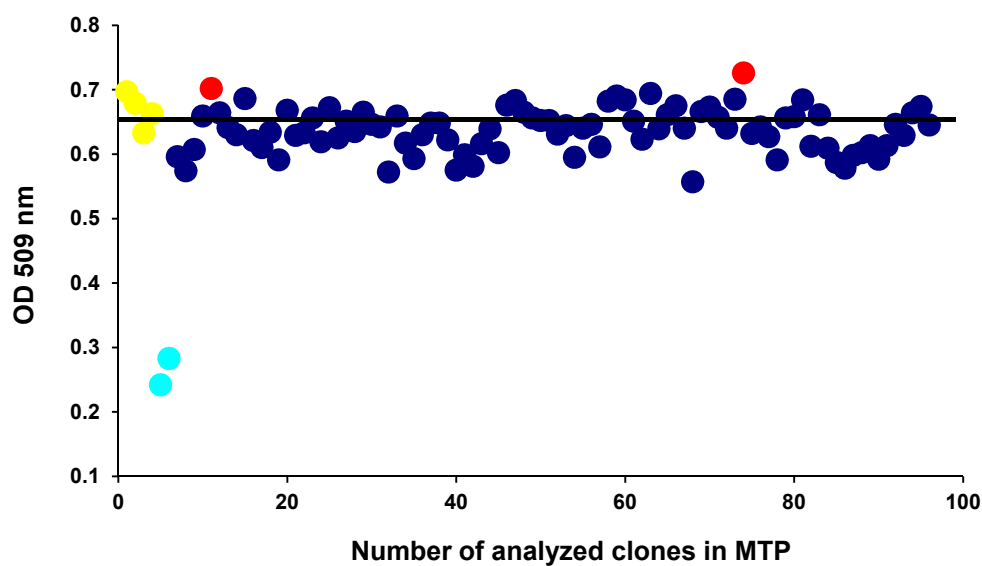


Fig. 73: Example of screening results from one 96 well plate from SSM 471 library. (●) clones from SSM library, (●) clones with improved activity, (●) wells with only media, (●) clones with parent gene Y51F T577G served as reference, (—) represents the arithmetic average of the activity from the starting variant, serving as threshold to select improved variants.

After re-screening of the best variants (10 % of each library), relative activities with crude lysate compared to the parent P450 BM3 Y51F T577G were determined (Fig. 74). Subsequently, two to four selected clones of each library were sent for sequencing to obtain an overview which AS substitutions were predominant (Fig. 75). Sequenced mutants (G488E; G488E; T533K A534E Y536S; Y536S; W574I) which showed an improved activity were subcloned by PCR (primer P6/P7, Table S1, Appendix 6.1) in pCWori(+) vector. The restriction sites BamHI/EcoRI and T4-ligase were used to ligate the insert in adequately prepared vector.

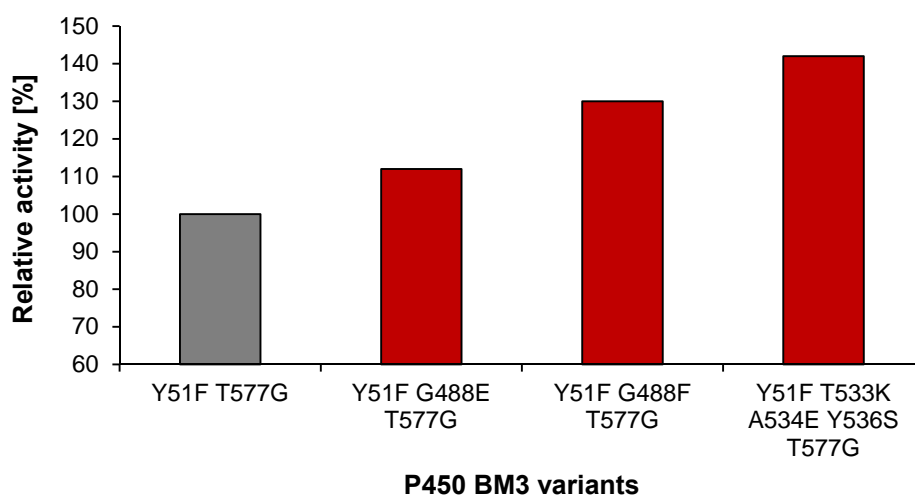


Fig. 74: Relative activities of several P450 mutants with the conducting polymer PEDOT/PSS and the 4-AAP assay compared to the parent P450 BM3 Y51F T577G. Variant P450 BM3 Y51F T577G was the starting variant and is labelled in grey.

Almost all amino acid exchanges were from hydrophobic to charged amino acids. Interestingly, the best variant (1.4 times the activity of the parent) carries two additional and unexpected amino acid exchanges at position 533 and 534 besides the anticipated substitution at position 536 (probably due to misannealing of the mutagenic primer).

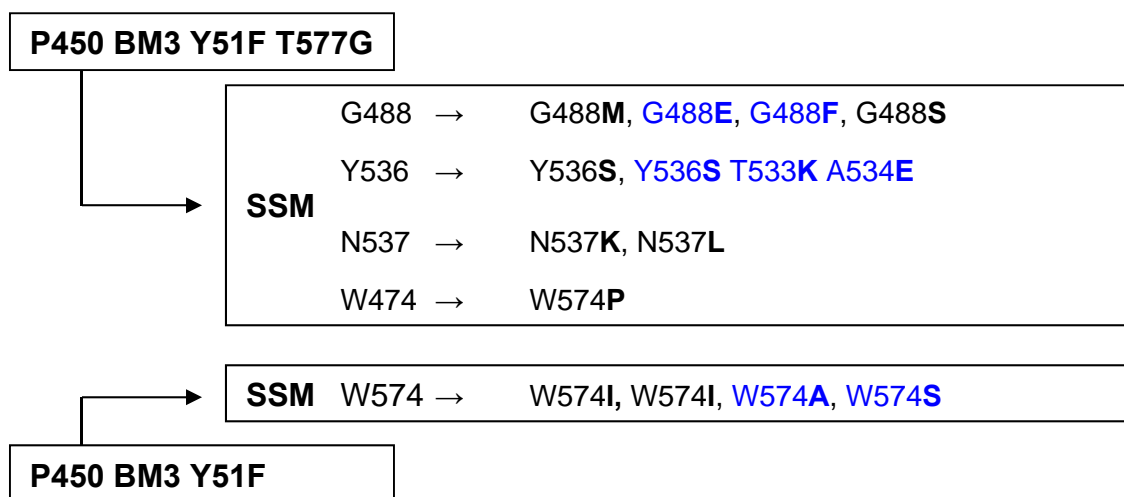
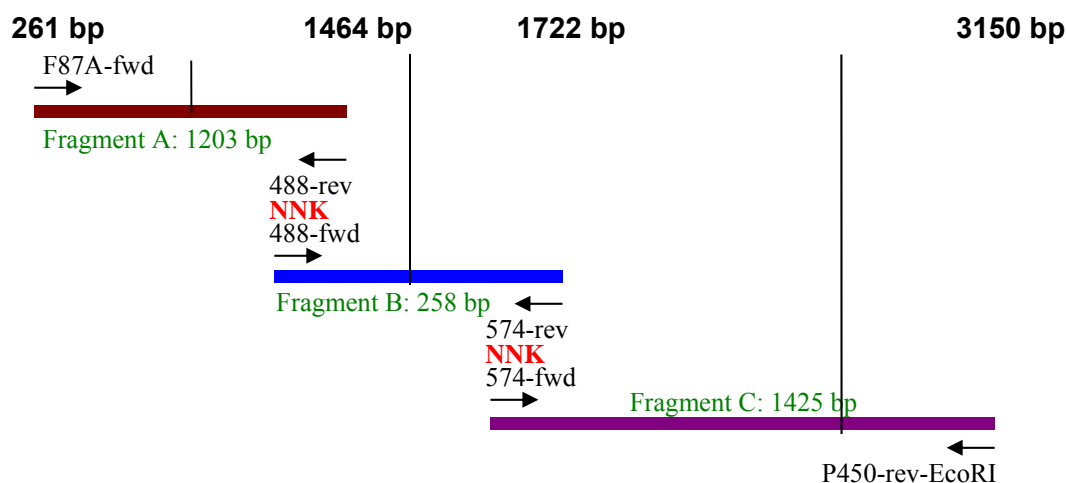


Fig. 75: Sequencing results of selected variants of structure guided mutant libraries. Blue labelled substitution showed a minor (>10 %) activity improvement.

2.2.2.2 Simultaneous saturation of position G488 and W574

In parallel to the consecutive SSM strategy (section 2.2.2.3) a simultaneous SSM was generated by overlap extension PCR. The position G488 and W574 lying in close proximity were simultaneously NNK saturated in the variant P450 BM3 Y536S T533E A534E which was selected in the focussed mutant library (section 2.2.2.1). The scheme in Fig. 76 describes the PCR setup. Three separated PCR fragments A, B and C were generated and purified by gel electrophoresis. The fragments were annealed and amplified by overlap extension PCR to generate a full length fragment of 2670 bp (Ho et al., 1989). The restriction sites MfeI/EcoRI and T4-ligase were used to ligate the insert in the variant P450 BM3 F87A to generate the full length gene (3150 bp). Screening of 1800 clones was done with the 4-AAP assay and the substrate 3-phenoxytoluene. The ratio of inactive clones in the mutant library was higher than 40%. Nevertheless, no variants with improved activity could be identified.



Step 1: Generation by PCR of three fragments A, B, C



Step 2: Overlap Extension PCR, annealing of the fragments (A, B, C)



Step 3: Restriction enzyme cloning of the full length gene by MfeI/EcoRI and T4-ligase

Fig. 76: Scheme of the overlap extension PCR used to generate a multiple SSM at position G488 and W574 in the variant P450 BM3 Y536S T533E A534E.

2.2.2.3 Iterative SSM libraries

The saturated positions (G488, Y536, N537, and W574) in section 2.2.2.1 were iteratively recombined, even if the obtained variants showed minor (1.1-1.4 fold) activity improvements. 400 clones of each generated library were screened with the 4-AAP assay and the substrate 3-phenoxytoluene and 10 % were re-screened. Finally, three clones were selected and sent for sequencing. Table 7 gives an overview of the generated libraries and the obtained results. Saturation of the position W574 (without T577G) in the Y536S and G488E variant did not lead to improved variants and the selected clone in case of Y536S-library revealed to be the template gene. Only two selected clones of the saturation at position 574 (with T577G) in the variant Y536S showed minor improvement (1.1-1.2 fold) compared to the starting gene Y51F

T577G, but the activity was comparable to the template gene (Y536S). The identified amino acid substitution was W574T and occurred in two sequenced clones.

Table 7: Overview and sequencing results of the generated iterative SSM libraries.

Template gene	SSM at position	Sequencing results of improved variants	Activity improvement
P450 BM3 Y51F G488E	574	-	no improvement
P450 BM3 Y51F G488F	574	-	no improvement
P450 BM3 Y51F Y536S T533K A534E	574	template gene	no improvement
P450 BM3 Y51F Y536S T533K A534E T577G	574	W574T (2 clones)	1.2 fold

Summarizing, this results covered the findings of the multiple site saturation mutagenesis (section 2.2.2.2) iteratively as simultaneous saturation of position G488 and W574 did not enhance the activity of P450 BM3 for the conductive polymer (Clevios P).

2.2.2.4 Summary of results from structure guided mutant libraries

Selected variants in the focussed mutant libraries were only compared after protein concentration normalized by the automated gel electrophoresis. This system could be identified as not suitable for the determination of the P450 concentration (see section 2.2.3.2 where the two methods to determine the concentration were compared). Therefore, the product formation rate of the selected variants were re-analysed with CO-normalized protein concentrations.

In summary, out of the 20 selected variants from the structure guided mutant libraries, which showed improved activities in the screening, nearly all revealed to be expression variants or showed after CO titration only minor improvements compared to the parent strain (4 out of 20 analyzed clones). Additionally, no variants with improved activity could be identified by screening the iterative SSM and the simultaneous SSM libraries at the position G488, Y536, N537 and W574. Only the SSM at position R471 revealed a variant (R471C) with 1.5 fold enhanced activity for the conductive polymer in crude cell lysate after CO normalization (Fig. 77).

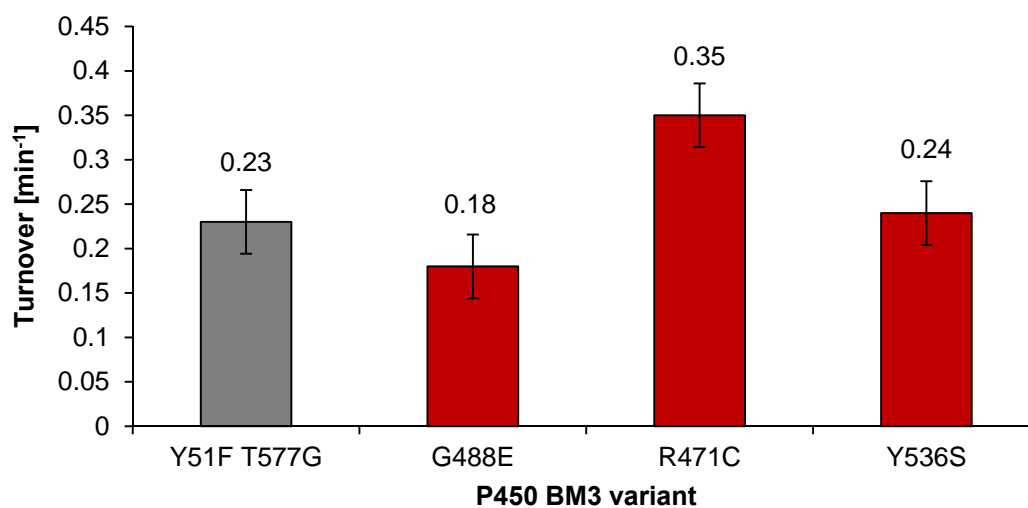


Fig. 77: Relative activity of improved variants in presence of the conductive polymer Clevios P compared to P450 BM3 Y51F T577G after CO normalization. Variant P450 BM3 Y51F T577G was the starting variant and is labelled in grey.

2.2.3 Random mutagenesis libraries

The semi rational evolution of P450 BM3 for DET was not successful; no significantly improved variants could be identified. Therefore, additionally to the structure guided mutant libraries, P450 BM3 was evolved for DET by a random mutagenesis approach to identify new hot spots. Two rounds of directed evolution were performed and screened in MTP for improved variants.

2.2.3.1 First round of directed evolution – mutagenesis and screening

In the first directed evolution round, random mutagenesis libraries were generated by error-prone PCR (epPCR) and screened with the 4-AAP assay for phenol detection (Wong et al., 2005b). Beside P450 BM3 Y51F T577G a pool of plasmid DNA from the structure guided mutant libraries (section 2.2.2) were used as template. In standard epPCR method the gene of interest is amplified by PCR under error prone conditions and afterwards ligated by restriction enzymes and ligase in the expression vector. In this thesis the standard protocol was followed for the epPCR (generation of the insert) but instead of restriction cloning the generated epPCR libraries were hybridized by PLICing in the expression vector (Blanusa et al., 2010b). For the insert amplification the primer PP3/PP4 and for the vector the primer PP1/PP2 were used (see Table S1, Appendix 6.1). The size of the PCR products were checked by agarose gel electrophoresis, no unspecific primer binding could be observed, since only one band of expected size was present (P450 BM3 = 3150 bp) (Fig. 78). The generated epPCR libraries were cloned into the commercially available expression vector pET28a(+) using the PLICing cloning technology (Blanusa et al., 2010b).

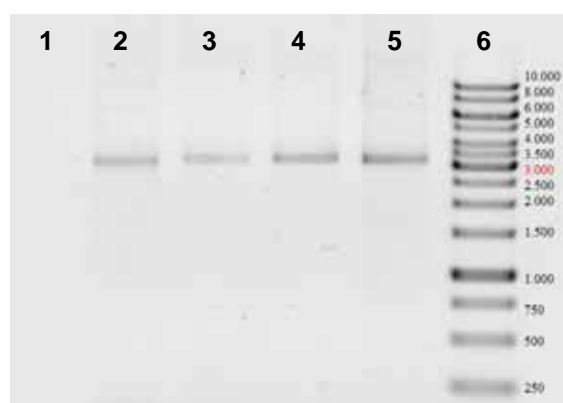


Fig. 78: Four epPCR products separated by agarose gel electrophoresis. Lane 1: negative control, PCR reaction mixture without template, Lane 2-5: Insert of the P450 BM3 epPCR libraries (3150 bp), respectively library I (0,05 mM MnCl₂ and 2,5 mM MgCl₂), library II (0,05 mM MnCl₂ and 5 mM MgCl₂), library III (0,1 mM MnCl₂ and 5 mM MgCl₂); Lane 6: Gene Ruler 1 kb DNA Ladder.

P450 BM3 variants were expressed in *E. coli* (DE3) Gold cells. The ratio of inactive clones for each library was determined with the 4-AAP assay in 96 well plate format.

The libraries had an inactivation ratio of 100% when compared to Y51F T577G which did not show activity. The coefficient of deviation was low; library I: 15.4%, library II: 13%, and library III: 12% and Y51F T577G: 13%, consequently, all three libraries were selected for screening. In total, 1000 clones from library I (balanced dNTPs, 0,05 mM MnCl₂ and 2,5 mM MgCl₂), 500 from library II (balanced dNTPs, 0,05 mM MnCl₂ and 5 mM MgCl₂) and 500 from library III (balanced dNTPs, 0,1 mM MnCl₂ and 5 mM MgCl₂) were screened with the 4-AAP assay. Five percent were re-screened and the arithmetic average of six measurements was calculated. For evaluation the adsorption at 600 nm was subtracted from the 509 nm values as well as the arithmetic average of the background signal (results of 4-AAP assay with cells expressing empty vector) according to Nazor at al. (Nazor, 2007). The arithmetic average $A_{509-600\text{ nm}}$ of P450 BM3 Y51F T577G was settled as 100 % and the relative activity of the muteins was calculated. (Fig. 79 shows as example the obtained screening results of one plate from the epPCR library.)

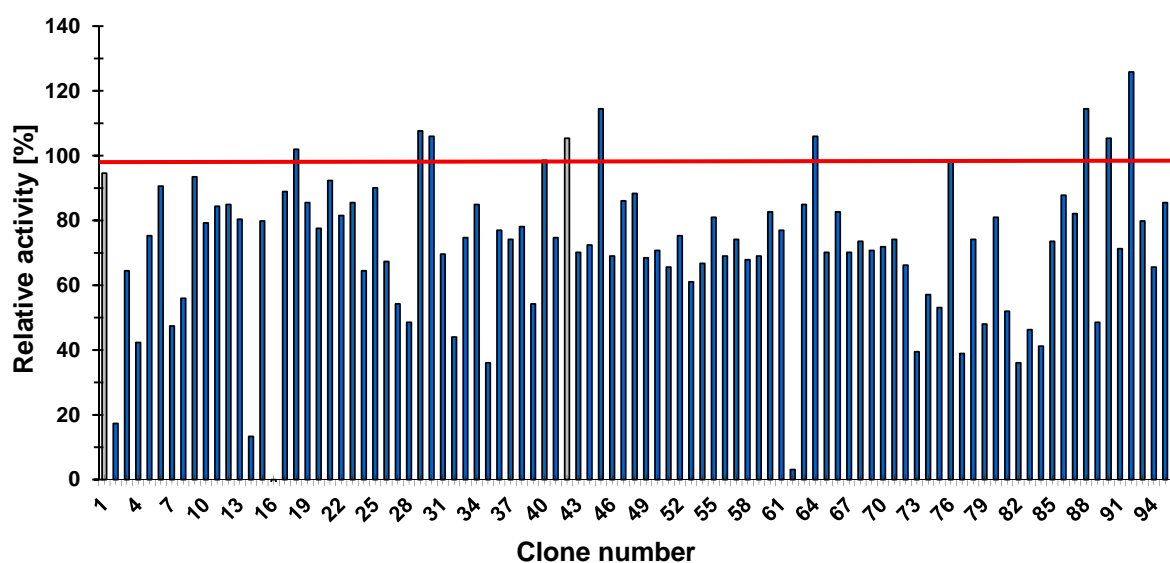


Fig. 79: The relative activity of the muteins compared to the template gene P450 BM3 Y51F T577G (colored grey) is displayed. The red bare indicates the arithmetic average of the starting variant P450 BM3 Y51F T577G activities, serving as threshold to select improved variants.

After re-screening, 11 variants were selected for further analysis and the protein expression was monitored by SDS-Page (Fig. 80), out of eleven mutants five did not show P450 expression. As none of the tested variants revealed a higher expression level as P450 BM3 Y51F T577G, the probability of expression mutant presence was decreased considering the total protein amount.

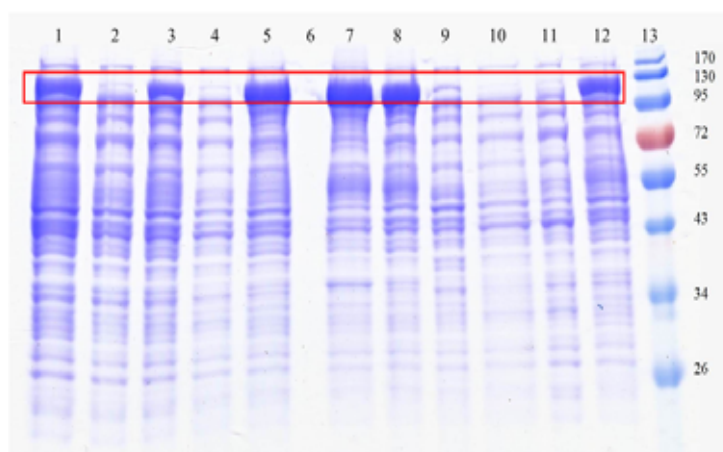


Fig. 80: SDS page of the expressed mutants from the first evolution round. The red box marks the expected 119 kDa band. Lane 1-12 respectively: P450 BM3 B1-P1-H2; P450 BM3 B2-P3-A2; P450 BM3 B1-P1-E12; P450 BM3 B3-P1-A5; P450 BM3 B1-P1-C5; pET28a(+); P450 BM3 Y51F T577G; P450 BM3 B3-P10-C6; P450 BM3 B3-P10-H4; P450 BM3 B3-P5-B10; P450 BM3 B2-P4-A3; P450 BM3 B3-P3-E2; Lane 13: PageRuler Prestained Protein Ladder in kDa.

After determination of the enzyme concentration by automated gel electrophoresis, the activity assay was repeated with adjusted catalyst amount. Only one variant called P450 BM3 B3-P10-C6 had a 10 % activity increase which was in the error range of the 4-AAP assay. This variant was selected for sequencing. For the first round of evolution, the template DNA was a pool of plasmids which comprise the amino acid substitutions: Y51F, Y488E, W574R, T577G. In addition, 6 further mutations were present in P450 BM3 B3-P10-C6, 3 silent mutations at positions L432, E688 und H932H and the amino acid substitution S305N, G577T und P898L. Accordingly this mutant (P450 BM3 B3-P10-C6) was named P450 BM3 Y51F S305N G488E W574R P898L.

2.2.3.2 Second round of directed evolution

Similar to the first evolution round a second random mutagenesis library was generated by epPCR and screened for improved DET. As template the variant from the first round (P450 BM3 Y51F S305N Y488E W574R P898L) and variant P450 BM3 Y51F T577G were used to generate epPCR libraries as described before. Due to the high mutational load in the first epPCR libraries milder condition (balanced dNTPs and 0.2 mM MnCl₂) were used. The pre-screening of 700 colonies and re-screening of 30 colonies was done with the 4-AAP assay as described in Material and Methods (section 2.13.1.2).

Comparison of methods used for determination of the P450 BM3 mtein concentrations

After screening and re-screening the selected variants which showed an activity improvement in presence of the conductive polymer Clevios P, were compared with normalized protein concentrations. Two methods to determine the protein concentration were applied, the automated gel electrophoresis and the P450 titration by CO-gassing. The activity improvement with P450 concentrations normalized by both methods were compared and evaluated to identify which method is most suitable for the determination of P450 concentration.

The comparison was performed on the example of the selected variants in the epPCR screening. Out of 26 selected variants in the re-screening 4 showed a minor improved activity (1.2-1.4 fold) compared to P450 BM3 Y51F T577G. To exclude expression mutants the 4 variants were analyzed with the Experion Pro260 Analysis kit (BioRad) (Fig. 81) for protein quantification. The expression of the variants P450 BM3 B4-P4-F2 and P450 BM3 B4-P3-G10 was 1.7 fold, respectively 1.5 fold lower as the starting variant. The variant P450 BM3 B4-P4-H2 had a comparable expression level ($\sim 4.2 \mu\text{g}/\mu\text{l}$) to the P450 BM3 Y51F T577G. Thus none of the variants were expression mutants.

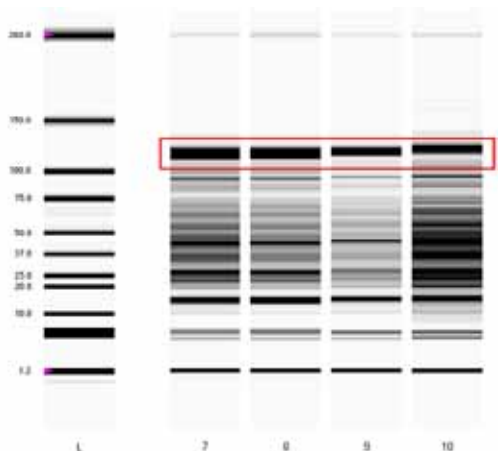


Fig. 81: Experion automated gel electrophoresis analysis of the selected improved variants from second directed evolution round. The red box indicates the expected band at 120 kDa, corresponding to P450 BM3. Lane L: Ladder in kDa; Lane 7: P450 BM3 Y51F T577G; Lane 8: P450 BM3 B4-P4-F2; Lane 9: P450 BM3 B4-P4-H2; Lane 10: P450 BM3 B4-P3-G10.

Additionally to the determination of the enzyme concentration by the automated gel electrophoresis system the active P450 concentration was quantified by CO titration (Fig. 82) (Omura and Sato, 1964a). The obtained absorbance spectra in Fig. 82 correspond to a typical P450 spectrum. Only variant C8 (—) had a higher ratio of inactive P450 (presence of a peak at 420 nm). The P450 BM3 concentration ranged from 12 and 35 μM .

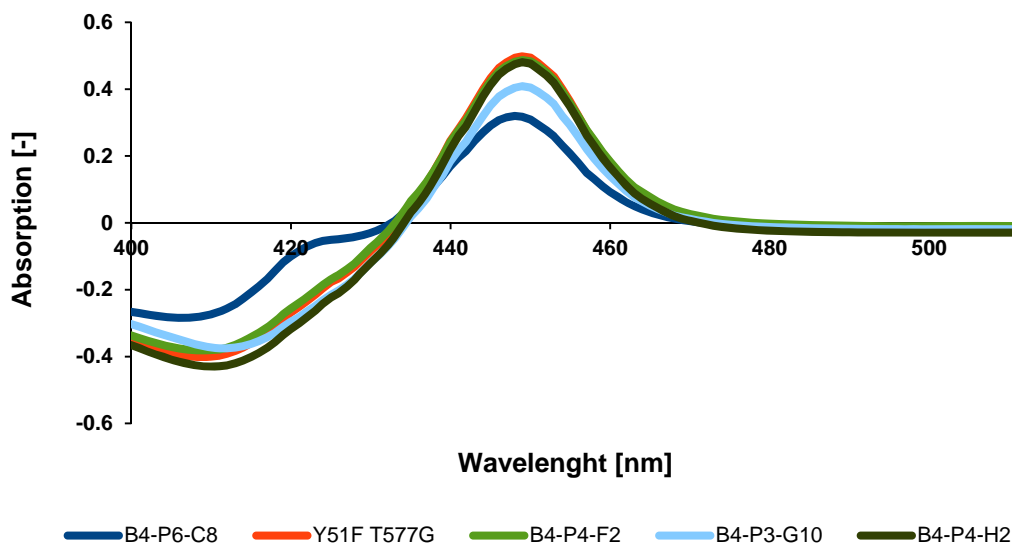
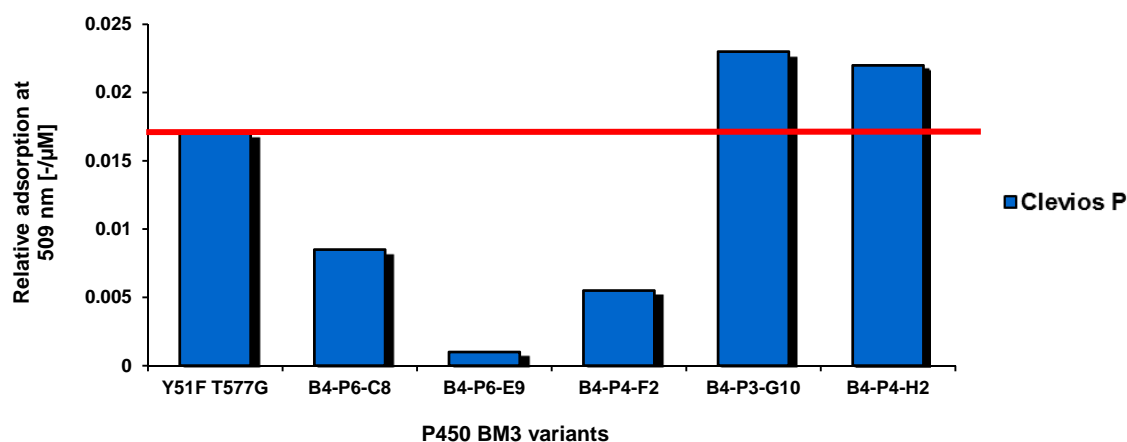


Fig. 82: Absorption spectra of the selected variants after CO-gassing used to determine the P450 concentration. Shown are the chromatograms after background subtraction (Reference without CO gassing is subtracted from the CO treated sample).

The activity assay was repeated at determined enzyme concentration with NADPH and the conductive polymer Clevios P. Fig. 83a shows the activity measurements correlated to the concentration determined by the automated gel electrophoresis system and Fig. 83b the activity normalized after concentration determined by CO-normalization. In all samples the activity with NADPH was higher compared to samples containing the conductive polymer as electron donor. A discrepancy between the two measurements was obtained. The enzyme concentration correlated by Experion system revealed that two variants were improved. The highest activity was observed for variants P450 BM3 B4-P3-G10 and P450 BM3 B4-P4-H2 (Fig. 83a). Contrary, the CO-normalization shows no improved variants. Thus the determination of the P450 concentration is reliable if proceed by titration with CO-gassing and the results are not comparable to the automated gel electrophoresis system.

(a) Activity normalized to enzyme concentration determined by automated gel electrophoresis



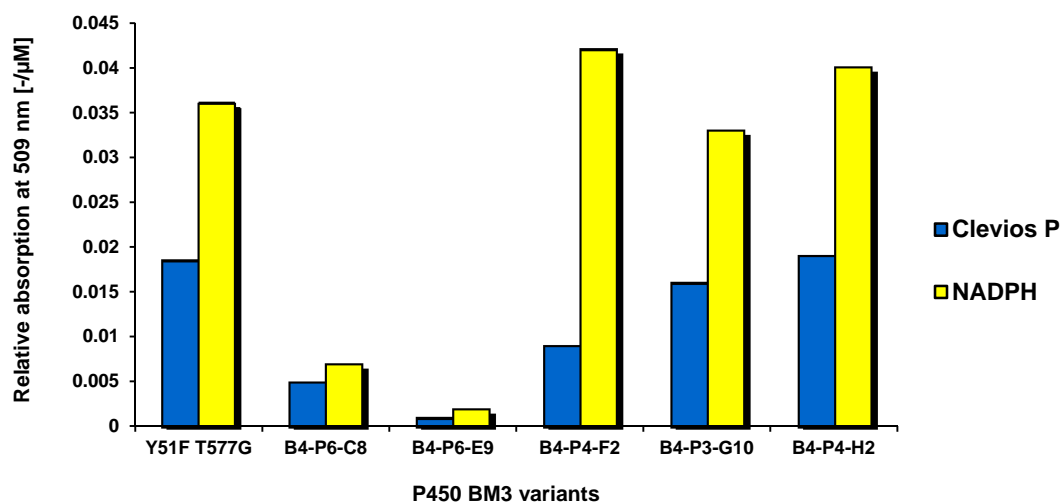
(a) Activity normalized to enzyme concentration determined CO-differenzspectroscopic

Fig. 83: Result of the 4-AAP activity assay with normalized enzyme concentration by automated gel electrophoresis system (a) or CO-normalized enzyme concentration (b). The Y-axis shows the $A_{509\text{ nm}}$ values with subtracted background (reaction mixture without substrate) and divided by the enzyme concentration.

Nevertheless, even if no variant with improved activity could be identified the activity assay was repeated with purified proteins to elucidate the obtained results. The variants P450 BM3 B4-P3-G10 und B4-P4-H2 were purified and the purity was monitored by SDS-page. Both proteins were active with NADPH, but no activity in presence of the conducting polymer Clevios P could be detected (Fig. 84). An inactivation during purification process could be excluded, otherwise P450 BM3 would display no activity with the natural cofactor. Further investigation concerning this observation can be found in the following section 2.3.

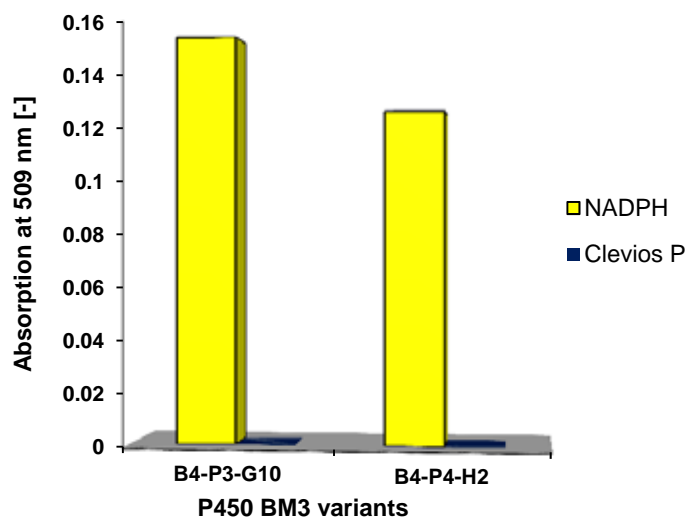


Fig. 84: Activity with NADPH and Clevios P of the purified variants selected in the epPCR library screening (B4-P3-G10 and B4-P4-H2) determined by the 4-AAP assay.

Sequencing results are summarized in Table 8. Sequencing of P450 BM3 B4-P3-G10 revealed two silent mutations at positions (L432 and K778) and amino acid substitutions

(L418V, R683Q and I864V). In the variant P450 BM3 B4-P4-H2 three mutations were present, beside two silent substitutions at positions L432 and G496, a substitution from alanin to valin at position 865 was observed. Accordingly P450 BM3 B4-P3-G10 was named P450 BM3 Y51F L418V T577G R683Q I864V and P450 BM3 B4-P4-H2 was named P450 BM3 Y51F T577G A865V.

Table 8: Sequencing results of the improved variants selected in the second directed evolution round.

Variant	Sequencing results	
	Silent mutations	Amino acid substitutions
P450 BM3 B4-P3-G10	L432, K778	L418V, R683Q, I864V
P450 BM3 B4-P4-H2	L432, G496	A865V

2.2.3.3 Summary of the random mutagenesis libraries

The random mutagenesis libraries were successfully generated by epPCR and cloned with the PLICing method. In two rounds of directed evolution 1700 colonies were screened with the 4-AAP assay for improved activity in the presence of the conductive polymer Clevios P. In the first round, a variant which had increased (1.1 fold) activity improvements could be selected (P450 BM3 Y51F S305N Y488E W574R P898L). The second evolution round was performed under milder PCR conditions and two variants with improved activity were selected whereas expression mutant could be excluded. The variants P450 BM3 Y51F L418V T577G R683Q I864V and P450 BM3 Y51F T577G A865V were purified and the activity with the natural cofactor NADPH and the conductive polymer as artificial electron source was determined.

In summary, the random mutagenesis approach to improve the activity with the conductive polymer did not lead to activity improved variants for DET. Three variants with minor improvements in the crude lysate could be selected but no activity with purified protein in the presence of the conductive polymer was observed. The activity with the natural cofactor NADPH remained unchanged and no activity improvement could be detected. Accordingly to this, the mutants could not be characterized using Clevios P as only electron donor. Mutagenic “hot spots” could not be selected but the substitution indicated that a modified interaction with the reductase domain might be present, as nearly all mutations were located in the reductase domain. The lacking activity with the purified protein and the location of the substitutions support the analyzed hypotheses (section 2.2) that no direct interactions between the conductive polymer and the protein is present. Nevertheless the comparison of the methods used to determine the P450 concentration revealed significant differences in the activity measurements.

2.2.4 Summary of the P450 BM3 evolution for improved DET

The evolution of P450 BM3 for improved DET was investigated by a structure guided focused mutagenesis approach as well as by random mutagenesis rounds. In total 8200 clones generated by 5 focused libraries SSM (450 clones/library), 4 libraries of combination of beneficial mutations (360 clones/library), 1 multiple SSM (1800 clones/library), and 2 random epPCR libraries (1700 clones) were screened with the 4-AAP assay. Summarizing, the activity improvement of the variants selected in the screening of the structure guided mutant libraries or in the random mutant libraries generated by epPCR were in the error range of the 4-AAP assay and did not exceed the standard deviation values. Only the variant R471C showed a minor improvement (1.5 fold). Improvements due to substitution at position R471 is very likely not related to an improved direct electron transfer but likelihood to an improved stability.

Surprisingly, all variants selected in the screening, displayed no activity as purified enzymes in presence of the conductive polymer. This interesting finding was investigated in detail and is reported in the following section (section 2.3). Altogether, neither a structure guided approach nor directed evolution could improve activity of P450 BM3 for DET. Concluding, the undetectable product formation of the starting variants and since no variant able to perform the direct electron transfer with Clevios P as electron source was identified, no electron transfer without regeneration system is feasible.

2.3 Activity measurements with purified protein in the presence of the conducting polymer Clevios P

As reported in section 2.2, the conversion of 3-phenoxytoluene with purified protein in presence of the conducting polymer Clevios P could not be observed. Already, the first activity measurements in presence of only Clevios P with the variant reported as improved, indicated that no product formation could be observed. This unexpected and interesting result was common in all selected variants in the screening (see section 2.2.4). Purification and analysis of selected variants in screening occurred, but never the starting variant P450 BM3 Y51F T577G was included which was reported as activity improved variant in presence of the conductive polymer Baytron P. Therefore, further investigations were performed to clarify why discrepancies in the activity measurements between purified protein and cell lysate are present. In the following sections, first the activity of purified P450 BM3 Y51F T577G was analysed and then the generated products in presence of the conducting polymer with cell lysate were detected by GC. Finally, the impact of mediators on the activity with purified protein was investigated by analysing a coupled enzyme reaction to exclude a NAPH based reaction.

2.3.1 Activity of purified P450 variant Y51F T577G

To compare and maybe elucidate the discrepancy of the activity measurements between purified P450 BM3 protein and cell lysates, the starting variant Y51F T577G was purified and the activity with the 4-AAP assay was monitored. Fig. 85 shows the activity with 3-phenoxytoluene in the NADPH consumption assay. As control, the same reaction with DMSO was carried along. The decrease in absorption at 340 nm in the sample with substrate compared to a constant adsorption when the substrate is replaced by DMSO, proves the presence of active P450 BM3 Y51F T577G enzyme with the natural cofactor NADPH.

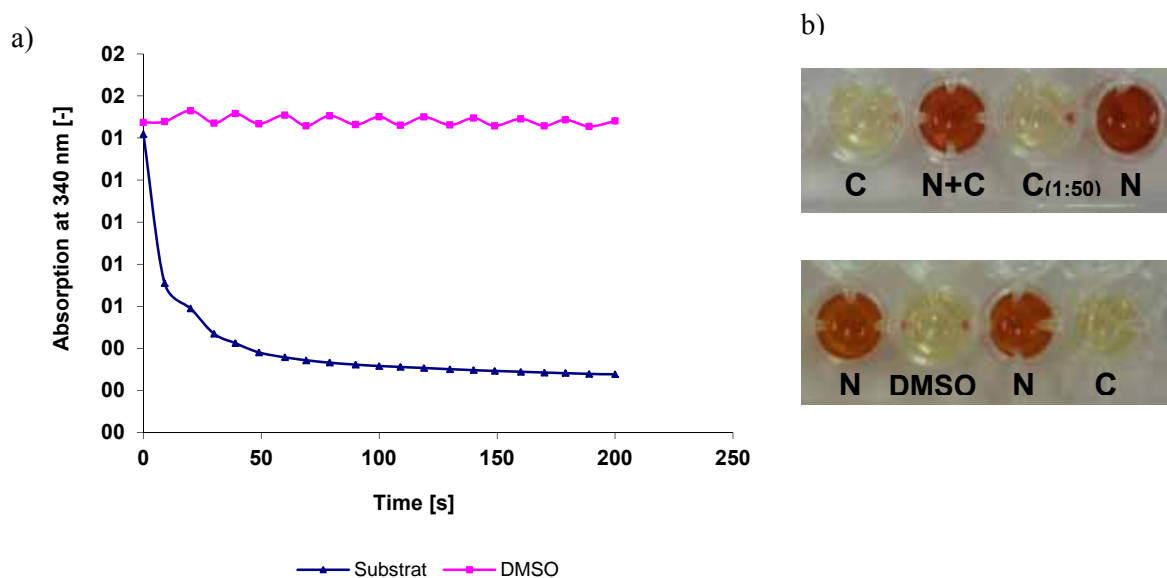


Fig. 85: a) NADPH consumption assay with purified P450 BM3 Y51F T577G. Conversion of the substrate 3-phenoxytoluene and negative control without substrate only DMSO addition, b) Detection of 3-phenoxytoluene conversion products by the 4-AAP assay with the natural cofactor NADPH (N), the alternative cofactor Clevios P (C) (C_{1:50}= Clevios P diluted 1:50), or without addition serving as negative control (DMSO).

The activity with NADPH demonstrates that the expression system and purification was effective and led to active and right folded proteins, even if substitution T577G is present. The same sample was analysed with the 4-AAP detection principle in presence of the conducting polymer Clevios P as alternative cofactor system or with addition of NADPH (Fig. 85). The colorimetric reaction proves that no activity in presence of the conductive polymer Clevios P was detected, but with NADPH. Nevertheless, activity in presence of the conductive polymer Baytron P was reported (Nazor, 2007). To exclude any influence coming from the expression system, or the substitution Y51F, the substitution T577G was introduced in WT P450 BM3 and in F87A variant. The purification and all measurements were done in duplicate. No activity for any of the constructed strains could be detected in presence of Clevios P, but the activity with NADPH remained.

Additionally, to exclude an influence of the selected detection method on the obtained data and to confirm the obtained data by other detection principles, the activity measurements were repeated and analyzed using alternative activity detection systems for P450 BM3. Three detection principles were applied: The pNCA assay, a fluorescent based assay and the 4-AAP assay with another substrate.

Changing the substrate to enhance the sensitivity of the assay included the subcloning of the variants (generated variants are listed in Table 9). The experiments were performed with the starting variant Y51F T577G and the 5 selected variants with the amino acid substitutions

identified in the screening of the focussed mutant libraries: Y536S T533K A534E W574T, G488E, Y536S T533K A534E, G488F, R471C).

Table 9: Generated variants used to compare the activity assay employed with purified protein.

Variant	Amino acid substitutions	Generated by
WT-T577G	T577G	SDM T577G in P450 BM3 WT
F87A-T577G	F87A T577G	SDM F87A in P450 BM3 WT-T577G
WT-Ethoxy-T577G	K187E I162G T577G	SDM in WT-T577G
WT-Ethoxy	K187E I162G	SDM in P450 BM3 WT
WT-G488E	T577G G488E	Subcloning by MfeI/NcoI in P450 BM3 WT
F87A-G488E	F87A T577G G488E	Subcloning by MfeI/NcoI in P450 BM3 F87A
F87A-W574T	Y51F Y536S T533K A534E T577G W574T	Subcloning by MfeI/NcoI in P450 BM3 F87A
F87A-Y536S	Y536S T533K A534E	Subcloning by MfeI/NcoI in P450 BM3 F87A
F87A-G488F	G488F	Subcloning by MfeI/NcoI in P450 BM3 F87A
WT-R471C	R471C	Subcloning by MfeI/NcoI in P450 BM3 WT
F87A-R471C	F87A R471C	Subcloning by MfeI/NcoI in P450 BM3 F87A

Detection of p-nitrophenol by the pNCA assay in presence of the conducting polymer

The pNCA assay was selected to investigate the hydroxylation of a natural like substrate in the presence of the conductive polymer. Product detection of the pNCA hydroxylation occurs at 405 nm and should not interfere with the absorption spectra of the conductive polymer. The substitution F87A was reported as beneficial for efficient conversion of pNCA (Schwaneberg et al., 1999a). For this purpose, the five selected variants and the Y51F T577G were subcloned in the F87A variant using the restriction sites MfeI/NcoI to exclude the Y51F mutation and to introduce the F87A substitution. The variants (F87A-G488E, F87A-W574T, F87A-Y536S, F87A-G488F, F87A-R471C, F87A-T577G) were purified and the pNCA conversion in presence of Clevios P assayed. The results obtained with the pNCA assay were similar to the obtained data with the 4-AAP assay. No activity with purified protein in presence of the conductive polymer Clevios P could be observed.

Detection of 11-phenoxyundecanoic acid conversion by the 4-AAP assay in presence of the conducting polymer

The conversion of the substrate 11-phenoxyundecanoic acid in presence of the conductive polymer was tested. The product of the 11-phenoxyundecanoic acid hydroxylation is a phenol and detectable with the 4-AAP assay. The experimental setup was comparable to the used screening system consisting of the 3-phenoxytoluene conversion and the 4-AAP detection principle (Wong et al., 2005b). Exchanging the substrate by keeping the detection principle constant allows excluding an influence of the substrate on the activity in presence of the conductive polymer. The activity in presence of Clevios P and NADPH of the six purified variants carrying the F87A mutations (F87A-G488E, F87A-W574T, F87A-Y536S, F87A-G488F, F87A-R471C, F87A-T577G) and 3 variants lacking the F87A and Y51F substitutions (WT-G488E, WT-R471C, WT-T577G) was recorded. However, no activity with purified protein in presence of the conductive polymer but with NADPH could be observed with this experimental setup.

Fluorescent activity assay in presence of the conducting polymer

Fluorescent based activity assays were setup to enhance the sensitivity of the detection principle. Fluorescent assays can detect product formation in nM scale compared to the colorimetric detection methods which are limited to product formation in μM scale (Arnold and Georgiou, 2003). This would exclude that the activity remained undetectable due to the detection limits of the tested colorimetric assays (pNCA and 4-AAP assay). First the reported fluorescent MTP-assay based on the hydroxylation of 7-hydroxycoumarin was performed (Park et al., 2010). For this reason, prerequisite was to introduce by SDM the substitution I162G and K187E allowing to convert the fluorescent substrate 7-hydroxycoumarin.

As second the conversion of BCCE was determined (see section II.1). Fundamental for the latter was no substitution at position Y51. Therefore the following mutants (WT-G488E, WT-R471C, WT-T577G, WT-Ethoxy-T577G, WT-Ethoxy) were constructed by SDM or subcloning with restriction enzymes.

The results of the conversion of both fluorescent substrates (7-hydroxycoumarin and BCCE) were similar with the eleven investigated variants (F87A-G488E, F87A-W574T, F87A-Y536S, F87A-G488F, F87A-R471C, F87A-T577G, WT-G488E, WT-R471C, WT-T577G, WT-Ethoxy-T577G, WT-Ethoxy). The result of the BCCE conversion by purified P450 BM3 WT-T577G in presence of NADPH and the conductive polymer is shown in Fig. 86 (λ_{ex} 400 nm, λ_{em} 440 nm).

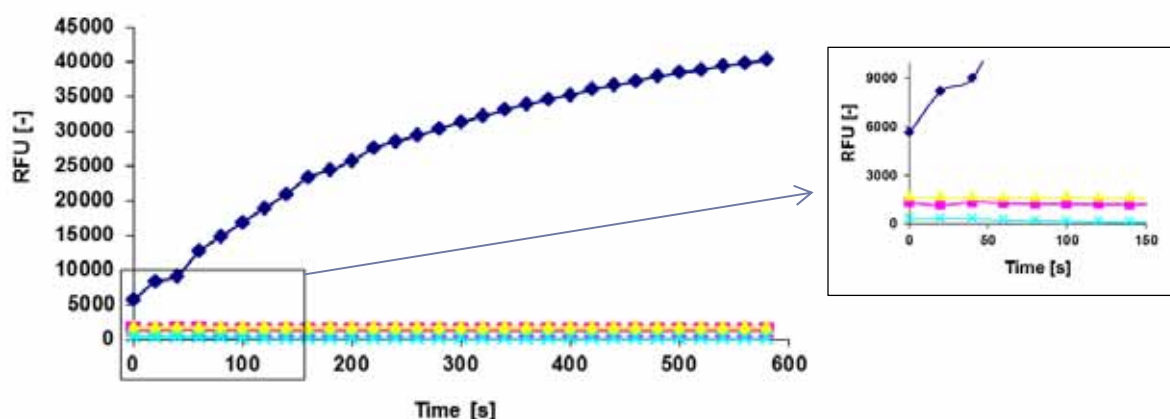


Fig. 86: BCCE conversion by purified P450 BM3 WT-T577G in presence of NADPH (\blacklozenge), the conductive polymer (\blacksquare) or without e-donor (\blacktriangle), and the reaction mixture without enzyme but with NADPH (\times), recorded at λ_{ex} 400 nm, λ_{em} 440 nm.

An increasing fluorescent signal with addition of NADPH but not in presence of Clevis P could be observed with purified protein. All variants only differ in the signal response with NADPH most likely due to an improved substrate conversion. The conductive polymer displayed furthermore quenching effects on the fluorescent signal or an inhibition of the enzyme. Although applying different variants as well as various fluorogenic substrates, no activity signal could be recorded using Clevis P as electron source for P450 BM3.

The fluorescent activity measurements were also proceeded with cell lysate (Fig. 87), indicating a fluorescent signal increase with, but also without addition of Clevis P. The signal was very low, when no addition occurred compared to the obtained RFU with addition of NADPH.

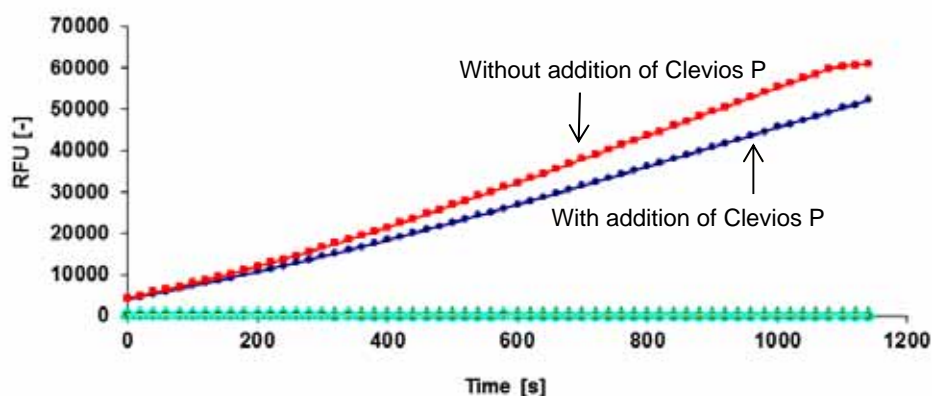


Fig. 87: BCCE conversion recorded at λ_{ex} 400 nm, λ_{em} 440 nm with P450 BM3 WT-T577G cell lysate, with addition of the conductive polymer Clevis P (\blacksquare) and without addition of Clevis P (\bullet), pET28a(+) cell lysate (\bullet) with addition of the conductive polymer Clevis P, purified P450 BM3 WT-T577G with addition of the conductive polymer Clevis P (\circ).

2.3.2 Product detection by GC and GC-MS

The product detection by GC and GC-MS was performed to elucidate if conversion is occurring in presence of the conductive polymer. Proving the product formation is essential as no activity with purified protein could be detected and the conversion rate with cell lysate in presence of the conducting polymer is very low and in the error range of the assay. The product detection by GC was repeated for all variants selected as improved in the screening and the reported variant P450 BM3 Y51F T577G. The conversion of 3-phenoxytoluene by freshly prepared cell lysate and in presence of Clevios P or the addition of NADPH was monitored on the GC. The chromatograms were similar for all analysed variants, thus only the results for P450 BM3 Y51F T577G are shown (Fig. 88)

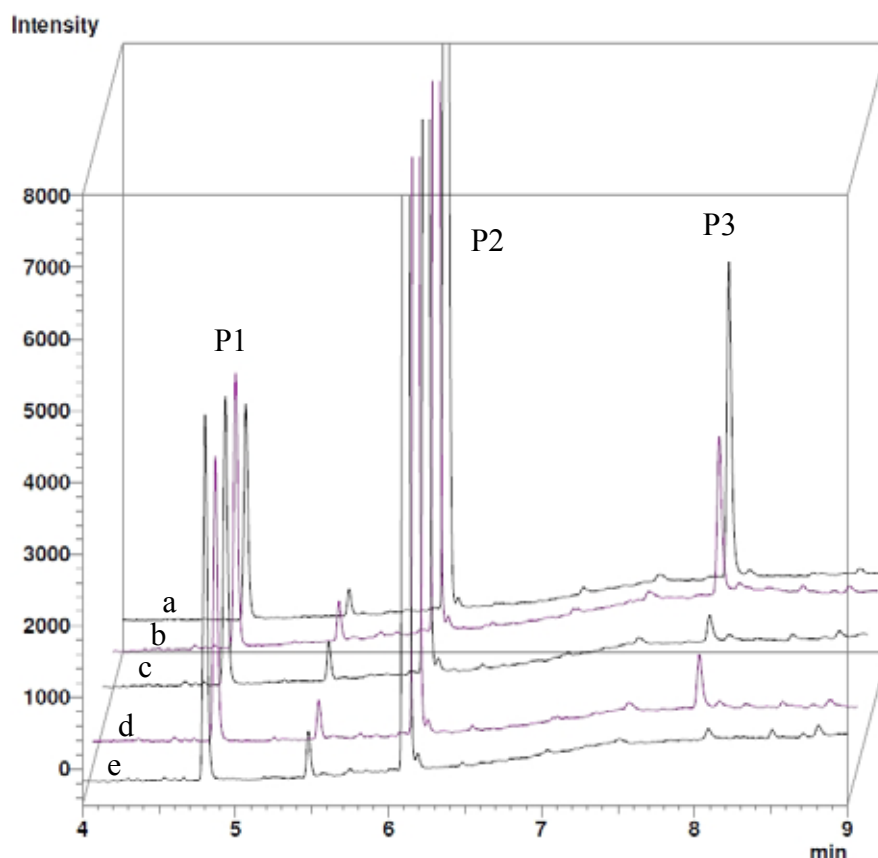
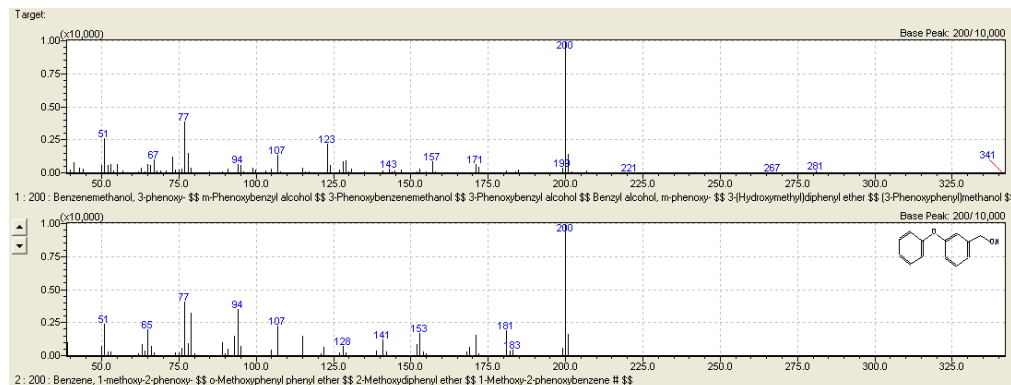


Fig. 88: GC chromatograms of the 3-phenoxytoluene conversion by P450 BM3. Reaction performed with cell lysate of Y51F T577G and with addition of NADPH (a), NADPH and Clevios P (b), Clevios P (c), no addition (d), cell lysate of pET28a(+) lacking the P450 gene (e). P1: Indol, P2: Substrate 3-phenoxytoluene, P3: Hydroxylated 3-phenoxytoluene.

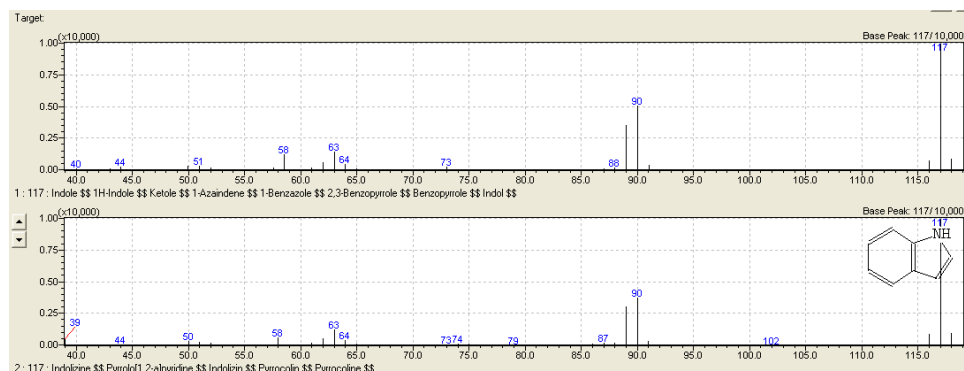
The presence of hydroxylated 3-phenoxytoluene (Peak 3 at RT:8 min) with NADPH addition or even without addition was clearly monitored. The peaks could be indicated by GC-MS with a similarity of 86% for 3-phenoxytoluene (Peak 2 in Fig. 88 and Fig. 89 a), 94% for

indol (Peak 1 in Fig. 88 and Fig. 89b), and 71% for hydroxylated 3-phenoxytoluene (Peak 3 in Fig. 88 and Fig. 89c).

(a) Peak 1: Hydroxylated 3-phenoxytoluene, similarity: 71%



(b) Peak 2: Indol, similarity: 94%



(c) Peak 2: 3-phenoxytoluene, similarity: 86%

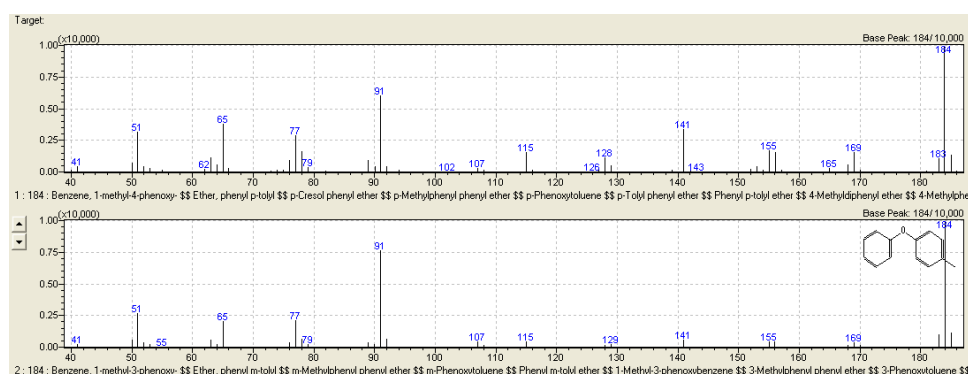


Fig. 89: GC-MS spectra used for the peak identification of the 3-phenoxytoluene conversion by P450 BM3.

However, the hydroxylate 3-phenoxytoluene could not be monitored in a reaction with cell lysate prepared from cells expressing the pET28a(+) lacking the P450 BM3 gene or *E. coli* BL21 (DE3) Gold cell lysate. Underlying that the substrate is not self-degraded or a site reaction catalysed by other enzymes present in the cell lysate is not occurring. The monitored

activity is not due to addition of the conducting polymer as the hydroxylated product could be monitored in the reaction mixture without supplemented electron donor indicating that a NADPH based reaction is occurring. Additionally, an inhibitory effect by the conductive polymer could be demonstrated. The GC peak areas were correlated to an internal standard and the reaction compared (Fig. 90). Reasoning, when Clevios P was added to the reaction catalysed by NADPH, the activity was lower compared to the one without addition of conductive polymer. This was already observed in the fluorescent activity measurements (section 2.3.1).

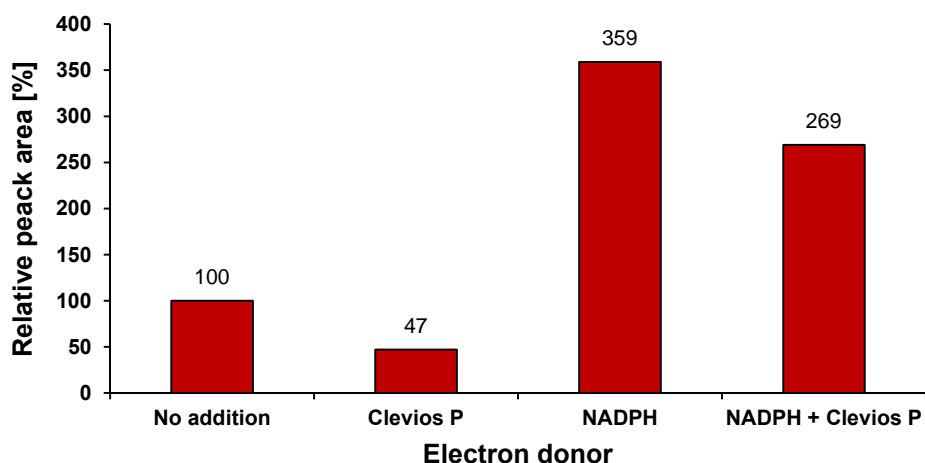


Fig. 90: GC peak area correlated to an internal standard to determine and compare the product formation rate of the 3-phenoxytolunene conversion in presence of Clevios P, no electron donor or NADPH.

2.4 NADPH or mediator based conversion

The colorimetric, the fluorescent and the GC measurements indicated the presence of a NADPH based reaction. Nevertheless, throughout the performed experiments a mediator based reaction could not be excluded. Feasible would be the conversion by P450 BM3 cell lysate due to the presence of the conducting polymer, but not as direct electron transfer but rather as a mediated electron transfer through an undefined constituent present in the cell lysate. This undefined constituent would be absent in the purified protein explaining why no activity can be detected. The three following experiments were performed to analyze if a NADPH or mediator based substrate conversion with cell lysate in the presence of the conductive polymer Clevios P is occurring.

1. First the prepared cell lysate was stored 48 h at 4°C and the activity was measured with the fluorescent assay. In freshly prepared cell lysate, the hydroxylation products could be detected using GC (section 2.3.2) as well as in the colorimetric detection systems (section 2.3.1). Indeed, after storage no activity could be observed with and without addition of Clevios P (See fig. 91 in comparison with Fig. 86). Nevertheless, the activity with supplemented NADPH remained, underlying that the monooxygenase was not inactivated by the storing procedure.

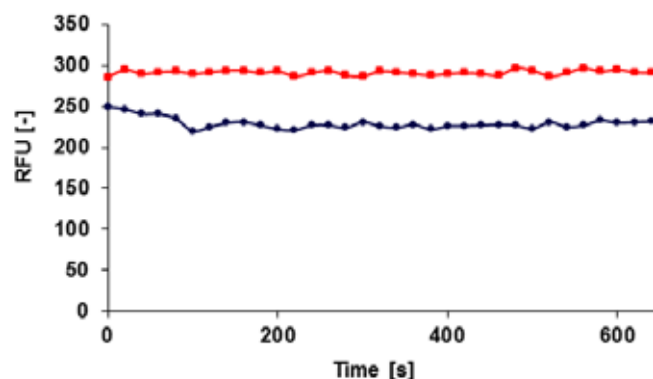


Fig. 91: BCCE conversion recorded at λ_{ex} 400 nm, λ_{em} 440 nm with P450 BM3 WT-T577G cell lysate, with addition of the conductive polymer Clevios P (■) and without addition of Clevios P (●), after storage of the cell lysate for 48h at 4°C.

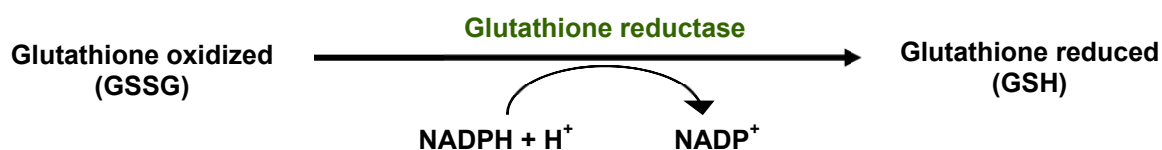
2. In the second experimental setup, the cell lysate was purified and the collected fractions were recombined before elution of the protein. The aim was to identify a compound separated by the purification process which could serve as mediator in the reaction system with Clevios P as observed in cell lysate (Fig. 92). The activity test was performed with the fluorescent assay after addition of the different fraction to the partially purified protein. NADPH is not binding to the purification matrix, ensuring a good separation of the cell lysate constituent (P450 BM3 and other enzymes) and the NADPH. Even when recombining all fractions no activity was detected with Clevios P. The fluorescent measurements are not shown; the result was identical to the obtained data in Fig. 86 and Fig. 91.

Additionally, cell lysate prepared from *E. coli* BL21 (DE3) Gold cells was supplemented to purified protein before performing the activity measurement. However, all attempts remained in no activity in the presence of the conductive polymer. If a mediator or an enzyme would be able to serve as electron shuttle between the conductive polymer and P450 BM3 that was present in the cell lysate, the system could have been reconstituted by adding cell lysate to the purified protein. A positive result of this experiment would question the hypothesis of a mediator based reaction with P450 BM3.



Fig. 92: SDS-page of the collected fraction during purification. Lane 1-4: fraction before protein elution; Lane 5-9: fraction after protein elution; Lane 11-14: protein elution fraction, red frame indicates P450 BM3 at 120 kDa; Lane 10: prestained protein ladder.

3. Finally the third control experiment was performed with a coupled enzyme assay. The NADPH in the cell lysate was consumed by the addition of a second enzyme, the Glutathione disulphide reductase. The Glutathione reductase converts oxidized Glutathione (GSSG) under consumption of NADPH to reduced Glutathione (GSH) (Michal, 1998).



After treatment of the cell lysate with the Glutathione reductase, this mixture was used with BCCE in presence of Clevios P to determine monooxygenase activity. No activity could be detected by addition of Clevios P (Fig. 93). Supplementing NADPH to the Glutathione reductase treated reaction, activity was monitored underlying the hypotheses that a NADPH based reaction is present.

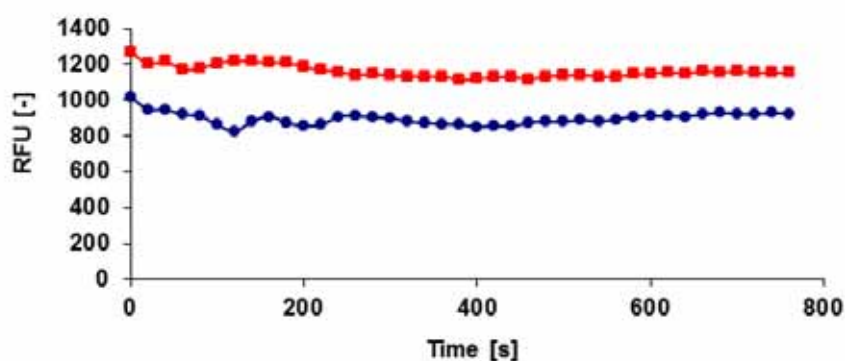


Fig. 93: BCCE conversion by P450 BM3 T577G crude extract after GSSG reductase treatment in presence of Clevios P (●) and without addition (■) recorded at λ_{ex} 400 nm, λ_{em} 440 nm.

Concluding, the activity detectable in the cell lysate by the fluorescent assay as well by the colorimetric assays is based on the NADPH present in the cell lysate and not due to the addition of the conductive polymer and/or the presence of a mediator.

The lack of activity in the absence of NADPH was underlined on the one hand by the NADPH consumption through a second enzymatic reaction (Glutathione reductase) or by storage procedure in which the enzymes present in the cell lysate consumed the remaining NADPH, on the other hand by the separation of the NADPH from the protein fractions during the purification process.

2.5 Discussion

In this chapter, the evolution of P450 BM3 towards improved Direct Electron Transfer by directed evolution was investigated. Starting variant for this work is the reported activity improved variant P450 BM3 Y51F T577G in the presence of the conductive polymer Baytron P (Nazor, 2007) for 3-phenoxytoluene. Preliminary conversion experiments showed that P450 BM3 could not hydroxylate efficiently the substrate 3-phenoxytoluene in presence of Clevios P as previously reported for Baytron P. The reported protocol for the 4-AAP screening system in presence of Baytron P could not be alienated to the use of Clevios P. Using this protocol, no activity in presence of Clevios P could be detected. Several mutants as well as several activity assays were applied to analyze the product formation rate. Leading to the conclusion that no direct electron could be detected. This is only due to the lack of a suitable electron donor, Clevios P without electrochemical reduction and without regeneration system cannot deliver electrons to the enzyme. The assay used for product detection (4-AAP assay) itself is working because when NADPH is supplemented to the reaction, a clear activity increase and difference between the empty vector and the P450 BM3 variant can be measured. The product formation could be proven by GC only when NADPH was supplemented.

Theoretical, the conductive polymer Clevios P, which is only soluble in the oxidized state cannot serve as electron donor and cannot reduce the Enzyme. A conductive polymer in the reduced state with a redoxpotential higher than -400 mV, which correspond to the redoxpotential of the enzyme and a regeneration system would be required to assure the efficient electron shuttle. Clevios P is not suitable for this approach, to use a conductive polymer in solution as exclusive electron source. An electrode coated with the conductive polymer and embedded P450 BM3 would be a suitable approach. On the electrode the

conductive polymer would be generated by electrochemical polymerization and build a thin film. Through the application of a redoxpotential lower than the enzyme redoxpotential the polymer would be in the reduced state and electrons could be shuttle to the enzyme enabling substrate conversion.

The non reproducible results from Nazor et al. were due to the employed conductive polymer. Beside the consideration mentioned above that theoretically Clevios P cannot serve as electron donor, the conductive polymer solution was questionable. The conductive polymer used in previous experiments was Baytron P produced by H.C. Starcks. In 2009 the Baytron P formulation was renamed as Clevios P by H.C Starcks, but the composition remained similar and unchanged in the ratio of PSS to PEDOT, as stated by the company. In this thesis, only the new batch of conductive polymer (Clevios P) was available and could be used. Subsequently, an unforeseeable event was the influence of the commercial available Clevios P, which was not identical to the previously employed Baytron P. The first alertness of an occurring change in the product was given by the different behaviour in the reported 4-AAP assay protocol. The conductive polymer Clevios P could not be precipitated after the enzymatic conversion by centrifugation (section 2.1.1.1). Clevios P stayed in solutions and interfered with the colorimetric reaction necessary to quantify the generated product amounts. Nevertheless, prerequisite for a successful directed protein evolution is a medium or high throughput screening assay allowing to sample the diversity of the generated libraries in an efficient and reliable way (Tee and Schwaneberg, 2007). To optimize the 4-AAP six conductive polymer formulations from H.C. Starcks with different properties were tested and compared to Clevios P. The aim was to identify one formulation with similar properties to that of Baytron P. Unfortunately, no activity or even no activity improvement could be detected applying all these polymers to P450 BM3 Y51F T577G. Several parameters, like buffer concentration, reaction volume, substrate concentration were modified without success. Finally, the main problem was solved after investigating additives and separation methods to effectively precipitate the polymer by the addition of lysozyme to the reaction mixture. The interaction principle of lysozyme and the conductive polymer in aqueous solution could not be explained.

Even if no activity could be detected, the 4-AAP assay in presence of the conductive polymer could be used for screening and selection of activity improved variants, because the coefficient of variation was determined to be between 3.7 and 7.5% depending on the

analyzed variant. Screening systems with standard deviation less than 15 % have successfully been used in directed evolution experiments (Schwaneberg et al., 1999a; Wong et al., 2005b).

Role of the FMN in P450 BM3 Y51F T577G

Screening of a site-saturation library at amino acid position T577 yielded a mutant bearing the amino acid exchange T577G with a significantly improved activity using the conducting polymer Baytron P (PEDOT/PSS) (Nazor, 2007). Nazor et al. proposed that the conductive polymer is binding in close proximity to the FMN binding site and could directly transmit electrons to the electron transfer chain. This rose up the importance of the bound FMN cofactor. The fluorescent and absorption spectra of truncated variants (FAD deficient mutants) were compared to the P450 BM3 WT. The FMN could clearly be detected, concluding that the FMN is not lost when the amino acid substitution T577G is present. Thus, a direct connection between the conducting polymer and amino acids in the FMN-binding cavity might not be due to the loss of the cofactor FMN. The hypothesis established by Nazor et al. that T577G substitution might lead to breaking of hydrogen bonds to W574 or FMN and the loss of either of them would allow more flexibility in the polypeptide backbone, leading to a destabilization of the FMN in its binding cavity could not be verified by the shown experiments.

Screening of Focused mutant libraries for improved DET

The evolution of P450 BM3 for DET was undertaken as promising results were published and the fact that Clevios P was not suitable to be applied without regeneration system as alternative cofactor system was recognized delayed.

The evolution of P450 BM3 for improved DET was performed first by screening of structure guided mutant libraries. Five residues (positions G488, Y536, N537 and W574) were selected which very likely interact with FMN through hydrogen bonds in the FMN-cavity of P450 BM3. The positions were NNK saturated and screened to enhance the activity of the monooxygenase with the conducting polymer Clevios P. The loop spanning residues Y536-P541 and its interactions with the cofactor in P450 BM3 are reported crucial for the stability and flexibility of the turn (Kasim et al., 2009). Almost all amino acids substitutions selected in the focused mutant libraries screened for improved DET were from hydrophobic to charged amino acids. These observations show that drastic structural changes in the FMN binding site, mainly towards charged amino acids, create an interface supporting a better connection to the conducting polymer (Nazor, 2007).

The asparagine residue on position 537 can form hydrogen bonds between the backbone amide and the FMN N5. Substitution at position N537 are reported to eliminate the asparagine side chain interactions (N537A) or to alter the turn stability (N537G) and structure (N537G/G538A, N537A/G538A) (Kasim et al., 2009). Position G538 is reported to be crucial in maintaining the type I turn conformation in the FMN binding cavity (Kasim et al., 2009). Therefore it is not unexpected that during the screening of focussed mutant libraries at position N537 no activity improvement could be observed.

Substitution at position Y536 to amino acids with basic residues (H or R) did not significantly influence the redox properties of the FMN or the accumulation of the anionic semiquinone but substitutions to charged amino acids (D) the FMN binding is affected, the variants contained less than half as much FMN as FAD and the FMN was lost during the purification (Kasim et al., 2009).

In the loop region Y536-P541 the tandem Pro-Pro sequence at position P540-P541 anchors and „regidifies“ the loop, these positions were not selected for mutagenesis as it was favorable to keep this design. The positions P540A/P541A are reported to alter the conformation and flexibility could not be reconstituted with the FMN cofactor (Kasim et al., 2009).

Amino acid G488 was selected for mutagenesis due to the beneficial impact observed in the MET results of position S489. Amino acid G488 is lying in close proximity to the considered loop Y536-P541. A probably loss of the hydrogen bond formation between N543 and S489 were observed in the variant N543S R471C with improved activity in presence of the alternative cofactor system Zn/Co(III)-sep. The screening of the saturation library at position G488 identified the amino acid substitution G488E and G488F which revealed only minor improved mutants.

Thus, several beneficial amino acid substitutions were identified by the screening of the SSM libraries at the position G488, Y536, N537 and W574. Altogether, no variants with significantly improved activity could be identified, as activity of all selected variants was in the error range of the assay. The coefficient of deviation was 7.5% for the 4-AAP (Y51F T577G) assay and the improvements were between 5-10%.

Only the SSM at position R471 revealed a variant (R471C) with 1.5 fold enhanced activity for the conductive polymer in crude cell lysate and after CO normalization. Position R471 was not reported in literature as important for the electron transfer or as crucial for interaction in the FMN binding cavity. Position R471 is located in the naturally occurring loop of the P450 BM3 (residues R471-N479), which is used to fuse the heme domain with the reductase

domain of non self-sufficient monooxygenase for engineering artificial redox chains by molecular 'Lego' (Sadeghi et al., 2000; Gilardi et al., 2002). Interestingly position R471 was also found in an epPCR library screened for improved MET (section III.1). R471C is reported as beneficial for DMSO resistance and explains why this mutation was identified in the improved variants. The variants were resistant to the applied DMSO concentration. DMSO was used as co-solvent to increase the substrate concentrations. Leading to the conclusion that R471C is not relevant for the DET and MET.

Screening of simultaneous and consecutive SSM for improved DET

Employing the 4-AAP assay and the substrate 3-phenoxytoluene, 1800 clones of the simultaneous saturation library were screened. The ratio of inactive clones in the mutant library was determined to be 60 %. Even if two clones were verified by sequencing to ensure a good annealing and revealed no mistake, the unfavourable annealing during the overlap extension PCR may be a reason for the high inactive ration. Additionally, a reason could be the cooperative effects obtained by combining substitutions at position W574 to substitutions in close proximity. A high inactive ratio was already observed in the single saturation at position W574 with around 12 %. Indicating that W574 is a crucial position for the cofactor binding. Position W574 has an important role in the flow of the electrons between the P450 BM3 heme and reductase domains and binds relatively high level of FMN (Klein and Fulco, 1993). Replacement of W574 with nonpolar residues has been shown to abolish FMN binding and conserved aromatic side chains, (Klein and Fulco, 1993). The variant W574Y displayed less activity compared to the WT enzyme and high activity of W574F mutant upon addition of as little as 10 μ M FMN, the cyt c reductase activity increased to a level about 15% above that of the P450 BM3 WT (Klein and Fulco, 1993). Screening of focussed libraries at position W574 revealed amino acids with polar uncharged side chain (W574S, W574T) and hydrophobic side chains (W574I, W574A).

In summary, iterative as well as simultaneous saturation of position G488 and W574 did not enhance the activity of P450 BM3 for the conductive polymer Clevios P. Both approaches were performed since in literature the simultaneous saturation is described beneficial compared to the iterative approaches (Reetz et al., 2006).

Screening of random mutagenesis libraries

The semi rational evolution of P450 BM3 for DET was not successful; no significantly improved variants could be identified. Therefore, additionally to the structured guided mutant

libraries, P450 BM3 was evolved for DET by a random mutagenesis approach to identify new hot spots. Two rounds of directed evolution were performed by generating epPCR libraries screened with the 4-AAP assay in the presence of Clevios P.

After the first round of mutagenesis and screening, only one P450 BM3 variant could be detected displaying a minor improvement in presence of the conductive polymer as alternative electron source. Drasticall substitutions from amino acids with polar side chain to basic were found at position S305, serin to asparagine in the variant P450 BM3 Y51F S305N G488E W574R P898L. Additionally at position P898 in the reductase domain, the substitution P898L (non-polar to hydrophobic) occurred. Position P896 is located near to the position S965, R966, K972 reported as crucial in the coenzyme selectivity in the P450 BM3 FAD/NADPH domain (Dunford et al., 2009).

The only partially available (AS 20-630) crystal structure of P450 BM3 WT restricted the analysis of the amino acid substitutions. The substitution at position L418 and S305 (variant selected in the first evolution round) could be displayed only as model (Fig. 94) and the remaining substitution (position: 864, 865, 683, 898) were located in the, till today, unsolved reductase domain.

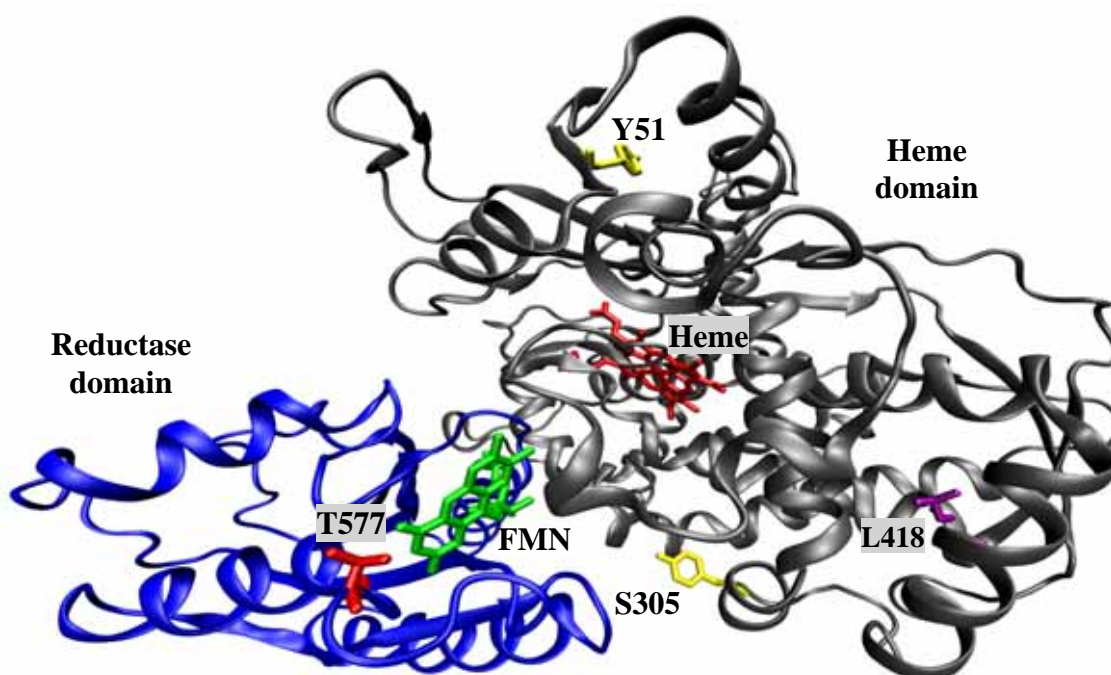


Fig. 94: Structure model of the P450 BM3. The heme domain is colored in gray with the Heme in red and the FMN domain is shown in blue with the FMN in green. The amino acid substitution T577 (red), S305 (yellow), Y51 (yellow) and L418 (purple) are highlighted.

Localization of the substitution in the reductase domain might indicate an improved or at least modified interaction with the cofactor NADPH. None of the mutations was located in the Heme-FMN (P472 – C592) interface which was defined as relevant in the electron transfer

pathway and the cofactor interaction (Klein and Fulco, 1993; Kasim et al., 2009). The lacking activity using the purified protein and the location of the substitutions supported the hypotheses that no direct interactions between the conductive polymer and the protein is present.

Comparison of methods used for determination of the protein concentration

The automated gel electrophoresis as well as the P450 titration by CO-gassing (Omura and Sato, 1964a) was employed and the activity profiles obtained after protein normalization of the variants selected from the epPCR libraries were compared.

Enzyme concentrations correlated by automated gel electrophoresis (Experion system from BioRad) revealed that 2 variants were activity improved in presence of Clevios P. The highest activity was observed for variants P450 BM 3 B4-P3-G10 and P450 BM 3 B4-P4-H2. Contrary, the CO-normalization shows no improved P450 BM3 variants. This can be explained by the fact that in the P450 BM3 titration by CO-gassing only active P450 BM3 is quantified, but in the automated gel electrophoresis the total amount of P450 BM3 protein is calculated. If the ratio of inactive to active protein differs in the selected variant, this leads to activity improved variants in the assay when the concentration is determined by the automated gel electrophoresis system. Concluding, the concentration determined by CO-gassing allows precise and reliable results. Therefore, all variants selected from focused mutant libraries were re-analyzed after CO-gassing and the comparison of product formation rate reconsidered.

In summary, the focused as well as the random mutagenesis approach to improve the activity with the conductive polymer did not lead to activity improved variants for DET. Variants with minor improvements in the crude lysate could be selected but no activity with purified protein in the presence of the conductive polymer was observed. The activity for the natural cofactor NADPH remained unchanged and no activity improvement could be detected for Clevios P. Accordingly to this, the mutants could not be characterized in detail using Clevios P as only electron source for P450 BM3.

NADPH or mediator based conversion

The hypothesis of an undefined component in the cell lysate which serves as mediator allowing activity improvement in presence of the conductive polymer was investigated by three experimental setups.

First the conversion of 3-phenoxytoluene with purified protein in presence of the conducting polymer Clevios P was analysed. No activity in presence of Clevios P could be observed, even though other colorimetric (pNCA) or fluorescent detection assay (7-Ethoxycoumarin and BCCE conversion) as well as several variants bearing the substitution F87A or K187E I162G were used for assaying P450 BM3 activity with the conductive polymer. Subsequently, the generated products in presence of the conducting polymer with cell lysate were detected by GC and GC-MS. The monitored activity is not due to addition of the conducting polymer as the hydroxylated product could be monitored in the reaction mixture without supplemented electron donor. This indicates that a NADPH based reaction is occurring. Additionally, an inhibitory effect by the conductive polymer could be demonstrated. The product could not be monitored in the reaction performed with cell lysate from cells lacking the P450 gene underlying that the substrate is not self-degraded or a site reaction catalysed by other enzymes present in the cell lysate is not occurring. Finally, the hypotheses of an undefined mediator present in the cell lysate and his impact on the activity was investigated.

When the NADPH remaining in the freshly prepared cell lysate is consumed by a coupled enzyme reaction with GSSG reductase or consumed in the storage procedure by other enzymes present in the cell lysate or separated from the protein during the purification, no activity in presence of Clevios P could be detected. These results supported the formulated hypotheses of an NADPH based activity and excluded a mediator present in the cell lysate. If a mediator separated by the purification process from the protein would have been present, the system could have been reconstituted by addition of prepared cell lysate to the purified protein.

All variants selected in the random mutagenesis and focused mutant libraries were probably improved in resistance to the conductive polymer which shows an inhibitory effect on the protein. The inhibitory effect was observed in the fluorescent measurements as well as for the product detection by GC. The product formation rate with NADPH supplemented with Clevios P was lower than compared to the addition of only NADPH. The obtained activity improvements by using different Clevios P formulations are most probably due to a reduced inhibition rather than an increase in activity. The improvements cannot be related to an activity increase rather than to a stability enhancement for variants including the amino acid exchange R471C or in the case of mutation in the reductase domain (epPCR mutants) to an efficient NADPH consumption. The presence of several amino acid substitutions in the reductase domain selected from epPCR libraries indicate a modified interactions with the NADPH. All variants selected as improved were in the error range of the assay and the

activity could not clearly be determined as improved, this is mainly due to the very low conversion. The NADPH remaining in the cell lysate is very low and could not serve as electron donor to convert significant amounts of substrate, leading to very low product formation rates, hardly detectable in the 96 well MTP format.

Nevertheless, even if no activity in presence of Clevios P with purified protein could be monitored, and the claimed 100 fold improved activity with Clevios P with purified Y51F T577G in presence of Baytron P could not be reproduced with Clevios P this results cannot be compared. The conductive polymer Clevios P was similar but could not be stated as identical to Baytron P. Concluding, the evolution of P450 BM3 in presence of the conductive polymer Clevios P could not be achieved. The remaining unsuccessful evolution of P450 BM3 leads to a deep literature research and contest the previous published results. This revealed that PEDOT/PSS solutions have a redoxpotential of around -400 mV and are generated by oxidative polymerization. Meaning that the applied polymer in the enzymatic reaction was in an oxidized state and didn't fulfil the requirements for an electron donor to P450 BM3. The reductase of P450 BM3 has a redoxpotential of -388 mV and requires a mediator in a reduced state (<-400 mV) coupled to an adequate regeneration system, otherwise no efficient electron transfer and substrate conversion would occur.

2.6 Conclusions

In this chapter of the thesis, the evolution of P450 BM3 towards improved Direct Electron Transfer by directed evolution was investigated.

Starting variant was the reported activity improved variant P450 BM3 Y51F T577G in the presence of the conductive polymer Baytron P. This results could not be confirmed as no activity in presence of Clevios P could be detected. Nevertheless, the evolution of P450 BM3 for DET was undertaken as promising results were published and the fact that Clevios P was not suitable to be applied without regeneration system as alternative cofactor system was recognized delayed.

The evolution was performed by a focused mutagenesis approach as well as by random mutagenesis. The generated libraries were screened with the 4-AAP assay for improved activity in presence of the conductive polymer Clevios P. Clevios P could not be precipitated by centrifugation like it occurred for Baytron P, therefore the 4-AAP assay was optimized. Several parameters, like buffer concentration, reaction volume, substrate concentration were varied. However, no improvement was achieved the product formation could not be increased and was not detectable. Then, six conductive polymer formulations from H.C. Starcks with

different properties were tested and compared to Clevios P to identify one formulation with similar properties as the Baytron P which could be used as artificial electron donor in the P450 hydroxylation reaction. None of the tested formulations affects significantly the activity. Finally, the main problem of an insufficient precipitation was solved after investigating additives and separation methods, and the polymer could effectively be precipitated by the addition of lysozyme to the reaction mixture. Using the improved protocol, the coefficient of variation was determined to be between 3.7 and 7.5% depending on the analyzed variant.

Besides the evolution of P450 BM3, the fate of FMN in the variant Y51F T577G was investigated. The FMN could clearly be detected in FAD deficient variants, concluding that the FMN is not lost when the amino acid substitution T577G is present. Thus, a direct connection between the conducting polymer and amino acids in the FMN-binding cavity might not be due to the loss of the cofactor FMN. The directed evolution of P450 BM3 to enhance the activity of the monooxygenase with the conducting polymer Clevios P was performed by a semi rational evolution approach as well as the random mutagenesis approach to identify new hot spots. The iteratively as well as the simultaneous saturation of position G488 and W574 in addition to the saturated position (positions G488, Y536, N537 and W574) and the screening of the epPCR libraries did not enhance the activity for the conductive polymer, no variants with improved activity could be identified. During the screening of epPCR libraries, the P450 titration by CO-gassing was compared to the P450 quantification by automated gel electrophoresis. Resulting, that the P450 concentration determined by CO-gassing allows more precise and reliable results. Transferring this observation to other protein, which are no monooxygenase indicates that the protein concentration determined by automated gel electrophoresis is not reliable to efficiently avoid expression mutants.

The subsequent identified lacking activity with the purified protein and the location of the substitutions supported the analyzed hypotheses that no direct interactions between the conductive polymer and the protein is present.

To exclude the presence of a mediator in the cell lysate and analyse if a NADPH or mediator based conversion is occurring, control experiments were performed. First the conversion of 3-phenoxytoluene with purified protein in presence of the conducting polymer Clevios P was analysed. No activity in presence of Clevios P could be observed, even though other colorimetric (pNCA) or fluorescent detection assays (7-Ethoxycoumarin and BCCE conversion). Subsequently, the generated products in presence of the conducting polymer with cell lysate were detected by GC and GC-MS. Concluding, the monitored activity is not

due to addition of the conducting polymer as the hydroxylated product could be monitored in the reaction mixture without supplemented electron donor indicating that a NADPH based reaction is occurring. Additionally, an inhibitory effect by the conductive polymer could be demonstrated. Finally, the hypothesis of an undefined mediator present in the cell lysate and his impact on the activity was investigated by recombining the cell lysate with purified protein. Concluding, the protein has no detectable activity with the conductive polymer Clevios P. Selected mutants from the screening were improved for resistance towards Clevios P or stability with NADPH but the activity for direct electron transfer and the electron transfer rate did not increase.

Subsequent analysis and discussion revealed that Clevios P could not be identified as a suitable alternative cofactor system when used alone in solution without regeneration system. The PEDOT/PSS polymer is generated through oxidative polymerization with Fe-salts and synthesized in its oxidized state, which would not be suitable to drive P450 BM3. The reductase of P450 BM3 has a formal redox potential of -388 mV. An efficient electron donor for P450 BM3 requires a redox potential, which is more negative than the P450 BM3's redox potential (< -400 mV). The formal redox potential of a PEDOT/PSS (Baytron P) solution is reported to be around -400 mV and because of existing reaction over potentials it is not suitable to function as electron donating "battery".

4. Appendix Chapter: Summarizing collaborative projects with P450 BM3

In this chapter of the thesis the research performed within the framework of the EU-Project Oxygreen besides the main topic of the P450 BM3 evolution for alternative cofactor systems is summarized. These projects were done in collaboration with the Dechema (Frankfurt, Germany), DWI (Aachen, Germany), TU Graz (Graz, Austria) and coworker from our group working on other work packages.

4.1 Directed Evolution of P 450 BM 3 into a p-Xylene Hydroxylase

Collaborator: Alexander Dennig (RWTH Aachen)

Publication: Directed Evolution of P 450 BM 3 into a p-Xylene Hydroxylase

Alexander Dennig, Jan Marienhagen, Anna Joelle Ruff, Lukas Guddat, Ulrich Schwaneberg

Abstract⁴: “2,5-Dimethylphenol (2,5-DMP) is of high interest for the production of temperature stable polymers (>500 K) as well as a building block for “next-generation” plastics. The presented reengineered P450 BM3 variant (R47I/Y51W/I401M) has a good catalytic activity (k_{cat} 1950 min⁻¹), excellent coupling efficiency (66 %) and selectivity (>98 %) for 2,5-DMP production.” (Dennig et al., 2012)

4.2 Electrochemical characterization of P450 BM3 variants

Collaborator: Claudia Ley, Dirk Holtmann, Jens Schrader (Dechema, Frankfurt)

The aim of the collaboration with the Karl-Winnacker Institute at the Dechema (Frankfurt, Germany) was to electrochemically evaluate the variants generated in this thesis for their MET transfer abilities. Besides the variants selected in the screening for improved MET, molecular biological tasks were realized to generate variants with attached tags for their electrochemical analysis. Several P450 BM3 variants were constructed, expressed and provided in mg scale for an evaluation with the recently developed eMTP (Ley et al., 2012, submitted).

⁴ Copied from Publication: Directed Evolution of P 450 BM 3 into a p-Xylene Hydroxylase, Alexander Dennig, Jan Marienhagen, Anna Joelle Ruff, Lukas Guddat, Ulrich Schwaneberg, ChemCatChem, 2012, 4, 771-773

- 1) P450 BM3 M4 and M5 were reconstituted by SDM as published by Nazor (Nazor et al., 2008) with the purpose to compare generated mutants to previously published data (Fig. 95).

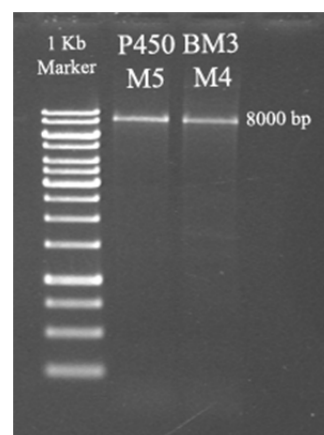


Fig. 95: PCR product of variant P450 BM3 M4 and M5 generated by SDM and separated by agarose gel electrophoresis.

- 2) P450 BM3 M3 with a N-terminal Lys-Taq was generated by PCR for evaluation of planned immobilization methods on the electrode. The sequence of the Lys-Tag as well as the used primers is given in Table S1 in the Appendix (section 6.1).
- 3) P450 BM3 variants with a HIS-tag (P450 BM3 M3, P450 BM3 F87A, P450 BM3 WT) were generated by PCR and confirmed by sequencing. The constructs were used to investigate the influence of charges on immobilization on electrodes according to the employed methods used by Ley (Ley et al., 2011).

4.3 Surface modification of P450 BM3 for immobilization on gold particles

Collaborator: Patrick van Rijn (DWI, Aachen)

Gold surfaces are reported to covalently bind monooxygenase via sulphur containing amino acids (Aryal et al., 2006; Ferrero et al., 2008; Mak et al., 2010). Rational introduction of amino acid substitutions to cysteine or lysins allow to orientate the monooxygenase on the electrode surface (Mak et al., 2010). P450 BM3 has many lysins (Fig. 96) but no cysteins on the surfaces. Aim of the project was to covalently attache P450 BM3 to gold Janus particles in an orientated manner to maintain the catalytic activity at interphase (hexane/aqueous buffer). The approach to use the lysins present on the surface failed, the particles were completely covered with P450 BM3 and no catalytic activity could be detected.

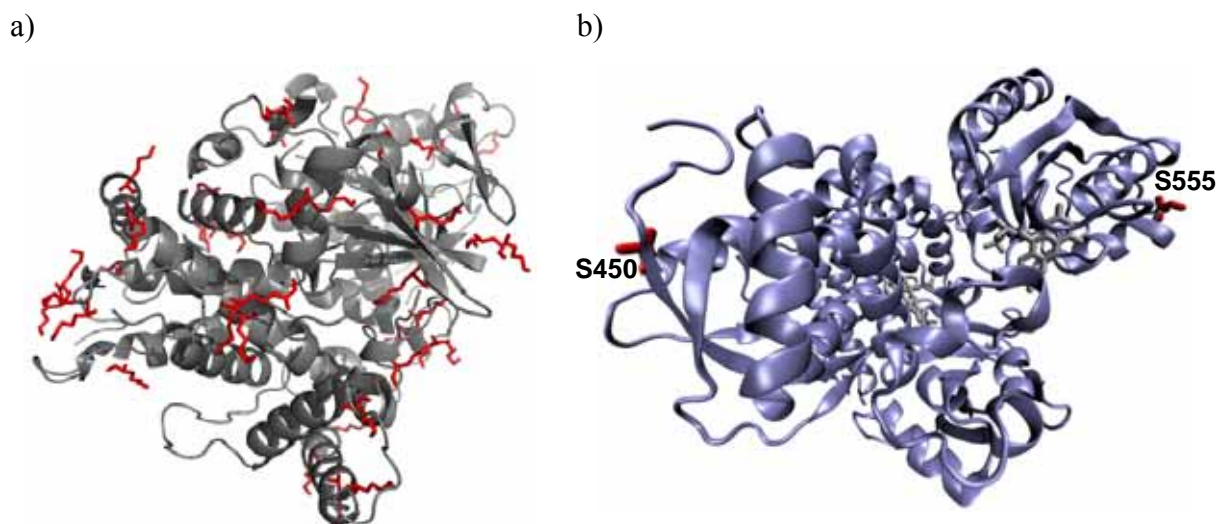


Fig. 96: a) Lysins displayed on the surfaces of P450 BM3. b) S450 and S555 located on the surfaces of P450 BM3 and displayed in red.

Therefore cystein modifications on the protein surface of P450 BM3 were performed to orientate the protein. The appointed substitution from serin to cysteine at position 450 located in the heme domain and position 555 located in the reductase domain were introduced by SDM. The variants were generated by SDM and purified according to standard protocols starting with the variant P450 BM3 I162G K187E improved for 7-Ethoxycoumarin conversion as well as for Indol hydroxylation (Park et al., 2010). Variant P450 BM3 I162G K187E was selected to enable the use of an easy to handle and sensitive fluorescent or robust colorimetric assay to determine the activity of the P450 BM3 I162G K187E in an immobilized state.

In collaboration with Patrick Van Rijn (DWI an der RWTH Aachen e.V.), the attachment of variant P450 BM3 I162G K187E S450C or P450 BM3 I162G K187E S555C to the gold surfaces was achieved and analysed. The immobilization was successful, but the catalytic activity of the generated assembly was lost.

4.4 Monooxygenase mutein database (MuteinDB)

The literature search, data collection and implementation in a format sheet which could be integrated in the Mutein DataBase (MuteinDB) was performed for P450 BM3; more than 50 publication were considered and 800 muteins were collected and integrated in the mutein database which was managed by A. Braun (TU Graz, Austria).

Collaborator: Andreas Braun (TU Graz, Austria)

Publication: MuteinDB: The mutein database linking substrates, products and enzymatic reactions directly with genetic variants of enzymes

Andreas Braun, Bettina Halwachs, Martina Geier, Katrin Weinhandl, Michael Guggemos, Jan Marienhagen, Anna Joelle Ruff, Ulrich Schwaneberg, Vincent Rabin, Daniel E. Torres Pazmino, Gerhard G. Thallinger, Anton Glieder

Abstract⁵: “Mutational events as well as the selection of the optimal variant are essential steps in the evolution of living organisms. The same principle is used in laboratory to extend the natural biodiversity to obtain better catalysts for applications in biomanufacturing or for improved biopharmaceuticals. Furthermore, single mutations in genes of drug metabolizing enzymes can also result in dramatic changes in pharmacokinetics. These changes are a major cause of patient-specific drug responses and are therefore the molecular basis for personalized medicine.

MuteinDB systematically links laboratory-generated enzyme variants (muteins) and natural isoforms with their biochemical properties including kinetic data of catalysed reactions. Detailed information about kinetic characteristics of muteins is available in a systematic way, and searchable for known mutations and catalysed reactions as well as their substrates and known products. MuteinDB is broadly applicable to any known protein and their variants and makes mutagenesis and biochemical data searchable and comparable in a simple and easy-to-use manner. For the import of new mutein data, a simple, standardised, spreadsheet-based data format has been defined. To demonstrate the broad applicability of the MuteinDB, first data sets have been incorporated for selected cytochrome P450 enzymes as well as for nitrilases and peroxidases.

Database URL: <http://www.MuteinDB.org>” (Braun et al., 2012)

⁵ Copied from Publication: MuteinDB: The mutein database linking substrates, products and enzymatic reactions directly with genetic variants of enzymes, Andreas Braun, Bettina Halwachs, Martina Geier, Katrin Weinhandl, Michael Guggemos, Jan Marienhagen, Anna Joelle Ruff, Ulrich Schwaneberg, Vincent Rabin, Daniel E. Torres Pazmino, Gerhard G. Thallinger, Anton Glieder, Database, 2012, Databases Vol. 2012, doi:10.1093/database/bas028

5. Summary

In this thesis entitled “Advances in directed monooxygenase evolution: From diversity generation and flow cytometry screening to tailor-made monooxygenases”, methodological advancements in the two key steps of directed protein evolution, the diversity generation and high throughput screening were achieved. The methodological advances were complemented by the directed protein evolution of P450 BM3 towards improved activity with alternative cofactor systems.

Directed evolution Step 1 consisting of generation of high quality mutant libraries was advanced by developing an improved SeSaM protocol in which a universal base complementary to the P-base was employed to generate more diverse libraries. Employing a second degenerated base allows for the first time to introduce transversion mutation at all four nucleotides. Step 2 was advanced by generating the first reported whole cell high throughput screening assay for monooxygenases allowing to efficiently sample the diversity generated in Step1. Subsequently, the SeSaM-R-base advanced protocol and the flow cytometry screening system were applied to evolve P450 BM3 for alternative cofactor systems in iterative rounds (Step 3) of diversity generation and screening. These developed methods (flow cytometer assay for P450 BM3 and advanced SeSaM method) are of main interest for the researchers focusing on protein engineering and contribute to improved directed evolution protocols which can be efficiently applied for protein engineering.

Chapter I of the thesis focus on the advancement of the SeSaM method. Herein, the application of the R-base as universal base complementary to the P-base was investigated to further increase the amino acid sequence space that can be generated by the SeSaM method is reported. SeSaM-P/R allows for the first time to introduce at all four nucleotides in a gene transversion mutations which are homogeneously distributed over the targeted gene and which mutates each nucleotide. Advancements compared to SeSaM-P lie in the more diverse fragmentations patterns, omitting the use of template-DNA (Step 3), doubling the mutation frequency, and chemical diversity due to parallel employment of the P- and R-base. The SeSaM-P/R method nearly doubles the number of by epPCR unobtainable amino acid substitutions when compared to previous SeSaM methods. Transversions cause amino acid substitutions that are naturally not or barely occurring leading to chemically diverse amino acids substitution patterns. The latter mutational bias might become beneficial for protein

reengineering challenges such as improving solubility of proteins in water, increasing thermal resistance or stability in organic solvents.

Second approach to advance the SeSaM method was tackled with modified bases on the 3' position of the sugar backbone through protecting groups to gain control over the number of added bases. The latter was not achieved efficiently.

Chapter II of the thesis reports the development of the first flow cytometer based ultra-high throughput screening platform that can be applied in directed evolution campaigns of P450 monooxygenases. The whole cell high throughput screening assay for P450 BM3 is based on a coumarin derivative (7-Benzoxo-3-Carboxy-Coumarin Ethyl ester (BCCE)) and allows sorting and enrichment of P450 variants at an excellent throughput of 500 events per second. Variants with up 7-fold increased activity (P450 BM3 DM-1) could be identified from a random mutant library. Furthermore, the presented BCCE screening platform is not only restricted to P450 monooxygenases, and will very likely be applicable to all P450 monooxygenases that can be expressed in *E. coli* and catalyze an *O*-dealkylation of coumarin derivatives (e.g. human CYP3A4). It could further be used in metagenomic screenings, improving protein expression and screening of recombination libraries of P450 monooxygenases as well as corresponding reductases.

A flow cytometer based ultra-high throughput screening assay for directed evolution of P450 BM3 towards improved mediated electron transfer with Zn-dust as electron source could not be settled despite that the entrapment of P450 BM3 expressing cells (permeabilized with polymixin B), of the substrate BCCE-acid, the water soluble mediator Co(III)-sep and Zn-dust in w/o/w emulsion was successful. Stable emulsion could be generated but no detectable activity was recorded. The inhibitory effect of the Zn-dust on the microbial grow was predominant and excluded the use of the double emulsion technology for the generation of an assay for the evolution of P450 BM3 for mediated electron transfer.

In Chapter III, the advanced methods developed in Chapter I and II were employed to generate P450 BM3 libraries to evolve the monooxygenase towards alternative cofactor systems (mediated and directed electron transfer). Random mutant libraries were generated with the SeSaM method and by epPCR, enriched with the flow cytometer assay and screened with the BCCE fluorescent assay in MTP for improved mediated electron transfer. P450 BM3 M3 could further be engineered towards increasing activity in presence of the alternative cofactor system Zn/Co(III)-sep. In the first step by the screening of focused saturation mutagenesis libraries at position N543 and R471, the variant P450 BM3 M3 N543SR471C could be selected with a 3 fold improved catalytic efficiency ($K_{\text{eff}} = 17 \text{ min}^{-1} \text{ mM}^{-1}$) compared

to the variant P450 BM3 M3 ($K_{\text{eff}} = 5 \text{ min}^{-1} \text{ mM}^{-1}$). Subsequent directed P450 BM3 M3 N543S R471C evolution yielded the variant P450 BM3 M3 DM-2 (R203H F423L I401V) which had a nearly 4 fold improved K_{cat} ($K_{\text{cat}} = 6.8 \text{ min}^{-1}$) vs. the engineered variant P450 BM3 M3 DM (N543S R471C) ($K_{\text{cat}} = 1.8 \text{ min}^{-1}$). Four new hot spots (255, 203, 423, 401) which were not reported before as relevant for the MET could be identified. Finally, the individual saturation of the identified position and the recombination of the beneficial amino acid substitution led to variants (Re-6 (R203V R255Q) and Re-B (F423L R255Q)) which were respectively 1.4 fold and 1.15 fold improved in activity compared to the selected variant in the first round of directed evolution (DM-2: R203H F423L I401V).

The second investigated alternative cofactor system, the Direct Electron Transfer was studied by directed P450 BM3 evolution to enhance activity in presence of the conducting polymer. The selected BM3 mutants were improved for resistance towards Clevios P or stability with NADPH but the activity for direct electron transfer and the electron transfer rate did not increase.

Furthermore, in this thesis related collaborative P450 BM3 projects within the Oxygreen funding networks are reported. These comprise the collection of data for the mutein database (MuteinDB), the reengineering of P450 BM3 for altered substrate specificity and surface modifications of P450 BM3 for electrochemical characterization.

6. Appendix

6.1 List of strains and primers

Table S1: Primer used in experimental section.

Primer	Sequence (5'-3')	Purpose used
PP1^b	CATGGGCATGACAATTAAGAAATGCCTCAG	PLICing P450 BM3
PP2^b	CGACGGAGCTCGAATTCTTATTACCCAGC	PLICing P450 BM3
PP3^b	CGAGCTCCGTCGACAAGCTTGCG	PLICing P450 BM3
PP4^b	GTCATGCCCATGGTATATCTCCTTC	PLICing P450 BM3
P1	GACCGGCGCTCAGTTGGAATTCTAG	SeSaM Chapter I
P2	CACACTACCGCACTCCGTCGGACCATGATTACGCCAAGCTTGC	SeSaM Chapter I
P3	GTGTGATGGCGTGAGGCAGCGACCGGCGCTCAGTTGGAATTCTAG	SeSaM Chapter I
P4^a	[Biotin] CAC ACT ACC GCA CTC CGT CG	SeSaM Chapter I
P5	CCTGTTACCAAGTGGCTGCTGCCAGTGG	SeSaM Chapter I
P6	CTATAGTGAGTCGTATTAATTTTCAACATGTGAGC	SeSaM Chapter I
P7	CTAACAAAGCCCAGAAAGGAAGCTGAGTTG	SeSaM Chapter I
P8	GCTATGAGAAAGCGCCACGCTTCCCG	SeSaM Chapter I
P9	GGCAAGATCCTGGTATCGGTCTGCG	SeSaM Chapter I
P10^b	CGTCGATTTTTGTGATGCTCGTCAG	SeSaM Chapter I
P11^b	CTAGCTAGGATCCGGTACCGGTATG	SeSaM Chapter I
P12	CTAGCTAGGATCCGGTACCGGTATGGTGR	SeSaM Chapter I
P13	CTAGCTAGGATCCGGTACCGGTATGGTGRR	SeSaM Chapter I
P14	CTAGCTAGGATCCGGTACCGGTATGGTGRRR	SeSaM Chapter I
P15^c	[FITC] GCAATACGCAAACAGTCTCTCT	SeSaM Chapter I
P16	TGGAATTCACCTTGTGGCCGTCTACTCGCGAGATCGTCGCCGTCCAGCTC GACCAGGATGGGCACCACCCCGGTGAACAGCTCCTCGCCCTTXXXCAC CATAACCGGTACC XXX = CCC, TTT, AAA, GGG, AGA, GAG	SeSaM Chapter I
P17	TAATACGACTCACTATAGGG	BM3 SEQUENCING-T7 promoter
P19	CTTTAACAGCTTTTACCGAGATCAGC	BM3 SEQUENCING-Primer 2.1
P20	CAGCTTAAATATGTCGGCATGGTC	BM3 SEQUENCING-Primer 3
P21	GTGCTATACGGTTCAAATATGG	BM3 SEQUENCING-Primer 4
P22	GTTTTCAACGAACGTCGTAGC	BM3 SEQUENCING-Primer 5
P23	GTCGATGAAAAACAAGCAAGC	BM3 SEQUENCING-Primer 6
P24	CGGAAAAGATCCAGAAAC	BM3 SEQUENCING-N-seq-2/4
P25	GCA ACGCTTGATTCACAC	BM3 SEQUENCING-N-seq-3/4
P26	CGGTCATCCGCCTGATNNNGCAAAGCAATTTGTCGAC	SSM 543-Fwd
P27	GTCGACAAATTGCTTTGCGNNNATCAGGCGGATGACCG	SSM 543-Rev
P28	CAGTCTGCTAAAAAAGTANNNAAGGCAGAAAACGCTC	SSM 471-Fwd
P29	GAGCGTTTTCTGCCTTTTTNNNTACTTTTTTAGCAGACTG	SSM 471-Rev
P30	GGATGCGGCGATAAAAACNNKGCTACTGGCTATCAAAAAG	SSM 574-T577G-Fwd
P31	CTTTTTGATAGCCAGTAGCMNNGTTTTTATCGCCGCATCC	SSM 574-T577G-Rev
P32	GCGCTGTATTTCTTAGGCAAAAATCCACATGTATTAC	SDM V281G-Fwd
P33	GTAATACATGTGGATTTTTGCCAAGAAATACAGCGC	SDM V281G-Rev
P34	GATCTAGCGGATCCATGACAATTAAGAAATG	Heme/FMN expression BamHI
P35	GATCTAGCGAATTCTTACCCAGCCACACGCTTTTTGC	P450 BM3 Rev EcoRI

P36	GCGGCTTAACTATCGCATT AACAGCTTTTACCGAGATCAG	Substrat 7-Ethoxycoumarin und coumarin SDM F162I
P37	CTGATCTCGGTAAGCTGTTAATGCGATAGTTAAAGCCGC	Substrat 7-Ethoxycoumarin und coumarin SDM F162I
P38	GGATGAAGCAATGAACGAAGTGCAGCGAGCAAATCC	Substrat 7-Ethoxycoumarin und coumarin SDM K187E
P39	GGATTTGCTCGCTGCAGTTCGTTTCATTGCTTCATCC	Substrat 7-Ethoxycoumarin und coumarin SDM K187E
P40	GATCTAGCCCATGGATGACAATTAAGAAATG	Heme-FMN bp 1-471 FAD DEFFICIENT MUTANT
P41	GATCTAGCGAATTCTTATTACGTTGAAAACGCACCGTG	Heme-FMN bp 1-664 FAD-defficient mutant
P42	GTTATCAGGCGGATGACCMNNATAAGACGCCGTTAC	SSM 537-Rev
P43	GTA ACG GCG TCT TAT NNK GGT CAT CCG CCT GAT AAC	SSM 537-Fwd
P44	GGATGCGGCGATAAAAACNNKGCTACTACGTATCAAAAAG	SSM 574-Fwd
P45	CTTTTTGATACGTAGTAGCMNNGTTTTATCGCCGCATCC	SSM 574-Rev
P46	CGCTGCTTGTGCTATACNNKTCAAATATGGGAACAGC	SSM 488-Fwd
P47	GCTGTTCCCATATTTGAMNNGTATAGCACAAGCAGCG	SSM 488-Rev
P48	GTATTAATTGTAACGGCGTCTNNKAACGGTCATCCGCCTG	SSM 536-Fwd
P49	CAGGCGGATGACCGTTMNNAGACGCCGTTACAATTAATAC	SSM 536-Rev
P50	GATACCATGGGCAAAAAGAAGAAAAGAAAATGACAATTAAGAAAT G	N-term Lys tag (Fwd)
P51	GGTCGTGTAACGCGCTTTTTATCAAGTCAGCGTC	SDM Y51F-Fwd
P52	GACGCTGACTTGATAAAAAGCGCGTTACACGACC	SDM Y51F-Rev
P53	GGCGATAAAAAGTGGGCTACTGGCTATCAAAAAGTG CCTGCT	SDM T577G-Fwd
P54	AGCAGGCACTTTTTGATAGCCAGTAGCCAGTTTTT ATC GCC	SDM T577G-Rev
P55	CCTCAGCTTCACCGTCATAAAACAATTTGGGGA	SDM D363H-Fwd
P56	TCCCCAAATTGTTTTATGACGGTGAAGCTGAGG	SDM D363H-Rev
P57	GCAGGAGACGGGTTAGCTACAAGCTGGACGCATG	SDM F87A-Fwd
P58	CATGCGTCCAGCTTGTAGCTAACCCGCTCCTGC	SDM F87A-Rev
P59	GAAAAAGGCGACGAACTAAGCGTTCTGATTCCCTCAG	SDM M354S-Fwd
P60	CTGAGGAATCAGAACGCTTAGTTCTGTCGCCTTTTTT	SDM M354S-Rev
P61	CAGTCTGCTAAAAAGTATGCAAAAAGGCAGAAAACGCT	SDM R471C-Fwd
P62	AGCGTTTTCTGCCTTTTTGCATACTTTTTTAGCAGACTG	SDM R471C-Rev
P63	CGGTCATCCGCCTGATAGCGCAAAGCAATTTGTCGAC	SDM N543S-Fwd
P64	GTCGACAAATTGCTTTGCGCTATCAGGCGGATGACCG	SDM N543S-Rev
P65	GGCTTTGTGGTAAAAGCAAAATGCAAAAATTCGCTTGCGGTATTC	SDM S450C-Fwd
P66	GAATACCGCCAAGCGGAATTTTTTGCATTTTCTTTTACCACAAAGCC	SDM S450C-Rev
P67	GTCGACTGGTTAGACCAAGCGTGTGCTGATGAAGTAAAAGGCGTTC	SDM S555C-Fwd
P68	GAACGCCTTTTACTTCATCAGCACACGCTTGGTCTAACCAGTCGAC	SDM S555C-Rev
P69	CGCTTGATGACGAGAACATTNNKTATCAAATTATTACATTC	SSM 255-Fwd
P70	GAATGTAATAATTTGATAMNNAATGTTCTCGTCATCAAGCG	SSM 255-Rev
P71	GCTTATGATGAAAACAAGNNKCAGTTTCAAGAAGATATCAAG	SSM 203-Fwd
P72	CTTGATATCTTCTTGAAACTGMNNTTGTTTTTCATCATAAGC	SSM 203-Rev
P73	GATGCTAAACACTTTGACNNKGAAGATCATAAACTACG	SSM 423-Fwd
P74	CGTAGTTTGTATGATCTTCMNNGTCAAAGTGTTTTAGCATC	SSM 423-Rev
P75	GCTTATGATGAAAACAAGGTGCAGTTTCAAGAAGATATCAAG	SDM R203V-Fwd
P76	CTTGATATCTTCTTGAAACTGCACCTTGTTTTTCATCATAAGC	SDM R203V-Rev

P77	CGCTTGATGACGAGAACATT NNK TATCAAATTATTACATTC	SDM R255H-Fwd
P78	GAATGTAATAATTTGATAM MNN AATGTTCTCGTCATCAAGCG	SDM R255H-Rev
P79	CGCCTGTCACCCGCTGCTTGTGCTATACGGTTC	SesSaM BM3 FMN-up
P80	CACACTACCGCACTCCGTCGCCGCTGCTTGTGCTATACGGTTC	SesSaM BM3 FMN-Fwd
P81	CGCTTGATGACGAGAACATT NNK TATCAAATTATTACATTC	SSM R255-Fwd
P82	GAATGTAATAATTTGATAM MNN AATGTTCTCGTCATCAAGCG	SSM R255-Rev
P83	GATGCTAAAACACTTTGAC CTG GAAGATCATACAAACTACG	SDM F423L-Fwd
P84	CGTAGTTTGTATGATCTT CAG GTCAAAGTGTTTTAGCATC	SDM F423L-Rev
P85	CAGCGTGCGTGT NNK GGTCAGCAGTTC	SSM 401-Fwd
P86	GAACTGCTGAC MNN ACACGCACGCTG	SSM 401-Rev
P87	CGACTCACTATAGGGGAATTGTGAGCGGA	Amplification MCS pET-vectors
P88	CGGGCTTTGTTAGCAGCCGGATCTCAG	Amplification MCS pET-vectors
P89	CACACTACCGCACTCCGTCGCGACTCACTATAGGGGAATTGTGAGCGGA	SeSaM library of genes cloned in pET-vectors
P90	GTGTGATGGCGTGAGGCAGCCGGGCTTTGTTAGCAGCCGGATCTCAG	SeSaM library of genes cloned in pET-vectors
P91	CGCCTGTCACCGACTCACTATAGGGGAATTGTGAGCGGA	SeSaM library of genes cloned in pET-vectors
P92	GCGGACAGTGCGGGCTTTGTTAGCAGCCGGATCTCAG	SeSaM library of genes cloned in pET-vectors
P93	[Biotin]CACACTACCGCACTCCGTCG	SeSaM library of genes cloned in pET-vectors
P94	[Biotin]GTGTGATGGCGTGAGGCAGC	SeSaM library of genes cloned in pET-vectors

^a [Biotin] represents 5'-biotin

^b bold letters represent phosphorothiolated nucleotides

^c [FITC] represent 5' fluorescein isothiocyanate

Table S2: List of strains used or generated in this work.

Strain	Origin
E. coli DH5a pET28a(+) P450 BM3 M4 (R47F F87A V281G M354S)	SDM V281G in pET28a(+) P450 BM3 M2
E. coli DH5a pET28a(+) P450 BM3 M5 (R47F F87A V281G M354S D363H)	SDM V281G in pET28a(+) P450 BM3 M3
E. coli DH5a pET28a(+) P450 BM3 Y51F	SDM Y51F in pET28a(+) P450 BM3 WT
E. coli DH5a pET28a(+) P450 BM3 Y51F T577G	SDM T577G in pET28a(+) P450 BM3 Y51F
E. coli BL21 (DE3) pET28a(+)P450 BM3 M2 (R47F F87A M354S)	Strain collection (Nazor et al., 2006)
E. coli BL21 (DE3) pET28a(+)P450 BM3 M3 (R47F F87A M354S D363H)	Strain collection (Nazor et al., 2006)
E. coli BL21 (DE3) pET28a(+)P450 BM3 M4 (R47F F87A V281G M354S)	Plasmid isolated from E.coli DH5a pET28a(+) P450 BM3 M4
E. coli BL21 (DE3) pET28a(+)P450 BM3 M5 (R47F F87A V281G M354S D363H)	E.coli BL21 (DE3) Gold pET28a(+) P450 BM3 M5
E. coli BL21 (DE3) Gold pET28a(+) P450 BM3 Y51F	Strain collection (Wong et al., 2008)
E. coli BL21 (DE3) Gold pET28a(+) P450 BM3 Y51F T577G	Strain collection (Nazor et al., 2006)
E. coli DH5a pCWORI P450 BM3 Y51F T577G	Strain collection (Nazor et al., 2006)
E. coli DH5a pCWORI P450 BM3 Y51F	Strain collection (Nazor et al., 2006)
E. coli BL21 (DE3) pET28a(+)	Commercial Vector from Merck
E. coli DH5a	Strain collection
E. coli BL21 (DE3) Gold	Strain collection
E. coli BL21 (DE3) lacIQ	Strain collection
E. coli BL21 (DE3) Gold pET28a(+) P450 BM3 F87A T577G	Restriction cloning MfeI/EcoRI from pET28a(+) P450 BM3 Y51F T577G in pET28a(+) P450 BM3 F87A
E. coli BL21 (DE3) Gold pET28a(+) P450 BM3 Y51F F162I K187E T577G	SDM F162I K187E in pET28a(+) P450 BM3 Y51F T577G
E. coli BL21 (DE3) Gold pET28a(+) P450 BM3 Y51F F162I T577G	SDM F162I in pET28a(+) P450 BM3 Y51F T577G
E. coli BL21 (DE3) Gold pET28a(+) P450 BM3 Y51F K187E T577G	SDM K187E in pET28a(+) P450 BM3 Y51F T577G
E. coli BL21 (DE3) Gold pET28a(+) P450 BM3 F162I K187E T577G	Restriction cloning MfeI/EcoRI from pET28a(+) P450 BM3 Y51F F162I K187E T577G in pET28a(+) P450 BM3 WT
E. coli BL21 (DE3) Gold pET28a(+) P450 BM3 F162I K187E T577G Y536S T533L A534G	Restriction cloning MfeI/EcoRI from pET28a(+) P450 BM3 Y51F F162I K187E T577G in pET28a(+) P450 BM3 WT
E. coli BL21 (DE3) Gold pET28a(+) P450 BM3 Y51F T577G Y536S T533L A534G	Generated in this thesis – SSM Y536S
E. coli BL21 (DE3) Gold pET28a(+) P450 BM3 F162I K187E T577G G488E	Restriction cloning MfeI/EcoRI
E. coli BL21 (DE3) Gold pET28a(+) P450 BM3 Y51F T577G G488E	SSM G488
E. coli BL21 (DE3) Gold pET28a(+) P450 BM3 T577G	SDM T577G in pET28a(+) P450 BM3 WT
E. coli BL21 (DE3) Gold pAlXtreme-1a P450 BM3 F87A	Subcloning from pET28a(+) P450 BM3 F87A
E. coli BL21 (DE3) Gold pET28a(+) P450 BM3 F87A T577G	SDM F87A in pET28a(+) P450 BM3 T577G
E. coli BL21 (DE3) Gold pALXtreme-1a P450 BM3	Strain collection
E. coli BL21 (DE3) Gold pET28a(+) P450 BM3 F162I K187E S450C T577G	SDM S450C in pET28a(+) P450 BM3 F162I K187E T577G
E. coli BL21 (DE3) Gold pET28a(+) P450 BM3 F162I K187E S555C T577G	SDM S555C in pET28a(+) P450 BM3 F162I K187E T577G
E. coli BL21 (DE3) Gold pET28a(+) P450 BM3 R471C T577G	SSM R471

E. coli BL21 (DE3) Gold pALXtreme-1a P450 BM3 M3 (R47F F87A M354S D363H)	Subcloning from pET28a(+) P450 BM3 M3
E. coli BL21 (DE3) Gold LacIQ pALXtreme-1a P450 BM3 M3 R471C	SSM R471
E. coli BL21 (DE3) Gold LacIQ pALXtreme-1a P450 BM3 M3 R471T	SSM R471
E. coli BL21 (DE3) Gold LacIQ pALXtreme-1a P450 BM3 M3 N543S	SDM N543S in pET28a(+) P450 BM3 M3
E. coli BL21 (DE3) Gold LacIQ pALXtreme-1a P450 BM3 M3 R471C N543S	SDM R471C in pET28a(+) P450 BM3 M3 N543S
E. coli BL21 (DE3) Gold pET28a(+) P450 BM3 M3 R471C N543S R203V I401V	Generated in this thesis – epPCR screening
E. coli BL21 (DE3) Gold pET28a(+) P450 BM3 M3 DM-2 (R47F F87A M354S D363H R471C N543S F423L I401V)	Generated in this thesis – epPCR screening
E. coli BL21 (DE3) Gold pET28a(+) P450 BM3 M3 R471C N543S I401V	SSM I401
E. coli BL21 (DE3) Gold pET28a(+) P450 BM3 M3 R471C N543S R255Q	SSM 255
E. coli BL21 (DE3) Gold pET28a(+) P450 BM3 M3 DM-1 (R47F F87A M354S D363H R471C N543S R255H)	Generated in this thesis – epPCR screening
E. coli BL21 (DE3) Gold pET28a(+) P450 BM3 M3 R471C N543S R203H F423L I401V	SDM pET28a(+) P450 BM3 M3 R471C N543S
E. coli BL21 (DE3) Gold pET28a(+) P450 BM3 M3 R471C N543S F423L I401V R255H	SDM pET28a(+) P450 BM3 M3 R471C N543S
E. coli BL21 (DE3) Gold pET28a(+) P450 BM3 M3 R471C N543S F423L R255H	SDM pET28a(+) P450 BM3 M3 R471C N543S
E. coli BL21 (DE3) Gold pET28a(+) P450 BM3 M3 R471C N543S F423L R255Q	SDM pET28a(+) P450 BM3 M3 R471C N543S
E. coli BL21 (DE3) Gold pET28a(+) P450 BM3 M3 R471C N543S R203H F423L I401V R255Q	SDM pET28a(+) P450 BM3 M3 R471C N543S
E. coli BL21 (DE3) Gold pET28a(+) P450 BM3 M3 R471C N543S R203H F423L I401V R255H	SDM pET28a(+) P450 BM3 M3 R471C N543S
E. coli BL21 (DE3) Gold pET28a(+) P450 BM3 M3 R471C N543S R203H F423L I401V	SDM pET28a(+) P450 BM3 M3 R471C N543S
E. coli BL21 (DE3) Gold pET28a(+) P450 BM3 M3 R471C N543S R203V R255Q	SDM pET28a(+) P450 BM3 M3 R471C N543S
E. coli BL21 (DE3) Gold pET28a(+) P450 BM3 M3 R471C N543S R203V R255H	SDM pET28a(+) P450 BM3 M3 R471C N543S
E. coli BL21 (DE3) Gold pET28a(+) P450 BM3 M3 R471C N543S R203V F423L I401V R255Q	SDM pET28a(+) P450 BM3 M3 R471C N543S
E. coli BL21 (DE3) Gold pET28a(+) P450 BM3 M3 R471C N543S R203V F423L I401V R255H	SDM pET28a(+) P450 BM3 M3 R471C N543S
E. coli BL21 (DE3) Gold pET28a(+) P450 BM3 M3 R471C N543S R203V F423L R255Q	SDM pET28a(+) P450 BM3 M3 R471C N543S
E. coli BL21 (DE3) Gold pET28a(+) P450 BM3 M3 R471C N543S R203V I401V R255H	SDM pET28a(+) P450 BM3 M3 R471C N543S

6.2 Supplementary information of Chapter I

Table S3: **Upper part:** Sequencing results of a SeSaM library with R base and in Step 3 employed Vent (exo-) polymerase. **Lower part:** Sequencing results of SeSaM library with R and P base and Vent (exo-) polymerase in Step 3. Gray underlined amino acid substitutions are unobtainable by epPCR.

Clone no.	Amino acid substitutions	Mutated codons	Transversion	Transition
1	K4T	AAG → ACG	+	
2	L196L	CTG → CTA		+
3	K108R	AAG → AGG		+
4	D118E	GAC → GAG	+	
5	F72L	TTC → CTC		+
6	V62G	GTG → GGG	+	
7	V62G	GTG → GGG	+	
8	I162I	ATC → ATT		+
9	R110H	CGC → CAC		+
10	F72L	TTC → CTC		+
11	D77G	GAC → GGC		+
12	V2A	GTG → GCG		+
	Y75N	TAC → AAC	+	
13	I15V	ATC → GTC		+
	V17G	GTC → GGC	+	
14	S31S	TCC → TCA	+	
	F72Y	TTC → TAC	+	
15	A88V	GCC → GTC		+
	I168T	ATC → ACC		+
16	I172I	ATC → ATT		+
	L222M	CTG → ATG	+	
17	H140Y	CAC → TAC		+
	F166L	TTC → CTC		+
18	L16M	CTG → ATG	+	
	R123G	CGC → GGC	+	
19	T98T	ACC → ACT		+
	I162I	ATC → ATT		+
20	P76S	CCC → TCC		+
	K114N	AAG → AAT	+	
	D191E	GAC → GAG	+	
21	T98I	ACC → ATC		+
	L138R	CTG → CGG	+	
	K163Q	AAG → CAG	+	

Clone no.	Amino acid substitutions	Mutated codons	Transversion	Transition
1	T226A	ACC → GCC		+
2	K167E	AAG → GAG		+
3	Q178Q	CAG → CAA		+
4	I153N	ATC → AAC	+	
5	G34C	GGC → TGC	+	
6	I172N	ATC → AAC	+	
7	L232H	CTC → CAC	+	
8	K127Q	AAG → CAG	+	
9	S206S	TCC → TCT		+
10	L138P	CTG → CCG		+
11	K4E	AAG → GAG		+
12	V2A	GTG → GCG		+
13	G34C	GGC → TGC	+	
	G175GS176R	GGC → GGA AGC → CGC	++	
14	M79T	ATG → ACG		+
	D156V	GAC → GTC	+	
15	L19L	CTG → TTG		+
	G34GE35Q	GGC → GGA GAG → CAG	++	
16	Y67N	TAC → AAC	+	
	R110H	CGC → CAC		+
17	G25G	GGC → GGG	+	
	G52G	GGC → GGG	+	
18	I153N	ATC → AAC	+	
	P14A	CCC → GCC	+	
19	D211V	GAC → GTC	+	
	F224I	TTC → ATC	+	
20	L142L	CTG → TTG		+
	M154T	ATG → ACG		+
21	N171R	AAC → AGA	+	+
	R169H	CGC → CAC		+
22	E6G	GAG → GGG		+
	G34C	GGC → TGC	+	
23	D37V	GAT → GTT	+	
	P193P	CCC → CCT		+
24	D77H	GAC → CAC	+	
	T119T	ACC → ACT		+

25	K4N	AAG	→	AAT	+	
	E7DL8L	GAG CTG	→	GAT TTG	+	+
26	H170R	CAC	→	CGC		+
	Y201C	TAC	→	TGC		+
27	F131C	TTC	→	TGC	+	
	S209G	AGC	→	GGC		+
28	V69A	GTG	→	GCG		+
	H170Y	CAC	→	TAC		+
29	D77H	GAC	→	CAC	+	
	T119T	ACC	→	ACT		+
30	M79T	ATG	→	ACG		+
	D156V	GAC	→	GTC	+	
31	T60A	ACC	→	GCC		+
	T98D	ACC	→	GAC	+	+
	T109S	ACC	→	TCC	+	
32	T60I	ACC	→	ATC		+
	V62E	GTG	→	GAG	+	
	Y152N	TAT	→	AAT	+	
33	F72Y	TTC	→	TAC	+	
	H82R	CAC	→	CGC		+
	Y201C	TAC	→	TGC		+
34	V30G	GTG	→	GGG	+	
	T51S	ACC	→	AGC	+	
	P90P	CCC	→	CCT		+
35	M1I	ATG	→	ATT	+	
	G5H	GGC	→	CAC	+	+
	N106H	AAC	→	CAC	+	
36	K4T	AAG	→	ACG	+	
	S31S	TCC	→	TCA	+	
	F72Y	TTC	→	TAC	+	
37	V56E	GTG	→	GAG	+	
	D118E	GAC	→	GAA	+	
	M234I	ATG	→	ATC		+
38	F72L	TTC	→	CTC		+
	R97L	CGC	→	CTG	+	
	F224S	TTC	→	TCC		+
39	P14A	CCC	→	GCC	+	
	L54L	CTG	→	CTA		+
	T66T	ACC	→	ACT		+

40	V94V	GTC	→	GTT		+
	V30E	GTG	→	GAG	+	
	T39I	ACC	→	ATC		+
	T60P	ACC	→	GCC		+
41	V69E	GTG	→	GAG	+	
	V113A	GTG	→	GCG		+
	N150D	AAC	→	GAC		+
	G161V	GGC	→	GTC	+	
42	V23V	GTA	→	GTG		+
	L43P	CTG	→	CCG		+
	P55P	CCC	→	CCA	+	
	L222P	CTG	→	CCG		+
43	I189T	ATC	→	ACC		+
	L43L	CTG	→	CTA		+
	T66T	ACC	→	ACT		+
	S87T	TCC	→	ACC	+	
44	I48I	ATC	→	ATT		+
	I124T	ATC	→	ACC		+
	N165D	AAC	→	GAC		+
	T204S	ACC	→	TCC	+	
	G233E	GGC	→	GAA	+	+
45	V69E	GTG	→	GAG	+	
	V113A	GTG	→	GCG		+
	N150S	AAC	→	AGC		+
	M154T	ATG	→	ACG		+
	G161V	GGC	→	GTC	+	
46	G117S	GGC	→	AGC		+
	I129F	ATC	→	TTC	+	
	K157R	AAG	→	AGG		+
	Q185L	CAG	→	CTG	+	
	L237V	CTG	→	GTG	+	

6.3 Vector maps

pET28a(+)

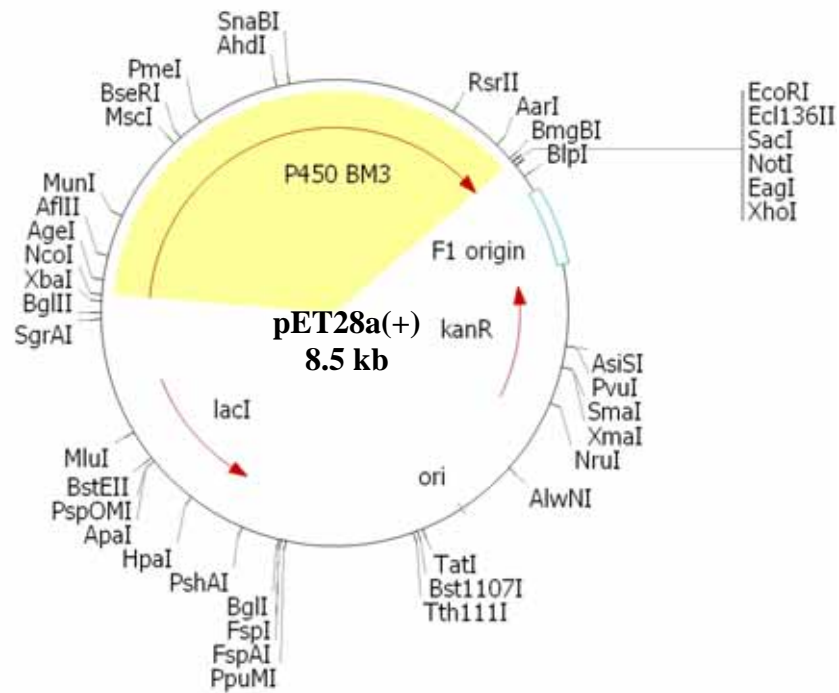


Fig. 97: Vector map of pET28a(+) (Merck, Darmstadt, Germany).

pCWori(+)

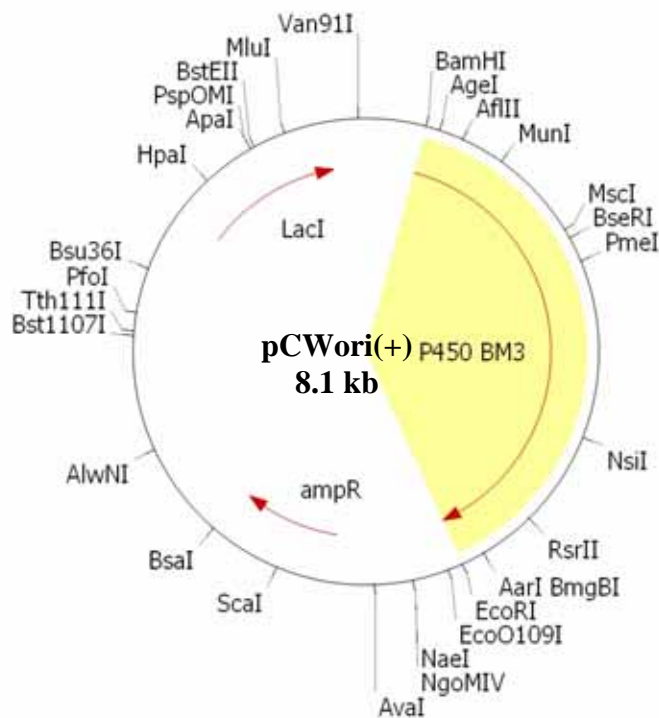


Fig. 98: Vector map of pCWori(+) a derivative of plasmid pHSe5 (Barnes, 1996).

pALXtreme-1a

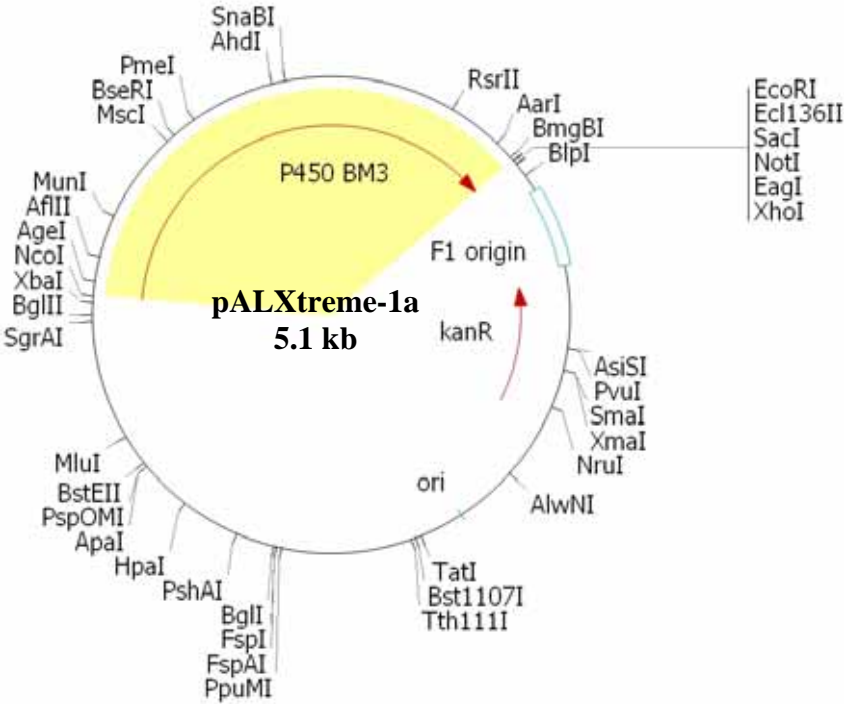


Fig. 99: Vector map of pALXtreme-1a, derivative of plasmid pET28a(+) (Dr. A. Schenk, Jacobs University Bremen, Bremen, Germany).

7. References

- Abécassis, V., Pompon, D., and Truan, G. (2000). High Efficiency Family Shuffling Based on Multi-Step PCR and in Vivo DNA Recombination in Yeast: Statistical and Functional Analysis of a Combinatorial Library Between Human Cytochrome P450 1A1 and 1A2. *Nucl. Acids Res.* 28, e88.
- Agresti, J.J., Antipov, E., Abate, A.R., Ahn, K., Rowat, A.C., Baret, J.-C., Marquez, M., Klibanov, A.M., Griffiths, A.D., and Weitz, D.A. (2010). Ultrahigh-throughput screening in drop-based microfluidics for directed evolution. *Proc. Natl. Acad. Sci. U.S.A.* 107, 4004–4009.
- Aharoni, A., Amitai, G., Bernath, K., Magdassi, S., and Tawfik, D.S. (2005a). High-throughput screening of enzyme libraries: thiolactonases evolved by fluorescence-activated sorting of single cells in emulsion compartments. *Chem. Biol.* 12, 1281–1289.
- Aharoni, A., Griffiths, A.D., and Tawfik, D.S. (2005b). High-throughput screens and selections of enzyme-encoding genes. *Curr. Opin. Chem. Biol.* 9, 210–216.
- An, Y., Ji, J., Wu, W., Lv, A., Huang, R., and Wei, Y. (2005). A rapid and efficient method for multiple-site mutagenesis with a modified overlap extension PCR. *Appl. Microbiol. Biotechnol.* 68, 774–778.
- Appel, D., Lutz-Wahl, S., Fischer, P., Schwaneberg, U., and Schmid, R.D. (2001). A P450 BM-3 mutant hydroxylates alkanes, cycloalkanes, arenes and heteroarenes. *J. Biotechnol.* 88, 167–171.
- Arnold, F.H., and Volkov, A.A. (1999). Directed evolution of biocatalysts. *Curr Opin Chem Biol* 3, 54–59.
- Arnold, F.H., and Georgiou, G. (2003). *Directed Enzyme Evolution: Screening and Selection Methods* (Humana Press).
- Aryal, S., R., Dharmaraj, N., Bhattarai, N., Kim, C.H., and Kim, H.Y. (2006). Spectroscopic identification of S-Au interaction in cysteine capped gold nanoparticles. *Spectrochim Acta A Mol Biomol Spectrosc* 63, 160–163.
- Barnes, H.J. (1996). Maximizing expression of eukaryotic cytochrome P450s in *Escherichia coli*. In *Cytochrome P450, Part B*, (Academic Press), 3–14.

- Beabealashvilli, R.S., Scamrov, A.V., Kutateladze, T.V., Mazo, A.M., Krayevsky, A.A., and Kukhanova, M.K. (1986). Nucleoside 5'-triphosphates modified at sugar residues as substrates for calf thymus terminal deoxynucleotidyl transferase and for AMV reverse transcriptase. *Biochim. Biophys. Acta* 868, 136–144.
- Bernath, K., Hai, M., Mastrobattista, E., Griffiths, A.D., Magdassi, S., and Tawfik, D.S. (2004a). In vitro compartmentalization by double emulsions: sorting and gene enrichment by fluorescence activated cell sorting. *Anal. Biochem.* 325, 151–157.
- Bernath, K., Magdassi, S., and Tawfik, D.S. (2004b). In vitro compartmentalization (IVC): A high-throughput screening technology using emulsions and FACS. *Discov Med* 4, 49–53.
- Bernhardt, R. (2006). Cytochromes P450 as versatile biocatalysts. *J. Biotechnol.* 124, 128–145.
- Bershtein, S., and Tawfik, D.S. (2008). Advances in laboratory evolution of enzymes. *Curr Opin Chem Biol* 12, 151–158.
- Biles, B.D., and Connolly, B.A. (2004). Low-fidelity *Pyrococcus furiosus* DNA polymerase mutants useful in error-prone PCR. *Nucleic Acids Res.* 32, e176.
- Blanusa, M. (2010a). Flow cytometry based screening system for finding and improving bioindustrial important biocatalysts – Cytochrome P450 BM3. Thesis, Jacobs University Bremen.
- Blanusa, M., Schenk, A., Sadeghi, H., Marienhagen, J., and Schwaneberg, U. (2010b). Phosphorothioate-based ligase-independent gene cloning (PLICing): An enzyme-free and sequence-independent cloning method. *Anal. Biochem.* 406, 141–146.
- Braun, A., Halwachs, B., Geier, M., Weinhandl, K., Guggemos, M., Marienhagen, J., Ruff, A.J., Schwaneberg, U., Rabin, V., Torres Pazmino, D.E., Thallinger, G., Glieder, A. (2012). MuteinDB: The mutein database linking substrates, products and enzymatic reactions directly with genetic variants of enzymes. *Databases* Vol. 2012, doi:10.1093/database/bas028.
- Bornscheuer, U.T., and Pohl, M. (2001). Improved biocatalysts by directed evolution and rational protein design. *Curr Opin Chem Biol* 5, 137–143.
- Brodie, B.B., Axelrod, J., Cooper, J.R., Gaudette, L., La Du, B.N., Mitoma, C., and Udenfriend, S. (1955). Detoxication of drugs and other foreign compounds by liver microsomes. *Science* 121, 603–604.
- Budde, M., Maurer, S.C., Schmid, R.D., and Urlacher, V.B. (2004). Cloning, expression and characterisation of CYP102A2, a self-sufficient P450 monooxygenase from *Bacillus subtilis*. *Appl. Microbiol. Biotechnol.* 66, 180–186.

- Budde, M., Morr, M., Schmid, R.D., and Urlacher, V.B. (2006). Selective hydroxylation of highly branched fatty acids and their derivatives by CYP102A1 from *Bacillus megaterium*. *Chembiochem* 7, 789–794.
- Cadwell, R.C., and Joyce, G.F. (1992). Randomization of genes by PCR mutagenesis. *PCR Methods Appl.* 2, 28–33.
- Campbell, N.A., and Reece, J.B. (2009). *Biologie* (PEARSON STUDIUM).
- Carmichael, A.B., and Wong, L.L. (2001). Protein engineering of *Bacillus megaterium* CYP102. The oxidation of polycyclic aromatic hydrocarbons. *Eur. J. Biochem.* 268, 3117–3125.
- Chang, L.M., and Bollum, F.J. (1990). Multiple roles of divalent cation in the terminal deoxynucleotidyltransferase reaction. *J. Biol. Chem.* 265, 17436–17440.
- Chefson, A., and Auclair, K. (2006). Progress towards the easier use of P450 enzymes. *Mol Biosyst* 2, 462–469.
- Cheng, Q., Sohl, C.D., and Guengerich, F.P. (2009). High-throughput fluorescence assay of cytochrome P450 3A4. *Nat Protoc* 4, 1258–1261.
- Chilvers, K.F., Perry, J.D., James, A.L., and Reed, R.H. (2001). Synthesis and evaluation of novel fluorogenic substrates for the detection of bacterial beta-galactosidase. *J. Appl. Microbiol.* 91, 1118–1130.
- Cirino, P.C., and Arnold, F.H. (2002). Protein engineering of oxygenases for biocatalysis. *Curr Opin Chem Biol* 6, 130–135.
- Cirino, P.C., Mayer, K.M., and Umeno, D. (2003). Generating mutant libraries using error-prone PCR. *Methods Mol. Biol.* 231, 3–9.
- Cline, J., Braman, J.C., and Hogrefe, H.H. (1996). PCR fidelity of pfu DNA polymerase and other thermostable DNA polymerases. *Nucleic Acids Res.* 24, 3546–3551.
- Crotty, S., Maag, D., Arnold, J.J., Zhong, W., Lau, J.Y., Hong, Z., Andino, R., and Cameron, C.E. (2000). The broad-spectrum antiviral ribonucleoside ribavirin is an RNA virus mutagen. *Nat. Med.* 6, 1375–1379.
- d'Abbadie, M., Hofreiter, M., Vaisman, A., Loakes, D., Gasparutto, D., Cadet, J., Woodgate, R., Pääbo, S., and Holliger, P. (2007). Molecular breeding of polymerases for amplification of ancient DNA. *Nat. Biotechnol.* 25, 939–943.
- de Saint-Aubin, C., Hemmerlé, J., Boulmedais, F., Vallat, M.-F., Nardin, M., and Schaaf, P. (2012). New 2-in-1 polyelectrolyte step-by-step film buildup without solution alternation: from PEDOT-PSS to polyelectrolyte complexes. *Langmuir: The ACS Journal of Surfaces and Colloids*.

- Delarue, M., Boulé, J.B., Lescar, J., Expert-Bezançon, N., Jourdan, N., Sukumar, N., Rougeon, F., and Papanicolaou, C. (2002). Crystal structures of a template-independent DNA polymerase: murine terminal deoxynucleotidyltransferase. *Embo J.* 21, 427–439.
- Dennig, A., Marienhagen, J., Ruff, A.J., Guddat, L., and Schwaneberg, U. (2012). Directed Evolution of P 450 BM 3 into a p-Xylene Hydroxylase. *ChemCatChem*, 4, 771-773.
- Dennig, A., Shivange, A.V., Marienhagen, J., and Schwaneberg, U. (2011). OmniChange: the sequence independent method for simultaneous site-saturation of five codons. *PLoS ONE* 6, e26222.
- Dunford, A.J., Girvan, H.M., Scrutton, N.S., and Munro, A.W. (2009). Probing the molecular determinants of coenzyme selectivity in the P450 BM3 FAD/NADPH domain. *Biochim. Biophys. Acta* 1794, 1181–1189.
- Estabrook, R.W., Faulkner, K.M., Shet, M.S., and Fisher, C.W. (1996). Application of electrochemistry for P450-catalyzed reactions. *Meth. Enzymol.* 272, 44–51.
- Farinas, E.T. (2006). Fluorescence activated cell sorting for enzymatic activity. *Comb. Chem. High Throughput Screen.* 9, 321–328.
- Farinas, E.T., Schwaneberg, U., Glieder, A., and Arnold, F.H. (2001). Directed Evolution of a Cytochrome P450 Monooxygenase for Alkane Oxidation. *Advanced Synthesis & Catalysis* 343, 601–606.
- Fasan, R., Meharena, Y.T., Snow, C.D., Poulos, T.L., and Arnold, F.H. (2008). Evolutionary history of a specialized p450 propane monooxygenase. *J. Mol. Biol.* 383, 1069–1080.
- Faust, S.D., and Mikulewicz, E.W. (1967). Factors influencing the condensation of 4-aminoantipyrine with derivatives of hydroxybenzene - II. Influence of hydronium ion concentration on absorptivity. *Water Research* 1, 509–522.
- Ferrero, V.E.V., Andolfi, L., Di Nardo, G., Sadeghi, S.J., Fantuzzi, A., Cannistraro, S., and Gilardi, G. (2008). Protein and electrode engineering for the covalent immobilization of P450 BMP on gold. *Anal. Chem.* 80, 8438–8446.
- Firth, A.E., and Patrick, W.M. (2008). GLUE-IT and PEDEL-AA: new programmes for analyzing protein diversity in randomized libraries. *Nucleic Acids Res.* 36, W281–285.
- Gilardi, G., Meharena, Y.T., Tsotsou, G.E., Sadeghi, S.J., Fairhead, M., and Giannini, S. (2002). Molecular Lego: design of molecular assemblies of P450 enzymes for nanobiotechnology. *Biosens Bioelectron* 17, 133–145.
- Glieder, A., Farinas, E.T., and Arnold, F.H. (2002). Laboratory evolution of a soluble, self-sufficient, highly active alkane hydroxylase. *Nat. Biotechnol.* 20, 1135–1139.

- Griffiths, A.D., and Tawfik, D.S. (2006). Miniaturising the laboratory in emulsion droplets. *Trends Biotechnol.* 24, 395–402.
- Groenendaal, L. (2000). Poly (3, 4-ethylenedioxythiophene) and its derivatives: past, present, and future. *Adv. Mater. Weinheim* 12, 481.
- Guengerich, F.P., Gillam, E.M., and Shimada, T. (1996). New applications of bacterial systems to problems in toxicology. *Crit. Rev. Toxicol.* 26, 551–583.
- Güven, G. (2011). *Engineering Bioelectrozymes for Bioelectronics Applications*. Thesis, Jacobs University Bremen.
- Güven, G., Prodanovic, R., and Schwaneberg, U. (2010). Protein Engineering – An Option for Enzymatic Biofuel Cell Design. *Electroanalysis* 22, 765–775.
- Hardiman, E., Gibbs, M., Reeves, R., and Bergquist, P. (2010). Directed evolution of a thermophilic beta-glucosidase for cellulosic bioethanol production. *Appl. Biochem. Biotechnol.* 161, 301–312.
- Henne, A., Schmitz, R.A., Bömeke, M., Gottschalk, G., and Daniel, R. (2000). Screening of environmental DNA libraries for the presence of genes conferring lipolytic activity on *Escherichia coli*. *Appl. Environ. Microbiol.* 66, 3113–3116.
- Ho, S.N., Hunt, H.D., Horton, R.M., Pullen, J.K., and Pease, L.R. (1989). Site-directed mutagenesis by overlap extension using the polymerase chain reaction. *Gene* 77, 51–59.
- Hogrefe, H.H., Cline, J., Youngblood, G.L., and Allen, R.M. (2002). Creating randomized amino acid libraries with the QuikChange Multi Site-Directed Mutagenesis Kit. *BioTechniques* 33, 1158–1160, 1162, 1164–1165.
- Hollmann, F., Arends, I.W.C.E., Buehler, K., Schallmeyer, A., and Buehler, B. (2011). Enzyme-mediated oxidations for the chemist. *Green Chem.* 13, 226–265.
- Holtmann, D., Mangold, K.-M., and Schrader, J. (2009). Entrapment of cytochrome P450 BM-3 in polypyrrole for electrochemically-driven biocatalysis. *Biotechnol. Lett.* 31, 765–770.
- Iijima, S., Ohishi, A., and Ohzeki, T. (2009). Cytochrome P450 oxidoreductase deficiency with Antley-Bixler syndrome: steroidogenic capacities. *J. Pediatr. Endocrinol. Metab.* 22, 469–475.
- Imaishi, H., and Ohkawa, H. (2002). Cytochrome P450 species specifically expressed in flower buds metabolize fatty acids. *International Congress Series* 1233, 115–120.
- Ingelman-Sundberg, M. (2004). Pharmacogenetics of cytochrome P450 and its applications in drug therapy: the past, present and future. *Trends Pharmacol. Sci.* 25, 193–200.

- Inoue, K., and Sakai, K. (1977). The synthesis of 11-substituted prostaglandin intermediates. *Tetrahedron Letters* 18, 4063–4066.
- Jiao, P., Hua, Y., Li, S., Huang, Y., and Cao, Z. (2001). Study on the cytochrome P450 activity in alkane converting process of *Candida tropicalis*. *Wei Sheng Wu Xue Bao* 41, 117–120.
- Joo, H., Lin, Z., and Arnold, F.H. (1999). Laboratory evolution of peroxide-mediated cytochrome P450 hydroxylation. *Nature* 399, 670–673.
- Joyce, M.G., Ekanem, I.S., Roitel, O., Dunford, A.J., Neeli, R., Girvan, H.M., Baker, G.J., Curtis, R.A., Munro, A.W., and Leys, D. (2012). The crystal structure of the FAD/NADPH-binding domain of flavocytochrome P450 BM3. *Febs J.* 279, 1694–1706.
- Juchau, M.R. (1990). Substrate specificities and functions of the P450 cytochromes. *Life Sci.* 47, 2385–2394.
- Kanaya, S., Koyanagi, T., and Kanaya, E. (1998). An esterase from *Escherichia coli* with a sequence similarity to hormone-sensitive lipase. *Biochem. J.* 332, 75–80.
- Kasim, M., Chen, H.-C., and Swenson, R.P. (2009). Functional characterization of the re-face loop spanning residues 536-541 and its interactions with the cofactor in the flavin mononucleotide-binding domain of flavocytochrome P450 from *Bacillus megaterium*. *Biochemistry* 48, 5131–5141.
- Kaur, J., and Sharma, R. (2006). Directed evolution: an approach to engineer enzymes. *Crit. Rev. Biotechnol.* 26, 165–199.
- Kazlauskaitė, J., Hill, H.A., Wilkins, P.C., and Dalton, H. (1996). Direct electrochemistry of the hydroxylase of soluble methane monooxygenase from *Methylococcus capsulatus* (Bath). *Eur. J. Biochem.* 241, 552–556.
- Kim, Y.C., Lee, H.S., Yoon, S., and Morrison, S.L. (2009). Transposon-directed base-exchange mutagenesis (TDEM): a novel method for multiple-nucleotide substitutions within a target gene. *BioTechniques* 46, 534–542.
- Klein, M.L., and Fulco, A.J. (1993). Critical residues involved in FMN binding and catalytic activity in cytochrome P450BM-3. *J. Biol. Chem.* 268, 7553–7561.
- Kocieński, P.J. (2005). *Protecting Groups* (Thieme).
- Laemmli, U.K. (1970). Cleavage of structural proteins during the assembly of the head of bacteriophage T4. *Nature* 227, 680–685.

- Lewis, D.F., and Lake, B.G. (1996). Molecular modelling of CYP1A subfamily members based on an alignment with CYP102: rationalization of CYP1A substrate specificity in terms of active site amino acid residues. *Xenobiotica* 26, 723–753.
- Ley, C., Holtmann, D., Mangold, K.-M., and Schrader, J. (2011). Immobilization of histidine-tagged proteins on electrodes. *Colloids Surf B Biointerfaces* 88, 539–551.
- Ley, C., Ruff, A.J., Schewe, H., Schwaneberg, U., Schrader, J., Holtmann, D. (2012). Fast method to optimize electroenzymatic processes with P450s. (in preparation)
- Li, H., Mei, L., Urlacher, V.B., and Schmid, R.D. (2008). Cytochrome P450 BM-3 evolved by random and saturation mutagenesis as an effective indole-hydroxylating catalyst. *Appl. Biochem. Biotechnol.* 144, 27–36.
- Li, Q.S., Ogawa, J., Schmid, R.D., and Shimizu, S. (2001a). Engineering cytochrome P450 BM-3 for oxidation of polycyclic aromatic hydrocarbons. *Appl. Environ. Microbiol.* 67, 5735–5739.
- Li, Q.-S., Schwaneberg, U., Fischer, M., Schmitt, J., Pleiss, J., Lutz-Wahl, S., and Schmid, R.D. (2001b). Rational evolution of a medium chain-specific cytochrome P-450 BM-3 variant. *Biochimica Et Biophysica Acta (BBA) - Protein Structure and Molecular Enzymology* 1545, 114–121.
- Li, Q.S., Schwaneberg, U., Fischer, P., and Schmid, R.D. (2000). Directed evolution of the fatty-acid hydroxylase P450 BM-3 into an indole-hydroxylating catalyst. *Chemistry* 6, 1531–1536.
- Link, A.J., Jeong, K.J., and Georgiou, G. (2007). Beyond toothpicks: new methods for isolating mutant bacteria. *Nat. Rev. Microbiol.* 5, 680–688.
- Luo, S.-C., Mohamed Ali, E., Tansil, N.C., Yu, H.-H., Gao, S., Kantchev, E.A.B., and Ying, J.Y. (2008). Poly(3,4-ethylenedioxythiophene) (PEDOT) nanobiointerfaces: thin, ultrasmooth, and functionalized PEDOT films with in vitro and in vivo biocompatibility. *Langmuir* 24, 8071–8077.
- Lussenburg, B.M.A., Babel, L.C., Vermeulen, N.P.E., and Commandeur, J.N.M. (2005). Evaluation of alkoxyresorufins as fluorescent substrates for cytochrome P450 BM3 and site-directed mutants. *Anal. Biochem.* 341, 148–155.
- Lutz, S., and Patrick, W.M. (2004). Novel methods for directed evolution of enzymes: quality, not quantity. *Curr. Opin. Biotechnol.* 15, 291–297.

- Maag, D., Castro, C., Hong, Z., and Cameron, C.E. (2001). Hepatitis C virus RNA-dependent RNA polymerase (NS5B) as a mediator of the antiviral activity of ribavirin. *J. Biol. Chem.* 276, 46094–46098.
- Mak, L.H., Sadeghi, S.J., Fantuzzi, A., and Gilardi, G. (2010). Control of human cytochrome P450 2E1 electrocatalytic response as a result of unique orientation on gold electrodes. *Anal. Chem.* 82, 5357–5362.
- Matsumura, I., and Rowe, L.A. (2005). Whole plasmid mutagenic PCR for directed protein evolution. *Biomol. Eng.* 22, 73–79.
- Michal, G. (1998). *Biochemical Pathways: Biochemie-Atlas* (Spektrum Akademischer Verlag).
- Miyazaki, K. (2003). Creating random mutagenesis libraries by megaprimer PCR of whole plasmid (MEGAWHOP). *Methods Mol. Biol.* 231, 23–28.
- Montellano, P.R.O.D. (2005). *Cytochrome P450: Structure, Mechanism, and Biochemistry* (Springer).
- Mouri, T., Michizoe, J., Ichinose, H., Kamiya, N., and Goto, M. (2006). A recombinant *Escherichia coli* whole cell biocatalyst harboring a cytochrome P450cam monooxygenase system coupled with enzymatic cofactor regeneration. *Appl. Microbiol. Biotechnol.* 72, 514–520.
- Mundhada, H., Marienhagen, J., Scacioc, A., Schenk, A., Roccatano, D., and Schwaneberg, U. (2011). SeSaM-Tv-II generates a protein sequence space that is unobtainable by epPCR. *Chembiochem* 12, 1595–1601.
- Munro, A.W., Leys, D.G., McLean, K.J., Marshall, K.R., Ost, T.W.B., Daff, S., Miles, C.S., Chapman, S.K., Lysek, D.A., Moser, C.C., et al. (2002). P450 BM3: the very model of a modern flavocytochrome. *Trends Biochem. Sci.* 27, 250–257.
- Narhi, L.O., Wen, L.P., and Fulco, A.J. (1988). Characterization of the protein expressed in *Escherichia coli* by a recombinant plasmid containing the *Bacillus megaterium* cytochrome P-450BM-3 gene. *Mol. Cell. Biochem.* 79, 63–71.
- Nazor, J. (2007). *Alternative Cofactor Systems driving P450 BM3*. Thesis, Jacobs University Bremen.
- Nazor, J., and Schwaneberg, U. (2006). Laboratory evolution of P450 BM-3 for mediated electron transfer. *Chembiochem* 7, 638–644.

- Nazor, J., Dannenmann, S., Adjei, R.O., Fordjour, Y.B., Ghampson, I.T., Blanusa, M., Roccatano, D., and Schwaneberg, U. (2008). Laboratory evolution of P450 BM3 for mediated electron transfer yielding an activity-improved and reductase-independent variant. *Protein Eng. Des. Sel.* 21, 29–35.
- Neeli, R., Roitel, O., Scrutton, N.S., and Munro, A.W. (2005). Switching Pyridine Nucleotide Specificity in P450 BM3 MECHANISTIC ANALYSIS OF THE W1046H AND W1046A ENZYMES. *J. Biol. Chem.* 280, 17634–17644.
- Nelson, D.R., Koymans, L., Kamataki, T., Stegeman, J.J., Feyereisen, R., Waxman, D.J., Waterman, M.R., Gotoh, O., Coon, M.J., Estabrook, R.W., et al. (1996). P450 superfamily: update on new sequences, gene mapping, accession numbers and nomenclature. *Pharmacogenetics* 6, 1–42.
- Neylon, C. (2004). Chemical and biochemical strategies for the randomization of protein encoding DNA sequences: library construction methods for directed evolution. *Nucleic Acids Res.* 32, 1448–1459.
- Olsen, M.J., Stephens, D., Griffiths, D., Daugherty, P., Georgiou, G., and Iverson, B.L. (2000). Function-based isolation of novel enzymes from a large library. *Nat. Biotechnol.* 18, 1071–1074.
- Omura, T. (1999). Forty years of cytochrome P450. *Biochem. Biophys. Res. Commun.* 266, 690–698.
- Omura, T., and Sato, R. (1964a). The carbon monoxide-binding pigment of liver microsomes. I. Evidence for its hemoprotein nature. *J. Biol. Chem.* 239, 2370–2378.
- Omura, T., and Sato, R. (1964b). The carbon monoxide-binding pigment of liver microsomes. II. Solubilization, purification, and properties. *J. Biol. Chem.* 239, 2379–2385.
- Park, S.-H., Kim, D.-H., Kim, D., Kim, D.-H., Jung, H.-C., Pan, J.-G., Ahn, T., Kim, D., and Yun, C.-H. (2010). Engineering bacterial cytochrome P450 (P450) BM3 into a prototype with human P450 enzyme activity using indigo formation. *Drug Metab. Dispos.* 38, 732–739.
- Paterson, I., Yeung, K.-S., Ward, R.A., Smith, J.D., Cuimming, J.G., and Lamboley, S. (1995). The total synthesis of swinholide A. Part 4: Synthesis of swinholide A and isoswinholide A from the protected monomeric seco acid, pre-swinholide A. *Tetrahedron* 51, 9467–9486.
- Peters, M.W., Meinhold, P., Glieder, A., and Arnold, F.H. (2003). Regio- and enantioselective alkane hydroxylation with engineered cytochromes P450 BM-3. *J. Am. Chem. Soc.* 125, 13442–13450.

- Petzoldt, K. (1982). Process for the preparation of 11-beta-hydroxy steroids. Patent 4353985.
- Picataggio, S., Rohrer, T., Deanda, K., Lanning, D., Reynolds, R., Mielenz, J., and Eirich, L.D. (1992). Metabolic engineering of *Candida tropicalis* for the production of long-chain dicarboxylic acids. *Biotechnology (N.Y.)* 10, 894–898.
- Powell, M.F., Wu, J.C., and Bruice, T.C. (1984). Ferricyanide oxidation of dihydropyridines and analogs. *J. Am. Chem. Soc.* 106, 3850–3856.
- Prodanovic, R., Ostafe, R., Scacioc, A., and Schwaneberg, U. (2011). Ultrahigh-throughput screening system for directed glucose oxidase evolution in yeast cells. *Comb. Chem. High Throughput Screen.* 14, 55–60.
- Rasila, T.S., Pajunen, M.I., and Savilahti, H. (2009). Critical evaluation of random mutagenesis by error-prone polymerase chain reaction protocols, *Escherichia coli* mutator strain, and hydroxylamine treatment. *Anal. Biochem.* 388, 71–80.
- Ravichandran, K.G., Boddupalli, S.S., Hasermann, C.A., Peterson, J.A., and Deisenhofer, J. (1993). Crystal structure of hemoprotein domain of P450BM-3, a prototype for microsomal P450's. *Science* 261, 731–736.
- Reetz, M.T., Kahakeaw, D., and Lohmer, R. (2008). Addressing the numbers problem in directed evolution. *Chembiochem* 9, 1797–1804.
- Reetz, M.T., Wang, L.-W., and Bocola, M. (2006). Directed evolution of enantioselective enzymes: iterative cycles of CASTing for probing protein-sequence space. *Angew. Chem. Int. Ed. Engl.* 45, 1236–1241.
- Reinen, J., Ferman, S., Vottero, E., Vermeulen, N.P.E., and Commandeur, J.N.M. (2011). Application of a fluorescence-based continuous-flow bioassay to screen for diversity of cytochrome P450 BM3 mutant libraries. *J Biomol Screen* 16, 239–250.
- Roccatano, D., Wong, T.S., Schwaneberg, U., and Zacharias, M. (2005). Structural and dynamic properties of cytochrome P450 BM-3 in pure water and in a dimethylsulfoxide/water mixture. *Biopolymers* 78, 259–267.
- Ruff, A.J., Marienhagen, J., Verma, R., Roccatano, D., Genieser, H.-G., Niemann, P., Shivange, A.V., and Schwaneberg, U. (2012a). dRTP and dPTP a complementary nucleotide couple for the Sequence Saturation Mutagenesis (SeSaM) method. *Journal of Molecular Catalysis B: Enzymatic* 84, 40–47.
- Ruff, A.J., Dennig, A., Wirtz, G., Blanusa, M., Schwaneberg, U. (2012b). Ultra-high throughput screening system for accelerated directed evolution of P450 monooxygenases. *ACS-Catalysis* 2, 2724–2728.

- Sadeghi, S.J., Meharena, Y.T., Fantuzzi, A., Valetti, F., and Gilardi, G. (2000). Engineering artificial redox chains by molecular “Lego”. *Faraday Discuss.* 135–153; discussion 171–190.
- Sambrook, J., and Russell, D.W. (2001). *Molecular Cloning: A Laboratory Manual* (Cold Spring Harbor Laboratory Press).
- Santoro, S.W., Wang, L., Herberich, B., King, D.S., and Schultz, P.G. (2002). An efficient system for the evolution of aminoacyl-tRNA synthetase specificity. *Nat. Biotechnol.* 20, 1044–1048.
- Schröder, G., Unterbusch, E., Kaltenbach, M., Schmidt, J., Strack, D., De Luca, V., and Schröder, J. (1999). Light-induced cytochrome P450-dependent enzyme in indole alkaloid biosynthesis: tabersonine 16-hydroxylase. *FEBS Letters* 458, 97–102.
- Schwaneberg, U., Appel, D., Schmitt, J., and Schmid, R.D. (2000). P450 in biotechnology: zinc driven omega-hydroxylation of p-nitrophenoxydodecanoic acid using P450 BM-3 F87A as a catalyst. *J. Biotechnol.* 84, 249–257.
- Schwaneberg, U., Schmidt-Dannert, C., Schmitt, J., and Schmid, R.D. (1999a). A continuous spectrophotometric assay for P450 BM-3, a fatty acid hydroxylating enzyme, and its mutant F87A. *Anal. Biochem.* 269, 359–366.
- Schwaneberg, U., Sprauer, A., Schmidt-Dannert, C., and Schmid, R.D. (1999b). P450 monooxygenase in biotechnology. I. Single-step, large-scale purification method for cytochrome P450 BM-3 by anion-exchange chromatography. *J Chromatogr A* 848, 149–159.
- Sevrioukova, I.F., Hazzard, J.T., Tollin, G., and Poulos, T.L. (1999a). The FMN to heme electron transfer in cytochrome P450BM-3. Effect of chemical modification of cysteines engineered at the FMN-heme domain interaction site. *J. Biol. Chem.* 274, 36097–36106.
- Sevrioukova, I.F., Li, H., Zhang, H., Peterson, J.A., and Poulos, T.L. (1999b). Structure of a cytochrome P450-redox partner electron-transfer complex. *Proc. Natl. Acad. Sci. U.S.A.* 96, 1863–1868.
- Shivange, A.V., Marienhagen, J., Mundhada, H., Schenk, A., and Schwaneberg, U. (2009). Advances in generating functional diversity for directed protein evolution. *Curr Opin Chem Biol* 13, 19–25.
- Singer, B., and Kuśmierk, J.T. (1982). Chemical mutagenesis. *Annu. Rev. Biochem.* 51, 655–693.

- Spee, J.H., de Vos, W.M., and Kuipers, O.P. (1993). Efficient random mutagenesis method with adjustable mutation frequency by use of PCR and dITP. *Nucleic Acids Res.* 21, 777–778.
- Stapleton, J.A., and Swartz, J.R. (2010). Development of an in vitro compartmentalization screen for high-throughput directed evolution of [FeFe] hydrogenases. *PLoS ONE* 5, e15275.
- Stemmer, W.P. (1994). DNA shuffling by random fragmentation and reassembly: in vitro recombination for molecular evolution. *Proc Natl Acad Sci U S A* 91, 10747–10751.
- Sun, Y.-F. (2008). *Imaging Sci. Photochem.* 26, 393–402.
- Tee, K.L., and Schwaneberg, U. (2006). A screening system for the directed evolution of epoxygenases: importance of position 184 in P450 BM3 for stereoselective styrene epoxidation. *Angew. Chem. Int. Ed. Engl.* 45, 5380–5383.
- Tee, K.L., and Schwaneberg, U. (2007). Directed evolution of oxygenases: screening systems, success stories and challenges. *Comb. Chem. High Throughput Screen.* 10, 197–217.
- Tu, R., Martinez, R., Prodanovic, R., Klein, M., and Schwaneberg, U. (2011). A flow cytometry-based screening system for directed evolution of proteases. *J Biomol Screen* 16, 285–294.
- Turner (2006). Agar Plate-based Assays. *Enzyme Assays: High-throughput Screening. Genetic Selection and Fingerprinting* (ed J.-L. Reymond) Chapter 5.
- Urlacher, V.B., and Eiben, S. (2006). Cytochrome P450 monooxygenases: perspectives for synthetic application. *Trends Biotechnol.* 24, 324–330.
- Urlacher, V.B., and Schmid, R.D. (2004). Protein engineering of the cytochrome P450 monooxygenase from *Bacillus megaterium*. *Meth. Enzymol.* 388, 208–224.
- Urlacher, V.B., Lutz-Wahl, S., and Schmid, R.D. (2004). Microbial P450 enzymes in biotechnology. *Appl. Microbiol. Biotechnol.* 64, 317–325.
- Vaghefi, M. (2005). *Nucleoside Triphosphates and their Analogs: Chemistry, Biotechnology, and Biological Applications* (CRC Press).
- Vanhercke, T., Ampe, C., Tirry, L., and Denolf, P. (2005). Reducing mutational bias in random protein libraries. *Anal. Biochem.* 339, 9–14.
- Viñas, P., Balsalobre, N., López-Erroz, C., and Hernández-Córdoba, M. (2004). Liquid chromatographic analysis of riboflavin vitamers in foods using fluorescence detection. *J. Agric. Food Chem.* 52, 1789–1794.
- Vo, N.V., Young, K.-C., and Lai, M.M.C. (2003). Mutagenic and inhibitory effects of ribavirin on hepatitis C virus RNA polymerase. *Biochemistry* 42, 10462–10471.

- Volles, M.J., and Lansbury, P.T., Jr (2005). A computer program for the estimation of protein and nucleic acid sequence diversity in random point mutagenesis libraries. *Nucleic Acids Res.* 33, 3667–3677.
- Weber, E., Seifert, A., Antonovici, M., Geinitz, C., Pleiss, J., and Urlacher, V.B. (2011). Screening of a minimal enriched P450 BM3 mutant library for hydroxylation of cyclic and acyclic alkanes. *Chem. Commun. (Camb.)* 47, 944–946.
- Whitehouse, C.J.C., Bell, S.G., and Wong, L.-L. (2012). P450(BM3) (CYP102A1): connecting the dots. *Chem Soc Rev* 41, 1218–1260.
- Whitehouse, C.J.C., Bell, S.G., Yang, W., Yorke, J.A., Blanford, C.F., Strong, A.J.F., Morse, E.J., Bartlam, M., Rao, Z., and Wong, L. (2009). A Highly Active Single-Mutation Variant of P450BM3 (CYP102A1). *ChemBioChem* 10, 1654–1656.
- Wong, T.S., and Schwaneberg, U. (2003). Protein engineering in bioelectrocatalysis. *Curr. Opin. Biotechnol.* 14, 590–596.
- Wong, T.S., Arnold, F.H., and Schwaneberg, U. (2004a). Laboratory evolution of cytochrome p450 BM-3 monooxygenase for organic cosolvents. *Biotechnol. Bioeng.* 85, 351–358.
- Wong, T.S., Tee, K.L., Hauer, B., and Schwaneberg, U. (2004b). Sequence saturation mutagenesis (SeSaM): a novel method for directed evolution. *Nucleic Acids Res.* 32, e26.
- Wong, T.S., Tee, K.L., Hauer, B., and Schwaneberg, U. (2005a). Sequence saturation mutagenesis with tunable mutation frequencies. *Anal. Biochem.* 341, 187–189.
- Wong, T.S., Wu, N., Roccatano, D., Zacharias, M., and Schwaneberg, U. (2005b). Sensitive Assay for Laboratory Evolution of Hydroxylases toward Aromatic and Heterocyclic Compounds. *Journal of Biomolecular Screening* 10, 246–252.
- Wong, T.S., Roccatano, D., Zacharias, M., and Schwaneberg, U. (2006a). A statistical analysis of random mutagenesis methods used for directed protein evolution. *J. Mol. Biol.* 355, 858–871.
- Wong, T.S., Zhurina, D., and Schwaneberg, U. (2006b). The diversity challenge in directed protein evolution. *Comb. Chem. High Throughput Screen.* 9, 271–288.
- Wong, T.S., Roccatano, D., and Schwaneberg, U. (2007a). Challenges of the genetic code for exploring sequence space in directed protein evolution. *Biocatalysis and Biotransformation* 25, 229–241.
- Wong, T.S., Roccatano, D., and Schwaneberg, U. (2007b). Steering directed protein evolution: strategies to manage combinatorial complexity of mutant libraries. *Environ. Microbiol.* 9, 2645–2659.

- Wong, T.S., Roccatano, D., and Schwaneberg, U. (2007c). Are transversion mutations better? A Mutagenesis Assistant Program analysis on P450 BM-3 heme domain. *Biotechnol J* 2, 133–142.
- Wong, T.S., Roccatano, D., Loakes, D., Tee, K.L., Schenk, A., Hauer, B., and Schwaneberg, U. (2008). Transversion-enriched sequence saturation mutagenesis (SeSaM-Tv+): a random mutagenesis method with consecutive nucleotide exchanges that complements the bias of error-prone PCR. *Biotechnol J* 3, 74–82.
- Wu, N., Courtois, F., Zhu, Y., Oakeshott, J., Easton, C., and Abell, C. (2010). Management of the diffusion of 4-methylumbelliferone across phases in microdroplet-based systems for in vitro protein evolution. *Electrophoresis* 31, 3121–3128.
- Yang, G., and Withers, S.G. (2009). Ultrahigh-throughput FACS-based screening for directed enzyme evolution. *Chembiochem* 10, 2704–2715.
- Yuan, L., Kurek, I., English, J., and Keenan, R. (2005). Laboratory-directed protein evolution. *Microbiol. Mol. Biol. Rev.* 69, 373–392.
- Zaccolo, M., Williams, D.M., Brown, D.M., and Gherardi, E. (1996). An approach to random mutagenesis of DNA using mixtures of triphosphate derivatives of nucleoside analogues. *J. Mol. Biol.* 255, 589–603.
- Zhao, H., Giver, L., Shao, Z., Affholter, J.A., and Arnold, F.H. (1998). Molecular evolution by staggered extension process (StEP) in vitro recombination. *Nat. Biotechnol.* 16, 258–261.
- Zhao, L., Güven, G., Li, Y., and Schwaneberg, U. (2011). First steps towards a Zn/Co(III)sep-driven P450 BM3 reactor. *Appl. Microbiol. Biotechnol.* 91, 989–999.
- Zhi-Hui, F., Yan-Bing, H., Quan-Min, S., Li-Fang, Q., Yan, L., Lei, Z., Xiao-Jun, L., Feng, T., Yong-Sheng, W., and Rui-Dong, X. (2010). Polymer solar cells based on a PEDOT:PSS layer spin-coated under the action of an electric field. *Chinese Physics B* 19, 038601.

Acknowledgments

First of all I take this opportunity to express my gratitude to the head of Institute Prof. Dr. Ulrich Schwaneberg for his extensive help and support in guiding me during my PhD-work. I thank him for allocation of these interesting topics, funding and in particular giving me the opportunity to present my work at international conferences.

Thanks to Prof. Dr. Miriam Agler-Rosenbaum (Juniorprofessorin) and Prof. Dr. Lothar Elling to be members of my thesis committee.

Coworkers of the Lehrstuhl für Biotechnologie is given a big thank for the agreeable working atmosphere and their cooperativeness. Especially, I would like to thank my colleague Alexander Dennig for his support and advices in the lab, my supervisor and subgroup leader Dr. Jan Marienhagen and Prof. Dr. Anett Schallmey (Juniorprofessorin) for their supervision and valuable suggestions, Dr. Monika Reiss for her permanent encouragement and Dr. Martin Zimmermann for his stimulation to go ahead.

I am also grateful for the support of the students during the entire lab work, Lukas Guddat (HIWI), Ina Milz (Internship), Ulrike Maitas (Master Thesis), and Georgette Wirtz (Internship and Master Thesis). I thank my sister Julie Ruff and Stephan Chang for supporting the organic synthesis.

Sincere thanks are given to all the members of the EU-project “Oxygreen” for fruitful discussions and scientific exchange, especially PD Dr. Jens Schrader, Dr. Dirk Holtmann and Claudia Ley (Dechema, Frankfurt), Dr. Percy Niemann and Dr. Hans-Gottfried Genieser (Biolog, Bremen), Dr. Iwona Kaluzna (DSM, Geleen), Martina Geier and Andreas Braun (TU Graz, Graz), and Dr. Amol V. Shivange. I thank Prof. Dr. Danilo Roccatano as well as Rajni Verma (Jacobs University Bremen) for discussing my results and supporting the analysis with the generation of the MAP Profiles. The Oxygreen meetings stay unforgettable.

This thesis would not have been possible without the constant support and understanding that I received during the past years from my parents to whom I would like to express my deepest gratitude.

“Hiermit versichere ich, dass ich die vorliegende Arbeit selbstständig verfasst und keine anderen als die angegebenen Quellen und Hilfsmittel benutzt habe, dass alle Stellen der Arbeit, die wörtlich oder sinngemäß aus anderen Quellen übernommen wurden, als solche kenntlich gemacht sind und dass die Arbeit in gleicher oder ähnlicher Form noch keiner Prüfungsbehörde vorgelegt wurde.“

Aachen, den

Anna Joëlle Ruff

Lebenslauf

Persönliches

Name	Anna Joëlle Ruff
Geburtsdatum und -ort	08.10.1985, Aachen
Staatsangehörigkeit	deutsch

Ausbildung

Ab 2009	Promotion an der RWTH Aachen University, Lehrstuhl für Biotechnologie
2003-2009	Studium der Biologie, RWTH Aachen University; Diplomarbeit: „Einsatz redoxsensitiver Varianten des grün fluoreszierenden Proteins zur Untersuchung des Glutathionstoffwechsels bei der Spaltheefe <i>Schizosaccharomyces pombe</i> .“ Abschluss: Diplom-Biologin
1997-2003	Collège Royal Marie Thérèse in Herve, Belgien Abschluss : Certificat d'enseignement secondaire supérieur (Abitur)
1991-1997	Ecole libre primaire et maternelle libre mixte in Charneux, Belgien. Abschluss : Certificat d'Etude de Base (Grundschule)